This is to certify that the
dissertation entitled

SAMPLING AND MASS SPECTROMETRY APPROACHES FOR THE DETECTION OF DRUGS AND FOREIGN CONTAMINANTS IN BREATH FOR HOMELAND SECURITY APPLICATIONS

presented by

Audrey Noreen Martin

has been accepted towards fulfillment
of the requirements for the

Doctoral degree in Chemistry

A. Paul Wilkins
Major Professor's Signature

March 6, 2009
Date

SAMPLING AND MASS SPECTROMETRY APPROACHES FOR THE DETECTION OF DRUGS AND FOREIGN CONTAMINANTS IN BREATH FOR HOMELAND SECURITY APPLICATIONS

By

Audrey Noreen Martin

A DISSERTATION

Submitted to
Michigan State University
in partial fulfillment of the requirements
for the degree of

DOCTOR OF PHILOSOPHY

Chemistry

2009

ABSTRACT

SAMPLING AND MASS SPECTROMETRY APPROACHES FOR THE DETECTION OF DRUGS AND FOREIGN CONTAMINANTS IN BREATH FOR HOMELAND SECURITY APPLICATIONS

By

Audrey Noreen Martin

Homeland security relies heavily on analytical chemistry to identify suspicious materials and persons. Traditionally this role has focused on attribution, determining the type and origin of an explosive, for example. But as technology advances, analytical chemistry can and will play an important role in the prevention and preemption of terrorist attacks. More sensitive and selective detection techniques can allow suspicious materials and persons to be identified even before a final destructive product is made. The work presented herein focuses on the use of commercial and novel detection techniques for application to the prevention of terrorist activities.

Although drugs are not commonly thought of when discussing terrorism, narcoterrorism has become a significant threat in the 21st century. The role of the drug trade in the funding of terrorist groups is prevalent; thus, reducing the trafficking of illegal drugs can play a role in the prevention of terrorism by cutting off much needed funding. To do so, sensitive, specific, and robust analytical equipment is needed to quickly identify a suspected drug sample no matter what matrix it is in. Single Particle Aerosol Mass Spectrometry (SPAMS) is a novel technique that has previously been applied to biological and chemical detection. The current work applies SPAMS to drug analysis, identifying the active ingredients in single component, multi-component, and multi-tablet drug samples in a relatively non-destructive manner. In order to do so, a sampling

apparatus was created to allow particle generation from drug tablets with on-line introduction to the SPAMS instrument. Rules trees were developed to automate the identification of drug samples on a single particle basis.

A novel analytical scheme was also developed to identify suspect individuals based on chemical signatures in human breath. Human breath was sampled using an RTube™ and the trace volatile organic compounds (VOCs) were preconcentrated using solid phase microextraction (SPME) and identified using gas chromatography – mass spectrometry (GC-MS). Modifications to the sampling apparatus allowed for increased VOC collection efficiency, and reduced the time of sampling and analysis by over 25%. The VOCs are present in breath due to either endogenous production, or exposure to an external source through absorption, inhalation, or ingestion. Detection of these exogenous chemicals can provide information on the prior location and activities of the subject. Breath samples collected before and after exposure in a hardware store and nail salon were analyzed to investigate the prior location of a subject; breath samples collected before and after oral exposure to terpenes and terpenoid compounds, pseudoephedrine, and inhalation exposure to hexamine and other explosive related compounds were analyzed to investigate the prior activity of a subject. The elimination of such compounds from the body was also monitored. In application, this technique may provide an early warning system to identify persons of interest in the prevention and preemption stages of homeland security.

ACKNOWLEDGEMENTS

As my road to the point of writing this dissertation was unusual, there are many people that deserve my deepest thanks for their help along the way.

I must start by thanking my research advisor, Dan Jones. When you received a call from a stranger out of the blue that I wanted to talk to you about joining your research group and promptly moving to California to do my work at LLNL, you didn't run the opposite direction. That belief from day one that we could make this arrangement work was, and is, much appreciated. Your going outside the box for me has allowed me to become what I am today, and I will always be forever grateful for that. Thank you.

To George Farquar and Matthias Frank, my other research advisors – your support and efforts made it possible for me to return to, and stay afloat at, LLNL. Without you both, this research wouldn't exist, so thank you. Thanks especially to George, you made my initial summer at LLNL enjoyable enough that I wanted to return, provided valuable mentorship for the past 2 years, and didn't make my life miserable as I got closer and closer to graduation.

Thank you to my dear friends, the Musketeers that are always there to cheer me up when I'm upset, to make me laugh, to deep-fry anything we can lift, and to remind me that there IS, in fact, a life outside the lab worth enjoying. Thanks to my St. Louis ladies who have been supportive of my being in school for the last two decades of my life, and have provided me with many words of wisdom to help me hang in there.

Thank you to my family – you're always there to silently support my decisions, and have helped me with some of the uphill battles I have faced over the last few years. Dad, you've always encouraged me to be the best I can be, and helped me to determine what that is. Mom, you're always supportive and interested in whatever I'm doing, and that keeps me going when I feel like nothing is going right. Alan, Ciara and Aaron, you've inspired me to keep on trucking through grad school, even if it is by way of teasing me for not being a 'real' doctor. John and Andi, you've helped me realize what the priorities in my life should be, each in your own way. . . and thank you for NOT being doctors.

To Devan – who would have known that a quick summer internship in California would lead me to you? For the past few years you've been my best friend, my voice of reason, you've supported me, written MatLAB scripts for me, kept Southwest Airlines in business with me, listened to me as I talked your ear off on days when I didn't encounter any people at work, and shown me how happy I can be. Thank you for being you.

Finally, I would like to acknowledge the funding sources that made my research possible. Part of this work was performed as a Department of Homeland Security (DHS) Fellow through a program administered by the Oak Ridge Institute for Science and Education (ORISE). The development of the SPAMS system at was funded through DARPA and TSWG in the Department of Defense, as well as through internal funding at LLNL. This work was performed under the auspices of the U.S. Department of Energy by Lawrence Livermore National Laboratory in part under Contract W-7405-Eng-48 and in part under Contract DE-AC52-07NA27344. LLNL-TH-410574.

TABLE OF CONTENTS

LIST OF TABLES

LIST OF FIGURES

LIST OF EQUATIONS

CHAPTER 1: Introduction

1-1: Motivations

Protection of the public from threats of violence in the 21st century is based upon the principles of deterrence, prevention, preemption, crisis management, consequence management, attribution, and response.[1] Deterrence of violence involves actions that prevent the terrorist from planning an attack.[2] These actions can include fear of retribution, as seen in the nuclear arms race of the Cold War. Prevention is needed when deterrence fails and a terrorist group moves ahead with an attack plan. Prevention takes place at ports of entry, border checkpoints, and in many law enforcement actions that can stop or mitigate a planned attack.[3] Preemption follows closely with prevention, and aims to stop an attack before it occurs. This often includes an action, such as a raid by law enforcement, to disrupt the action of the terrorist.[4] If an attack does occur, crisis and consequence management become key functions in the protection of public safety. Strong leadership is required to coordinate multiple agencies responding to a crisis and ensure information is shared. Consequence management attempts to mitigate the effects of an attack. This occurs simultaneously with crisis management, and for example, would involve the coordination and actions of public health personnel after a biological attack. Attributing a terrorist attack involves identifying and confirming the parties who participated in the event.[5] This involves not only the forensic analysis of the scene of the attack, but also analysis of money and paper trails that may identify silent partners.[6] The ability to quickly and effectively attribute an attack also feeds back into deterrence, as being identified as the attackers may prevent an organization from planning an attack. Finally, response to violence is the final principle of protecting the public. It includes not

only focusing on the current identified threat, but also preventing potential criminals and terrorists from engaging in future violent activity. All of the principles rely on studying the aggressors, i.e., the social science of studying the psychology of terrorist groups, identifying the aggressors, i.e., law enforcement efforts, as well as the science and technology of understanding and identifying the threats.

The science and technology necessary for protecting the public from violence relies heavily on analytical chemistry to identify suspicious materials and persons. Traditionally this role has been more in the attribution phase, determining the type and origin of an explosive, for example. But, as technology has advanced and new techniques have been created, analytical chemistry can and will play an important role in the prevention and preemption of terrorist attacks. More sensitive and selective detection techniques can allow suspicious materials to be identified even before a final destructive product is made. The work presented herein focuses on the use of commercial and novel detection techniques for application to the prevention of terrorist activities.

1-2: Overview

Chapter 2 will discuss advances in the detection of drugs using Single Particle Aerosol Mass Spectrometry (SPAMS), which is a rapid, sensitive, and information-rich analytical tool. Although drugs are not commonly thought of when discussing terrorism, narcoterrorism has become a significant threat in the 21st century. The role of the illicit drug trade in the funding of terrorist groups is prevalent, thus, reducing the trafficking of illegal drugs can play a role in the prevention of terrorism by cutting off much needed funding. To do so, sensitive, specific, and robust analytical equipment is needed to

quickly identify a suspected drug sample no matter what matrix it is in. SPAMS is a novel technique that has previously been applied to biological and chemical detection; this chapter will discuss efforts to apply the technique to the identification of a variety of constituents in drug tablets.

Chapters 3 and 4 will discuss a novel analytical scheme to identify potential terrorists and criminals using a commercial gas chromatography-mass spectrometry (GC-MS) system. Human breath is sampled, breath constituents are concentrated, and the sensitivity of the GC-MS allows for trace volatile organic compounds (VOCs) to be identified in the breath. These VOCs are present in breath owing either to their production *in vivo*, or exposure to an external source of VOCs through absorption, inhalation, or ingestion. Those chemicals arising from exposure can provide information about the prior location and activities of the subject; thus, activities such as synthesis of explosive materials may be detected through analysis of substances in breath. In application, this technique may provide an early warning system to identify persons of interest in the prevention and preemption stages of homeland security. Chapter 3 will discuss the development of the analytical method, including instrument settings, breath sampling procedures and optimization, as well as repeatability of the analysis. Chapter 4 will present findings from several experiments when a subject had a known chemical exposure. Information on the uptake and decay of several VOCs is included in this chapter.

Chapter 5 will summarize conclusions from this body of work, as well as milestones that have been achieved. Information about the potential applications of the techniques developed in these studies will be included.

1-3: References

(1) *Combating Terrorism: Protecting the United States - Part I*; Hearing Before the Subcomm. on National Security, Veterans' Affairs, and International Relations of the House Comm. on Gov. Reform, 107th Cong. (March 23, 2002) (Statement of Col. R. J. Larson (USAF, Ret.) Director, ANSER Institute for Homeland Security).

(2) *Deterrence, Protection, and Preparation: The New Transportation Security Imperative, Special Report 270*; Transportation Research Board, **2002**.

(3) Smith, J. M. In *10th Annual Research Results Conference*: Colorado Springs, CO, **2003**.

(4) *Countering the Changing Threat of International Terrorism*; National Commission on Terrorism, **2000**.

(5) R. J. Larsen; David, R. A. *Homeland Security* **2000**, 1-8.

(6) Colby, E. A. *Expanded Deterrence* In Policy Review, **2008**.

CHAPTER 2: Single Particle Aerosol Mass Spectrometry of Drug Samples

2-1: Motivations and Introduction

The manufacture, sale, and use of legal and illegal drugs are major issues in the world today. The science of pharmaceutical development and quality control/quality assurance has consistently been a pursuit of the chemist. Analytical techniques that can identify the active and inactive ingredients of legal drugs, including over-the-counter and prescription medications, are necessary as it critical to know the components in the drug formulation and optimize the efficacy of a treatment. Counterfeit prescription drug synthesis and sale is increasingly becoming a major problem,[7] especially with the increase in the number and availability of online pharmacies and rising drug prices. For example, a study that analyzed anti-malarial formulations marketed as containing chloroquine as the active ingredient obtained from street vendors in Cameroon determined that 32% of the samples analyzed were counterfeit and contained no chloroquine.[8] The lack of active ingredient in such drugs can cause the spread of diseases such as malaria, and well as create new health concerns.

The motivation for the analysis of illegal drugs is more criminal in nature. The active and inactive ingredients are still important to identify, but many byproducts, cutting agents, and contaminants are usually present in illegal drugs, as synthesis is often done with off the shelf ingredients and apparati, in clandestine locations. These ingredients may confound the analysis, thus insensitivity to matrix effects is an important quality of an analytical technique. Another aspect of detecting illicit drugs is that the criminal may attempt to destroy evidence before analysis, such as rinsing the drugs down the drain or destroying them in some manner. Analysis of residual particles would then be

advantageous to determine what the prior contents of a bottle or distillation flask were, or the identity of a powder on the floor or table of a suspected drug house.

Drug trade contributes to the threat of terrorism as profits from drug exportation and sale often fund organizations that commit violence against the public. For example, the Revolutionary Armed Forces of Colombia, FARC, is accused of being a narcoterrorist organization, monetarily benefiting from the production and sale of cocaine.[9] It is important to have an analytical technique that can identify illicit drugs with speed, sensitivity, and selectivity in any environment, including border crossings to prevent the importation of illegal drugs into the United States and combat the drug trade.

This chapter will describe efforts made to use the Single Particle Aerosol Mass Spectrometer to detect and identify drugs. For safety and regulatory reasons, over-the-counter drugs are used in lieu of illicit drugs, but the results are transferable across different classes of drugs. Several over-the-counter drugs such as pseudoephedrine are used as starting materials in the synthesis of illegal drugs, thus their identification is important for identifying processes used in clandestine synthesis of drugs. Also, many over-the-counter drug formulations are used as cutting agents in counterfeit and illegal drugs, so their identification would aid investigators identify tablets and their sources. An anti-malarial drug is also analyzed as proof-of-concept for counterfeit drug detection.

2-2: Background on Drug Analysis

Sensitive and specific analysis of drug tablets has a broad range of applications including pharmaceutical quality control and forensic analysis of counterfeit drugs or illicit

substances. In a pharmaceutical context, it is important to identify the drug ingredient as well as any impurities that affect quality control. In forensic investigations, it is important to identify the drug ingredients and impurities while maintaining the physical integrity of a tablet. Both industries depend on fast and accurate analytical methods in order to process a large sample load.

Preliminary forensic tests of a tablet rely first on visual inspection to identify any differences in shape, color, or markings from an authentic pill, or similarities to other drug seizures for prosecution reasons.[7, 10] Confirmatory testing requires that the active ingredient be identified and characterized. In fact, the World Health Organization (WHO) states that "the principal requirement for a suitable screening procedure is the identification of the active drug substance".[10] To this end, forensic laboratories as well as pharmaceutical companies are faced with an ever increasing sample load, stressing the importance of fast high-throughput analysis. Thus, a simple, fast detection system with little sample preparation that can identify the active ingredient in a tablet while preserving the integrity of its structure and visual identifiers would be advantageous.

Several methods have been used to separate and/or detect drug samples alone, as mixtures, or in complex samples. Capillary electrophoresis[11, 12] and infrared (IR) spectroscopy have often been used for drug detection, although sample preparation can be time-consuming.[13-15] To circumvent this issue, near IR reflectance spectroscopy has been used to directly analyze drug tablets.[13, 15] While sensitive, the main limitation to IR is the training required for the interpretation of the complex spectra the technique yields. Gas and liquid chromatography (GC and LC)[16-18] have both been used for drug analysis when coupled to mass spectrometry (MS). The most common technique currently in use

for drug analysis is GC-MS. This technique has the advantage of providing orthogonal data from one analytical scheme which fulfills the Scientific Working Group for the Analysis of Seized Drugs (SWGDRUG) recommendations for forensic analysis of seized drugs.[19] The main drawbacks of GC-MS are that an extraction step is required which lengthens the time of analysis, uses consumable reagents, destroys the physical integrity of the solid sample, many drugs require derivatization because of their low volatility, and the chromatography itself has an inherent time requirement that can lead to an individual analysis taking over ten minutes.[16] Chromatography is also used to analyze drugs in complex samples. Water samples[16, 20, 21] and biological samples[17, 18] have been analyzed using LC-MS/MS, high performance LC-MS, GC with a nitrogen-phosphorus detector, and GC-MS. Antonic and Heath demonstrated the use of GC-MS in the determination of several drugs in river sediments after extraction and the addition of a derivatizing agent to increase the volatility of the drugs.[16]

Because of the sample preparation time required for GC-MS, other options for sample introduction into a mass spectrometer have been explored. The recently developed ionization methods direct analysis in real time (DART), desorption atmospheric pressure chemical ionization (DAPCI) and direct electrospray ionization (DESI) have been used in conjunction with mass spectrometry to identify active ingredients in prescription, non-prescription and illicit drugs by placing the tablet in the ionization stream of the instrument.[22-30] Although many groups break or scrape the tablets before analysis[26, 27, 31] in order to sample the contents of the center of a coated tablet, little to no sample preparation is necessary. Molecular fragmentation is commonly minimal; the ions predominantly obtained are $[M+H]^+$ or $[M-H]^-$ which allow for facile identification of the

active ingredients.[22, 30] Van Berkel *et al.* have coupled DESI-MS to TLC separation of extracted drug ingredients creating an orthogonal approach to drug analysis.[32] While these techniques are promising advances in drug analysis, they do not sample the heterogeneous body of a tablet, only the small area that interacts with the ion or droplet stream, which may allow a drug component to go undetected.

Single Particle Aerosol Mass Spectrometry (SPAMS) is an on-line detection system that individually analyzes single micrometer-sized particles and provides real-time data including sizing and simultaneously obtained positive and negative ion mass spectra.[33-35] SPAMS has been applied in a variety of environments,[33, 34] and is capable of low concentration detection of target particles in a high background environment. It was hypothesized that SPAMS would also provide a fast, simple, sample preparation-free method of analyzing drugs in tablet form. The application of SPAMS to the rapid detection of over-the-counter drug samples is described herein. Although SPAMS has previously been applied primarily to aerosolized liquids, this work shows the direct analysis of solid particles without the need for solvent extraction, and demonstrates the applicability of SPAMS to drug detection and identification.

2-3: Background of SPAMS

Single Particle Aerosol Mass Spectrometry (SPAMS) is a technique based on the original work of Davis in the 1970s.[36] Davis' system allowed aerosol particles to impinge on a heated Rhenium ribbon causing ions to be formed and released for analysis in a magnetic sector mass analyzer; the maximum particle yield, defined as the number of particles producing ions as compared to the number of particles per cm^3 of air, was reported as

0.3%.[36] Over the past several decades, many modifications and improvements have been made to Davis' original system, which have been reviewed by Noble and Prather,[37] resulting in the current commercially available aerosol mass spectrometer from TSI Inc. (Shoreview, MN). This instrument incorporates two time of flight mass analyzers which simultaneously analyze both the positive and negative ions produced in the source region,[33] with a particle sizing region that calculates particle size based on the timing of scattering effects of 2 continuous wave (CW) lasers through which each particle passes. Since the 1990s, work at Lawrence Livermore National Laboratory (LLNL) has focused on modifying and improving this commercial instrument to function as a sensitive and selective biological agent detection system under the name of Bioaerosol Mass Spectrometry (BAMS). Through this work the particle sizing region on the front end of the instrument, as well as the operating software, was modified, incorporating up to 6 CW lasers allowing a more accurate determination of the aerodynamic diameter of each particle.[35] This added a degree of selectivity, because particles of a size of interest could be selectively ionized in the source region, preventing excessive amounts of non-useful data from taking up disk space as well as time to be thoroughly analyzed. A laser induced fluorescence (LIF) region was also added, allowing the fluorescence of each particle excited at 266 nm to be determined. Advances in data acquisition and storage have also been made. In the past two years, an additional LIF stage was incorporated to also measure the fluorescence of each particle excited at 355 nm, as well as a stage to determine the charge on each particle. These stages can be operated to pre-select particles of interest for mass spectrometric analysis. In the current configuration, particle yield, when defined in the same manner as in Davis' experiments of the 1970s, can be as

high as 90%. The operating software for the LLNL system is very powerful. After 'training' the system on a particular target particle type by collecting many spectra of a standard sample, alarm files can be made and the instrument will record an alarm whenever a user-set threshold number of particles identified by the software as containing that specific compound described by the alarm file in a set period of time are detected. This allows the instrument to operate autonomously with little user interaction for air monitoring studies.

Although originally applied to the detection of such defense threat analytes as *Bacillus* spores,[38-44] viruses, [41] toxin simulants,[41] fungi,[39] and Mycobacteria,[44] work at LLNL has expanded the application of the BAMS system to include explosives,[45] chemical warfare agent simulants,[46] and even stretched into medical applications.[44, 47] Because of this broader sample application, the name BAMS was officially changed to SPAMS[45] to present a more universal detection system.

A significant advantage of SPAMS is its ability to analyze solid and liquid samples with no sample preparation. Vapor phase samples can also be analyzed, but do require some sample preparation to create particles large enough to detect.[48] It is also able to detect a small number of particles with a particular chemical signature in the midst of a large number of particles that do not share the same chemistry. This ability is aided by the capacity to pre-select particles for mass spectrometric analysis using the fluorescence and/or charge stages.

2-4: SPAMS Description

A schematic of the SPAMS instrument used at LLNL is shown in Figure 2- 1.[39]

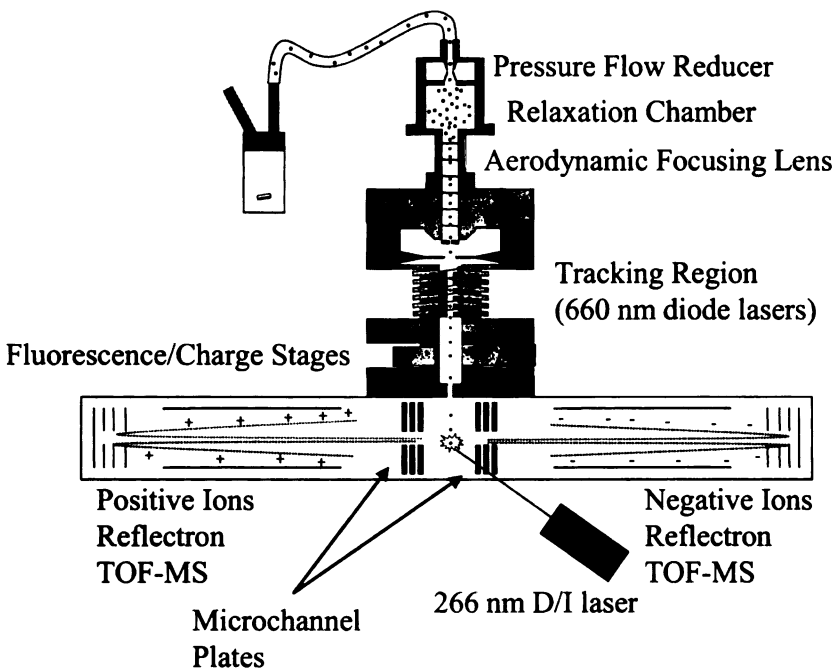

Figure 2- 1: Schematic of the Single Particle Aerosol Mass Spectrometer. Particles are generated using the modified glass vial and transferred to the SPAMS via conductive tubing. After passing through a pressure flow reducer with a relaxation chamber and aerodynamic focusing lens, the pressure is lowered and the beam is focused into a linear beam. Particles are then tracked, where the aerodynamic velocity and size are determined. Laser induced fluorescence at two wavelengths (266 and 355 nm) as well as particle charge is then determined before the particle enters the source region of the mass spectrometer. The particle is desorbed and ionized by an Nd:YAG laser operating at 266 nm, and the positive and negative ions created are concurrently accelerated in linearly opposing directions into two reflectron time-of-flight mass analyzers, where two mass spectra are recorded for each particle.

Particles released from the analyte in the solid sampling vial (discussed below) are carried to the SPAMS via 3/8" conductive tubing and enter the pressure flow reducer which reduces the pressure of the analyte stream for introduction to the higher vacuum chambers by passing the particles into two facing conical apertures, thereby cutting the flow significantly. On the other side of the apertures the particles lose their directionality in the relaxation chamber. From this chamber, the particles pass into the aerodynamic focusing lens, which centers the particles into a thin stream by passing them through a series of nine consecutively thinner lenses with orifices of decreasing diameter. The particles then pass into the tracking region of the SPAMS, where their aerodynamic diameter ($d_{p,a}$) is determined. As the particles travel through this region of the instrument, the larger particles move more slowly than the smaller particles; thus size can be extrapolated from a calculation of the particle's speed. The tracking region ($\sim 10^{-4}$ Torr) contains up to 6 diode lasers (660 nm, continuous wave) each paired with a channel photomultiplier tube (CPMTs, part c962, Perkin Elmer Optoelectronics, Santa Clara, CA). As the particle travels through the laser beams, the light is scattered from its normal path, and a change in laser light intensity is detected by the CPMTs. The time of each scattering event is recorded, and the series of scattering events can be used to determine the particle's velocity and therefore aerodynamic size using a field-programmable gate array. Incorporating 6 lasers provides several scattering events per particle that would allow for the deconvolution of velocities of two particles traveling through the tracking region simultaneously. The size measurement is calibrated by analysis of spherical standards (polymeric beads, Bangs Laboratories, Inc., Fishers, IN, and Duke Scientific Corp, Fremont, CA) of known size. Aerodynamic diameter, and not actual diameter, is

used to describe aerosol particles. Aerodynamic diameter is the diameter of a unit-density spherical object that moves with the same velocity through a fluid[49] and relates to Stokes' diameter, which assumes a particle is spherical, by Equation 2- 1:

$$d_{p,a} = d_{p,S}\sqrt{\delta}_p$$

Equation 2- 1: Relationship between aerodynamic diameter and Stokes' Diameter,

where $d_{p,a}$ is the aerodynamic diameter of a particle, $d_{p,S}$ is the Stokes' diameter of the particle, and δ_p is the density of the particle.

After size is determined, the particle enters the source region of the mass spectrometer (~10^{-6} Torr). The previously determined particle velocity is used to calculate the exact time the particle will be centered in the source region, and internal electronics trigger the desorption/ionization (D/I) laser to fire at this precise moment. The laser, a Q-switched frequency-quadrupled Nd:YAG (Ultra CFR, Big Sky Laser Technologies, Inc., Bozeman, MT), operates at 266 nm with 7 ns FWHM pulses and can fire at up to 20 Hz with fluences between 0.05-8.4 nJ/μm^2. When fired, the laser imparts a significant amount of energy to the particle, desorbing and ionizing it to create both positive and negative ions. These ions are simultaneously accelerated by an electric field in linearly opposing directions into two linear reflectron time-of-flight (TOF) mass analyzers,[50] each 536 mm in length. The TOF mass analyzer operates by determining an ion's mass/charge by measuring the time between acceleration and arrival at the detection plate as it travels through a field-free drift region.[50, 51] The reflectron aspect of the TOF was developed to

improve the resolution of the time of arrival of ions of equal masses which have slightly different flight times owing to the variation in their ionization time, initial position, and initial kinetic energy.[51] It involves the addition of retarding plates at the end of the flight tube which deflect the ions and reverse their direction to pass back through the flight tube to ring microchannel plate detectors (MCP, Burle Technologies, Inc., Lancaster, PA) surrounding the exit from the source region. Ions that were imparted with larger kinetic energies or were closer to the flight tube during ionization and acceleration travel deeper into the retarding field than do those with lower kinetic energies or those that were further from the flight tube; thus, the faster ions are slowed slightly, allowing both types of ions to reach the detector simultaneously. Time is then related to the mass-to-charge ratio (m/z) by Equation 2- 2: [51]

$$t^2 = \frac{md^2}{2zeV_S}$$

Equation 2- 2: Relationship between time and mass-to-charge ratio in a time-of-flight mass analyzer,

where m is the mass of the ion (kg), d is the distance the ion travels to the detector (m), z is the charge on the ion, e is the charge on an electron (C), and V_S is the accelerating voltage (V). The signal from the MCPs is digitized (Signatec, Inc., Newport Beach, CA, PDA1000) at 500 MHz, 8 bits with 256 arbitrary units (a.u.) on a 333 mV scale, yielding a mass spectrum from both polarities of ions, providing a significant amount of information on each single particle.

2-5: Laser Optics

Figure 2- 2 shows a schematic of the optics used to create the D/I laser beam in the source region.

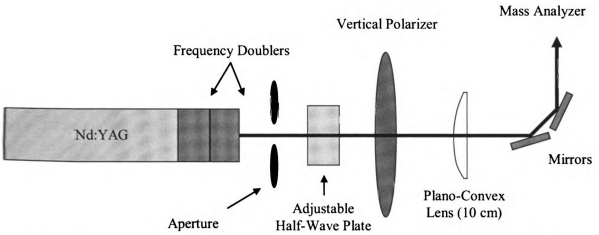

Figure 2- 2: Diagram of the desorption/ionization laser optics. A Nd:YAG laser is frequency quadrupled to generate a 266 nm beam which is then passed through an aperture, adjustable half-wave plate and vertical polarizer before being imaged by a plano-convex lens with a 10 cm focus length onto two planar mirrors which direct the image into the source region of the mass spectrometer.

The Nd:YAG laser beam, originally 1064 nm in wavelength, is passed through 2 frequency doublers to form a 266 nm beam. The beam then passes through an aperture and a half-wave plate, which is manually rotatable to control the polarization of the beam. Only vertically polarized light is then passed through the vertical polarizer; thus, the half-wave plate and polarizer together control the energy of the transmitted beam. The beam passes through a 10 cm plano-convex lens which creates an image of the aperture that is reflected into the source region on 2 planar mirrors. The position of the mirrors is

controlled by manual calipers which manipulate the position of the image on the x-y plane. The resulting beam is ~ 330 μm in diameter in the center of the source region, and maintains a relatively flat-topped energy profile,[41] although weaker areas do exist, particularly near the beam edges. The energy of each laser pulse is measured at the back of the source region using a digital laser energy meter (Coherent, Inc., Santa Clara, CA, J25LP-MUV). The laser energy is averaged over 50 particles to give statistically significant values for energy, with the pulse-to-pulse variation generally being <5%. Laser fluence is often reported, and is equivalent to the laser energy per beam area, which in the current system is 0.086 mm^2.

2-6. *Solid Sampling Materials*

Figure 2- 3 shows the modified glass vial used to introduce solid samples, particularly drug tablets, to the SPAMS.

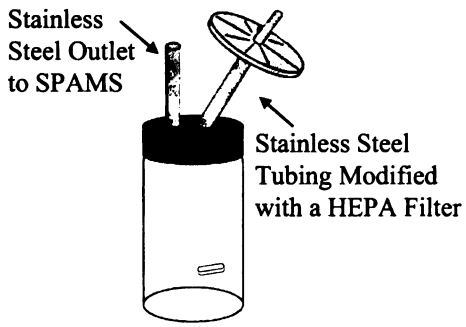

Figure 2- 3: Diagram of modified glass vial used to generate particles from solid samples for analysis by SPAMS. The plastic cap was modified using stainless steel tubing to create a port to transfer the sample to the SPAMS as well as a second port to which a HEPA filter was attached. The solid sample is placed in the vial which is then shaken or vortexed; particles are generated by the collisions induced by the shaking.

A ~20 mL glass vial with a plastic cap was modified using stainless steel tubing to create a port to allow connection of 3/8" conductive tubing to connect to the SPAMS instrument. A second piece of steel tubing was also modified into the plastic cap to allow connection of a HEPA filter to the vial. Particles are created by manually shaking or vortexing the vial, causing collisions between the vial contents and the vial walls.

2-7: Data Collection and Analysis

Operation of the SPAMS system and recording of the data obtained is performed using a program developed at LLNL by Vincent Riot. Data can be collected using all analysis stages or any combination thereof, with the minimum requirement that two tracking lasers are used for accurate velocity determination. The current experiments used only the sizing (3 tracking lasers) and mass spectral regions, generating smaller data files. The software can be set to acquire a specific number of mass spectral 'hits;' a 'hit' occurs when mass spectral data is obtained that surpasses a user-define threshold, typically ~120 mV on the 333 mV scale. Hundreds if not thousands of particles per sample are analyzed, typically collecting 1000 mass spectral 'hits'. Once the data is obtained, spectral analysis occurs using another program developed in house by Paul Steele, Gary Armstrong, and David Fergenson, 'Irene,' which was written in MatLAB. By using 'Irene,' spectra can be averaged, sorted by peak area at a particular m/z value, integrated, and statistically analyzed.

The mass spectrum for each particle is analyzed using 'Irene' to determine its composition by comparison against user-generated alarm files. The alarm files used with SPAMS are typically created using an algorithm based on pattern matching, where the

350-order vector of the mass spectrum of a single particle is compared to the average vector from the mass spectra of a known material contained in the alarm file.[52, 53] Further refinement of the alarm files is then done by creating rules trees to further discriminate particles. In a rules tree, each 'branch' is created by probing a specific mass vector to determine if it is greater than or less than a specific value. If the particle passes onto a specific branch, another mass vector may be probed, i.e. a second 'branch', etc. until sufficient differentiation has occurred. Rules trees analyze normalized vector values so that an increase in overall signal from the MCPs does not affect the classification. Contributions from mass vectors typically seen in all particles, such as m/z 23 and 39, due to sodium and potassium, respectively, are eliminated to facilitate comparisons of mass spectra.

Analysis of the heterogeneous drug samples provided many particles that contained numerous active ingredients, as discussed below, precluding accurate pattern matching without creating alarm files and thus a training set requiring a standard mixture for every possible combination of drug ingredients. Therefore, alarm files for this study were created using only rules trees, where specific m/z values, or mass vectors, could be used to categorize the components of the particle. A rules tree was created to identify each drug using m/z values corresponding to characteristic peaks seen in the mass spectra of each compound. Using a unique alarm file for each drug allowed detection of any combination of 1, 2, 3, 4, etc. of these compounds in a single particle, as well as reduced confounding by any filler materials and inactive ingredients. When discriminated with a single alarm file, each particle is thus processed through all 'branches' of the rules tree, and is identified as containing that specific drug, or not containing that specific drug

(Null). All particles are then subjected to the rules tree for the second drug, etc., until all alarms have been run, allowing a single particle to be identified by multiple alarm files. The rules trees used for the identification of ibuprofen is shown in Figure 2- 4, and subsequent rules trees for other drug components are included in Appendix A.

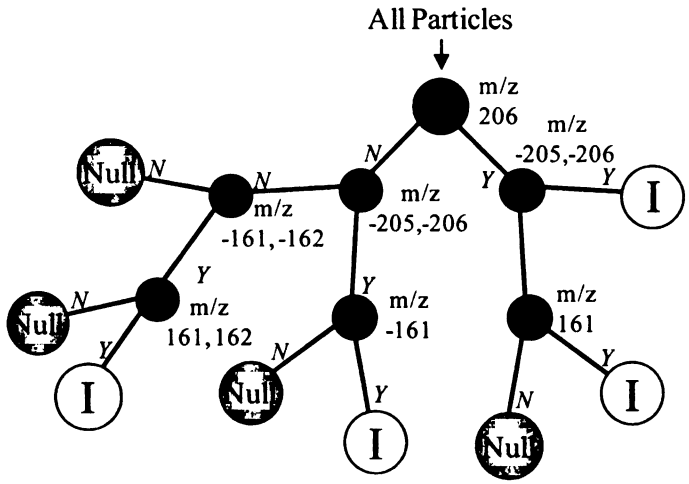

Figure 2- 4: Rules tree for classification of ibuprofen. The mass vectors probed at each branch division are shown, with 'Y' indicating a positive response and 'N' indicating a negative response. Circles labeled 'I' indicate a positive identification for ibuprofen; circles labeled 'Null' indicate a negative response. M/z 206 corresponds to the $[M]^+$ ion, m/z -205 and -206 correspond to the $[M]^-$ and $[M-H]^-$ ion, m/z 161 corresponds to the $[M-COOH]^+$ ion, and m/z -161 corresponds to the $[M-COOH]^-$ ion.

It should be noted that although only mass vectors are used to create the alarm files in this work, particle size, fluorescence (266 nm and 355 nm excitation), and/or charge could be incorporated into the alarm file in the future to further enhance the confidence in identification after an alarm is reported to further the selectivity.

2-8: Drug Material Preparation

Single ingredient over-the-counter medications containing acetaminophen (analgesic/antipyretic), aspirin (NSAID), clemastine (antihistamine), diphenhydramine (antihistamine, sedative), ibuprofen (NSAID), loratadine (antihistamine), phenylephrine (decongestant), or pseudoephedrine (decongestant) were obtained as tablets from commercial grocery chains. Tablets containing chloroquine (antimalarial) were obtained from a commercial pharmacy in Belize City, Belize. Multi-ingredient medications were also obtained from commercial grocery chains: Tylenol Cold™ and Tylenol PM™, containing acetaminophen and diphenhydramine, Tylenol Severe Congestion™, containing acetaminophen, diphenhydramine, pseudoephedrine, and guaifenesin (expectorant), and Advil Cold and Sinus™, containing ibuprofen and pseudoephedrine.

For the single tablet experiments, a single tablet was placed in the modified glass vial and attached to the SPAMS using 3/8" conductive tubing. The glass vial was either manually shaken or placed on a vortexer (Fisher Scientific, Inc.); the collisions of the tablet with the sides of the glass vial created sufficient particles for analysis. In fact, manual shaking typically generated and transferred more particles to the SPAMS instrument than could be analyzed at the 20 Hz frequency of the D/I laser. Placing the vial on the vortexer at a low setting provided a steadier stream of particles to the instrument, without constant saturation of the sampling rate of the instrument. For the multiple tablet experiments, several tablets were simultaneously placed in the vial, each containing a different active ingredient. These tablets were then removed from the vial and the emptied vial again analyzed. A fluence of 2.7 $nJ/\mu m^2$ (SD=0.1) was used for all samples. The drugs studied are shown in Table 2- 1, including their molecular weights and chemical structures.

Table 2- 1: Structures and molecular weights of drug compounds studied.

Drug	Structure	Drug	Structure
Acetaminophen MW 151.06	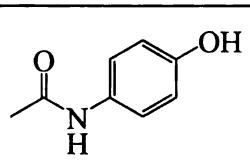	Diphenhydramine MW 255.16	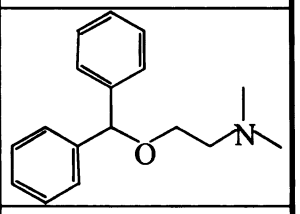
Aspirin MW 180.16	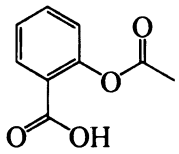	Guaifenesin MW 198.09	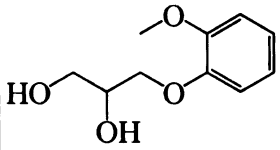
Chloroquine MW 319.18	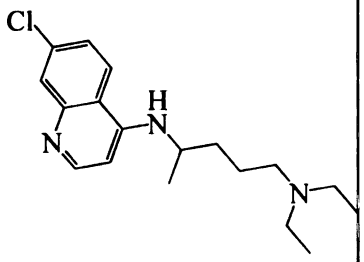	Ibuprofen MW 206.28	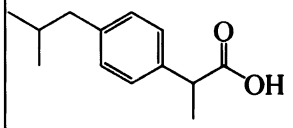
Chlorpheniramine MW 274.12	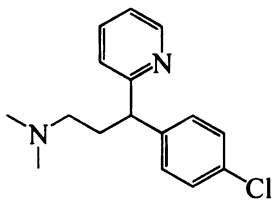	Loratadine MW 382.15	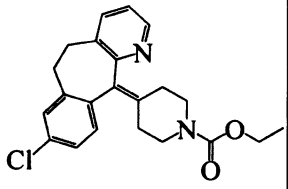
Clemastine MW 343.17	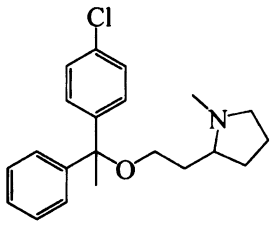	Phenylephrine MW 167.21	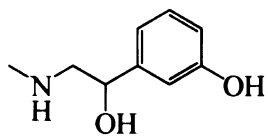
Dextromethorphan MW 271.19	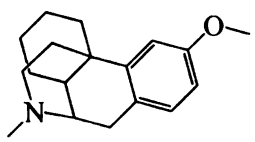	Pseudoephedrine MW 165.23	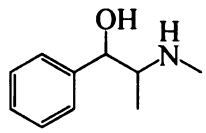

2-9: Drug Analysis Using SPAMS

2-9-1: Bayer™ Aspirin

The resulting dual-polarity mass spectrum obtained from a single Bayer™ tablet containing 325 mg of aspirin is shown in Figure 2- 5.

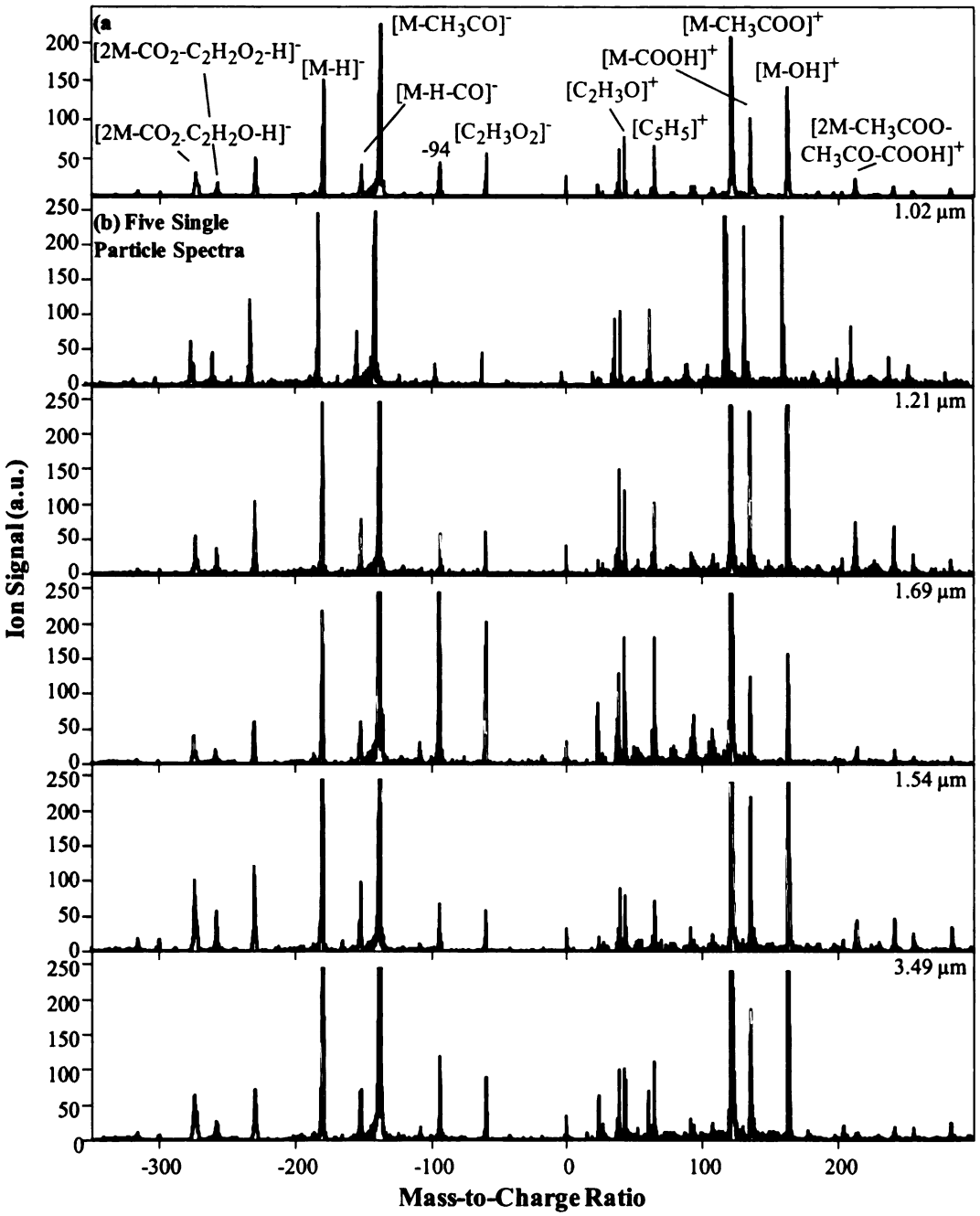

Figure 2- 5: (a) Average single particle aerosol mass spectra of 999 aspirin particles, and (b) five consecutively obtained aspirin particles (aerodynamic diameter displayed in upper right of each spectrum). The single particle spectra contain all peaks used to identify aspirin. The spectra from these particles were obtained in less than five seconds.

Figure 2- 5(a) shows the average mass spectrum of 999 particles generated from the tablet obtained at a rate of 1 spectrum every 1.26 seconds. The average aerodynamic diameter of the particles was 1.54 μm (RSD 71.7%). The large size distribution (0.59 – 8.71 μm) was expected owing to the method of particle formation, and particle size did not affect the relative ion abundances. The major ions observed in the positive and negative mass spectra are characteristic of the aspirin (acetylsalicylic acid) present in the tablet. Peaks at m/z -179, -151, and -137, due to $[M-H]^-$, $[M-H-CO]^-$, and $[M-CH_3CO]^-$, respectively, and major peaks in the negative ion spectrum, and have been previously documented in solid tablet analysis using DESI in negative ion mode to analyze the broken surface of a tablet[25, 26] The spectrum also contains several significant peaks hypothesized to arise from the formation and fragmentation of an acetylsalicylic acid dimer formed via hydrogen-bonding ($[2M-CO_2-C_2H_2O-H)]^-$ and $[2M-CO_2-C_2H_2O_2-H]^-$, at m/z -273, and -257, respectively) which can also aid in identification of the active ingredient. The main peaks in the positive ion spectrum are present at m/z +121, +135, and +163 ($[M-CH_3COO]^+$, $[M-COOH]^+$, and $[M+H-H_2O]^+$, respectively) the latter of which has been previously described using DART, DESI and DAPCI in positive ion mode to analyze the broken surface of a tablet.[31] Small peaks attributed to the dimer are also seen in the positive ion spectrum at m/z +213, 241, 255, and 283, assigned as $[2M-CH_3COO-CH_3CO-COOH]^+$, $[2M-2CH_3COO-H]^+$, $[2M-CH_3COO-COOH-H]^+$, and $[2M-COOH-CH_3-OH]^+$, respectively. Figure 2- 5(b) shows the mass spectra obtained from five consecutive single particles of the aspirin tablet. Note the presence of all identifying peaks in the single spectra as well as the consistency in the signal obtained, allowing the presence of aspirin in the table to be confirmed from a single particle. The speed with

which the mass spectra are obtained is demonstrated by the fact that the spectra shown in the figure were obtained in less than five seconds. Software developed in-house has the capability to identify a sample in real-time based on single spectra and could be trained to identify and alarm when a specific drug was detected.[53]

2-9-2: Chloroquine Diphosphate

Figure 2- 6a shows the average dual-polarity mass spectrum obtained from a single tablet containing 250 mg of an anti-malarial drug, chloroquine diphosphate. 1000 particles were analyzed in 182 s.

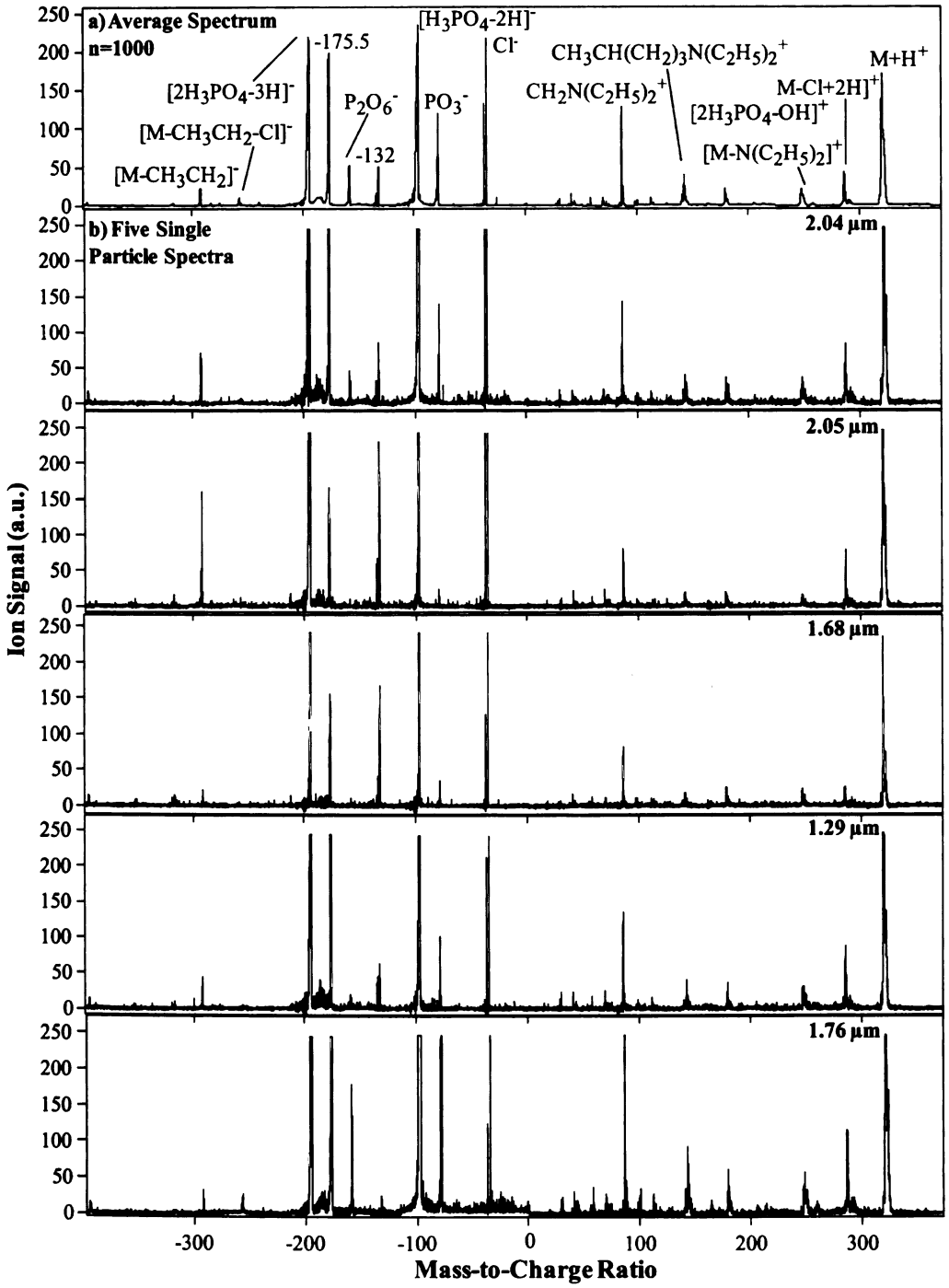

Figure 2- 6: a) average dual-polarity mass spectrum of 1000 particles dislodged from a single chloroquine phosphate tablet, b) mass spectra obtained from 5 individual particles of chloroquine phosphate dislodged from the tablet. Particle size is notated.

The average aerodynamic diameter of the particles was 1.88 μm (RSD 43.7%). Most peaks in the positive and negative polarities can be attributed to the parent or fragment ions of the drug compound (7-chloro-4-((4-(diethylamino)-1-methylbutyl)amino)-quinoline = M, MW 319.18). The $[M+H]^+$ ion is the most abundant ion in the positive spectrum at m/z 320, followed by the $[CH_2N(C_2H_5)_2]^+$ fragment at m/z 86. Other fragments due to the loss of chlorine and addition of hydrogen (m/z 286), the loss of $N(C_2H_5)_2$ (m/z 247), and $[CH_3CH(CH_2)_3N(C_2H_5)_2]^+$ (m/z 142) are also seen in the positive spectrum. The final major fragment seen in the positive ion spectrum is due to the phosphate salt of the drug, $[2H_3PO_4\text{-}OH]^+$ at m/z 179. Several peaks are also seen in the negative ion spectrum that can be attributed to phosphate salts. $P_2O_6^-$, PO_3^-, $[2H_3PO_4\text{-}H]^-$, $[2H_3PO_4\text{-}H_3O]^-$, and $H_2PO_4^-$ are seen at m/z -158, -79, -195, -177, and -97, respectively. Peaks indicative of chloroquine are also seen in the negative spectrum; loss of an ethyl group is seen at m/z -290. All of these fragment ions are consistent with the presence of the active ingredient, chloroquine, in the sample. Figure 2- 6b shows the dual-polarity mass spectra from five individual particles containing chloroquine. Although there is some variation in the intensity of the peaks, the characteristic peaks are present in all spectra, and chloroquine can be easily recognized as a component of the tablet. The high quality and reproducibility of these mass spectra allow accurate rules trees to be created, which, when used with the software developed in house, provide automated identification of the compound with none of the alarm files for the other drugs tests provided a positive alarm.

2-9-3: Clemastine Fumarate

An allergy medication containing 1.34 mg of clemastine fumarate was then studied. An equivalent value of 1 mg of clemastine free base was present in the tablet. The average aerodynamic diameter of 999 particles was 1.82 μm (RSD 45.4%). Figure 2- 7shows the dual-polarity mass spectrum obtained from a single particle of the tablet. This particle was 2.09 μm in diameter.

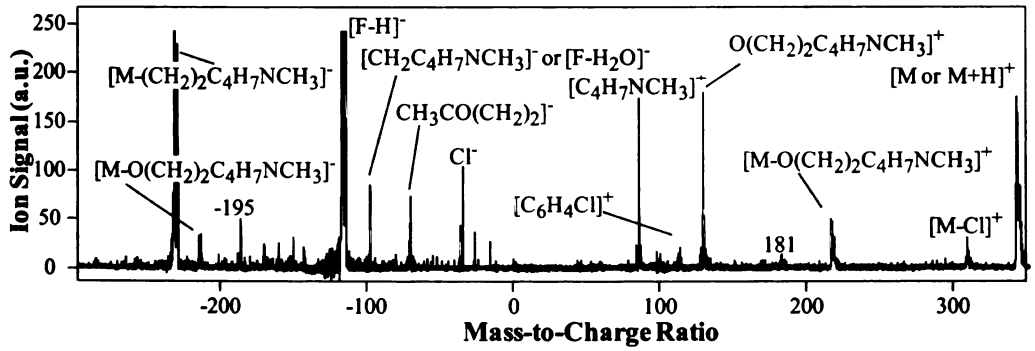

Figure 2- 7: Average mass spectrum of a single particle dislodged from a clemastine tablet (aerodynamic diameter 2.09 μm).

Many fragments are present, owing to the fragmentation of the bonds connecting the 3 rings of the molecule. A series of fragments attributed to the consecutive breakage of C-C bonds on the alkane chain connecting the pyrrolidine ring to the molecule are present: $[C_4H_7NCH_3]^+$, $[CH_2C_4H_7NCH_3]^-$, $[M\text{-}(CH_2)_2C_4H_7NCH_3]^-$, $[O(CH_2)_2C_4H_7NCH_3]^+$ and $[M\text{-}O(CH_2)_2C_4H_7NCH_3]^+$ and $[M\text{-}H\text{-}O(CH_2)_2C_4H_7NCH_3]^-$, at m/z 84, -98, -231, 128, 215, and -215, respectively. The fragment at m/z -71 is formed by the removal of both the aromatic rings and the pyrrolidine ring, $[CH_3CO(CH_2)_2]^-$. The chlorine atom is also removed from the molecule, leading to fragment ions at m/z -35, Cl^-, and m/z 308,

assigned as $[M-Cl]^+$. A peak assigned as a molecular ion is seen in the positive spectrum; however, limitations in the data acquisition range prevent accurate mass calibration in this region, so it is unknown whether the peak is at m/z 344, assigned as the $[M]^+$ ion, or m/z 345, due to $[M+H]^+$. This peak, as well as all peaks due to ions containing the chlorine atom, shows a consistent and appropriate isotopic distribution. A peak due to the fumarate salt is also seen in the negative ion spectrum: $[F-H]^-$ at m/z -115. An additional peak at m/z -98 may be due to $[F-H_2O]^-$, although this is more probably due to the clemastine fragment described above.

2-9-4: Benadryl™ (Diphenhydramine)

Next, an antihistamine and sedative Benadryl™ tablet containing 25 mg diphenhydramine was studied using SPAMS. The average aerodynamic diameter of 999 particles was 1.81 μm (RSD 80.6%). Figure 2- 8 shows the mass spectrum of an individual particle generated from a single tablet.

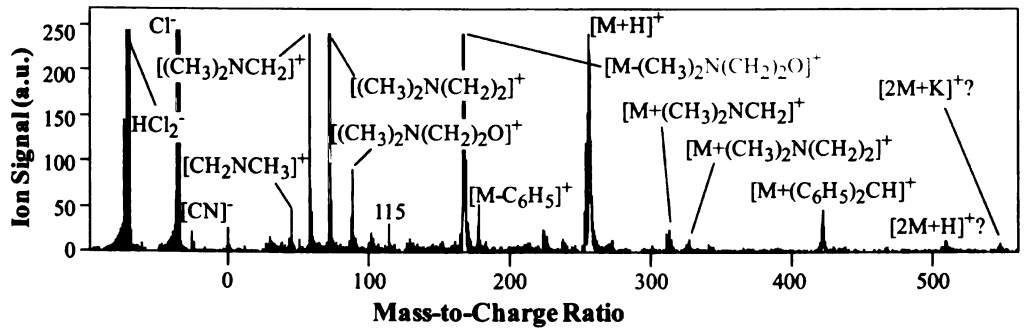

Figure 2- 8: Single particle aerosol mass spectrum of an individual diphenhydramine particle (aerodynamic diameter 1.14 μm).

Minimal structural information is present in the negative ion spectrum; only the fragment attributed to $[CN]^-$ is identified. A peak attributed to HCl_2^- is also seen, with the corresponding chlorine isotope ratio at m/z -71, -73, and -75. However, many peaks indicative of diphenhydramine are present in the positive ion spectrum. The most prominent peaks are assigned as loss of the side-chain from the parent molecule: $[(CH_3)_2N(CH_2)_2O]^+$, $[(CH_3)_2N(CH_2)_2]^+$, and $[(CH_3)_2NCH_2]^+$ at m/z +88, +72, and +58, as well as $[M\text{-}(CH_3)_2N(CH_2)_2O]^+$ (m/z +167); the latter three have been previously reported using GC-MS (+EI),[54] and LC-MS-MS (+CID).[55] Peaks corresponding to the addition of these fragments to the molecular species as well as the protonated intact molecule are also present: $[M+(CH_3)_2NCH_2]^+$ (m/z +313), $[M+(CH_3)_2N(CH_2)_2]^+$ (m/z +327), $[M+(C_6H_5)_2CH]^+$ (m/z +422) and $[M+H]^+$ (m/z +256). Two peaks separated by 38 mass units are seen in the high mass region of the positive mass spectrum. These peaks have been tentatively attributed to the protonated dimer and potassiated dimer, which would yield m/z +511 and +549, respectively, but the mass calibration at these high masses is unreliable, so final assignments cannot be made. The peaks seen in the mass spectrum of diphenhydramine allow for the positive identification of diphenhydramine in the tablet.

2-9-5: Loratadine

An antihistamine tablet containing 10 mg of loratadine was analyzed using SPAMS. The average aerodynamic diameter of 999 particles was 1.67 μm (RSD 80.9%). A mass spectrum of an individual particle generated from the single tablet is shown in Figure 2-9.

Ion Signal (a.u.)

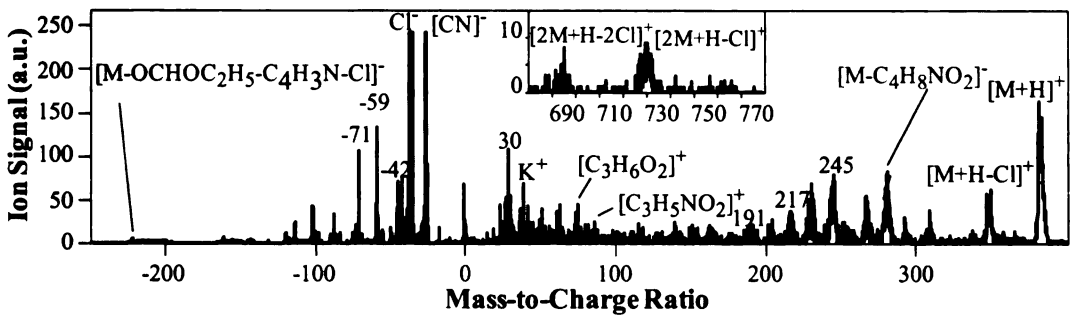

Figure 2- 9: Single particle aerosol mass spectrum of an individual loratadine particle (aerodynamic diameter 3.95 μm). Inset shows high mass peaks due to loratadine dimers.

The negative ion spectrum shows several peaks characteristic of loratadine, including those assigned as the fragments $[M\text{-}OCHOC_2H_5\text{-}C_4H_3N\text{-}Cl]^-$, and $[CN]^-$, at m/z -221 and -26, respectively. The positive ion spectrum also shows peaks due to several fragments, including $[M\text{-}C_4H_8NO_2]^+$ at m/z +280; however, more significantly, peaks at m/z +348 and +383, assigned as $[M+H\text{-}Cl]^+$ and $[M+H]^+$ are seen. The $[M+H]^+$ has been previously reported.[22, 25] The inset in Figure 2-9 shows the high mass region between m/z +680 and +780. Although the intensity is low, significant peaks are seen with sufficient signal-to-noise ratios at m/z +695 and +730, possibly due to loratadine dimers $[2M+H\text{-}2Cl]^+$ and $[2M+H\text{-}Cl]^+$. These peaks are the highest mass peaks that have been clearly resolved on the instrument used in this study.

2-9-6: Generic Ibuprofen

Figure 2- 10 shows the mass spectrum of an individual particle generated from a single tablet containing ibuprofen (200 mg). Although 999 spectra were obtained to ensure the

consistency of the data recorded, the single particle spectrum is representative of the data obtained and was randomly selected.

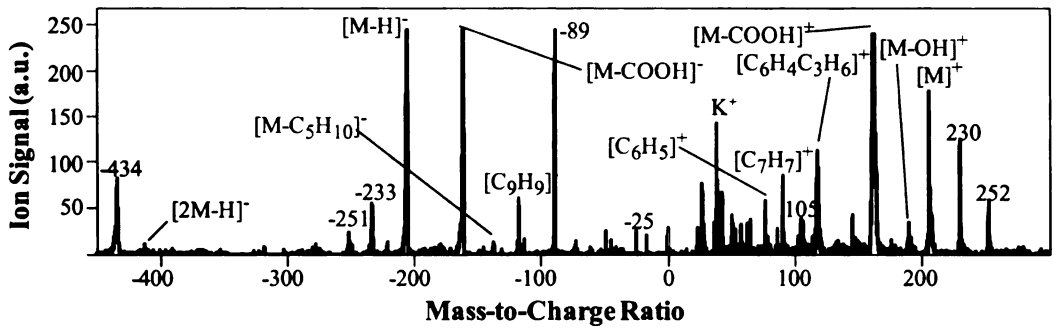

Figure 2- 10: Single particle aerosol mass spectrum of a randomly selected individual ibuprofen particle (aerodynamic diameter 1.21 μm). Note the presence of the $[M]^+$ and $[M-H]^-$ peaks to allow for simple identification.

The average aerodynamic diameter of the 999 particles was 1.83 μm (RSD 65.3%), again with the large size distribution due to the method of particle formation. The aerodynamic diameter of the particle displayed was 1.21 μm. The negative ion spectrum is dominated by peaks at m/z -205 and -161, due to $[M-H]^-$ and $[M-COOH]^-$, respectively.[20, 26, 31] A peak at m/z -411 is attributed to the deprotonated dimer, $[2M-H]^-$, also seen by Williams and Scribens using DESI with a quadrupole-TOFMS.[26] The positive ion spectrum contains many peaks, including those due to the $[M]^+$ ion as well as peaks due to the loss of -OH, and -COOH[21] (m/z +206, +189, +161). A slight peak due to the $[M+H]^+$ ion is also seen in some mass spectra; however the $[M]^+$ ion does dwarf this peak in all the spectra. The pseudomolecular ion of ibuprofen was also not seen in studies using LC-ESI-MS for the analysis of several drug samples. The presence of the $[M]^+$ and $[M-H]^-$ peaks allows for the simple identification of ibuprofen in the sample using either the

positive or negative ion spectrum; the dual-polarity nature of the data provides additional confirmation of the active ingredient.

2-9-7: Generic Pseudoephedrine and Phenylephrine

Several decongestant tablets were analyzed using SPAMS. Pseudoephedrine is a decongestant commonly sold under the brand name of Sudafed™. Since the enactment of the Combat Methamphetamine Epidemic Act of 2005, the quantity of pseudoephedrine purchased by an individual has been restricted to no more than 3.6 g per day and no more than 9 g in any 30 day period due to its use as a starting material for methamphetamine synthesis.[56] This legislation has increased the promotion and availability of alternative decongestants, such as phenylephrine (commonly sold as Sudafed PE™). Figure 2- 11 shows a mass spectrum of a single particle generated from (a) a pseudoephedrine (30 mg) containing tablet and (b) a phenylephrine (10 mg) containing tablet.

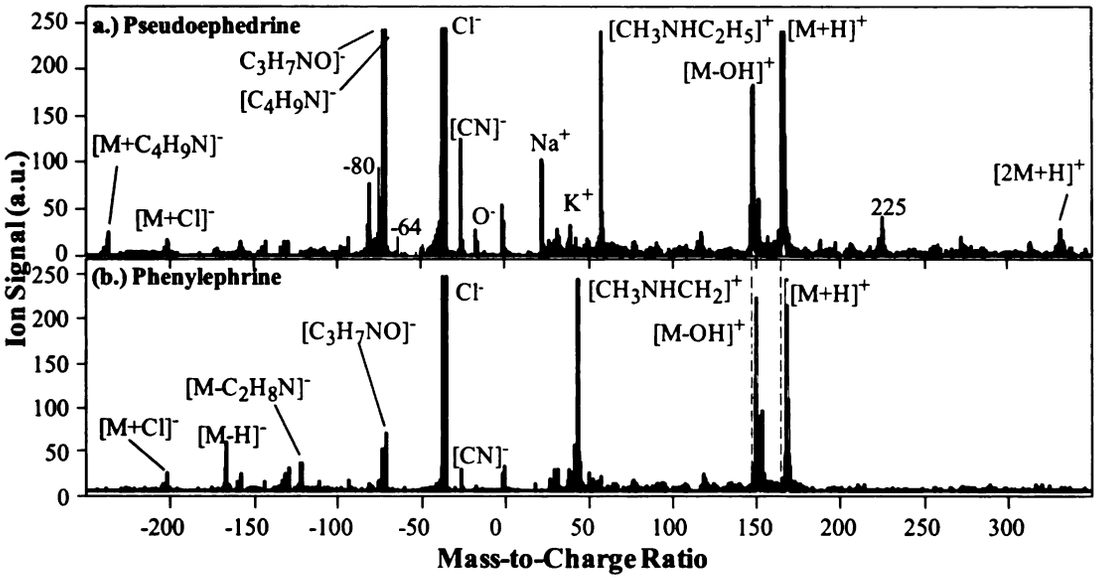

Figure 2- 11: (a) Single particle aerosol mass spectrum of an individual pseudoephedrine particle (aerodynamic diameter 1.08 μm) and (b) an individual phenylephrine particle (aerodynamic diameter 0.96 μm). Although similar in structure and mass, these two compounds can be differentiated using SPAMS based on molecular and fragment ion species.

Molecular masses of pseudoephedrine and phenylephrine are 165.23 and 167.21 Da, respectively. The average aerodynamic diameter of 999 particles of each drug was 1.81 μm (69.5% RSD) for pseudoephedrine and 1.23 μm (58.0% RSD) for phenylephrine. The positive ion spectra of the two substances show similar fragment ions and losses owing to the similar structures of the compounds. Peaks corresponding to the base peaks in the NIST standard mass spectra of pseudoephedrine ($[CH_3NHC_2H_5]^+$, m/z 58) and phenylephrine ($[CH_3NHCH_2]^+$, m/z 44) are present in high yield in the current spectra; however, peaks assigned to $[M+H]^+$ and $[M-OH]^+$ are also seen in both drug samples, have been previously reported,[57-60] and provide more confirmatory identification of the drug. Pseudoephedrine also shows evidence of dimer formation with $[2M+H]^+$ (m/z +331). The negative ion spectra of these two compounds again show similarities. Peaks

due to $[M+Cl]^-$ are seen in both compounds, as well as peaks attributed to $[C_3H_7NO]^-$ (m/z -73) and $[CN]^-$ (m/z -26). Several other fragments are also present that contribute to the signature of each drug.

2-9-8: Bayer™ Aspirin versus Certified™ Aspirin

SPAMS can also be used to identify differences between brands of tablets containing a single drug. Although intended to have the same medicinal effects, differences in manufacturing processes, equipment, and inactive ingredients in the tablets impart a different chemical signature to the tablets. Figure 2- 12 compares three regions of the mass spectra obtained from two tablets containing aspirin: the average mass spectrum of 999 particles dislodged from a Bayer™ brand tablet (325 mg aspirin) and a Certified™ brand tablet (81 mg aspirin).

Ion Signal (a.u.)
Ion Signal (a.u.)
Ion Signal (a.u.)

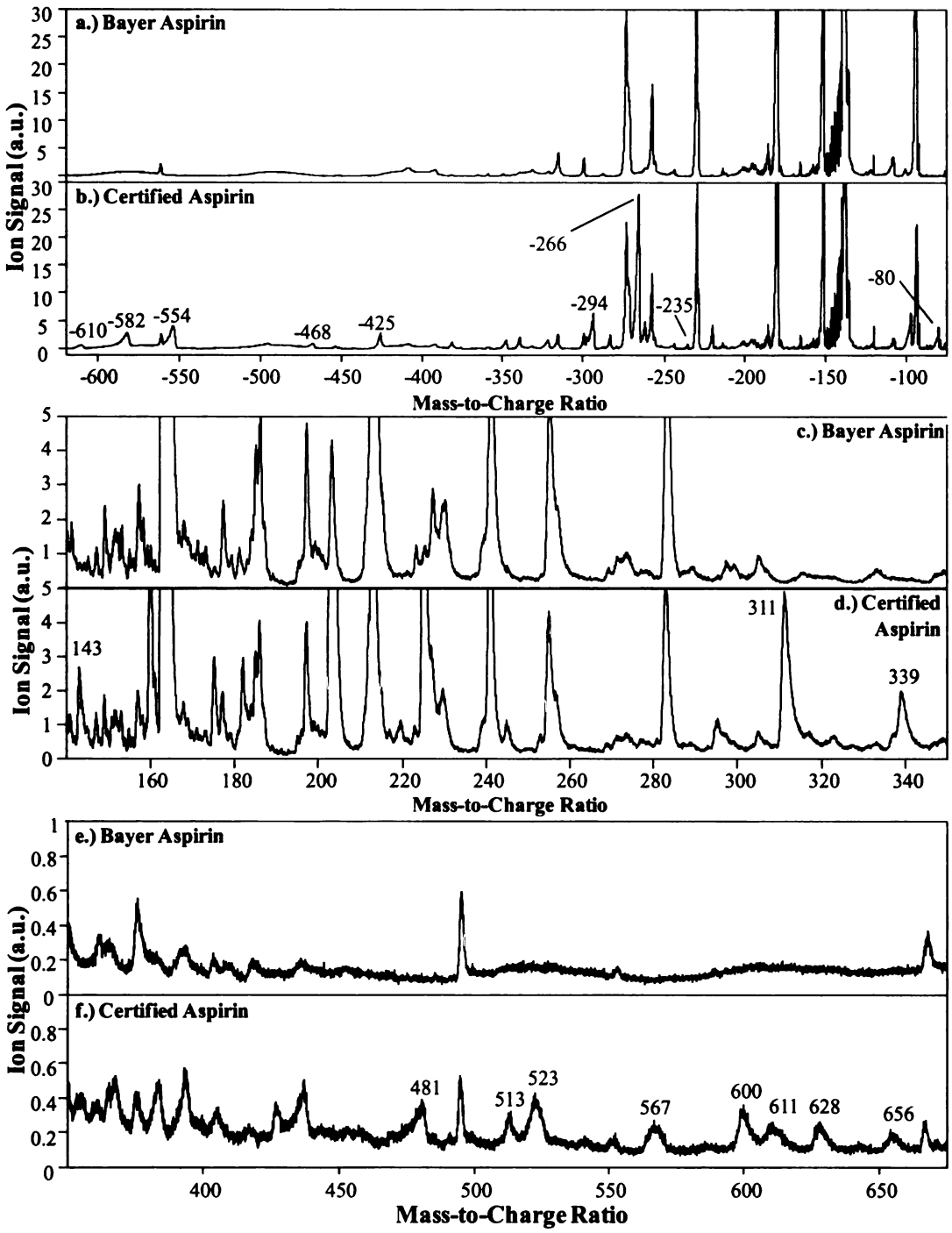

Figure 2- 12: Average mass spectra of 1000 particles of Bayer™ brand aspirin (a,c,e) and Certified™ brand aspirin (b,d,f) in three separate mass regions. Note the presence of additional peaks in the Certified™ Brand aspirin, attributed to fillers and impurities in the sample that can be used to distinguish the two brands.

The peaks previously discussed (Figure 2- 5) as being indicative of aspirin are present in both spectra; however other features in the spectra differ. The labeled peaks in the figure indicate peaks (S/N≥5) present only in the Certified™ brand tablet. In fact, these peaks are not present even in single particle spectra of the Bayer™ brand aspirin sorted for that particular mass. Although small in amplitude, the presence of these peaks can be used to qualitatively distinguish between these two brands of aspirin. These peaks are hypothesized to be due to fragments originating from an unknown filler material in the tablets.

2-9-9: Tylenol Extra Strength™ (Acetaminophen)

Many varieties of tablets can be analyzed using SPAMS. Tablets with a harder shell coating to slow tablet dissolution may take a longer analysis time, as the active ingredient may or may not be present in this shell. Several over the counter and prescription medications are coated with an enteric coating to aid in digestion and to ensure the tablet reaches the appropriate body compartment before releasing the active ingredient (e.g. stomach or small intestine). If this coating does not contain the active ingredient, analysis may take a longer time; particles containing the active ingredient must be dislodged from the tablet, so many spectra may be obtained that do not contain the active ingredient, formed from this coating. One such medication studied was Tylenol Extra Strength™ (EX) geltabs, containing 500 mg acetaminophen. Figure 2- 13shows (a) the average mass spectrum obtained from 799 particles (d_a=2.33 μm, RSD 52.7%) dislodged from a Tylenol EX™ tablet and (b) the average mass spectrum obtained from the 50

particles having the highest mass spectral signal at m/z 152, corresponding to the $[M+H]^+$ ion of acetaminophen.

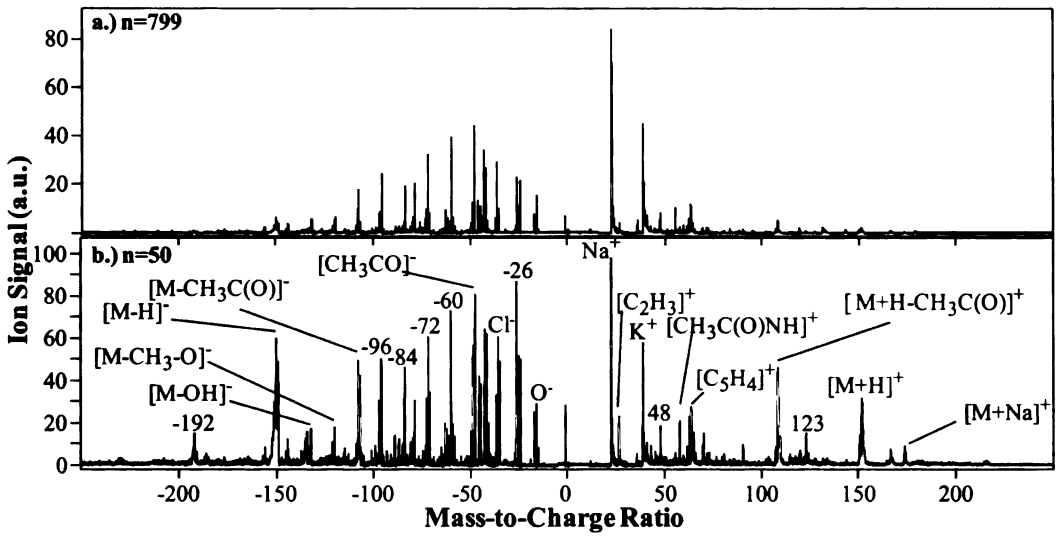

Figure 2- 13: Average mass spectrum from 50 particles dislodged from a Tylenol EX tablet. The 50 particles shown were selected by sorting 799 particles for the highest peak area at m/z 152.

Although peaks due to the active ingredient are seen in the averaged spectrum (n=799), the intensity is low, impeding the facile identification of the substance. However, after sorting the spectra for a particular peak known to be caused by acetaminophen, the active ingredient is easily distinguished from the background material. Thus, even coated tablets can be analyzed successfully with SPAMS. Other ions indicative of acetaminophen are also seen in the spectra. The sodiated ion, $[M+Na]^+$ is seen at m/z 174, as well as the fragment $[M+H-CH_3C(O)]^+$, caused by cleavage of the C-N bond, at m/z 109, $[CH_3C(O)NH]^+$ at m/z 58, is assigned as a fragment from the acetamide group, and, and $[C_2H_3]^+$ at m/z 27 is likely a fragment of the aromatic ring. The negative ion

mass spectrum also has identifying peaks: $[M-H]^-$, $[M-OH]^-$, $[M-O-CH_3]^-$, $[M-CH_3C(O)]^-$, and $[C_4]^-$ at m/z -150, -134, -120, -108, and -48, respectively. Other peaks, attributed to anionic carbon clusters (C_n^-), are seen in the negative spectrum at -96, -84, -72, -60, -48, and -36.

2-9-10: Tylenol Cold™ (Acetaminophen + Diphenhydramine)

SPAMS can also be used to identify multiple ingredients in a single tablet. Several multicomponent tablets were analyzed and presented below. Figure 2- 14b shows the average mass spectrum obtained from 999 particles (d_a= 1.57 μm, RSD 44.9%) dislodged from a Tylenol Cold™ tablet.

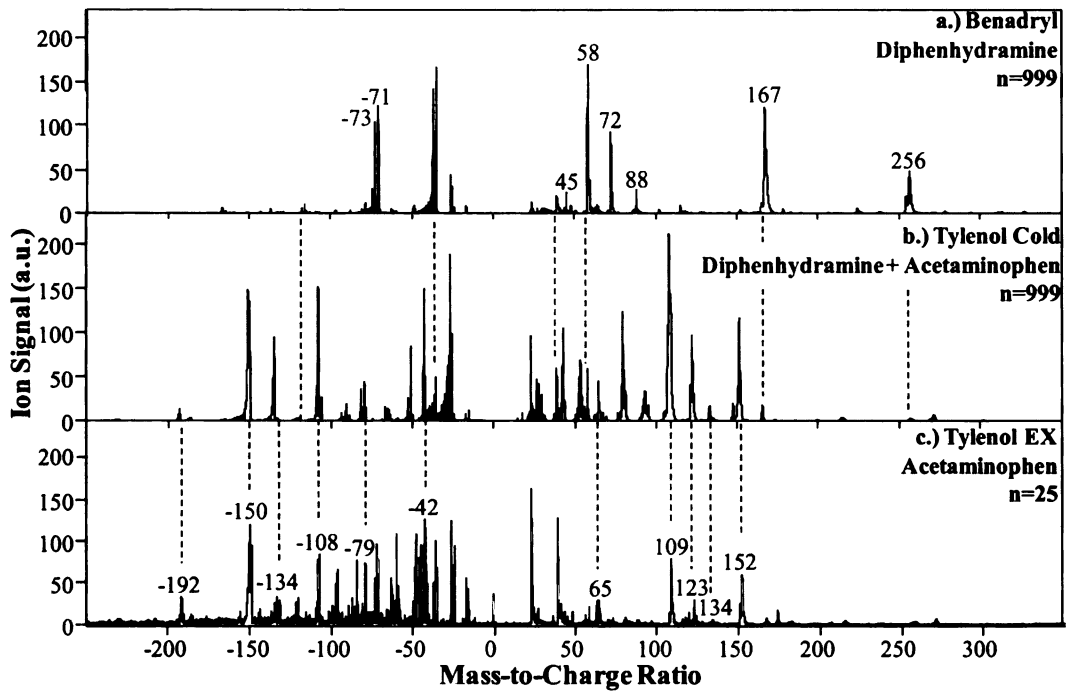

Figure 2- 14: Average mass spectra of particles dislodged from a.) a Benadryl tablet containing diphenhydramine (n=999), b.) a Tylenol Cold tablet containing acetaminophen and diphenhydramine (n=999), and c.) a Tylenol EX tablet containing acetaminophen (n=25). Dashed lines indicate peaks in the Tylenol Cold sample that can be attributed to either acetaminophen or diphenhydramine.

Tylenol Cold™ contains 500 mg of acetaminophen and 12.5 mg of diphenhydramine. Diphenhydramine is the active ingredient in Benadryl™, so the average mass spectrum of 999 particles from a Benadryl™ tablet is shown (Figure 2- 14a) as well as the average mass spectrum of 25 particles from a Tylenol EX™ tablet (Figure 2- 14c). Dashed lines indicate the peaks in the Tylenol Cold™ spectrum that have been attributed to either diphenhydramine or acetaminophen. Numerous peaks are present due to each compound; especially of note are the $[M+H]^+$ ions from each drug, at m/z 152 for acetaminophen, and m/z 256 for diphenhydramine. The presence of two active ingredients does not affect

the ability to identify these substances. The acetaminophen alarm file identified 953 particles as containing acetaminophen. Other peaks are also seen in the Tylenol Cold spectrum that cannot be attributed to either active ingredient. These peaks are hypothesized to be due to the additional filler compounds in the tablet.

2-9-11: Tylenol PM™ – Caplet versus Tablet (Acetaminophen + Diphenhydramine)

Figure 2- 15 shows mass spectra obtained from two varieties of Tylenol PM – a caplet and a tablet.

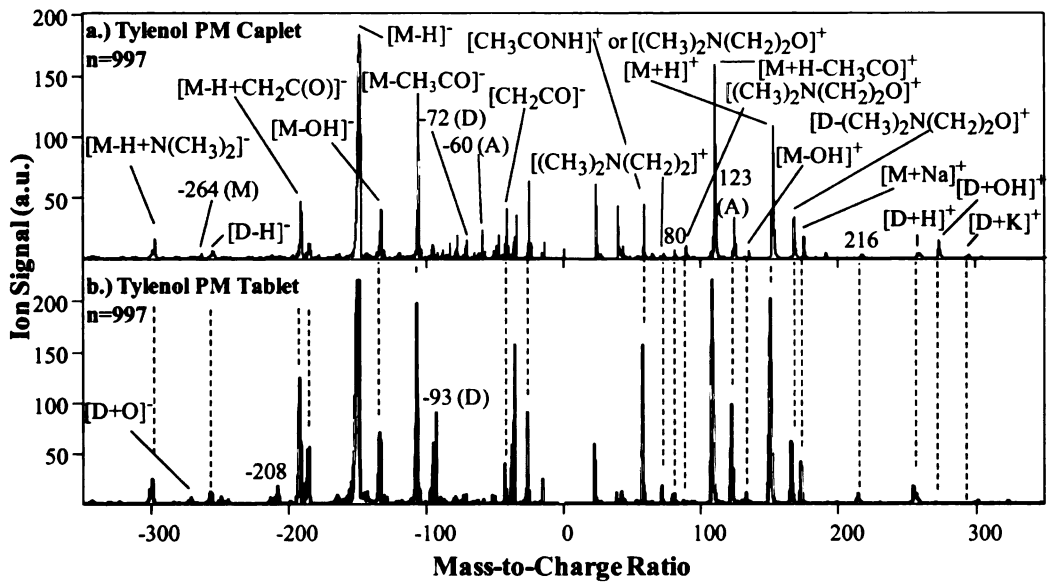

Figure 2- 15: Average mass spectra obtained from 997 particles dislodged from a.) a Tylenol PM caplet and b.) a Tylenol PM tablet. While many peaks indicative of the active ingredients, acetaminophen and diphenhydramine, are seen, other peaks are also present in either sample, allowing differentiation between the two formulations.

Both formulations also contain both acetaminophen (500 mg) and diphenhydramine (25 mg). Again, peaks attributed to the acetaminophen: $[M+Na]^+$, $[M+H]^+$, $[M\text{-}OH]^+$, $[M+H\text{-}CH_3O]^+$, $[CH_3C(O)NH]^+$, $[CH_3CO]^-$, $[M+CH_3CO]^-$, $[M\text{-}CH_3\text{-}O]^-$, $[M\text{-}OH]^-$, $[M\text{-}H]^-$ and $[M\text{-}H+CH_2C(O)]^-$ are seen at m/z 174, 152, 134, 109, 58, -48, -108, -120, -134, -150, and -192 respectively and those attributed to diphenhydramine, $[D+K]^+$, $[D+H]^+$, $[D\text{-}(CH_3)_2N(CH_2)_2O]^+$, $[(CH_3)_2N(CH_2)_2O]^+$, $[(CH_3)_2N(CH_2)_2]^+$, $[(CH_3)_2NCH_2]^+$, and $[D\text{-}H]^-$, at m/z 294, 256, 167, 88, 72, 58, -254, and -271, respectively are seen in both samples. The tablet formulation also contains peaks at m/z -271 attributed to $[D+O]^-$, -208 unattributed, and -93, which is also unattributed but also seen in a Benadryl tablet, containing only diphenhydramine. The caplet formulation contains additional peaks at m/z -264, -72, and -60 which were also seen in the Tylenol EX sample attributed to acetaminophen and m/z 310, which was seen in the Benadryl tablet. This variation in peaks present allows the different formulations of the same drug produced by a single brand to be distinguished, highlighting another ability of SPAMS. The alarm files for both acetaminophen and diphenhydramine were run again all particles. 853 particles in the caplet were identified as containing acetaminophen, and 390 were identified as containing diphenhydramine. In the tablet, 898 particles were identified as containing acetaminophen, while 584 particles were identified as containing diphenhydramine. Thus, many particles must contain both drug components.

2-9-12: Advil Cold and Sinus™ (Ibuprofen + Pseudoephedrine)

Figure 2- 16 shows an average mass spectrum of 50 particles from a multicomponent tablet, Advil Cold and Sinus™. This tablet contains 200 mg ibuprofen and 30 mg pseudoephedrine. The 50 particles shown were chosen by sorting 797 particles (d_a=1.68 μm, RSD 48.6%) by peak area at m/z 166, and selecting the top 50 particles. While many peaks have been attributed to either ibuprofen (I) or pseudoephedrine (P), including $[I]^+$, $[P+H]^+$, and $[I-H]^-$ at m/z 206, 166, and -205, many additional peaks are seen that have not been attributed. Again, these peaks, such as those at m/z -264, -97, 56, and 64 are thought to be due to the unknown filler compounds in the tablet.

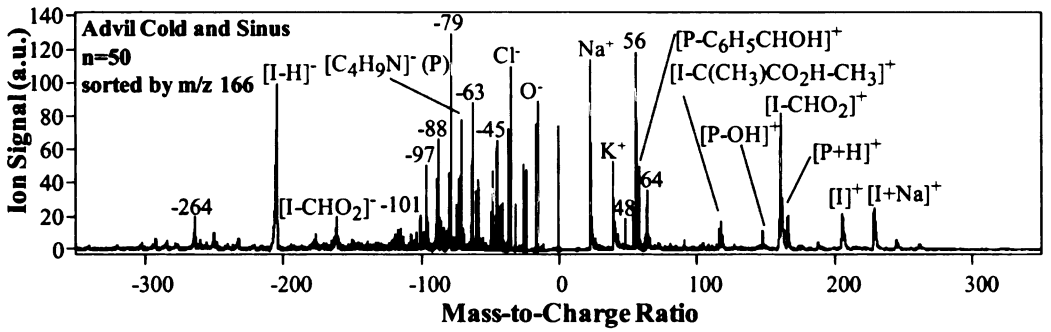

Figure 2- 16: Average mass spectrum obtained from 50 particles dislodged from an Advil Cold and Sinus tablet. The 50 particles were selected by sorting 797 particles for the highest mass area at m/z 166.

2-9-13: Tylenol Severe Congestion™ (Acetaminophen + Dextromethorphan + Guaifenesin + Pseudoephedrine)

A single Tylenol Severe Congestion™ tablet containing four active ingredients: acetaminophen (325 mg), dextromethorphan (15 mg), guaifenesin (200 mg), and pseudoephedrine (30 mg), was analyzed. Figure 2- 17a shows the average dual-polarity

mass spectrum obtained from 1000 particles (d_a= 1.46 μm, RSD 49.0%) from this tablet.

Figure 2- 17b-e show spectra of the individual components for comparison.

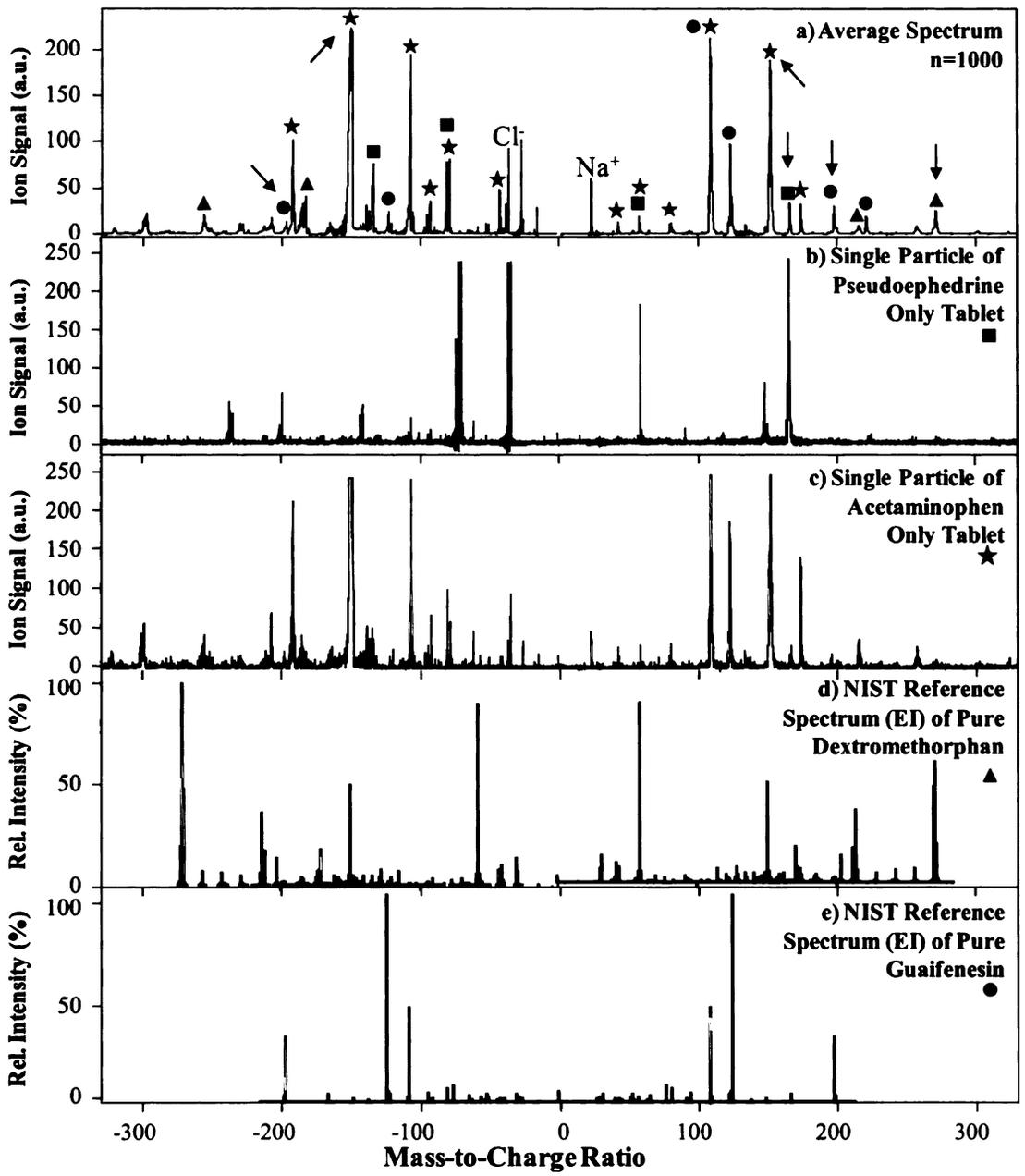

Figure 2- 17: a) Average mass spectrum of 1000 particles dislodged from a single Tylenol Severe Congestion tablet containing pseudoephedrine, acetaminophen, dextromethorphan, and guaifenesin as the active ingredients, b-c) mass spectra obtained from a single particle dislodged from a tablet containing only pseudoephedrine or acetaminophen, respectively, as the active ingredient, d-e) concatenated standard NIST mass spectra of dextromethorphan and guaifenesin, respectively. Single component tablets containing these ingredients were not readily available.

A tablet containing pseudoephedrine as the active ingredient as well as a tablet containing acetaminophen as the active ingredient were analyzed to create the spectra shown in Figure 2- 17b-c; Single component tablets containing dextromethorphan or guaifenesin were not available during the study, therefore standard 70 eV electron ionization (EI) spectra from the NIST reference library are shown (Figure 2- 17d-e), and concatenated to display all ions as potentially-formed positive and negative ions. Note that peaks attributed to the molecular or fragment ions of each component are present in the average (Figure 2- 17a). Pseudomolecular ions of each compound are present and indicated by the arrows: $[M-H]^-$ and $[M+H]^+$ for acetaminophen, $[M+H]^+$ for dextromethorphan, $[M+H]^+$ and M^- for guaifenesin, and $[M+H]^+$ for pseudoephedrine. After analysis of 1000 particles, the mass of the tablet was reduced by only 0.025%, and all markings were clearly visible on the tablet.

The 1000 particles were then processed through the rules trees for all the drug compounds in this study. 953 particles produced a positive identification for acetaminophen, 571 for pseudoephedrine, 907 for dextromethorphan, and 804 for guaifenesin. No false positives were obtained for aspirin, loratadine, phenylephrine, ibuprofen, or chloroquine. This averages to 3.2 drug compounds per particle. The heterogeneous nature of this multi-ingredient tablet allowed for varying combinations of drug compounds to be detected in single particles and demonstrates that the ingredients of such a heterogeneous tablet can be rapidly identified using SPAMS.

2.4.3 Multip

Net. SPAM

engaged. A

ng were pla

shows the

spectrum fr

Figure 2-

a.) Ph

n=24

b.) A

n="

c.) A

n=24

Raw Signal (a.u.)

Figure 2-

Phenylephri

single appro

particles d

aspirin pe

2-9-14: Multiple Tablets: Phenylephrine and Aspirin

Next, SPAMS was tested to determine if multiple tablets could be simultaneously analyzed. A single phenylephrine tablet (10 mg) and a single generic aspirin tablet (81 mg) were placed in a single vial and introduced to the SPAMS system. Figure 2- 18 shows the average of 798 mass spectra obtained from this sample (Figure 2- 18b) and a spectrum from 249 particles of phenylephrine alone (Figure 2- 18a) and aspirin alone (Figure 2- 18c).

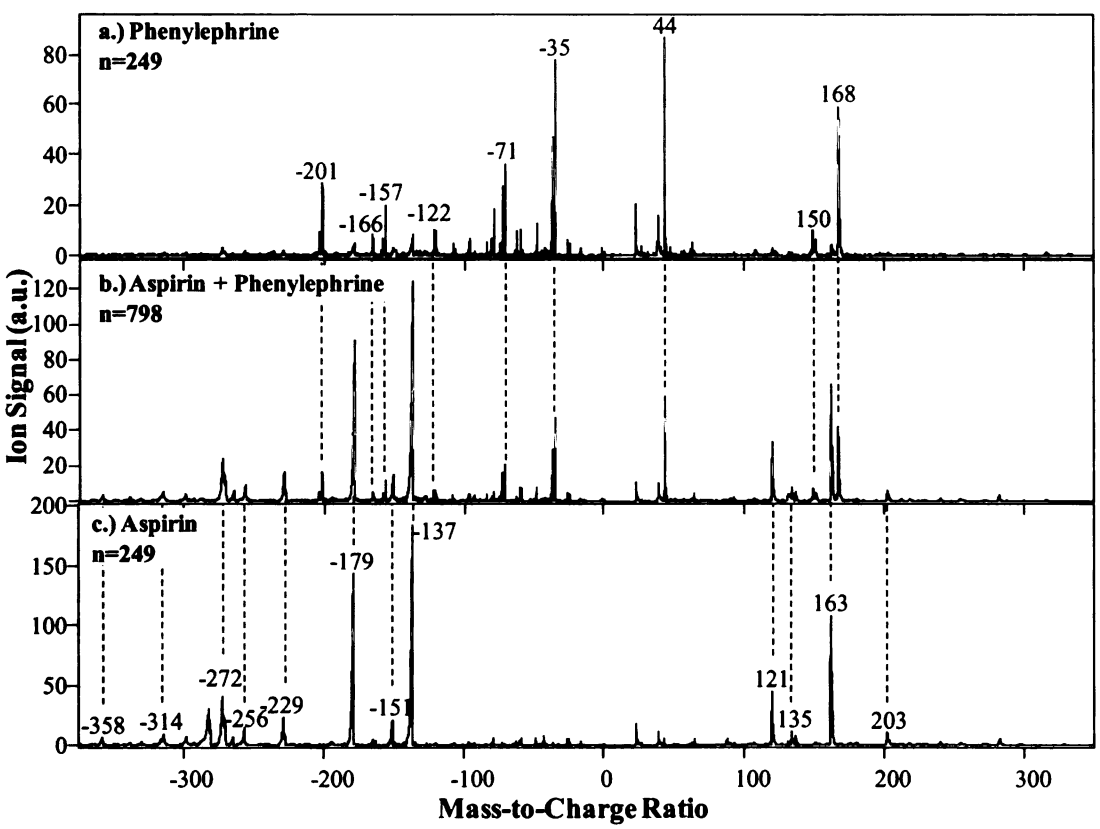

Figure 2- 18: Average mass spectrum obtained from a.) 249 particles dislodged from a phenylephrine tablet, b.) 798 particles dislodged from a single phenylephrine tablet and a single aspirin tablet placed in the same glass vial and sampled simultaneously, c.) 249 particles dislodged from a single aspirin tablet. Note that both phenylephrine and aspirin peaks are seen in the mixed tablet spectrum.

The presence of each component is seen in peaks attributed to the molecular and fragment ions of each compound, all of which have been previously identified and are indicated by the dashed lines. When the data are analyzed on a particle by particle basis, most particles can be identified as containing only one drug, but approximately 5% are identified by the rules trees as containing both compounds. It is thought that these are indeed individual single particles formed by a collision inside of the glass vial and are not due to several particles being concurrently desorbed/ionized in a single pulse, as the probability of more than one particle being present in the D/I laser beam when it is fired is 0.5%, based on a sample containing 1000 particles/mL and sampling rate of 1 L/min.[61] This hypothesis is addressed further in Section 2-9-15. Visual analysis of the tablets after sampling reveals small particles present on the outside of the tablets, thought to be residual particles from the other tablet in sample. Particles formed during tablet-tablet collisions may contain fragments from both tablets.

2-9-15: Multiple Tablets – Separate Vials: Phenylephrine and Aspirin

In order to test the hypothesis of tablet-tablet collisions causing the multi-component particles, 2 tablets were simultaneously introduced to the instrument using 2 separate sampling vials. A single tablet of loratadine was placed in a modified glass vial, while a single tablet of pseudoephedrine was placed in a second vial. Both vials were connected to the SPAMS inlet using a y-shaped connector for the conductive tubing. By placing the tablets in separate vials, tablet collisions are eliminated as a source of this phenomenon, while maintaining all other parameters as consistent. Mass spectra were collected for 498 particles using this setup, and analyzed on a particle by particle basis. No spectra were

seen that containing peaks indicative of both drugs, which supports the hypothesis of mixed drug particles forming within the sampling vial.

2-9-16: Multiple Tablets: Phenylephrine, Aspirin, Ibuprofen, Loratadine, Pseudoephedrine

It is also important to ensure that drug components in a bulk sample containing more than 1 or 2 types of tablets could be accurately detected and identified. Thus, a greater number of tablets, 5, were placed in a single vial: aspirin (81 mg), ibuprofen (200 mg), loratadine (10 mg), phenylephrine (10 mg), and pseudoephedrine (30 mg) and simultaneously analyzed. Figure 2- 19a shows the average dual-polarity mass spectrum of 799 particles.

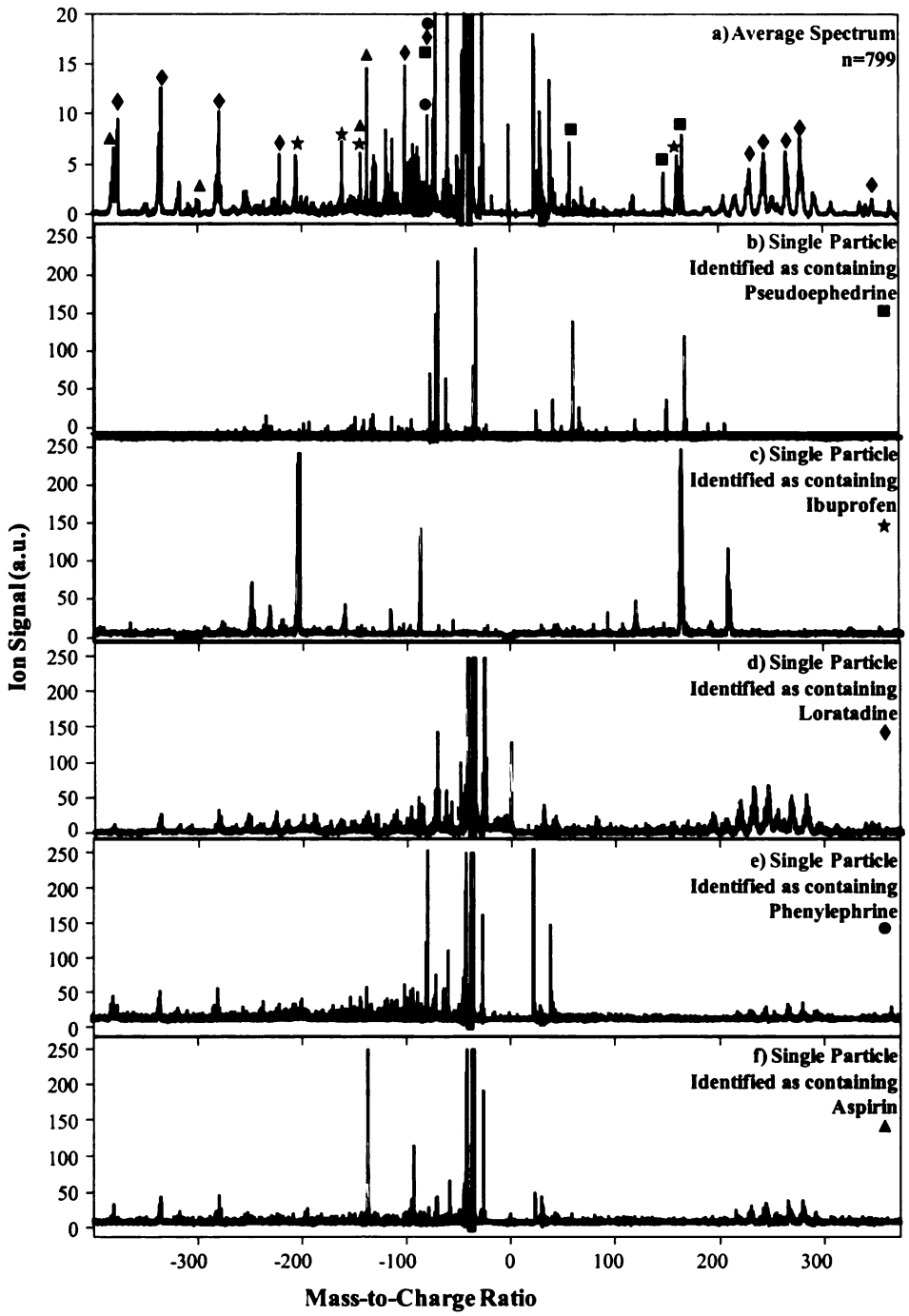

Figure 2- 19: a) average mass spectrum obtained from 799 particles introduced from a complex sample containing 5 single active ingredient tablets including aspirin, ibuprofen, loratadine, phenylephrine, and pseudoephedrine, b-f) single particles selected from the 799 particles collected that were identified as containing primarily pseudoephedrine, ibuprofen, loratadine, phenylephrine, or aspirin, respectively.

The presence of each component is seen in peaks attributed to the parent and fragment ions of each compound, all of which have been previously identified. Figure 2- 19b-f shows single particles of the 799 particles analyzed. These particles were selected as representative of each drug component. Again, many particles do contain only one drug, but many others seem to contain remnants of several of the drug tablets. This is again hypothesized to be due to the tablet-tablet collisions forming mixed component particles.

The alarm algorithm also successfully identified the components of this drug mixture. 534 particles were identified as containing aspirin, 606 as loratadine, 13 as phenylephrine, 581 as pseudoephedrine, and 206 as ibuprofen. No false positives were detected for dextromethorphan, guaifenesin, acetaminophen, or chloroquine. This averages to 2.4 identified components per particle, thought to be due to the tablet collisions.

2-9-17: Emptied Vial

The prior contents of a vial can also be detected with this system. After analysis, the five tablets were removed from the sampling vial, and the empty vial reanalyzed. While the number of residual particles dislodged from the empty vial was limited, over 500 particles were analyzed. Figure 2- 20b shows the resulting average mass spectrum from 500 particles. Figure 2- 20a shows 500 randomly selected particles from the vial containing the five tablets for comparison. Although the ion abundances vary, all the identifying peaks are still detected for each drug tablet. 328, 348, 7, 353, and 155 particles were identified as containing aspirin, loratadine, phenylephrine,

pseudoephedrine, or ibuprofen, respectively, with no false positives, again, indicating formation of multi-component particles.

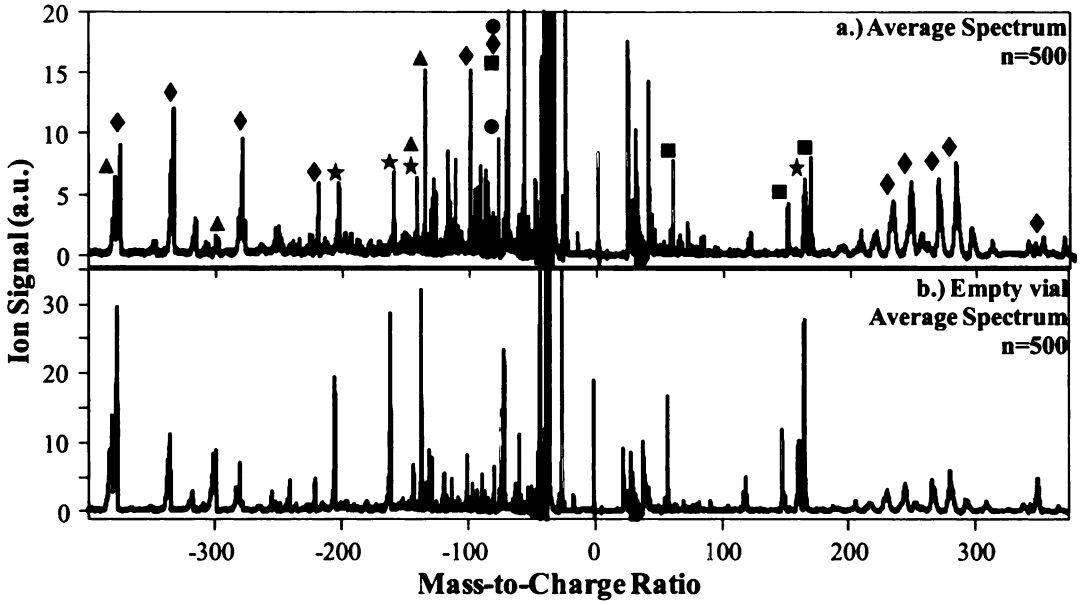

Figure 2- 20: a) average mass spectrum of 500 particles introduced from the complex sample containing 5 single active ingredient tablets including aspirin, ibuprofen, loratadine, phenylephrine, and pseudoephedrine, b) average mass spectrum of 500 residual particles introduced from the emptied sampling vial.

2-9-18: In Situ Sampling: Chloroquine Diphosphate and Loratadine

The SPAMS technique is also successful when used to sample tablets *in situ*, *i.e.* in their actual commercial bottle. 11 chloroquine phosphate tablets remaining in their original bottle were sampled by taping the modified vial cap to the opening of the jar. Mass spectra of 100 particles dislodged from these 11 tablets were analyzed in 64 seconds (fluence=2.4 nJ/μm^2); all spectra were equivalent to those shown in Figure 2- 6 and all particles were identified by the rules trees as only containing chloroquine, with no false positives. Finally, a single loratadine tablet was added to the eleven chloroquine phosphate tablets in this container to simulate the presence of a single illicit tablet in a

container of licit materials. The loratadine tablet accounted for 1.2% of the weight of the tablets in the container. Using this same sampling method, particles were again identified as chloroquine, with mass spectra matching those in Figure 2- 6. However, a particle identified as loratadine was detected 117 seconds after sampling began. Figure 2- 21a shows the mass spectrum obtained from this single loratadine particle and Figure 2- 21b shows the averaged mass spectrum previously obtained from 100 loratadine particles sampled from a single tablet for comparison. All identifying peaks are present, especially the $[M-H]^-$ and $[M+H]^+$ ions which greatly facilitate identification. The rules tree for loratadine identified this single particle, with no false identifications for the other drugs studied.

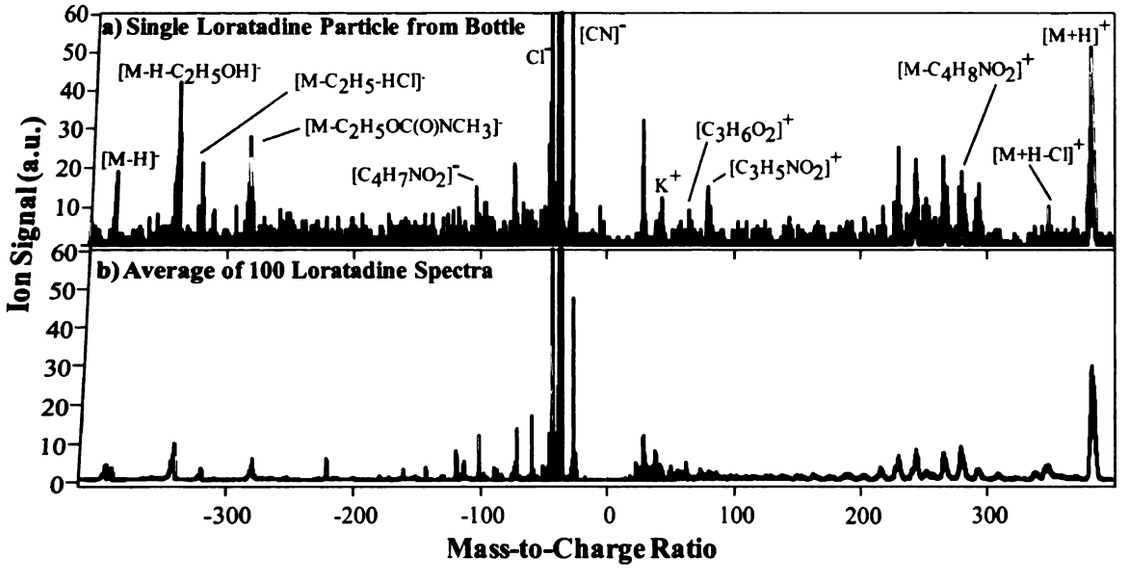

Figure 2- 21: a) Mass spectrum of a single particle of loratadine detected in an original bottle containing 11 chloroquine phosphate tablets, b) average mass spectrum of 100 loratadine particles previously collected for comparison.

2-10: Conclusions

As a technique that has previously proven successful for the detection of biological, explosive, and chemical warfare agent samples, it was hypothesized that SPAMS would also be an ideal detection system for drugs. A novel sample formation and introduction system had to be developed for this application; the modified glass vial was an efficient, simple, and effective method for creating particles from solid samples due to their collisions with each other and the sides of the glass vial, and the slight vacuum of the SPAMS system allowed for the particles to be pulled into the system with no additional power requirements. Many single component over-the-counter medications were analyzed and effectively characterized using SPAMS, including acetaminophen, aspirin, clemastine, diphenhydramine, ibuprofen, loratadine, phenylephrine, and pseudoephedrine. These tablets were analyzed without destroying other forensically useful information, such as their shape, color, and markings. Chloroquine was also identified in tablets, demonstrating the ability of SPAMS to be used for the identification of counterfeit drugs. Additionally, multi-component medications were also analyzed, showing indicative peaks from all active ingredients. These studies also included chlorpheniramine, dextromethorphan, and guaifenesin. Multiple single component tablets were then simultaneously analyzed to show the ability of SPAMS to serve as a general screening device. While many particles analyzed contained one drug, many also contained multiple drugs, and further experiments showed that this was caused by tablet-tablet collisions in the glass vial, and not by multiple particles being simultaneously desorbed/ionized in the source region. The study also highlights the ability of SPAMS to detect drug compounds even after they have been removed from the container. This has

forensic applications to situations in which a suspected drug sample was discarded before seizure, leaving only the emptied container as possible evidence. Enough residual particles were present in the emptied vial to allow for the collection and analysis of over 500 particles. Proof of concept *in situ* analysis experiments were performed by attaching the modified glass vial cap to a commercial chloroquine bottle. The chloroquine was still effectively sampled and analyzed, reducing consumables and analysis time. Finally, a single loratadine tablet placed in a bottle with multiple chloroquine tablets was successfully detected, even though it only made up 1.2% weight of the sample, demonstrating that SPAMS is a useful technique for detecting a single illicit tablet in a large batch of licit materials. SPAMS has been successfully demonstrated as a useful and effective drug detection technique with over-the-counter medications, and it is hypothesized that it will also be an effective system for sensitive and rapid illicit drug detection. As such, SPAMS may be a powerful tool for border control and customs applications to provide almost instantaneous identifying information about the components in drug tablets.

11: References

(1) **Newton, P.** N.; Green, M. D.; Fernandez, F. M.; Day, N. P. J.; White, N. J. *The Lancet Infectious Diseases* **2006**, *6*, 602-613.

(2) **Basco, L. K.** *The American Journal of Tropical Medicine and Hygiene* **2004**, *70*, 145-250.

(3) *Foreign Terrorist Organizations*, Office of the Coordinator for Counterterrorism, Washington, D.C., **2008**.

(4) *Counterfeit drugs: Guidelines for the development of measures to combat counterfeit drugs*, Geneva: World Health Organization, **1999**.

(5) Azhagvuel, S.; Sekar, R. *J. Pharm. Biomed. Anal.* **2007**, *43*, 873-878.

(6) Tanyanyiwa, J.; Hauser, P. C. *Anal. Chem.* **2002**, *74*, 6378-6382.

(7) Borer, M. W.; Zhou, X. J.; Hays, D. M.; Hofer, J. D.; White, K. C. *J. Pharm. Biomed. Anal.* **1998**, *17*, 641-650.

(8) Bondesson, L.; Mikkelsen, K. V.; Luo, Y.; Garberg, P.; Agren, H. *Spectrochimica Acta Part A-Molecular and Biomolecular Spectroscopy* **2007**, *66*, 213-224.

(9) Meza, C. P.; Santos, M. A.; Romanach, R. J. *Aaps Pharmscitech* **2006**, *7*, E1-E9.

(10) Antonić, J.; Heath, E. *Anal. Bioanal. Chem.* **2007**, *387*, 1337-1342.

(11) Hardt, J. *Fresenius' Journal of Analytical Chemistry* **2001**, *371*, 787-790.

(12) Tseng, Y. L.; Shieh, M.-H.; Kuo, F.-H. *Forensic Science International* **2006**, *157*, 149-155.

(13) Ma, W.; Liu, X. Y.; Pawliszyn, J. *Anal. Biochem.* **2006**, *385*, 1398-1408.

(14) Hernando, M. D.; Heath, E.; Petrovic, M.; Barceló, D. *Anal. Bioanal. Chem.* **2006**, *385*, 985-991.

15) **Cahill, J. D.**; Furlong, E. T.; Burkhardt, M. R.; Kolpin, D.; Anderson, L. G. *J. Chromatogr. A* **2004**, *1041*, 171-180.

16) **Takats, Z.**; Wiseman, J. M.; Gologan, B.; Cooks, R. G. *Science* **2004**, *306*, 471-473.

(17) **Cody, R. B.**; Laramee, J. A.; Nilles, J. M.; Durst, H. D. *JEOL News* **2005**, *40*, 8-12.

(18) **Wood, M.**; Laloup, M.; Samyn, N.; del Mar Ramirez Fernandez, M.; de Bruijn, E. A.; **Maes, R. A. A.**; De Boeck, G. *J. Chromatogr. A* **2006**, *1130*, 3-15.

(19) **Chen, H.**; Talaty, N. N.; Takats, Z.; Cooks, R. G. *Anal. Chem.* **2005**, *77*, 6915-6927.

(20) Williams, J. P.; Scrivens, J. H. *Rapid Commun. Mass Spectrom.* **2005**, *19*, 3643-3650.

(21) Leuthold, L. A.; Mandscheff, J. F.; Fathi, M.; Giroud, C.; Augsburger, M.; Varesio, E.; Hopfgartner, G. *Rapid Commun. Mass Spectrom.* **2006**, *20*, 103-110.

(22) Rodriguez-Cruz, S. E. *Rapid Commun. Mass Spectrom.* **2006**, *20*, 53-60.

(23) Weston, D. J.; Bateman, R.; Wilson, I. D.; Wood, T. R.; Creaser, C. S. *Anal. Chem.* **2005**, *77*, 7572-7580.

(24) Cody, R. B.; Laramee, J. A.; Durst, H. D. *Anal. Chem.* **2005**, *77*, 2297-2302.

(25) Williams, J. P.; Patel, V. J.; Holland, R.; Scrivens, J. H. *Rapid Commun. Mass Spectrom.* **2006**, *20*, 1447-1456.

(26) VanBerkel, G. J.; Ford, M. J.; Deibel, M. A. *Anal. Chem.* **2005**, *77*, 1207-1215.

(27) Gard, E.; Mayer, J. E.; Morrical, B. D.; Dienes, T.; Fergenson, D. P.; Prather, K. A. *Anal. Chem.* **1997**, *69*, 4083-4091.

(28) Noble, C. A.; Prather, K. A. *Environ. Sci. Technol.* **1996**, *30*, 2667-2680.

9) Sinha, M. P. *Rev. Sci. Instrum.* **1984**, *55*, 886-891.

0) Davis, W. D. *Environ. Sci. Technol.* **1977**, *11*, 587-592.

1) Noble, C. A.; Prather, K. A. *Mass Spectrom. Rev.* **2000**, *19*, 248-274.

(32) Czerwieniec, G. A.; Russell, S. C.; Tobias, H. J.; Pitesky, M. E.; Fergenson, D. P.; Steele, P.; Srivastava, A.; Horn, J. M.; Frank, M.; Gard, E. E.; Lebrilla, C. B. *Anal. Chem.* **2005**, *77*, 1081-1087.

(33) Fergenson, D. P.; Pitesky, M. E.; Tobias, H. J.; Steele, P. T.; Czerwieniec, G. A.; Russell, S. C.; Lebrilla, C. B.; Horn, J. M.; Coffee, K. R.; Srivastava, A.; Pillai, S. P.; Shih, M.-T. P.; Hall, H. L.; Ramponi, A. J.; Chang, J. T.; Langlois, R. G.; Estacio, P. L.; Hadley, R. T.; Frank, M.; Gard, E. E. *Anal. Chem.* **2004**, *76*, 373-378.

(34) Srivastava, A.; Pitesky, M. E.; Steele, P. T.; Tobias, H. J.; Fergenson, D. P.; Horn, J. M.; Russell, S. C.; Czerwieniec, G. A.; Lebrilla, C. B.; Gard, E. E.; Frank, M. *Anal. Chem.* **2005**, *77*, 3315-3323.

(35) Steele, P. T.; Srivastava, A.; Pitesky, M. E.; Fergenson, D. P.; Tobias, H. J.; Gard, E. E.; Frank, M. *Anal. Chem.* **2005**, *77*, 7448-7454.

(36) Steele, P. T.; Tobias, H. J.; Fergenson, D. P.; Pitesky, M. E.; Horn, J. M.; Czerwieniec, G. A.; Russell, S. C.; Lebrilla, C. B.; Gard, E. E.; Frank, M. *Anal. Chem.* **2003**, *75*, 5480-5487.

(37) Tobias, H. J.; Pitesky, M. E.; Fergenson, D. P.; Steele, P. T.; Horn, J.; Frank, M.; Gard, E. E. *J. Microbiol. Methods* **2006**, *67*, 56-63.

(38) Tobias, H. J.; Schafer, M. P.; Pitesky, M.; Fergenson, D. P.; Horn, J.; Frank, M.; Gard, E. E. *Applied and Environmental Microbiology* **2005**, *71*, 6086-6095.

(39) Martin, A. N.; Farquar, G. R.; Gard, E. E.; Frank, M.; Fergenson, D. P. *Anal. Chem.* **2007**, *79*, 1918-1925.

(40) Martin, A. N.; Farquar, G. R.; Frank, M.; Gard, E. E.; Fergenson, D. P. *Anal. Chem.* **2007**, *79*, 6368-6375.

(41) Adams, K. L.; Steele, P. T.; Bogan, M. J.; Sadler, N. M.; Martin, S. I.; Martin, A. N.; Frank, M. *Anal. Chem.* **2008**, *80*, 5350-5357.

(42) Martin, A. N., Michigan State University, East Lansing, MI, **2006**.

(43) Dockery, D. W.; Pope III, C. A. *Annual Review of Public Health* **1994**, *15*, 107-132.

(44) Wiley, W. C.; McLaren, I. H. *Rev. Sci. Instrum.* **1955**, *26*, 1150-1157.

(45) de Hoffman, E.; Stroobant, V. *Mass Spectrometry: Principles and Applications*; John Wiley & Sons, Ltd.: New York, **2002**.

(46) Riot, V.; Coffee, K.; Gard, E.; Fergenson, D.; Ramani, S.; Steele, P., Waltham, MA **2006**; Proceedings of the Fourth IEEE Workshop on Sensor Array and Multichannel Signal Processing; 98-101.

(47) Steele, P. T.; Farquar, G. R.; Martin, A. N.; Coffee, K. R.; Riot, V. J.; Martin, S. I.; Fergenson, D. P.; Gard, E. E.; Frank, M. *Anal. Chem.* **2008**, *80*, 4583-4589.

(48) Hasegawa, C.; Kumazawa, T.; Lee, X. P.; Fujishiro, M.; Kuriki, A.; Marumo, A.; Seno, H.; Sato, K. *Rapid Commun. Mass Spectrom.* **2006**, *20*, 537-543.

(49) Zhu, L.; Chen, X. Y.; Zhang, Y. F.; Yu, H. L.; Zhong, D. F. *Journal of Chromatography B-Analytical Technologies in the Biomedical and Life Sciences* **2005**, *820*, 175-182.

(50) U.S. Drug Enforcement Agency, **2005**; Vol. Title VII, P.L. 109-177.

(51) Beyer, J.; Peters, F. T.; Kraemer, T.; Maurer, H. H. *J. Mass Spectrom.* **2007**, *42*, 150-160.

(52) Marin, A.; Barbas, C. *J. Pharm. Biomed. Anal.* **2004**, *35*, 1035-1045.

(53) Ming, M.; Fang, F.; Yulan, S.; Shuangjin, C.; Han, L. *Journal of Chromatography B-Analytical Technologies in the Biomedical and Life Sciences* **2007**, *846*, 105-111.

(54) Nirogi, R. V. S.; Kandikere, V. N.; Shukla, M.; Mudigonda, K.; Maurya, S.; Komarneni, P. *Rapid Commun. Mass Spectrom.* **2006**, *20*, 3030-3038.

(55) Farquar, G. R.; Steele, P. T.; McJimpsey, E. L.; Lebrilla, C. B.; Tobias, H. J.; Gard, E. E.; Frank, M.; Coffee, K. R.; Riot, V. J.; Fergenson, D. P. *J. Aerosol Sci* **2008**, *39*, 10-18.

CHAPTER 3: Breath Analysis – Method Developments

3-1: Motivations and Introduction

Although breathing is an involuntary action of the human body that often occurs unnoticed, it is one of the ways that the human body interacts with the world. Gas exchange occurs each second, with oxygen being inhaled from the air, into the lung, transferring into the blood, and being delivered to muscles and organs throughout the body. Carbon dioxide is then removed from the body in the reverse action. However, more than O_2-CO_2 exchange is occurring at this blood-air barrier. Other compounds, both volatile and non-volatile, are constantly being brought into and expelled from the body. These compounds may range from being inhaled and exhaled with no interaction with the body, or may be inhaled, interact with the body and then be exhaled, or they may even be inhaled and metabolized before elimination. Some compounds are also produced in the body and subsequently exhaled. These compounds may provide insight into the processes regularly occurring in the body, from metabolism to oxidation.

The non-invasive nature of breath analysis has generated significant interest in using profiles of breath constituents to derive information about physiological functions and interactions with the environment. Applications including medical diagnostics, assessment of environmental contamination, and physiological monitoring are common interests in the breath analysis community.[62] Homeland security applications of breath analysis have been suggested.[62, 63] Investigation of whether breath analysis could be used to detect the prior activity of an individual, or even biometric applications have gained momentum recently.

Whatever the targeted application of breath analysis, fundamental studies are necessary to ensure the reliability of data obtained from breath analysis in such applications. These fundamental studies must identify the problems and weaknesses in breath analysis, with the aim of solving some of these problems. This chapter will describe efforts made to develop a breath analysis scheme capable of breath sampling, preconcentration, analysis, and interpretation. Each of these segments of the scheme present individual challenges and options, many of which are addressed. Several breath collection modifications are presented, and several detection challenges are discussed. The next chapter will address more applications of breath analysis once a reliable system and method is established herein.

3-2: Background on Breath Analysis

Breath analysis has existed in a qualitative form for thousands of years. Hippocrates described the process of diagnosing disease based on the odor of the breath of patients in the 4th century B.C..[64] In the 18th century, the French scientist Antoine Lavoisier and colleagues measured the breath of guinea pigs to discover the presence of carbon dioxide in exhaled breath using a precipitation reaction.[64, 65] The 19th century brought additional information on exhaled breath, as colorimetric tests were used to detect acetone in the breath of a diabetic patient and alcohol in the breath of a subject after consumption.[65] The detection of alcohol in breath grew in the 20th century, as the automotive industry boomed and impaired driving became an issue. Bogen's work in 1927 to quantify the ethanol in the blood by measuring the ethanol in the breath began the development of breathalyzers for legal and medical purposes.[66] The larger scale application of breath

analysis garnered renewed interest with the work of Pauling in 1971. In this work, Pauling *et al.* described that several hundred volatile organic compounds (VOCs) were present in breath in low, but measurable quantities.[67] Since this work, these VOCs have been the subject of much research in medical and environmental realms.

From a medical perspective breath analysis is appealing owing to the non-invasive diagnostic nature of the technique. Thus far, over 3000 VOCs have been detected in human breath,[68] and variations in particular markers have been studied in relation to asthma,[69-73] chronic obstructive pulmonary disease,[74, 75] breast cancer,[76-78] lung cancer,[79-85] lung infection,[73, 86, 87] transplant rejection,[88-90] and diabetes.[91, 92] Breath samples are easily collected, and have been simplified to the point that the subjects can collect the breath privately in their own homes.[93] From an environmental perspective, breath analysis has focused on detecting exposure to pollutants and industrial chemicals.[94-101] Several Environmental Protection Agency (EPA) studies have measured the breath of subjects throughout the United States, documenting exposure to chemicals such as automotive exhaust and cigarette smoke.[97, 100-103]

No matter what the application, breath analysis relies on the principle that the lung alveolar air can be treated as the headspace of the blood stream, given the constant partitioning of volatile organic compounds (VOCs) between the two compartments via the alveolar pulmonary membrane (Figure 3- 1).[68, 104]

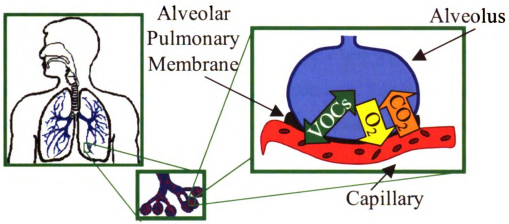

Figure 3- 1: Diagram of the alveolar-capillary interface. Alveolar air sacks within the bronchioles of the lung are in close contact with the blood stream via the alveolar-pulmonary membrane. Oxygen and carbon dioxide, as well as VOCs, partition across this membrane, making the alveolar air function as a headspace of the blood. (Image originally in color)

For medical diagnostics, the compounds of interest are the endogenous compounds in breath that are formed by metabolic processes taking place in vivo.[68, 105] For environmental applications the other compounds present in breath, including exogenous compounds that are inhaled, are of interest. Once inhaled, these compounds can be passed across the alveolar membrane and be distributed throughout the body via the bloodstream. These compounds can then be cleared via many pathways, including respiration. Breath analysis therefore presents an interesting and non-invasive method of detecting chemical exposure as well as monitoring the clearance of such chemicals.

3-3: Breath Collection Methods

Several commercial and laboratory-based devices have been used for breath collection. The RTube™ (Respiratory Research, Inc., Charlottesville, VA) is one such device, a commercially available, FDA approved, disposable exhaled breath condensate (EBC) collection system (Figure 3- 2). The RTube™ consists of a polypropylene tube fitted to a polyethylene mouthpiece. The subject inhales through the mouthpiece via a one-way valve (valve A) fitted with a saliva trap to prevent sample contamination. The subject then exhales through the mouthpiece into a polypropylene collection tube via a second one-way valve (valve B). The polypropylene collection tube is placed inside an aluminum sleeve cooled in a freezer (-20 or -80 °C) prior to collection (not shown). In this configuration, breath passing through the collection tube condenses and collects at the base of polypropylene tube.

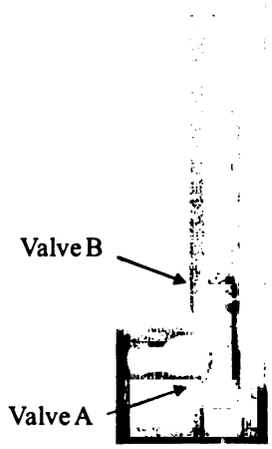

Figure 3- 2: Picture of the RTube™. The RTube™ is used for EBC collection and can be chilled with a previously frozen aluminum sleeve. ***(Image originally in color)***

The ECoScreen II (VIASYS Healthcare, Yorba Linda, CA) is a third generation EBC collection system that also incorporates a spirometer to control either volume or time during collection (Figure 3- 3). The subject exhales through the mouthpiece into a pneumotachograph, where the rate of airflow is measured, and the breath is then passed into a polyethylene collector, stored in a temperature-controlled unit. A unique feature of the ECoScreen II is the optional use of a second collector, thus allowing separation of alveolar air from dead space air. A portable version is also available, the ECoScreen Turbo, which uses a Peltier cooler to maintain the temperature of the breath collectors.

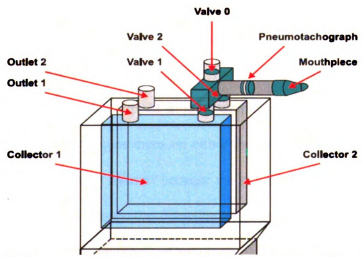

Figure 3- 3: Diagram of the ECoScreen II. This device is used to collect EBC and can also control the volume or time of sample collection. (Image originally in color)

Summa canisters are also used for breath collection. A Summa canister is a stainless steel container whose inner surfaces are passivated by electropolishing with chemical deactivation. Summa canisters are held under vacuum before sample collection, so they

may be stored for up to 30 days before use. These canisters were used for the extensive experiments of the EPA's environmental studies.[98, 100-102, 106-109]

3-4: Volatile and Non-Volatile Components

Breath analysis has focused on both the volatile and non-volatile components in breath. Though they have various sources, both classes of components provide interesting information about the subject. The volatile components in breath range from oxygen, nitrogen, and carbon dioxide, which compose over 99% of inhaled air, to the low concentrations (ppbv and below) of acetone, methanol, and many alkanes and methylated alkanes. The non-volatile components of breath are often proteins, oxidation or nitration products, cytokines, eicosanoids, and mediators.[110] One of the most abundant constituents of breath is water, which is exhaled in the form of respiratory droplets; aerosol particles can become trapped in these droplets, allowing them to be expelled.[111] Most breath analysis techniques focus on either the volatile or non-volatile components. Work by Zenobi *et al.* is of interest because the extractive electrospray ionization used with mass spectrometry allows the detection of volatile and non-volatile components simultaneously from the same breath of air.[112]

3-5: Breath Analysis Techniques

Many techniques have been pursued for analysis of exhaled breath including enzyme-linked immunosorbent assay (ELISA),[113, 114] colorimetric tests,[115, 116] optical spectroscopy,[116, 117] high performance liquid chromatography, [72, 116] ion mobility

spectrometry,[87] liquid chromatography-mass spectrometry (LC-MS),[72, 74, 75] GC with flame ionization detection (GC-FID),[19, 118-120] and GC-MS.[68, 76, 79-84, 86, 88, 89, 92, 99, 100, 105, 120-127] Ekips Technologies has developed a system approved by the FDA for research studies called the Breathmeter.[70] The Breathmeter uses tunable diode later spectroscopy to detect both organic and inorganic components in breath. The mid-IR absorption of many compounds allows for internal calibration and wide-range detection with laser tuning. Aerocine Inc. markets the first FDA-approved system called NIOX Flex which uses chemiluminescence to monitor NO in exhaled breath with a detection limit of 2 ppb.[128] Toda *et al.* developed a breath isoprene detection system based on its chemiluminescence after reaction with ozone with a limit of detection of 0.6 ppbv.[129] Plodinec and Wang used cavity ring-down spectroscopy for the detection of breath acetone in a single breath.[130] Amirav *et al.* demonstrated the use of gas chromatography – electrolyzer-fed FID (GC-EFID) for breath detection of ethanol, isoprene, pentane, and acetone.[131] This system generated its own combustion gases from water and thus was gas cylinder-free making it more field-portable.[131] Sacks *et al.* used GC-GC for breath detection, achieving limits of detection in the ppt range.[132] The most common breath detection system currently used is gas chromatography-mass spectrometry (GC-MS).

Gas chromatography-mass spectrometry (GC-MS) has shown great potential for breath analysis, due to its selectivity and sensitivity.[68, 76, 79-84, 86, 88, 89, 92, 99, 100, 104, 120-127] Indeed, a breath analysis apparatus using GC-MS, Heartsbreath, developed by Menssana Research, Inc. has recently been approved by the FDA as a test for heart transplant rejection.[89] Chemical exposure has also been detected using GC-MS.[100-102, 125, 133] Sofia *et al.* studied toluene in the exhaled breath condensate (EBC) of individuals exposed to the chemical

via inhalation.[99] A relationship between concentration in the environment and EBC was determined, and the toluene concentration in the EBC decreased with time after the exposure ended.[99] However, no efforts were made to ensure that additional exposure, e.g. from clothing, did not inadvertently occur during sampling.

3-6: Issues in Breath Analysis

3-6-1: Preconcentration

A major difficulty in accurate breath analysis is the low concentrations of the VOCs that are present in breath samples (ppbv and below). This issue is compounded by issues including the dilution of VOCs by extraneous air as well as loss of VOCs during condensation if EBC is to be collected. To circumvent this issue, several techniques have been developed to preconcentrate a breath sample before analysis. Gordin and Amirav have developed the 'Snifprobe' as a novel preconcentration method.[134] The Snifprobe consists of a small length of capillary or porous layer open tubular (PLOT) column that preconcentrates the sample. Breath was sampled for 5 s through the Snifprobe, after which the entire column segment was placed inside a direct/dirty sample introduction device (DSI) which was then inserted into the GC injector for thermal desorption.[134] A limit of detection for ethanol was stated in the low ppb (v/v) level.[134] Several researchers have also used a sorbent material to sample from a bag or chamber containing a breath sample.[19, 81, 83, 100, 118, 127, 129] In this manner, preconcentration takes place after breath collection. Other groups have created in-line preconcentration methods.[100, 122, 125, 126, 135, 136] Phillips, for example, has developed a breath collection apparatus (BCA) which incorporates a sorbent trap in-line with the breath flow so that VOCs are preconcentrated

as the breath sample is collected.[68, 76, 79, 80, 82, 86, 89, 92, 122-124] Several generations of this instrument have been developed, the latest being the BCA 6.0 (Menssana Research, Inc.).[137] A promising tool for breath VOC preconcentration is solid phase microextraction (SPME) which was included in a recent review.[94]

SPME was developed in 1989 by Belardi and Pawliszyn[138] as a method to quickly, inexpensively, and easily preconcentrate chemicals of interest. The SPME fiber is typically an inch-long piece of fused silica coated with various polymeric materials depending on the target compounds for preconcentration. The SPME fiber is housed in a standard injection needle, so introduction to the GC is simple, and desorption occurs in the heated injection port. Compounds are absorbed or adsorbed to the fiber from the sample. The SPME fiber can be directly exposed to a liquid sample, where the analyte will partition between the liquid phase of the sample and the liquid phase of the SPME fiber coating, or exposed in the headspace of a sample, where the analyte partitions between the sample, the gaseous phase above the sample, and the SPME fiber coating. SPME can be used quantitatively as the amount of analyte absorbed/adsorbed to the fiber is proportional to the concentration of the analyte in the sample.

An analyte partitions into a SPME fiber according to Equation 3- 1:[139, 140]

$$n_f = \frac{\kappa_{fs} V_f V_s C_o}{\kappa_{fs} V_f + \kappa_{hs} V_h + V_s}$$

Equation 3- 1: Equation describing the partitioning of an analyte into a SPME fiber coating.

Where n_f is the amount of analyte extracted into the SPME fiber, κ_{fs} is the distribution constant of the analyte between the liquid sample and the SPME coating, V_f is the volume of the SPME coating, V_s is the volume of the liquid sample, C_o is the concentration of the analyte in the sample, κ_{hs} is the distribution constant of the analyte between the gaseous phase and the SPME coating, V_h is the gas volume of the vial, and V_s is the volume of the liquid sample.

SPME sampling can be passive, where a breath sample is obtained and later exposed to a SPME fiber, or active, where a breath sample is exposed to a SPME fiber as it is obtained.[105] Wang *et al.* used passive sampling to preconcentrate breath samples obtained in Tedlar® sampling bags, obtaining sub ng/mL detection limits for many VOCs.[119] Mutti *et al.* used a similar technique, collecting breath samples into Teflon bulbs into which a SPME fiber was inserted for preconcentration, with limits of detection on the order of 10^{-12} M.[84] Grote and Pawliszyn have used SPME for active breath sampling.[141] The SPME fiber was inserted into an inert tube serving as a mouthpiece, and acetone, isoprene, and ethanol were analyzed using GC-MS.[141]

3-6-2: Contamination

Because of the influence of exogenous VOCs on the air exhaled by a subject, some emphasis has been placed on ensuring the inhaled air supply of a subject is clean. One solution is to provide a closed source of air for the subject.[81, 83, 96, 127, 142, 143] Although effective, this method is reagent consuming and makes the testing apparatus importable.

Others have required subjects to sit in the sampling environment for a set period of time to allow equilibration with the environmental air.[92, 119, 124] This is very time consuming for the subjects and requires a single sampling location to compare groups of subjects. Others still have attempted to clean the ambient air using charcoal filters[133, 143] Many studies do not cleanse the inhaled air supply;[19, 72, 75, 85, 87, 113, 116, 118-120, 129, 136, 144-147] commonly a background sample of the ambient air is sampled at the same time as the subject who has reached equilibrium with the room air donates a breath sample and calculation of the alveolar gradient (concentration in the breath – concentration in the ambient air) is thought to eliminate any effects of contaminated inhaled air.[68, 76, 79, 80, 82, 86, 89, 92, 122, 123, 126 124, 148] A positive alveolar gradient suggests that VOC was manufactured in the body while a negative alveolar gradient indicates the source of the VOC is external to the body.[149] While this technique has advantages in the determination of kinetics and metabolomics, it does require that equilibrium exists for all VOCs in the body and the ambient air – a condition that may be difficult to achieve in select situations. Also, important information about occupational and incidental chemical exposure can be gained by studying the real-time exposure of a subject.

This work presents the use of a commercial respirator cartridge or PVC tubing for purifying the inhaled air. This reduces the amount and concentration of exogenous substances a subject inhales during sample collection, but can also reduce exposure via clothing or skin after exposure.

3-7: Background of Gas Chromatography-Mass Spectrometry

Gas Chromatography-Mass Spectrometry (GC-MS) is an orthogonal detection technique that combines the separation ability of chromatography with the specificity of mass spectrometry. GC is used to separate complex mixtures into more simple or pure components as a method of sample clean-up and/or to prepare more pure materials for sample analysis. The comparison of the retention time of a compound on 2 columns of differing polarities with that of an unknown sample is a presumptive method of compound identification. Mass spectrometry is used to analyze the components in a sample, allowing identification based on the fragmentation patterns of the analyte. Gas chromatography was first coupled to mass spectrometry in 1958 and has evolved over the last 5 decades into a common bench-top technique used in many standard operating procedures in environmental, forensic, and research laboratories.[150]

3-7-1: Gas Chromatography Theory

Gas chromatography was first described by Martin and Synge in 1941 and demonstrated in 1952 by Martin and James.[151, 152] Gas chromatography, or gas-liquid chromatography, relies on a gaseous mobile phase carrying an analyte through a column fitted with a liquid stationary phase supported by a solid material. Gas-solid chromatography has also been described, but has not garnered as much success or attention as gas-liquid chromatography. As the solute passes through the column, it partitions between the stationary and mobile phases. The equilibrium constant of this process, K_D, depends on

the solute, the stationary phase, and the temperature, and can be relate to the partition ratio (k) and phase ratio (β) of the separation according to Equation 3- 2.

$$K_D = \frac{[stationary(liquid)phase]}{[mobile(gas)phase]} = k\beta$$

Equation 3- 2: Description of the equilibrium constant of an analyte as it partitions between the stationary and mobile phases during separation.

The partition ratio is a measure of how long an analyte spends in the stationary phase, and is related to the retention time, t_R, which is the time an analyte spends in the column before elution. The standard compound, methane, is used as a comparison for partition ratios, since methane is considered to not be retained by a stationary phase, and spends all the time in the column in the mobile phase, and thus has the minimum retention time possible in a column. Thus,

$$k = \frac{t_R - t_M}{t_M} = \frac{t_R'}{t_M}$$

Equation 3- 3: Relationship between the partition ratio and retention time.

where k is the partition ratio, t_R is the retention time of the analyte, t_M is the retention time of methane and t_R' is the time an analyte spends in the mobile phase. The phase ratio (β) can be defined as the ratio between the volume of gas in the column and the volume of the liquid stationary phase,

$$\beta = \frac{r}{2d_f}$$

Equation 3- 4: Definition of the phase ratio.

where r is the radius of the column and d_f is the thickness of the film of the stationary phase.

The efficiency of a chromatographic column can be expressed in terms of theoretical plates, or effective theoretical plates. The use of the term 'theoretical plates' refers to the early fractionating distillation columns which indeed had discrete plates to perform the separation; chromatographic columns of today do not have discrete plates, so 'theoretical plates' is used to describe the efficiency in a relative manner. Theoretical plates (n) were originally used to define efficiency:

$$n = 5.54\left(\frac{t_R}{W_H}\right)^2$$

Equation 3- 5: Definition of the number of theoretical plates.

with W_H being the width at half height of a peak. Effective theoretical plates (N) are used to describe the actual time that an analyte is in the mobile phase of the column, thus modifying Equation 3- 5 to be:

$$N = 5.54\left(\frac{t'_R}{W_H}\right)^2$$

Equation 3- 6: Definition of the effective number of theoretical plates.

3-7-2: Mass Spectrometry Theory

The roots of mass spectrometry are based in the late 19th century with the analysis of positive ions using magnetic deflection by Wien.[150] Although there are many types of mass spectrometry, all mass spectrometers detect ions, positive or negative. A sample must be introduced to the system (sample introduction), ions must be formed (ionization region), separated (mass analyzer), and detected (detector), and the data must be processed and output into an understandable form (readout).

There are a variety of sample introduction methods, all requiring introduction of a sample to the mass spectrometer in the gas phase, which must be held under high vacuum in order to reduce ion-molecule collisions. These collisions may cause the ions to lose their charge, thus losing their ability to be detected, cause ions to undergo reactions, or deflect ion trajectories. Therefore to reduce these ion collisions, the mean free path of an ion is important. The mean free path (L, cm), is defined as:

$$L = \frac{1}{\sqrt{2}p n \sigma^2}$$

Equation 3- 7: Definition of the mean free path of an ion.

where p is the pressure (Pa), n is the number of moles per cm^3 and σ is the collision diameter (cm). The mean free path of an ion should be at least 1 m in most mass spectrometry applications, which requires a pressure of 66 nbar or lower as shown in Equation 3- 8:

$$L \approx \frac{0.66}{p}$$

Equation 3- 8: Approximation of the mean free path of an ion at 300 K and $3.8x10^{-10}$ molecules/cm^3.

approximated for 300 K and $\sigma = 3.8x10^{-10}$ molecules/cm^3. Often chromatographic methods are used for sample introduction as they allow for compound separation and sample cleanup. Other options include bleeding a gaseous sample into the ionization region, or novel methods such as Direct Electrospray Ionization (DESI) or Direct Analysis in Real Time (DART) that combine the sample introduction, gasification, and ionization steps.

The ionization region produces ions from the sample for analysis. Several ionization sources are available, most commonly electron ionization (EI) or chemical ionization (CI) are used in GC-MS, but other ionization sources exist for other applications. In electron ionization, the sample is ionized by interactions with electrons. The electrons are produced by heating a filament, and accelerated towards an anodic plate. As the electrons travel through the source, they encounter the gaseous sample, and if the wavelength of the electron approaches the bond length of the molecules in the sample, energy transfer may occur, and an electron is expelled from the molecule, creating a

positive ion. Typical electron energy of 70 eV is used for the ionization of organic molecules, which maximizes the ionization efficiency to ~0.1% on average because of the similar de Broglie wavelength of the electrons and bond length of the organic molecules (~ 0.14 nm). Only the positive molecular ion is formed using EI, as the energy of the electrons is too high for electron capture to occur. Fragmentation of the molecule is common using EI, creating fragment ions which are also detected.

Another common ionization method is chemical ionization (CI) which involves the introduction of a reagent gas, such as methane, which is ionized using electron ionization. The ions produced will then collide and react with other molecules of reagent gas, creating a series of ions in the source region. These reagent gas ions will then react with the sample molecules, ionizing them in a 'soft' ionization process that causes minimal fragmentation. Deposition of energy into analyte ions is much less than for EI because it depends on the thermodynamics of the ion-molecule reaction.

After ions are produced they must be separated before detection. This separation occurs in the mass analyzer, which is commonly a quadrupole mass analyzer for GC-MS and is the mass analyzer used in the instruments used in these experiments. A quadrupole mass analyzer consists of 4 parallel hyperbolic rods, although circular rods are more commonly used. An electric field consisting of a quadrupolar oscillating field superimposed on a constant electric field exists in the center of the analyzer, following:

$$\Phi_0 = (U - V\cos\omega t)$$
$$-\Phi_0 = -(U - V\cos\omega t)$$

Equation 3- 9: Equations describing the electric field formed in the center of a quadrupole mass analyzer.

where Φ_0 is the potential applied to the rods, ω is the angular frequency, and U is the constant potential and V is the peak amplitude of the RF voltage. The angular frequency is related to the frequency of the RF field by Equation 3- 10:

$$\omega = 2\pi f$$

Equation 3- 10: Relationship between angular frequency and RF field frequency.

where f is the frequency of the RF field. Ions created in the source region are accelerated along the z-axis via focusing lenses into the space between the rods. The electric field induces forces on the ions in the x and y directions, causing the ion to move away from and towards the rods. If the ion does not change directions quickly enough with the oscillation of the RF field, it will collide with the rod and be discharged. If the ion direction oscillates with the RF field the entire time it is within the rods, it will pass through to the detector with its charge intact. Thus, by modifying the electric field, i.e. controlling U and V, ions of a specified mass-to-charge ratio can be selectively passed through to the detector. For detection of a wide range of m/z, U and V must be scanned to allow ions of successive m/z to be passed through the mass analyzer. Generally, the U/V ratio is kept constant to allow this successive detection.

The ions that pass through the mass analyzer are converted to electrons by collisions with a conversion dynode, and these secondary electrons are detected using an electron multiplier, typically a continuous dynode electron multiplier. In an electron multiplier, the charged particle collides with a metal or lead oxide coated surface of low work function, inducing the emission of 1-3 electrons. These electrons are then accelerated onto another plate, inducing an additional 1-3 electrons each. This process is repeated numerous times until a gain in signal of about 10^5 is realized. The current induced in this process is measured as a voltage drop across a resistor, and this voltage is converted to a digital value and stored on a computer. A mass calibration function assigns m/z values to each ion based on the U and V potentials that are applied coincident with the arrival time of each ion.

3-7-3: GC-MS Description

A schematic of a GC-MS instrument used at LLNL is shown in Figure 3- 4.

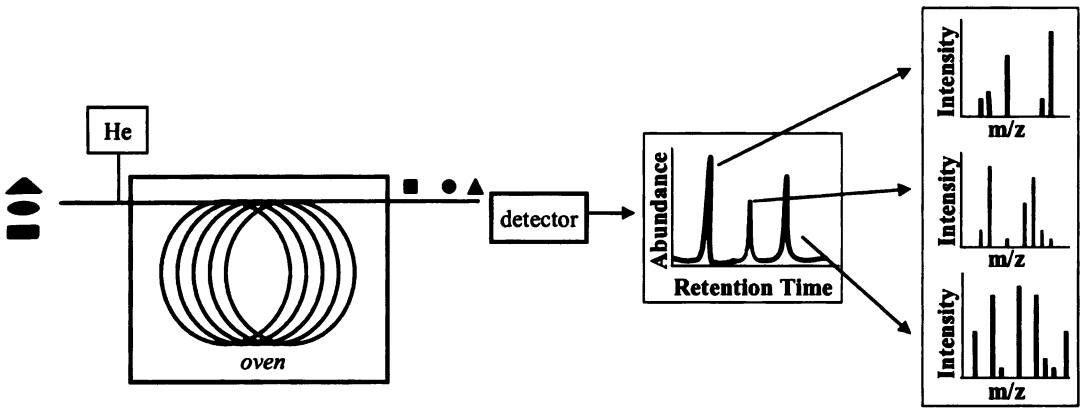

Figure 3- 4: Schematic of a gas chromatograph-mass spectrometer (GC-MS). A sample is injected onto a capillary column held inside a temperature programmed oven. As the sample passes through the column, components separate based on partitioning between the mobile and stationary phases of the column, aided by the temperature ramp in the oven. The components exit the column directly into the source region of the mass spectrometer, where they are ionized, fragmented, and pass into the mass analyzer, where the fragments are detected. The resulting data includes a chromatogram with a corresponding mass spectrum for each time point. (Image originally in color)

The sample is introduced to the instrument through a temperature controlled injection port using a syringe (liquid samples) or a solid phase microextraction (SPME) fiber, discussed previously, where a solid preconcentrating material is injected via syringe needle and the adsorbed sample is thermally desorbed from the material. The sample is vaporized and carried onto the capillary column by a flow of carrier gas, typically helium. The column is stored in a temperature controlled oven, and the initial temperature is typically held at a point lower than that of the injection port, causing the vaporized sample to condense at the head of the column. The carrier gas carries the sample through the column and the analytes partition between the mobile (carrier gas) and stationary phases (column coating) to different extents. Compounds that partition more into the

mobile phase are transported through the column faster than compounds retained more in the stationary phase, causing the separation to occur. The temperature of the oven is often increased with time, aiding volatilization of less volatile analytes. The end of the column is positioned inside the ionization chamber of the mass spectrometer, where the pressure is held in the range of 10^{-6}-10^{-5} Torr. Each analyte is ionized via electron ionization (EI) as it elutes from the column. The resulting ions are accelerated through the quadrupole mass analyzer and are detected by the electron multiplier. The signal is digitized and the data readout provided through the commercial software that also operates the instrument.

The current study demonstrates an in-house modification of a standard exhaled breath condensate collection device, the RTube™ (Respiratory Research, Inc., Charlottesville, VA). This modification reduces the time of analysis from sampling to results to 27 minutes, as well as eliminates the need for a freezer, making the sampling device more field-friendly, and increases the sensitivity. This study also shows the need for purification of inhaled air in some cases and describes additional RTube™ modifications that meet this need.

3-8. *Instrument Description*

3-8-1: Agilent System

An Agilent (Santa Clara, CA) 6890N GC equipped with a SPME inlet sleeve and an Agilent J&W DB-5MS column (30 m x 0.25 mm x 0.25 μm, equivalent to 5% phenyl, 95% methylpolysiloxane) was used for the separation of all compounds. Helium (99.999%, Praxair, Inc., Danbury, CT) was used as a carrier gas and the GC was operated

in constant pressure mode (10 psi). The injector temperature was held at 250 °C, and the oven temperature was held at 40°C for 1 min, then ramped at 20°C/min to 300°C, where it was held for 3 min. Detection was carried out with an Agilent 5973 MS detector (Santa Clara, CA), using 70 eV electron ionization and operated in scan mode (m/z 40 – 450) at 3.54 scans/s, with the source held at 230°C and the mass analyzer (quadrupole) held at 150°C. ChemStation software was used for data collection and analysis.

3-8-2: Shimadzu System

A Shimadzu (Pleasanton, CA) QP2010 with a SPME inlet sleeve and fitted with an Agilent J&W DB-5MS column was used. The same method was used as in the Agilent system. GCMS Solutions software was used for data collection and analysis.

Compounds were identified based on comparison of their mass spectra with those in the NIST Mass Spectral Library (RMatch >700, NIST MS Search 2.0, NIST, Gaithersburg, MD) as well as mass spectra published in the literature, and comparison of retention time with pure chemicals when available.

3-9: *Materials*

Frozen lemonade concentrate (Safeway/Vons Lemonade, Safeway, Inc., Pleasanton, CA) was purchased from a local supermarket and reconstituted according the manufacturer's instructions. Samples were used the day of reconstitution after reaching room temperature (24 °C). Nail Polish (ORLY Nail Color, Orly International, Inc., Los Angeles, CA) was obtained from commercial sources and used as is. Gasoline (89 octane

automotive grade) was obtained from a local gas station. D-Camphor was obtained from J.T. Baker, Inc. (Phillipsburg, NJ). A 65.3 mM solution was made in a 1:4 solution of H_2O:methanol and stored in a glass vial. (1S)-(-)-β-pinene (99%) was obtained from Alfa Aesar (Ward Hill, MA) and +/- α-limonene (95%) was obtained from TCI America, Inc. (Portland, OR).

3-10: Subjects

Fourteen healthy adults were recruited as subjects for this study. All subjects had no known respiratory ailments and did not report any routine chemical exposure on a questionnaire. The Institutional Review Board (IRB) at Lawrence Livermore National Laboratory (LLNL) as well as the IRB at Michigan State University approved the study and formal written informed consent was obtained from each subject prior to participation.

3-11: Original Sample Collection (EBC)

Exhaled breath condensate (EBC) was originally collected as per the RTube™ manufacturer's instructions. The aluminum sleeve was cooled in a -80°C freezer overnight, and then placed in the insulating sleeve on the RTube™ body. The subject held the RTube™ and inhaled and exhaled through the mouthpiece, causing the exhaled breath to condense on the walls of the cooled polypropylene tube. Breath samples were collected for 10 minutes, after which the mouthpiece apparatus was removed from the RTube™, and the polypropylene tube placed on a plunger which caused the liquid

condensate to be collected in a small volume area of the tube. The liquid was then divided into 500 µL aliquots in microcentrifuge vials and the excess vials refrigerated. A single EBC aliquot was sampled using a SPME fiber under direct exposure for 10 minutes which was then injected into the GC-MS. The SPME fiber was predesorbed during a 'blank' GC-MS run each morning before any breath sampling occurred. After collection the RTube™ was washed with methanol followed by water, followed by D.I. water and dried before reuse. Studies demonstrated there was no carryover effect from reusing the RTube™ after cleaning.

3-12- GC-MS Method Development

3-12-1: GC Method Optimization

Experiments were performed to optimize the GC-MS method used for analysis. Mass spectra were acquired over m/z 40-450. The temperature ramp of the GC oven was modified to create different methods to optimize the separation of a breath sample. EBC was used in order to have a single sample that could be analyzed using each method. Four methods were created and are shown in Table 3- 1.

A single EBC sample was collected from the subject, and split into 4 0.5 mL aliquots. A SPME fiber was directly exposed to the liquid condensate for 10 min. Figure 3- 5 shows total ion chromatograms obtained using each method. Overall peak area is consistent throughout methods 1-3, with 8.3% RSD for the total integrated area under the curve; however, the total area under the curve for method 4 was approximately 3 times larger than for the other methods. The peak area for the peak attributed to acetone, at approximately 1.4 min, revealed an RSD of only 4.9% across all 4 methods. Integration

using the ChemStation Software (RTE Integrator, 6000 count area minimum) identified 61, 48, 52, and 11 peaks, respectively for each method. Method 1 was therefore selected to provide an optimal separation method based on number of peaks detected and time of analysis.

Table 3- 1: Description of method parameters for methods tested to optimize the separation of breath samples.

	Method 1	Method 2	Method 3	Method 4
Starting Temp	40°C (1 min)	40°C (1 min)	40°C (1 min)	40°C (1 min)
Ramp Rate	20°C/min	15°C/min	10°C/min	1°C/min
Final Temp	300 (5 min)	300 (5 min)	300 (5 min)	300 (5 min)

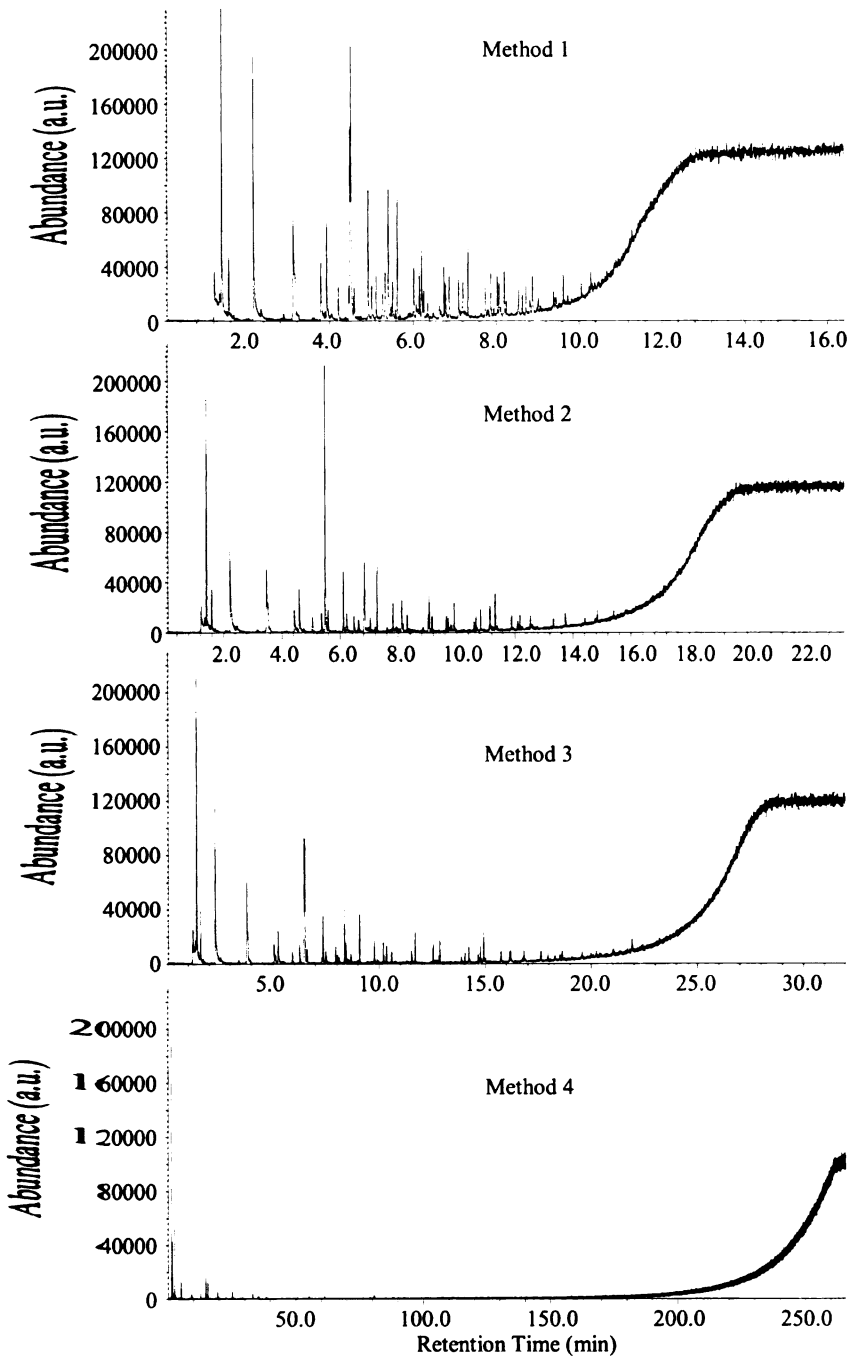

Figure 3- 5: GC-MS total ion chromatograms obtained from a single breath sample analyzed with the 4 methods shown in Table 3- 1. Method 1 was selected as the optimal detection method.

3-12-2: SPME Exposure Time Optimization

The SPME PDMS/DVB fiber coating was selected based on the literature using SPME for breath analysis[141, 153] and the need to preconcentrate mostly semi-volatile compounds, and was confirmed based on conversations with other researchers in the breath analysis field.[154] The exposure time was optimized in two sets of experiments, one using EBC and one using EBV. Figure 3- 6 shows the peak area of three peaks detected in EBV collected for 0.5, 1, 2, 5, and 10 min. These compounds, an unidentified branched alkane (RT=7.83 min), decanal (RT=7.29 min), and an unidentified alcohol (RT=10.67 min), were selected to represent an alkane, an aldehyde, and an alcohol, respectively. Data points are the average of 3 replicates taken in a single day. A sampling time of 10 min was optimal and used for the remainder of the experiments.[155]

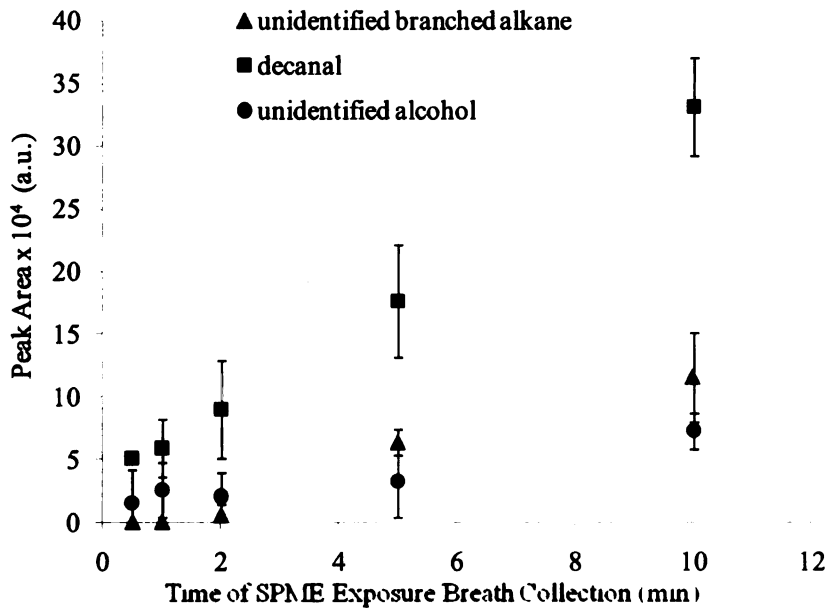

Figure 3- 6: Comparison of TIC peak area to exposure time of SPME fiber. The exposure time of the SPME fiber is equivalent to the breath collection time for these EBV samples. (Image originally in color)

3-13: Comparison of Breath to Background Air

It is important to understand the source of inhaled air to determine whether a compound detected on breath is exogenous or endogenous. The inhaled air was measured by exposing a SPME fiber for 10 minutes on a desk in the room where breath samples were obtained. This SPME fiber was then analyzed using the standard GC-MS method. Figure 3- 7a shows the chromatogram obtained after exposure to room air. There are several peaks present in the sample. Table 3- 2 shows the tentative identification as well as retention time of these peaks. Figure 3- 7b shows a representative breath sample (EBC) collected from a single subject. Figure 3- 7c shows this same sample with the contribution from the room air subtracted. While many peaks in the room air and seen in the breath, the concentration is much larger in breath.

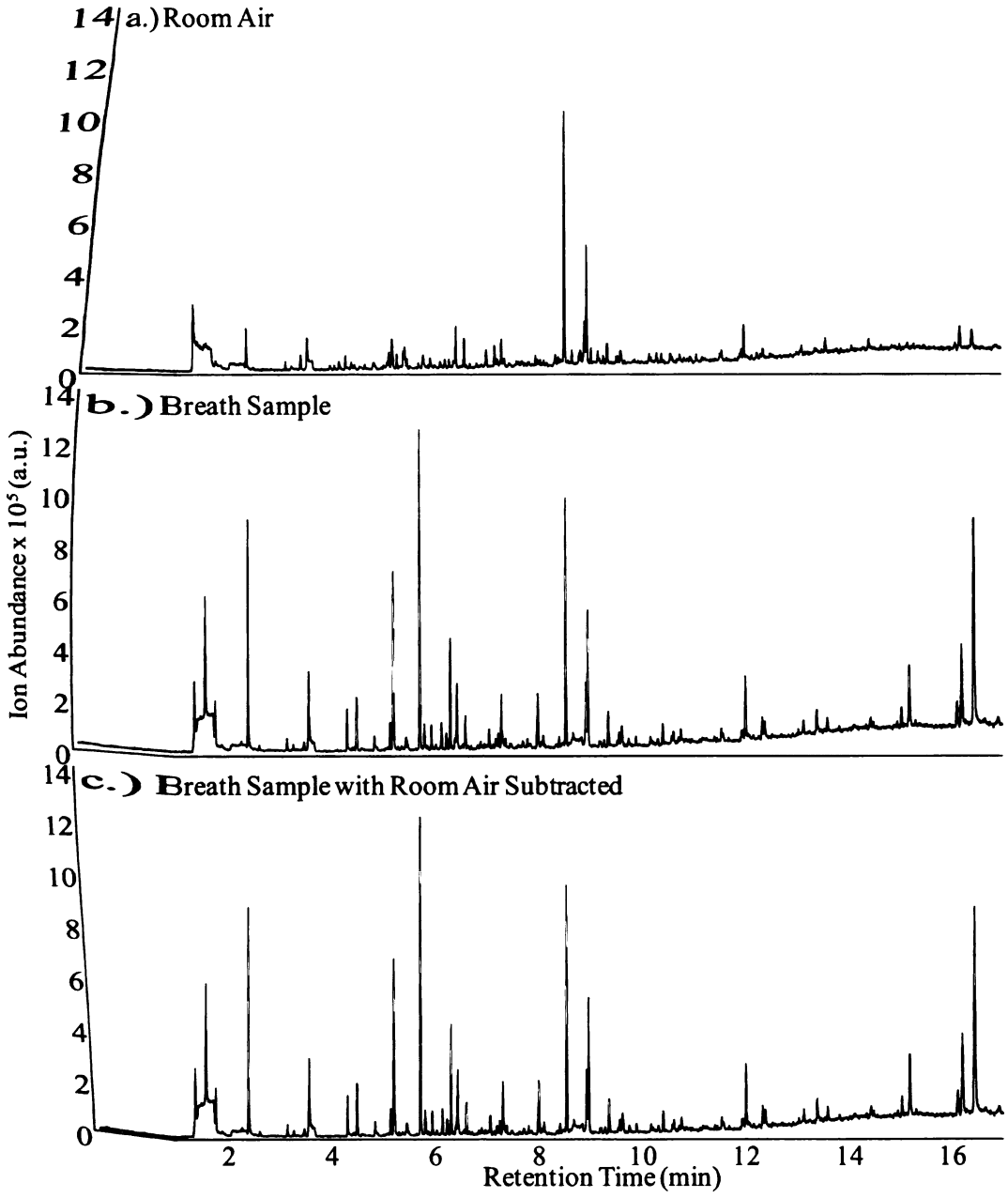

Figure 3- 7: Chromatograms obtained from (a) 10 minute exposure of the SPME fiber to the ambient room air at the collection site, (b) a representative breath sample (EBC), and (c) the difference between the chromatograms in a and b. Note that the majority of peaks in breath are in much greater concentration than those in the room air.

Table 3- 2: Compounds and corresponding retention times tentatively identified in a SPME sample of room air.

Peak	Compound	RT	Peak	Compound	RT
1	Carbon dioxide	1.33	14	3-ethyl-Benzaldehyde	7.01
2	Dimethyl silanediol	2.35	15	4-ethyl-Benzaldehyde	7.17
3	Butanoic acid, ethyl ester	3.42	16	Decanal	7.30
4	Hexamethyl cyclotricyloxane	3.55	17	2,4-diisocyanato-1-methyl-benzene	8.52
5	Unidentified aromatic	4.29	18	1,3-dihydro-5-methyl-2H-benzimidazol-2-one	8.91
6	Benzaldehyde	5.12	19	1,3-dihydro-5-methyl-2H-benzimidazol-2-one	8.95
7	Octamethyl Cylcotetrasiloxane	5.18	20	Unidentified compound	9.04
8	6-methyl-5-Hepten-2-one	5.28	21	1-tridecanol	9.35
9	Hexanoic acid, ethyl ester	5.40	22	6-undecylamine	12.00
10	2-(2-ethoxyethoxy)-ethanol	5.43	23	Bisphenol A	13.59
11	Benzyl alcohol	5.79	24	Unidentified Compound	16.19
12	Nonanal	6.42	25	2-hydroxy-1-(hydroxymethyl) ethyl ester-octadecanoic acid	16.43
13	Decamethyl-cyclopentasiloxane	6.58			

3-14: Reproducibility Studies

3-14-1: Repeatability of Measurement

A study was undertaken to determine the injection to injection repeatability of the measurement. Since breath itself is a variable matrix, sensitive to storage and the activity of each subject, a standard of diethyl ethylphosphonate (DEEP) was spiked into samples for measurement; thus, the matrix effects of breath were still present. In order to generate a larger volume of sample, EBC was simultaneously collected from two subjects, and combined for a total of approximately 5.7 mL of EBC. 15 µL of a 0.031 M solution of DEEP in methanol was spiked into 5.5 mL of this combined EBC sample. The sample was then divided into eleven, 0.5 µL aliquots, each of which was refrigerated until analysis by GC-MS. Samples were analyzed 19, 79, 139, 199, 260, and 441 minutes, as well as 24.3, 48.9, 49.3, 72.9, and 96.1 hours after sample collection. Chromatograms obtained from the samples at 48.9 and 72.9 hours after exposure were eliminated because the SPME fiber was exposed to the sample longer than intended. Peak areas were calculated by manually integrating the area of the peak at 6.23 min due to DEEP in each sample. The relative standard deviation (RSD) was determined to be 11.7%. This measurement includes error in sample dilution, SPME fiber exposure time, and instrument variation.

3-14-2: Single Subject, Single Day

Intra-subject variation is a concern when developing an analytical method relying on biological samples. Natural variation between samples may cause a false positive or false negative test if it is not understood. This variation may occur on a short time scale, being

present within multiple samples collected in a single day, or on a longer time scale, being present within samples collected over the course of weeks or months. In order to study the short-term variation, EBV samples were collected from a single subject throughout the day. 19 samples were analyzed using the standard GC-MS method immediately after collection. The GC-MS data files were processed using MarkerLynx, which extracts XIC peak areas for nontargeted analytes, in this case extracting an integrated area for a single m/z from each detected peak. Method parameters for XIC peak area extraction are shown in Table 3- 3.

Table 3- 3.- MarkerLynx method parameters for peak area extraction

Retention Time Window	0-17 min
Mass Range	40-450 Da
Mass Tolerance	0.30 Da
Use Relative Retention Time	No
Peak Width at 5% Height	1 s (automatic)
Peak-to-Peak Baseline Noise	0 (automatic)
Masses per Retention Time	1
Minimum Intensity	1% of base peak intensity
Mass Window	0.3
Retention Time Window	0.2
Noise Elimination Level	0
Deisotope Data	No
Peak Area Normalization	None
Peak Area Scaling	None

Markers at m/z 45, 73, 77, and 207 were excluded as they arise from septum and column bleed, and m/z 93 was also excluded as this is the major m/z peak in terpenes, which the

subject consumed in lemonade the day of sampling. Ninety marker compounds were reported. The standard error of the mean (SEM) of the raw peak area of each marker for the 19 samples was calculated. 27.8% (25) of the markers had a SEM of <5%, 8.9% (8) had an SEM between 5% and 10%, 10.0% (9) had an SEM between 10% and 15%, 5.6% (5) had an SEM between 15-20%, 7.8% (7) had an SEM between 20-25%, and 21.1% (19) had an SEM >50%. Of the markers with an SEM <5%, 72.0% (18) had an SEM <1%. These results show that the intra-subject variation during a single day is less than 25% for the majority of markers. The variance is lower for those markers with lower average peak areas, with those with an SEM<1% ranging from 0.157-2.31 a.u., those with SEM<5% ranging from 3.61-5.69 a.u., SEM<10% ranging from 6.59-298 a.u., SEM<15% ranging from 11.5-364 a.u., SEM<20% ranging from 29.5-45.8 a.u., SEM<25% ranging from 33.8-564 a.u., and SEM>50% ranging from 93.0-11800 a.u..

3-14-3: Single Subject, Multiple Days

Intra-subject variation is not only caused by the variation in the breath composition throughout a single day, but also by the long-term variation in the breath. This type of variation could be caused by more major lifestyle changes, including diet, exercise, environment, and stress.[155] This long-term variation was studied by collecting 25 EBV samples from a single subject over the course of 1 month. Samples were analyzed using the standard GC-MS method immediately after collection and analyzed using MarkerLynx as described in section 3-14-2 and Table 3- 3 with the exclusion of only the markers at m/z 45, 73, 77, and 207. The software reported data for 233 markers. The standard error of the mean (SEM) for the raw peak areas of 25 samples was calculated for

each marker. 43.8% (102) of the markers had a SEM of <5%, 9.4% (22) had an SEM between 5% and 10%, 6.4% (15) had an SEM between 10% and 15%, 3.0% (7) had an SEM between 15-20%, 3.86% (9) had an SEM between 20-25%, and 20.2% (47) had an SEM >50%. Of the 102 markers with an SEM <5%, 58.8% (60) had an SEM <1%; however, these 60 markers had very small average peak areas, the maximum being 0.28 a.u., and they were not present in all samples, so they may be meaningless as markers. These results show that the intra-subject variation over a period of a month is minimal for the majority of markers.

3-15: Optimization of Breath Sample Collection

3-15-1: Exhaled Breath Condensate (EBC) and Exhaled Breath Vapor at -80°C (EBV-80°C) Collection

The RTube™ was slightly modified to allow for simultaneous vapor collection above the EBC. A plastic fitting was constructed from a second RTube™ (Figure 3- 8b) which attached directly to the top of the RTube™ and served as a mount for a SPME sampler. A SPME fiber (65 μm PDMS/DVB Stableflex fiber, Sigma-Aldrich, St. Louis, MO), previously thermally conditioned in the GC injection port per manufacturer's instructions, was fitted into this mount and extended into the polypropylene tube, the end of the fiber extending approximately 3.7 cm into the tube. The subjects breathed at normal frequency and tidal volume through the mouthpiece for 10 or 15 min, typically yielding 0.7-2.5 mL of EBC. After collection, the exhaled breath vapor (EBV-80°C) collected on the SPME fiber was analyzed immediately by GC-MS, and a standard volume, 0.5 mL, of EBC was aliquoted into a disposable polypropylene microcentrifuge tube (Fisher Scientific, Pittsburgh, PA). After analysis of the EBV-80°C was complete,

the SPME fiber was directly inserted into the aliquot of EBC for 10 minutes (direct exposure), followed by injection into the GC-MS.

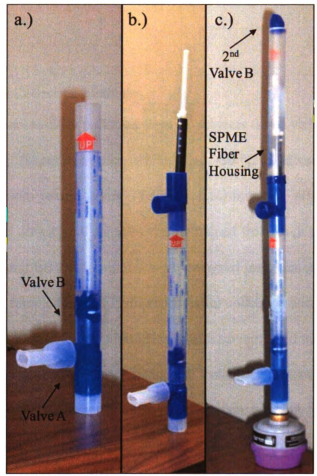

Figure 3- 8: Exhaled breath condensate (EBC) and vapor (EBV) collection devices. a.) the commercially available RTube™; b.) the RTube™ was modified for EBV collection by the addition of a plastic fitting to hold a SPME fiber for active sampling; c.) the additional modification of the RTube™ to provide an enclosed environment for SPME sampling as well as the addition of a respirator to purify inhaled air. ***(Image originally in color)***

3-15-2: Exhaled Breath Vapor – Room Temperature (EBV-RT) Collection

EBV-RT was collected using the modified RTube™ (Figure 3- 8b) at room temperature, using no aluminum condenser. The subject breathed at a normal frequency and tidal

volume through the mouthpiece of the RTube™ for 10 min while the SPME fiber was exposed inside the polypropylene tube. After collection, the sample was immediately analyzed.

3-15-3: Comparison of Collection Methods

Breath samples were successfully collected from all subjects (n=4) yielding EBC (-80 °C condenser), EBV-80°C (vapor collection while using -80 °C condenser), and EBV-RT (vapor collection at room temperature). To reduce confounding effects such as diet, ambient intake air, and activity, all samples were obtained from each subject within one hour. All EBV-80°C and EBV-RT samples were analyzed immediately after collection; all EBC samples were sampled using SPME shortly after collection and then immediately injected. Noticeable warming of the aluminum condenser occurred during sampling, as has been previously documented.[114] A typical EBC collection yielded 0.7-2.5 mL EBC during the 10 minute collection time. EBV-RT collection typically yielded < 200 µL condensate which was discarded. Figure 3- 9 shows example total ion chromatograms (TIC) from breath samples of a single subject collected using EBC, EBV-80 °C, and EBV-RT.

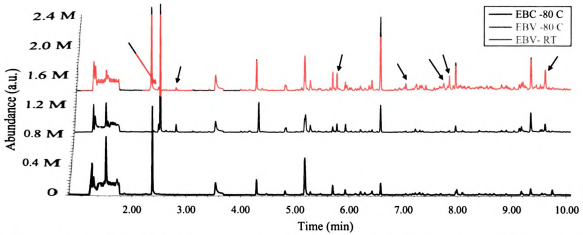

Figure 3- 9: Total ion chromatograms of breath samples from a single subject. Samples were obtained using several collection methods: EBC with a -80 °C condenser (black trace, bottom), EBV-80°C (green trace, middle), and EBV-RT (red trace, top). Arrows indicate several peaks with increased signal in the EBV samples compared to the EBC sample. Chromatograms are offset for clarity. (Image originally in color)

The EBV-RT samples yielded an average of 23% more peaks than the EBC samples from the same subject using the same integration parameters, several of which are indicated by the arrows. Table 3- 4 shows a list of observed compounds and their retention times tentatively identified in EBV-RT breath samples.

Table 3- 4: Breath VOCs and corresponding retention times tentatively identified in a typical EBV-RT sample (no known exposure).

Peak	Compound	RT	Peak	Compound	RT
1	Carbon dioxide	1.3	38	α-terpinene	6.3
2	Acetone	1.54	39	α-p-dimethylstyrene	6.34
3	Acetic acid	1.85	40	Nonanal	6.43
4	Allyl methyl sulfide	2.5	41	D-fenchyl alcohol	6.64
5	Unidentified Compound	2.63	42	4,7,7-Trimethylbicyclo [4.1.0]heptan-3-ol	6.76
6	(Z)-1-(methylthio)-1-propene	2.82	43	L-isopulegol	6.89
7	Methyl isobutyl ketone	2.86	44	Camphor	6.92
8	Formic acid	3.0	45	Menthone	6.96
9	Toluene	3.13	46	Isopregol	7.0
10	4,4-dimethyl-2-pentene	3.4	47	Ethyl benzoate	7.05
11	Butyl ester acetic acid	3.55	48	4-isopropyl-1-methylcyclohexanol	7.13
12	3-furaldehyde	3.77	49	4-terpineol	7.18
13	4-hydroxy-4-methyl-2-pentanone	3.86	50	α-terpineol	7.29
14	2-furanmethanol	3.97	51	4-ethyl octane	7.35
15	o-xylene	4.08	52	5-hydroxymethylfurfural	7.43
16	p-xylene	4.18	53	Undecane	7.58
17	Unidentified Aromatic	4.31	54	3-methyl-dodecane	7.67
18	Styrene	4.4	55	Tridecane	7.75
19	Ethylene glycol monoisobutyl ether	4.49	56	2,6,10-trimethyl-dodecane	7.82
20	2-methyl-bicyclo[3.1.0]hex-2-ene	4.75	57	Unidentified Alkane	7.85
21	6,6-dimethyl-2-methylenebicyclo[3.1.1]heptane	4.84	58	Isomenthol acetate	8.02
22	Benzaldehyde	5.13	59	Unidentified Alkane	8.54
23	Phenol	5.19	60	Unidentified Alkane	8.6
24	6-methyl-5-hepten-2-one	5.29	61	Unidentified Alkane	8.63
25	Cyclofenchene	5.30	62	Unidentified Alkane	8.81
26	beta-pinene	5.34	63	Unidentified Alkane	8.9
27	Isopentyl ether	5.46	64	Dihydropseudoionone	9.18
28	alpha-terpinene	5.66	65	2,6-dimethyl heptadecane	9.25
29	2-ethyl-1-hexanol	5.7	66	1-dodecanol	9.35
30	o-cymene	5.73	67	Unidentified Compound	9.48
31	α-limonene	5.78	68	Hexyloctylether	9.53
32	Eucalyptol	5.83	69	Butylated hydroxytoluene	9.62
33	2-methyl tridecane	5.96	70	Diethyl phthalate	10.1
34	4,6-dimethyl-undecane	6.01	71	Heptadecane	10.2
35	gamma-terpinene	6.04	72	2,2-dimethyl-3-octanone	10.8
36	Isooctylvinyl ether	6.16	73	2,2-dimethyl-4-Octen-3-ol	11.1
37	2,5-furandicarboxaldehyde	6.19			

The vapor samples also provided increased peak areas for many peaks. For example, α-limonene showed a ten-fold increase in peak area when a vapor phase sample was collected and analyzed. The area increase of several such peaks is shown in Table 3- 5. Thus, for many compounds, vapor phase collection of exhaled breath provides increased signal and increased information.

Table 3- 5: Peak area of several compounds tentatively identified in total ion current chromatograms of breath samples collected as EBV-80°C or EBV-RT versus peak area of EBC total ion current chromatograms. These peaks are indicated by the arrows in Figure 3- 9.

		Factor Increase in Measured Peak Area vs. EBC-80°C	
Compound	**R.T. (min)**	**EBV-80°C**	**EBV-RT**
Allyl methyl sulfide	2.50	5.0	2.1
(Z)-1-(methylthio)-1-propene	2.82	9.9	3.7
α-Limonene	5.78	6.8	10.2
Ethyl benzoate	7.05	1.6	4.6
Tridecane	7.75	2.0	8.4
Unidentified Alkane	7.85	2.1	9.0
Butylated Hydroxytoluene	9.62	4.9	8.4

3-16: *Efforts to Control the Inhaled Air of a Subject*

3-16-1: RTube™ Modification with PVC Tubing

A method to provide clean air to a subject was developed using approximately twelve feet of FDA-approved clear PVC tubing (0.5 in I.D., 0.75 in O.D., VWR, Inc., West Chester, PA) fitted to the base of valve A on the modified RTube™ (Figure 3- 8b) using

a plastic fitting. Tubing was stretched into a different room (air space) than that in which the samples were obtained. This provided inhaled air free from contamination from the skin or clothing of the individual, and eliminated contamination by the localized environment of the subject. The subject breathed at normal frequency and tidal volume through the mouthpiece while holding their nose for 10 min. After collection, the EBV-RT collected on the SPME fiber was analyzed immediately.

The headspace of the plastic tubing was sampled using SPME in order to understand any background that may be present in the tubing. A SPME fiber was placed inside the tubing for 10 minutes, and analyzed using GC-MS. The major compounds detected were 2-ethyl-1-hexanol, and butylated hydroxytoluene, a solvent and stabilizer used in the production of plastics, respectively. An increase in the peak area of these compounds in chromatograms obtained using the plastic tubing to provide inhaled air relative to samples obtained without the tubing was found, but both compounds are present in many products that an individual is exposed to on a daily basis; thus they are normally found in breath obtained with or without the tubing. These peak areas decrease over time as more air is passed through the plastic tube, thus, the tube was flushed with compressed air before use.

3-16-2: Nail Salon Inhalation with PVC Tubing

Breath samples (EBC) from a single subject with a fresh manicure were obtained at regular intervals over the course of a single day (7 hours) using the RTube™ modified with PVC tubing. Immediately after the manicure, the concentration of several compounds, tentatively identified as isopropyl alcohol, camphor, and diacetone alcohol,

increased and then exponentially decayed with time (data not shown). Isopropyl alcohol and camphor were listed as ingredients on the nail polish used; diacetone alcohol was not a listed ingredient, but is commonly formed via an aldol condensation of acetone,[156] which was a listed ingredient. The breath sample obtained 215 minutes after the manicure showed minimal detectable signal from these compounds. An additional sample was then taken 317 minutes post-manicure using an unmodified RTube™ (no tubing). This chromatogram again showed the increased concentrations of isopropyl alcohol, camphor, and diacetone alcohol. Extracted ion chromatograms for each of these peaks are shown in Figure 3- 10.

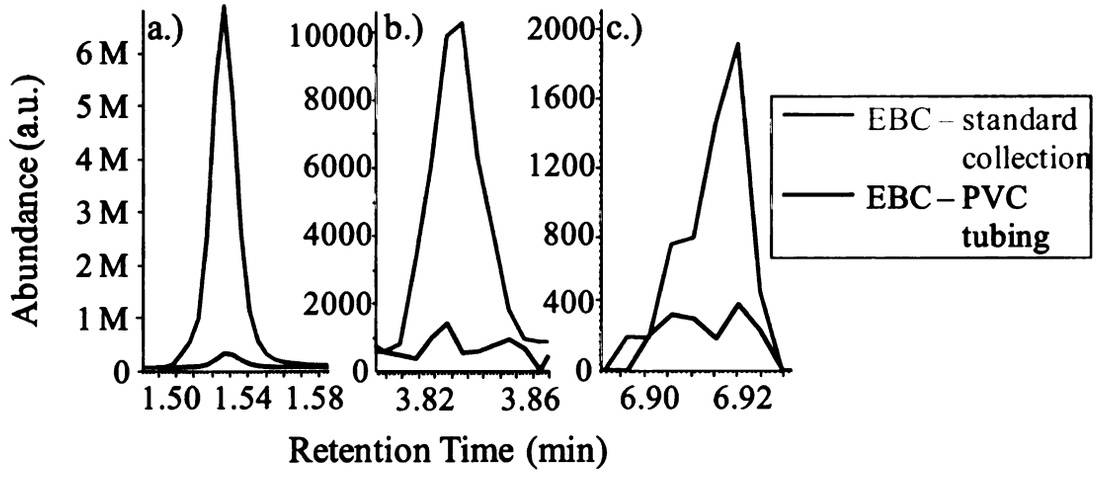

Figure 3- 10: Extracted ion chromatograms (XIC) of breath samples from a single subject (EBC). One sample was collected 215 minutes after the subject received a manicure with an RTube™ modified with PVC tubing which provided inhaled air from a separate room (black trace, bottom). Another sample was obtained 317 minutes after receiving the manicure, and was obtained with the standard unmodified RTube™ (red trace, top). a.) the XIC of m/z 45, identified as a major fragment ion from isopropyl alcohol, b.) the XIC of m/z 43, corresponding to a major fragment ion from diacetone alcohol, and c.) the XIC of m/z 152 corresponding to the molecular ion of camphor. (Image originally in color)

By holding the RTube™ to obtain the breath sample, the subject's hands (i.e. painted fingernails) were in close proximity to the mouth/nose, inadvertently causing the subject to inhale a higher concentration of compounds directly from the nail polish. The use of the PVC tubing to provide an air source removed from the subject's person eliminated these localized situational effects.

Alveolar gradients were calculated for isopropyl alcohol, camphor, and diacetone alcohol in both breath samples. The breath sample collected using the traditional RTube™ method (317 min after exposure) yielded positive values for all three compounds, implying that they were manufactured inside the body.[122, 124, 149] However, the sample obtained using the RTube™ modified with PVC tubing (215 min after exposure) yielded negative alveolar gradient values for camphor and diacetone alcohol, indicating they were not synthesized in the body. The alveolar gradient for isopropyl alcohol remained positive, but was 96.3% smaller than in the contaminated sample.

3-16-3: RTube™ Modification with Respirator Cartridge

A commercial organic vapor respirator cartridge with a P100 Particulate Filter (99.97% minimum filter efficiency, Lab Safety Supply Inc., Janesville, WI) was fitted to the plastic fitting holding valve A via a Viton® o-ring (approximately 2.5 cm diameter) and a machined brass fitting. Plastic caps, the polypropylene tube, and valve B from a second RTube™ were used to isolate the SPME fiber from the outside air as shown in Figure 3-8c. The subject breathed at normal frequency and tidal volume through the mouthpiece while holding their nose for 10 min. After collection, the EBV-RT collected on the SPME

fiber was analyzed immediately. A second respirator can also be attached in series to provide additional filtration in selected studies described below.

3-16-4: Nail Polish Inhalation with Respirator Cartridge

Breath samples were then collected from a single subject while painting a standardized 1.5 in x 1.5 in cardboard square covered in packaging tape with nail polish. The cardboard was used to simulate a fingernail while preventing the possibility of dermal absorption of the compounds. Breath samples (EBV-RT) were obtained i) with no modification to the inhaled air, ii) with the inhaled air passing through an organic vapor respirator, and iii) with the inhaled air passing through PVC tubing from a separate room. Figure 3- 11 shows the chromatograms obtained in each case.

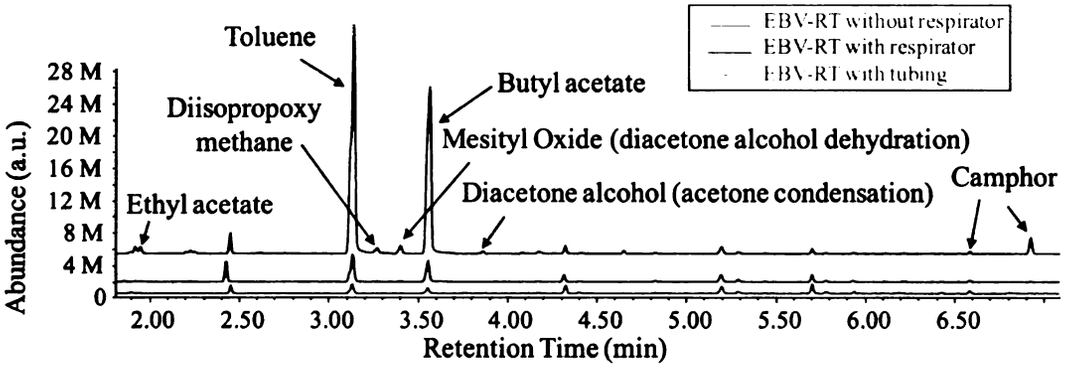

Figure 3- 11: Total ion current chromatograms of breath samples from a single subject (EBV-RT) collected using a variety of inhaled air sources: ambient air (red trace, top), ambient air through a respirator (blue trace, middle), and ambient air from a separate room than sampling (green trace, bottom). The subject painted a simulated fingernail with commercial nail polish during sampling. Compounds labeled are listed ingredients of the nail polish or byproducts of ingredients. Chromatograms are offset for clarity. ***(Image originally in color)***

It is immediately apparent that many foreign compounds are present in the breath samples. The ingredients of the nail polish used were listed as butyl acetate, ethyl acetate, toluene, nitrocellulose, tosylamide/formaldehyde resin, dibutyl phthalate, isopropyl alcohol, stearalkonium hectorite, camphor, phthalic anhydride/trimellitic anhydride/glycols copolymer, benzophenone-1, and guanine; many of these compounds are seen in the chromatograms. Table 3- 6 shows the relative reduction in XIC peak area of several compounds caused by the use of the respirator or PVC tubing.

Table 3- 6: Reduction in peak area for several ingredients of nail polish detected in human breath obtained with respirator or PVC tubing. Peak areas were calculated by integration of the XIC for each compound, and are displayed relative to the XIC peak area value obtained without modifying the inhaled air source.

		Peak Area Reduction (%)	
Compound	**Extracted Ion (m/z)**	**With Respirator**	**With Tubing**
Isopropyl Alcohol	45	90	96
Ethyl Acetate	88	92	94
Diisopropoxy methane	73	89	96
Toluene	91	94	98
Mesityl oxide	83	94	99
Butyl acetate	56	92	98
Diacetone alcohol	43	96	94
Camphor (1)	152	95	100
Camphor (2)	152	97	99

There is a trend that compounds with a higher vapor pressure are less effectively removed from the intake air by the respirator (e.g. VP of isopropyl alcohol = 30.75 torr; VP of

camphor = 0.15 torr)[157, 158]. The large reductions in peak area (> 90%) demonstrate the advantages of controlling the inhaled air of a subject. Two additional subjects repeated the experiment using a respirator with similar results (peak area reduction RSD 0-17%).

3-16-5: Lemonade Inhalation with Respirator Cartridge

Figure 3- 12 shows the extracted ion chromatograms (m/z 93) of breath samples obtained from a single subject inhaling directly above a glass containing approximately 125 mL of room temperature lemonade, which contains many flavor and aroma compounds. Breath samples were obtained with and without the use of a respirator to cleanse the inhaled air.

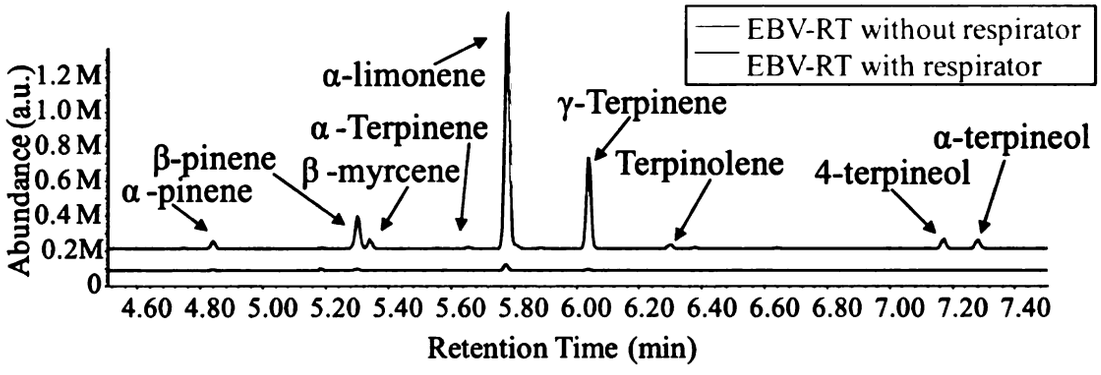

Figure 3- 12: Extracted ion chromatograms (XIC m/z 93) of breath samples from a single subject (EBV-RT). One sample was collected over 4 oz. of lemonade with no modification to the inhaled air (red trace, top) and another sample was collected over 4 oz. of lemonade using a respirator (blue trace, bottom). Peaks labeled are identified as monoterpenes and monoterpene alcohols, flavor ingredients present in lemonade. (Image originally in color)

A large reduction in peak area is seen for all compounds present. The peak area percent reduction relative to the sample without the respirator is shown in Table 3- 7. These data

show the effectiveness of the respirator for removing naturally-derived compounds, such as monoterpenes, from the inhaled air.

Table 3- 7: Reduction in peak area for the monoterpenes detected in EBV-RT samples obtained over lemonade. Peak areas were calculated by integration of the XIC for each compound, and are displayed relative to the peak area value obtained without modifying the inhaled air source.

Compound	**Peak Area Reduction (%) With Respirator**	**Compound**	**Peak Area Reduction (%) With Respirator**
α-pinene	82	3-carene	91
β-pinene	93	γ-terpinene	98
β-myrcene	95	Terpinolene	98
α-terpinene	96	4-terpineol	100
α-limonene	97	α-terpineol	99

3-16-6: Gasoline Inhalation with Respirator Cartridge and Synthetic Lung Substitute Development

Tests were then performed to determine the efficiency of the respirator-modified RTube™ when obtaining breath samples in a very dirty environment. Automobile-grade gasoline was used to simulate dirty sampling conditions. To prevent unnecessary exposure to harmful chemicals a human subject was not used to collect these data; a polyethylene synthetic lung substitute was developed to simulate human respiration. The synthetic lung substitute was fabricated to approximate adult tidal volume (500 mL)[159] and was pumped to simulate the inhalation and exhalation of a normal adult respiratory pattern over the gasoline and through an RTube™.

Figure 3- 13 shows a portion of the total ion chromatogram of this synthetic breath sample obtained using the synthetic lung substitute at a constant and steady respiration rate. Many peaks are present in this chromatogram – numerous compounds have been tentatively identified in Table 3- 8.

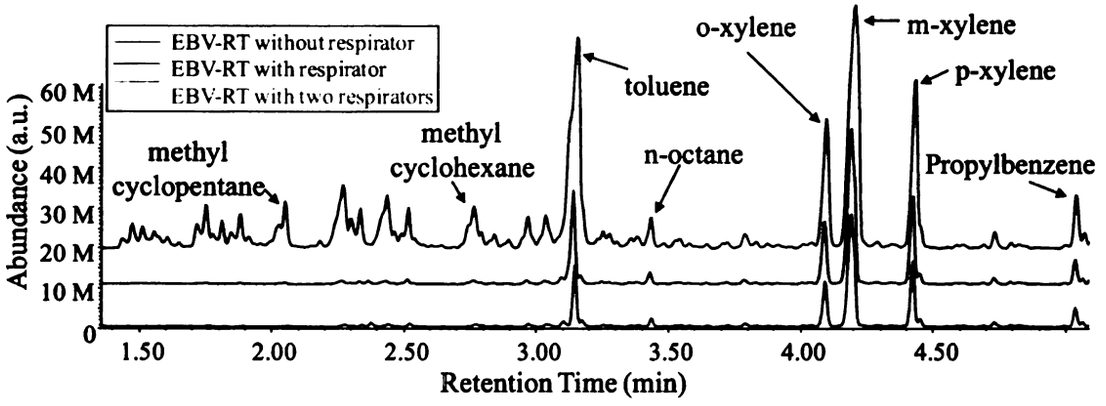

Figure 3- 13: Total ion current chromatograms of 'breath' samples obtained using a synthetic lung substitute over gasoline (EBV-RT). One sample was collected with no modification to the inhaled air (red trace, top), a second sample was collected using a single respirator (blue trace, middle), and a final sample was collected using two respirators in series (green trace, bottom) Chromatograms are offset for clarity. ***(Image originally in color)***

Additional synthetic breath samples were obtained by attaching a single respirator cartridge to the intake valve of the RTube™ and repeating the synthetic lung substitute's respiration over gasoline, as well as attaching two respirator cartridges in series by removing the particulate filter from one cartridge in order to attach the second. These chromatograms are also shown in Figure 3- 13. The percent reduction in peak area of the compounds detected in the sample obtained with one respirator cartridge versus no respirator cartridge is shown in Table 3- 8. The peak area was reduced by 56-98% when a single respirator is used, specifically with a greater decrease in peak area for smaller

molecular weight compounds. With the addition of the second respirator cartridge, additional reductions in peak areas were determined versus the sample obtained with one respirator cartridge (Table 3- 8).

Table 3- 8: Reduction in peak area for the tentatively identified compounds detected in EBV-RT samples generated with a synthetic lung substitute respirated over gasoline. Peak areas were calculated by integration of the TIC for each compound, and are displayed relative to the peak area value obtained without modifying the inhaled air source. The additional peak area reduction demonstrated by the use of two respirators was calculated compared to those values when using one respirator to demonstrate the additional benefit of the respirator series.

RT	Compound	Area Reduction (%) One Respirator	Additional Area Reduction (%) Two vs. One Respirator
1.44	Ethanol	93	86
1.48	Unidentified compound	97	82
1.51	2-methylbutane	97	102
1.56	Pentane	96	82
1.61	2-methyl-2-butene	94	94
1.65	2,2-dimethylbutane	91	95
1.72	2-methylpentane	97	59
1.75	2,3-dimethylbutane	97	60
1.77	Unidentified alkane	98	100
1.81	3-methylpentane	98	59
1.85	2,2-dimethylheptane	98	34
1.88	Hexane	97	52
1.91	2,3-dimethyl-2-butene	97	68
2.03	2-cyclopropylpropane	98	22
2.05	Methylcyclopentane	97	70
2.18	1-methylcyclopentene	96	49
2.27	Unidentified alkane	96	42
2.30	2,3-dimethylpentane	96	70
2.34	3-methylhexane	87	81
2.44	2,2,3,3-tetramethylbutane	95	68
2.52	Heptane	90	61
2.76	Methylcyclohexane	92	50
2.78	3-methylheptane	91	109
2.84	Ethylcyclopentane	93	69
2.90	1,2,4-Trimethylcyclopentane	92	77
2.97	2,3,4-Trimethylpentane	91	68
3.04	2,3,3-Trimethylpentane	90	68

Table 3-8 (cont'd).

3.15	Toluene	77	60
3.25	3,5,5-trimethyl-1-hexene	86	64
3.28	1,3-dimethylcyclohexane	87	75
3.36	1-ethyl-3-methylcyclopentane	83	56
3.38	(2,2-Dimethyl propylidene)cyclopropane	81	72
3.43	n-octane	68	66
3.79	2,5-dimethylheptane	71	71
4.10	o-xylene	61	66
4.29	m-xylene	68	79
4.43	p-xylene	58	70
4.73	Isopropylbenzene	64	75
5.04	Propylbenzene	59	74
5.07	4-methylnonane	56	59

Depending on the concentration of contaminants in the ambient air, the respirator is useful in reducing the amount of carryover of the contamination into a breath sample, and more than one can be used in extremely dirty environments. While not a perfect solution to entirely eliminating background components from a breath sample, this method allows for fast and facile sampling and analysis, with no power (freezer) requirements.

3-17: Conclusions

The data from this study demonstrate that real-time sampling of EBV is an effective and advantageous method for breath analysis. As an active sampling method, collection is fast; because sampling and preconcentration occur concurrently, the overall collection and analysis time of a breath sample is reduced ~30% compared to EBC collection. Sampling and SPME exposure time were optimized to yield the highest signal from the GC-MS. Comparisons were made between the traditional EBC collection at -80°C, EBV

collection at -80°C, and EBV collection at room temperature. This study has shown that EBV is more sensitive than EBC, yielding 23% more compounds than traditionally collected EBC, as well as up to a 10-fold increase in peak area for many compounds. This modification is simple and thus maintains the disposable and inexpensive nature of the RTube™. The sampling technique is field portable as it requires minimal user training and has zero power requirements or need for a frozen condenser. Also demonstrated herein was the need to control the quality and cleanliness of inhaled air when collecting a breath sample in a dirty environment. The use of PVC tubing or a respirator cartridge was established as a simple and effective method of providing inhaled air yielding breath samples with 89-100% reduction in peak area for compounds inhaled from nail polish, and 82-100% reduction in peak are for terpenes inhaled from lemonade. The use of multiple respirator cartridges was also demonstrated, showing an additional reduction in peak area of 22-109% when a simulated breath sample was obtained over gasoline. Caution must be paid to the localized situational environment created at a subject's point of inhalation; compounds may be inadvertently inhaled at concentrations greater than that in the general ambient air causing error in alveolar gradient calculations. Collection and analysis of EBV using the methods described in this study will provide valuable information for future breath analysis.

3-18: References

(1) *Breath Analysis for Biomedicine and National Security Sensor Design Issues and Strategies for Biomarker Discovery*, Davis, CA **2008**.

(2) *DARPA Workshop: Breath Signatures*, Livermore, CA **2008**.

(3) Stix, G. *Sci. Am.* **2003**, *289*.

(4) Phillips, M. *Sci. Am.* **1992**, *267*, 74-79.

(5) Bogen, E. *California and Western Medicine* **1927**, *26*, 778-783.

(6) Pauling, L.; Robinson, A. B.; Teranish.R; Cary, P. *Proc. Natl. Acad. Sci. U. S. A.* **1971**, *68*, 2374-&.

(7) Phillips, M.; Herrera, J.; Krishnan, S.; Zain, M.; Greenberg, J.; Cataneo, R. N. *J. Chromatogr. B* **1999**, *729*, 75-88.

(8) Mukhopadhyay, R. *Anal. Chem.* **2004**, *76*, 273A-276A.

(9) Namjou, K.; Roller, C. B.; McCann, P. J. *IEEE Circuits & Devices Magazine* **2006**, *22*, 22-28.

(10) Hunt, J. F.; Fang, K.; Malik, R.; Snyder, A.; Malhotra, N.; Platts-Mills, T. A. E.; Gaston, B. *Am. J. Respir. Crit. Care Med.* **2000**, *161*, 694-499.

(11) Corradi, M.; Folesani, G.; Andreoli, R.; Manini, P.; Bodini, A.; Piacentini, G.; Carraro, S.; Zanconato, S.; Baraldi, E. *Am. J. Respir. Crit. Care Med.* **2003**, *167*, 395-399.

(12) Wood, L. G.; Gibson, P. G.; Garg, M. L. *Eur. Respir. J.* **2003**, *21*, 177-186.

(13) Corradi, M.; Rubinstein, I.; Andreoli, R.; Manini, P.; Caglieri, A.; Poli, D.; Alinovi, R.; Mutti, A. *Am. J. Respir. Crit. Care Med.* **2003**, *167*, 1380-1386.

(14) Gonzalez-Reche, L. M.; Kucharczyk, A.; Musiol, A. K.; Kraus, T. *Rapid Commun. Mass Spectrom.* **2006**, *20*, 2747-2752.

(15) Phillips, M.; Cataneo, R. N.; Ditkoff, B. A.; Fisher, P.; Greenberg, J.; Gunawardena, R.; Kwon, C. S.; Tietje, O.; Wong, C. *Breast Cancer Res. Treat.* **2006**, *99*, 19-21.

(16) Phillips, M.; Cataneo, R. N.; Ditkoff, B. A.; Fisher, P.; Greenberg, J.; Gunawardena, R.; Kwon, C. S.; Rahbari-Oskoui, F.; Wong, C. *The Breast Journal* **2003**, *9*, 184-191.

(17) Phillips, M.; Cataneo, R. N.; Greenberg, J.; Gunawardena, R.; Naidu, A.; Rahbari-Oskoui, F. *J. Lab. Clin. Med.* **2000**, *136*, 243-249.

(18) Phillips, M.; Altorki, N.; Austin, J. H. M.; Cameron, R. B.; Cataneo, R. N.; Greenberg, J.; Kloss, R.; Maxfield, R. A.; Munawar, M. I.; Pass, H. I.; Rashid, A.; Rom, W. N.; Schmitt, P. *Cancer Biomarkers* **2007**, *3*, 95-109.

(19) Phillips, M.; Cataneo, R. N.; Cummin, A. R. C.; Gagliardi, A. J.; Gleeson, K.; Greenberg, J.; Maxfield, R. A.; Rom, W. N. *Chest* **2003**, *123*, 2115-2123.

(20) Gordon, S. M.; Szidon, J. P.; Krotoszynski, B. K.; Gibbons, R. D.; Oneill, H. J. *Clin. Chem.* **1985**, *31*, 1278-1282.

(21) Phillips, M.; Gleeson, K.; Hughes, J. M. B.; Greenberg, J.; Cataneo, R. N.; Baker, L.; McVay, W. P. *The Lancet* **1999**, *353*, 1930-1933.

(22) Oneill, H. J.; Gordon, S. M.; Oneill, M. H.; Gibbons, R. D.; Szidon, J. P. *Clin. Chem.* **1988**, *34*, 1613-1618.

(23) Poli, D.; Carbognani, P.; Corradi, M.; Goldoni, M.; Acampa, O.; Balbi, B.; Bianchi, L.; Rusca, M.; Mutti, A. *Respiratory Research* **2005**, *6*.

(24) Di Natale, C.; Macagnano, A.; Martinelli, E.; Paolesse, R.; D'Arcangelo, G.; Roscioni, C.; Finazzi-Agro, A.; D'Amico, A. *Biosens. Bioelectron.* **2003**, *18*, 1209-1218.

(25) Phillips, M.; Cataneo, R. N.; Condos, R.; Erickson, G. A. R.; Greenberg, J.; La Bombardi, V.; Munawar, M. I.; Tietje, O. *Tuberculosis* **2007**, *87*, 44-52.

(26) Ruzsanyi, V.; Baumbach, J. I.; Sielemann, S.; Litterst, P.; Westhoff, M.; Freitag, L. *J. Chromatogr. A* **2005**, *1084*, 145-151.

(27) Phillips, M.; Boehmer, J. P.; Cataneo, R. N.; Cheema, T.; Eisen, H. J.; Fallon, J. T.; Fisher, P. E.; Gass, A.; Greenberg, J.; Kobashigawa, J.; Mancini, D.; Rayburn, B.; Zucker, M. J. *Am. J. Cardiol.* **2004**, *94*, 1593-1594.

(28) Phillips, M.; Boehmer, J. P.; Cataneo, R. N.; Cheema, T.; Eisen, H. J.; Fallon, J. T.; Fisher, P. E.; Gass, A.; Greenberg, J.; Kobashigawa, J.; Mancini, D.; Rayburn, B.; Zucker, M. J. *J. Heart Lung Transplant.* **2004**, *23*, 701-708.

(29) Sobotka, P. A.; Gupta, D. K.; Lansky, D. M.; Costanzo, M. R.; Zarling, E. J. *J. Heart Lung Transplant.* **1994**, *13*, 224-229.

(30) Deng, C.; Zhang, J.; Yu, X.; Zhang, W.; Zhang, X. *J. Chromatogr. B* **2004**, *810*, 269-275.

(31) Phillips, M.; Cataneo, R. N.; Cheema, T.; Greenberg, J. *Clin. Chim. Acta* **2004**, *344*, 189-194.

(32) *Exhaled Breath Condensate*; Respiratory Research, Inc.: Charlottesville, VA, **2005**.

(33) Amorim, L. C. A.; Cardeal, Z. d. L. *J. Chromatogr. B* **2007**, *853*, 1-9.

(34) Chinery, R. L.; Gleason, A. K., **1993**; Vol. 13, pp 51-62.

(35) Giardino, N. J.; Gordon, S. M.; Brinkman, M. C.; Callahan, P. J.; Kenny, D. V. *Epidemiology* **1999**, *10*, S72-S72.

(36) Lindstrom, A. B.; Pleil, J. D. *J. Air Waste Manage. Assoc.* **1996**, *46*, 676-682.

(37) Lindstrom, A. B.; Pleil, J. D.; Berkoff, D. C. *Environ. Health Perspect.* **1997**, *105*, 636-642.

(38) Maniscalco, M.; De Laurentiis, G.; Pentella, C.; Mormile, M.; Sanduzzi, A.; Carratu, P.; Sofia, M. *Biomarkers* **2006**, *11*, 233-240.

(39) Raymer, J. H.; Pellizzari, E. D.; Thomas, K. W.; Cooper, S. D. *J. Expo. Anal. Environ. Epidemiol.* **1991**, *1*, 439-451.

(40) Wallace, L. A. *Annual Review of Energy and the Environment* **2001**, *26*, 269-301.

(41) Wallace, L. *Environ. Health Perspect.* **1996**, *104*, 1129-1136.

(42) Wallace, L.; Pellizzari, E.; Gordon, S. *J. Expo. Anal. Environ. Epidemiol.* **1993**, *3*, 75-102.

(43) Giardina, M.; Olesik, S. V. *Anal. Chem.* **2003**, *75*, 1604-1614.

(44) Giardina, M.; Olesik, S. V. *Anal. Chem.* **2003**, *75*, 1604-1614.

(45) Pleil, J. D.; Lindstrom, A. B. *Journal of Chromatography B-Biomedical Applications* **1995**, *665*, 271-279.

(46) Pleil, J. D.; Fisher, J. W.; Lindstrom, A. B. *Environ. Health Perspect.* **1998**, *106*, 573-580.

(47) Pleil, J. D.; Smith, L. B.; Zelnick, S. D. *Environ. Health Perspect.* **2000**, *108*, 183-192.

(48) Wallace, L. A.; Nelson, W. C.; Pellizzari, E. D.; Raymer, J. H. *J. Expo. Anal. Environ. Epidemiol.* **1997**, *7*, 141-163.

(49) "Exhaled Breath Condensate and Other Markers in Exhaled Air" In *Pediatric Pulmonary Function Testing*; Eber, H. J., Ed.; Karger, **2005**; Vol. 33, pp 190-202.

(50) Schneideler, l.; Manke, H. G.; Schwulera, U.; Imacker, P.; Hammerle, H. *Am. Rev. Respir. Dis.* **1993**, *148*, 778-784.

(51) Chen, H. W.; Wortmann, A.; Zhang, W. H.; Zenobi, R. *Angewandte Chemie-International Edition* **2007**, *46*, 580-583.

(52) Cunningham, S.; McColm, J. R.; Ho, L. P.; Greening, A. P.; Marshall, T. G. *Eur. Respir. J.* **2000**, *15*, 955-957.

(53) Soyer, O. U.; Dizdar, E. A.; Keskin, O.; Lilly, C.; Kalayci, O. *Allergy* **2006**, *61*, 1016-1018.

(54) Reinhold, P.; Jaeger, J.; Schroeder, C. *Biomarkers* **2006**, *11*, 118-142.

(55) Vass, G.; Huszar, E.; Barat, E.; Valyon, M.; Kiss, D.; Penzes, L.; Augusztinovicz, M.; Horvath, I. *Am. J. Respir. Crit. Care Med.* **2003**, *167*, 850-855.

(56) Skeldon, K. D.; Patterson, C.; Wyse, C. A.; Gibson, G. M.; Padgett, M. J.; Longbottom, C.; McMillan, L. C. *J. Opt. A* **2005**, *7*, S376-S384.

(57) Lord, H.; Yu, Y. F.; Segal, A.; Pawliszyn, J. *Anal. Chem.* **2002**, *74*, 5650-5657.

(58) Ma, W.; Liu, X. Y.; Pawliszyn, J. *Anal. Biochem.* **2006**, *385*, 1398-1408.

(59) Yu, H.; Xu, L.; Wang, P. *J. Chromatogr. B* **2005**, *826*, 69-74.

(60) Lawson, L. D.; Wang, Z. J. *J. Agric. Food Chem.* **2005**, *53*, 1974-1983.

(61) Carpenter, C. T.; Price, P. V.; Christman, B. W. *Chest* **1998**, *114*.

(62) Phillips, M. *Anal. Biochem.* **1997**, *247*, 272-278.

(63) Phillips, M.; Cataneo, R. N.; Greenberg, J.; Grodman, R.; Gunawardena, R.; Naidu, A. *Eur. Respir. J.* **2003**, *21*, 48-51.

(64) Phillips, M.; Greenberg, J.; Cataneo, R. N. *Free Radic. Res.* **2000**, *33*, 57-63.

(65) Raymer, J. H.; Pellizzari, E. D.; Thomas, K. W.; Kizakevich, P.; Cooper, S. D. *J. Expo. Anal. Environ. Epidemiol.* **1992**, *2*, 67-83.

(66) Statheropoulos, M.; Agapiou, A.; Georgiadou, A. *J. Chromatogr. B* **2006**, *832*, 274-279.

(67) Wallace, L. A.; Pellizzari, E. D. *Environ. Health Perspect.* **1995**, *103*, 95-98.

(68) *NIOX Flex: Technical Specification*; Aerocrine AB: Solna, Sweden.

(69) Ohira, S. I.; Li, J. H.; Lonneman, W. A.; Dasgupta, P. K.; Toda, K. *Anal. Chem.* **2007**, *79*, 2641-2649.

(70) Walsh, J. *Spectroscopy* **2004**, *19*, 49-50.

(71) Frishman, G.; Tzanani, N.; Amirav, A. *Field Anal. Chem. Tech.* **2001**, *5*, 107-115.

(72) Libardoni, M.; Stevens, P. T.; Waite, J. H.; Sacks, R. *J. Chromatogr. B* **2006**, *842*, 13-21.

(73) Raymer, J. H.; Thomas, K. W.; Cooper, S. D.; Whitaker, D. A.; Pellizzari, E. D. *J. Anal. Toxicol.* **1990**, *14*, 337-344.

(74) Gordin, A.; Amirav, A. *J. Chromatogr. A* **2000**, *903*, 155-172.

(75) Sanchez, J. M.; Sacks, R. D. *Anal. Chem.* **2003**, *75*, 2231-2236.

(76) Sanchez, J. M.; Sacks, R. D. *Anal. Chem.* **2006**, *78*, 3046-3054.

(77) Menssana Research, Inc.:Breathtaking Technology,

(78) Berlardi, R.; Pawliszyn, J. *Water Pollution Research Journal of Canada* **1989**, *24*, 179-191.

(79) Zhang, Z.; Pawliszyn, J. *Anal. Chem.* **1993**, *65*, 1843-1852.

(80) Louch, D.; Mothlagh, S.; Pawliszyn, J. *Anal. Chem.* **1992**, *64*, 1187-1199.

(81) Grote, C.; Pawliszyn, J. *Anal. Chem.* **1997**, *69*, 587-596.

(82) Phillips, M.; Greenberg, J. *Clin. Chem.* **1992**, *38*, 60-65.

(83) Wallace, L.; Buckley, T.; Pellizzari, E.; Gordon, S. *Environ. Health Perspect.* **1996**, *104*, 861-869.

(84) Effros, R. M.; Biller, J.; Foss, B.; Hoagland, K.; Dunning, M. B.; Castillo, D.; Bosbous, M.; Sun, F.; Shaker, R. *Am. J. Respir. Crit. Care Med.* **2003**, *168*, 1500-1505.

(85) Wanner, A.; Mendes, E. S.; Atkins, N. D. *J. Appl. Physiol.* **2006**, *100*, 1674-1678.

(86) Muhlberger, F.; Streibel, T.; Wieser, J.; Ulrich, A.; Zimmermann, R. *Anal. Chem.* **2005**, *77*, 7408-7414.

(87) "An Improved Method for the Biological Monitoring of Volatile Compounds" In *Environmental Health in Central and Eastern Europe*; Donnelly, K. C., Cizmas, L. H., Eds.; Springer: Dordrecht, The Netherlands, **2006**, pp 65-71.

(88) Phillips, M.; Greenberg, J.; Awad, J. *J. Clin. Pathol.* **1994**, *47*, 1052-1053.

(89) Phillips, M.; Greenberg, J.; Sabas, M. *Free Radic. Res.* **1994**, *20*, 333-337.

(90) De Hoffman, E.; Charette, J.; Stroobant, V. *Mass Spectrometry: Principles and Applications*; John Wiley & Sons: New York, **1996**.

(91) James, A. T.; Martin, A. J. P. *Biochem. J.* **1952**, *50*, 679-690.

(92) Martin, A. J. P.; Synge, R. L. M. *Biochem. J.* **1941**, *35*, 1358-1368.

(93) Merrick, W., Massachusetts Institute of Technology, Cambridge, MA, **2004**.

(94) Oser, H.; SRI International: Davis, CA, **2008**.

(95) Hyspler, R.; Crhová, S.; Gasparic, J.; Zadák, Z.; Cízková, M.; Balasová, V. *Journal of Chromatography B: Biomedical Sciences and Applications* **2000**, *739*, 183-190.

(96) Ahluwalia, V. K.; Parashar, R. K. *Organic Reaction Mechanisms*, 2nd ed.; Alpha Science International Ltd.: Harrow, U.K., **2005**.

(97) *Knovel Critical Tables*; Knovel, **2003**.

(98) Wickstrom, E. **1988**; INCHEM.

(99) Palsson, B. P.; Hubbell, J. A.; Plonsey, R.; Bronzino, J. D. *Tissue Engineering*; CRC Press: San Diego, CA, **2003**.

CHAPTER 4: Measuring Chemical Exposure using Breath Analysis

4-1: Motivations and Introduction

Human exposure to environmental chemicals is a reality; the presence of chemicals in the work place, in food, and in association with common human activities, such as visiting a gas station, or using moth balls for clothing storage, puts all humans in contact with many chemicals. While exposure to some of these chemicals may be harmless, some compounds elicit toxicity in individuals exposed to high doses. Rapid assessment and monitoring of chemical exposure is important in order to diagnose the exposure and select the appropriate medical treatment to minimize its physiological effects. The ideal technique would provide instantaneous identification of the chemical in question, provide information on its concentration within the subject, monitor the rise and fall of this concentration, provide information about the route of exposure, and monitor the subject to ensure no further exposure is occurring. If the chemical of interest is toxic, this information can be used to determine the appropriate treatment plan for the subject; if the chemical is non-toxic, it is still useful to monitor its uptake and elimination in the body in order to learn about metabolic and excretion processes. If the substance is a chemical of interest for forensic and homeland security applications, the presence of the chemical documents that exposure has occurred. However, it would also be useful to gain some information about the time and extent of exposure. Detection of chemicals unique to a particular environment may also provide information on the prior location of an individual and could be used to place a subject at a particular location for forensic purposes.

This chapter will describe several studies designed to test the abilities of breath analysis for use as a means to detect chemical exposure. This chemical exposure is targeted in an effort to document occupational exposure, determine the chemical signature of unique locations, or determine the prior location or activity of an individual. These experiments will demonstrate that breath analysis is an effective technique for all of these purposes, and the implications of sensitive analysis of breath constituents will also be discussed in regards to a field study for the detection of industrial chemicals.

4-2: Background

Regardless of the exposure route (e.g. dermal, inhalation, oral), breath analysis provides an alternative method of monitoring exposure of humans to chemicals. The non-invasive nature of breath sampling allows a greater number of samples to be collected from a subject owing to the higher tolerance of subjects to the collection method compared to subject willingness to provide blood samples, which is commonly painful. Another advantage of breath collection is that the biological waste is limited. Research at the US Environmental Protection Agency (EPA) has shown that exhaled breath can be an accurate surrogate for blood analysis when monitoring chemical exposure to trichloroethene.[1] Exhaled breath comes from the lungs, where the inspired air diffuses through tissues and into the blood. Chemicals in the blood strive for equilibrium between the alveolar air and the capillaries in the lung, passing through the pulmonary alveolar membrane in order to achieve this. Therefore, volatile compounds that are in circulation in the bloodstream can be detected by sampling exhaled breath.

Breath analysis has been extensively reported in the literature for medical applications, but additional studies focused on the exogenous compounds in breath – specifically those due to a chemical exposure,[2-9] have been reviewed by Wallace.[10] Many studies of chemical exposure focus on the dermal and inhalation routes of exposure. Raymer *et al.* studied the effect of inhalation exposure in several microenvironments, including common work places including a woodworking shop; 21 VOCs were monitored and their elimination from the body was described by a two-compartment model of the body.[11] Work at the US EPA has focused on methods development for monitoring inhalation exposures in several microenvironments in part through the Total Exposure Assessment Methodology (TEAM) program[12, 13] and in part through controlled exposures.[12-17] The TEAM program developed breath sampling methods to analyze the VOCs in human breath of subjects in various cities in the United States, testing levels of VOCs in their normal environments as well as after exposure in several environments or to several household products, and again fit the acquired data of elimination using a two-compartment model of the body.[13] Dermal exposure was also probed in these studies, for example, comparisons were made between the levels of chloroform in breath samples collected while the subjects showered with and without rubber suits, isolating inhalation exposure versus inhalation and dermal exposure, where the levels detected were twice that detected while the rubber suits were worn.[12] Several studies have also researched trihalomethane exposure from sources such as chlorinated water in showers or swimming pools and modeled the uptake and decay of such compounds with a 3-compartment model.[1, 6, 18, 19] These studies provided insight into the VOCs detected in breath, common environmental sources of exposure, as well as common routes of exposure.

4-2-1: Industrial/Commercial Exposure

One example of industrial chemical exposure occurs in the nail salon. Nail salons are poorly regulated, and safety procedures are recommended, but not enforced, and there is a general lack of concern of chemical exposure by salon technicians.[20] Chemical exposure in the nail salon can occur from the nail polish, nail polish remover, acrylic nails and other sources. Workers in the salon may wear a mask, but generally not one that would seal against the face and prevent inhalation exposure. During the application of acrylic nails, ethyl methacrylate and silica exposure can be high for the technicians, whose breathing zone is 6-12 in from the fingernails. The filing and sanding of such nails can produce much dust containing acrylic monomers, fiberglass, and silica. Exposure to such chemicals has been shown to cause asthma, contact dermatitis, and even silicosis.[21, 22] A study by the Illinois Department of Public Health assessed exposures of several nail technicians in salons throughout Illinois. In this study, none of the subjects exceeded the National Institute for Occupational Safety and Health (NIOSH) Recommended Exposure Limits (REL) or the Occupational Safety and Health Administration (OSHA) Permissible Exposure Limits (PEL) for respirable silica dust exposures,[23] but the proximity of the technician to the chemicals as well as an intense smell of ethyl methacrylate was noted.

The EPA has also issued comments about the health and chemical exposures of nail salon technicians. They identify acetone, benzoyl peroxide, butyl acetate, butyl methacrylate, camphor, dibutyl phthalate, ethyl acetate, ethyl cyanoacrylate, ethyl methacrylate, formalin, hydroquinone, isobutyl methacrylate, methacrylic acid, 4-methoxyphenol, methyl ethyl ketone, methyl methacrylate, poly (ethyl/methyl methacrylate), titanium

dioxide, toluene, and tosylamide formaldehyde resin as common ingredients in nail care products.[24] Exposure may occur through inhalation or absorption via the skin and fingernails, and may cause medical trouble including asthma, cancer, lung fibrosis, or shortness of breath. Monitoring exposure to such chemicals would provide valuable information about the risks posed to the health of the subject, as well as the amount of time spent in a particular location.

Other industrial and commercial locations also pose the risk of dangerous chemical exposure. Manufacturing plants and well as retailers of chemicals may present high levels of solvents in vapor or liquid form. These locations are regulated by OSHA and NIOSH, but chemical signatures unique to these locations may be present and may provide information on the prior location of an individual if detected on breath.

4-2-2: Exposure via Ingestion – Terpenes and Terpenoid Compounds

Terpenoid compounds are natural organic compounds, which are derived from several isoprene building blocks, $(C_5H_8)_n$. Terpenoids and terpenes are present in many natural products, including fruit oils, flowers, and turpentine. Several studies have described the elimination of monoterpenes from the human body after exposure to these compounds. Levin *et al.* showed that 8% of inhaled α-pinene was eliminated unmetabolized in exhaled breath, with less than 0.001% excreted via the kidneys, thus leaving the majority of inhaled α-pinene stored in the body or excreted as a metabolite.[25] Falk-Fillipson reported that the respiratory clearance of 3-carene was significantly higher when the subject was exposed to the pure monoterpene, rather than a mixture of monoterpenes in turpentine.[26] The decay of three monoterpenes in blood was also fit to a 3-compartment

model.[26] Such a model describes how the organs and processes of the body are simplified; a 1-compartment model assumes that a substance is uniformly distributed throughout the body via the same kinetic processes. A 2-compartment model assumes that the organs with highest blood flow form the central compartment and have uniform rapid distribution of a substance, then the rest of the body forms the peripheral compartment which experiences a slower rate of distribution. Likewise, a 3-compartment model assume that the central compartment distributes into two compartments with slower, and different, kinetics.[27] Wallace *et al.* fit the decay of signal in exhaled breath after inhalation exposure to α-limonene to a 3-compartment model, but were unable to gather information on the first compartment decay due to its short half-life.[14] Few studies have described the pharmacokinetics of monoterpenes and terpenoid compounds after oral ingestion, especially after consumption of a mixture of compounds. When orally dosed, first-pass metabolism in the liver affects the amount of unmetabolized compound present in the bloodstream.[27] Chen *et al.* orally dosed rates with α-limonene, fitting the resulting decay curve in blood to a biexponential model.[28] It has been reported that although the monoterpenes are metabolized in the body, these metabolites were detected only in the urine and only the original monoterpenes were detected in the blood.[29]

4-2-3: Research Directions

Due to the ubiquitous nature of VOCs in several environments, detection of these VOCs in the breath of a subject may provide insight into their prior location or activities. Although visiting a nail salon or hardware store is not an activity of forensic interest, these systems may be used as surrogates for exposure to VOCs in more illicit

environments, or to more toxic VOCs. The accessible nature of these environments makes them ideal to study the presence and elimination of such VOCs in the breath of a subject. The results from these studies can then be used to predict the uptake and elimination of other VOCs of interest in the breath of subjects that have been exposed. Similarly, while the detection of terpenes in breath is not indicative of any criminal activity, these compounds are easily accessible and provide further insight into the uptake and elimination of VOCs in breath. As presented below, the detection of terpenes in breath allows many data points to be acquired during the elimination of the compounds from the body, allowing greater information on the half-lives and elimination processes of these chemicals in breath to be elucidated.

4-3: Materials and Methods

4-3-1: Materials

D-Camphor was obtained from J.T. Baker, Inc. (Phillipsburg, NJ). A 65.3 mM solution was made in a 1:4 (v:v) solution of H_2O:methanol and stored in a glass vial. Hexamine (hexamethylenetetramine) was obtained from Chem Service, Inc. (West Chester, PA). Frozen lemonade concentrate (Safeway/Vons Lemonade, Safeway, Inc., Pleasanton, CA) was purchased from local sources. Original lemonade was mixed according to the manufacturer's instructions. Concentrated lemonade was mixed using half the water required by the manufacturer's instructions. Mediterranean lemonade was made by mixing 10 thinly sliced lemons, 2 cups of sugar, and 5 cups of water. (1S)-(-)-β-pinene (99%) was obtained from Alfa Aesar (Ward Hill, MA) and +/- α-limonene (95%) was

obtained from TCI America, Inc. (Portland, OR). Serial dilutions of both compounds were made using deionized water.

4-3-2: Methods

The RTube™ (Respiratory Research, Inc., Charlottesville, VA), was used to collect all breath samples. The subject inhales via a mouthpiece through a one-way valve that prevents salivary contamination of the EBC or EBV sample. The subject then exhales through the same mouthpiece via a second one-way valve at the base of a polypropylene tube which serves as the EBC or EBV collection media. The polypropylene tube is used at room temperature (EBV) or cooled by a previously frozen (-80 C) aluminum sleeve (EBC). The subject breathes at a normal tidal volume and frequency though the RTube™. Subjects in the environmental exposure study held their nose during collection.

When EBC is collected, 0.5 mL of EBC was aliquoted into a disposable polypropylene microcentrifuge tube (Fisher Scientific, Pittsburgh, PA). A previously thermally conditioned SPME fiber (65 μm PDMS/DVB Stableflex fiber, Sigma-Aldrich, St. Louis, MO), was inserted directly into this aliquot of EBC for 10 minutes, followed by injection into the GC-MS. When EBV is studied, the breath sample is simultaneously collected and preconcentrated on the SPME fiber, which is then injected into the GC-MS.

An Agilent (Santa Clara, CA) 6890N GC with an Agilent 5973N mass spectrometer (Santa Clara, CA), or a Shimadzu (Pleasanton, CA) QP2010 GC-MS were used for analysis. In both instruments, the Helium carrier gas was held at a flow rate of 1.3 L min^{-1} (99.999%, Praxair, Inc., Danbury, CT). Both instruments were operated using 70 eV

electron ionization, 3.54 scans s^{-1}, operated in scan mode (m/z 40 – 450). ChemStation software was used for data collection and analysis with the Agilent system; GCMS Solutions software was used with the Shimadzu system for data processing. An Agilent J&W DB-5MS column (30 m x 0.25 mm x 0.25 μm, equivalent to 5% phenyl, 95% methylpolysiloxane) was used for all experiments.

Compounds were identified by comparing mass spectra obtained in these experiments with those found in the NIST Mass Spectral Library (RMatch >700, NIST MS Search 2.0, NIST, Gaithersburg, MD) and the literature, as well as comparison of retention time and mass spectra obtained from pure chemicals when available.

4-4: Subjects

Thirteen healthy adults with no known respiratory ailments were recruited for this study. Subjects were asked to report any chemical exposure (none) and gave formal written consent prior to sample collection. The Institutional Review Boards (IRB) at Lawrence Livermore National Laboratory (LLNL) and Michigan State University approved experimental protocols used for this study.

4-5: Nail Salon Study

In order to provide an isolated inhaled air source and prevent contamination from localized chemical exposures (i.e. chemical residues remaining on clothing or skin/fingernails), the RTube™ was modified as follows. Approximately twelve feet of FDA-approved plastic tubing (0.5 in I.D., 0.75 in O.D., VWR, Inc., West Chester, PA)

was attached to the base of the intake valve on the RTube™ using a plastic fitting. This tubing was extended into a different air space (room) than that in which the subject donated a breath sample. The breath sample (EBC) was obtained using the standard procedure with the aluminum sleeve cooled to -80 C, or EBV was obtained using the modified procedure with no aluminum sleeve.

A 10 minute breath sample was obtained from a subject early in the morning. The subject then visited a nail salon; after approximately 45 minutes in the salon, the subject returned to the sampling area and gave additional 10 minute breath samples over a 4 hour period. Figure 4- 1 shows the chromatogram obtained from the breath sample obtained before visiting the salon versus that obtained 12 minutes after leaving the salon (inverted for comparison). The majority of peaks observed in the GC-MS total ion chromatograms are present in both samples, and are attributed to endogenous compounds in the subject's breath; however additional peaks, such as those highlighted by the arrows, are present in the sample obtained after salon exposure. The use of the plastic tubing adapter connected to the RTube™ during breath collection provided inhaled air from a different room. This prevented inadvertent chemical exposure of the subject while obtaining a breath sample, as chemicals from the nail salon may have absorbed onto the clothing of the subject, as well as remained on the fingernails of the subject. Previous data have shown that this approach provides effective prevention of subject inhalation of the local chemical source (substances applied to fingernails).

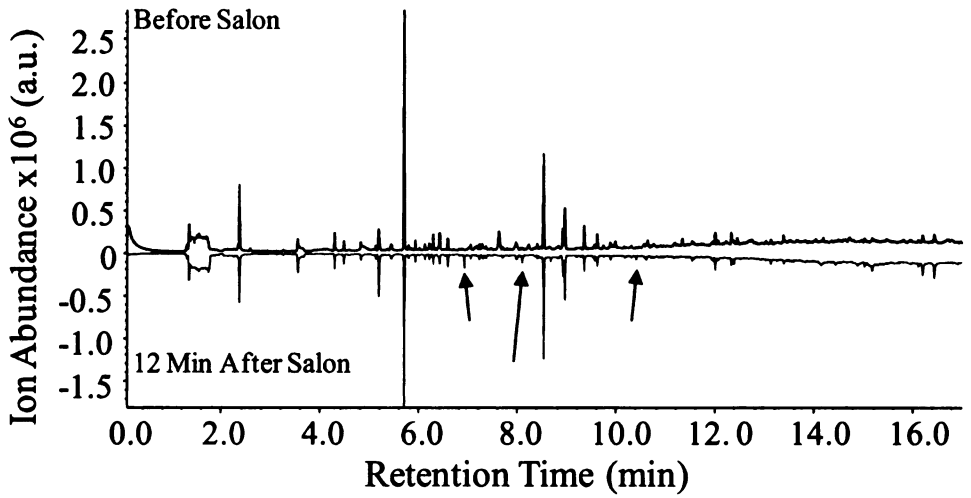

Figure 4- 1: GC-MS total ion chromatograms of sampled breath constituents obtained before salon exposure (top) and 12 minutes after leaving the salon (bottom). The signal obtained after leaving the salon was inverted for clarity. Many peaks endogenous to breath are present in both samples. Additional peaks are present in the sample taken after the subject left the salon, such as those indicated by the arrows. (Image originally in color)

Figure 4- 2 shows a narrow retention time window in the chromatograms generated from breath samples from a human subject collected before visiting the salon, and 12, 50, 99, 152, and 214 minutes after leaving the salon. There is a sharp increase in the total ion chromatogram signal in this region immediately after salon exposure, which decays back to near baseline over several hours. The source of this peak was identified as camphor, a common ingredient in nail polish, and listed as an ingredient in the particular polish used on the subject. Camphor was also identified in a SPME sample obtained from the ambient air in the salon, confirming that the subject's inhaled air contained this compound. The area of the peak due to camphor was calculated using the extracted ion chromatogram (XIC) of m/z 152. The decay of the peak area can be fit to an exponential

(R^2=0.999), as is shown in Figure 4- 2b. The half-life of the decay was calculated to be 23.5 min.

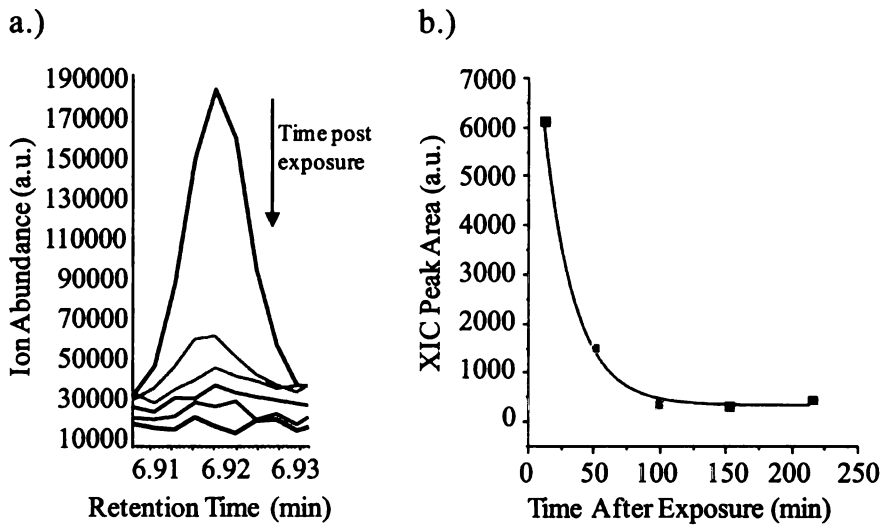

Figure 4- 2: (a) Selected window of GC-MS total ion chromatograms obtained before salon exposure (black), and 12, 50, 99, 152, and 214 minutes after leaving the salon. The source of the peak was identified as a common nail polish ingredient, camphor. Chromatograms are slightly offset for clarity. (b) Exponential decay, R^2= 0.999, of the area of the peak due to camphor, calculated from the XIC (m/z 152) for the molecular ion (chromatogram not shown). (Image originally in color)

The subject made an additional visit to the nail salon, and a polish without camphor as a listed ingredient was applied to the subject's fingernails. Breath samples were obtained using EBV collection with the plastic tubing supplying inhaled air from a separate location than the subject. A single breath sample was obtained from a subject early in the morning. The subject then visited the nail salon; after approximately 45 minutes in the salon, the subject returned to the sampling area and gave additional breath samples over a 5 hour period. Figure 4- 3a shows the retention time window in the XICs for m/z 91

generated from samples obtained before visiting the salon, and 11, 25, 52, 79, 121, 168, 222, 285, and 313 minutes after leaving the salon. There is a sharp increase in signal in this region immediately after salon exposure, which decays back to near baseline over several hours. The source of this peak was identified as toluene, which is also a common ingredient in nail polish and is listed on the polish used on the subject. Toluene was also seen in the sample obtained from the headspace of the salon. The area of this peak was calculated using the XIC for m/z 91. The decay of the peak area was fit to an exponential (R^2=0.960), as is shown in Figure 4- 3b. The half-life of the decay was calculated to be 21.4 min. A small amount of camphor was detected in the sample collected 11 minutes after exposure in the salon. Though it was not a constituent in the polish used, camphor was still present in the air of the salon, so the subject was exposed even when care was taken to use a polish free of camphor.

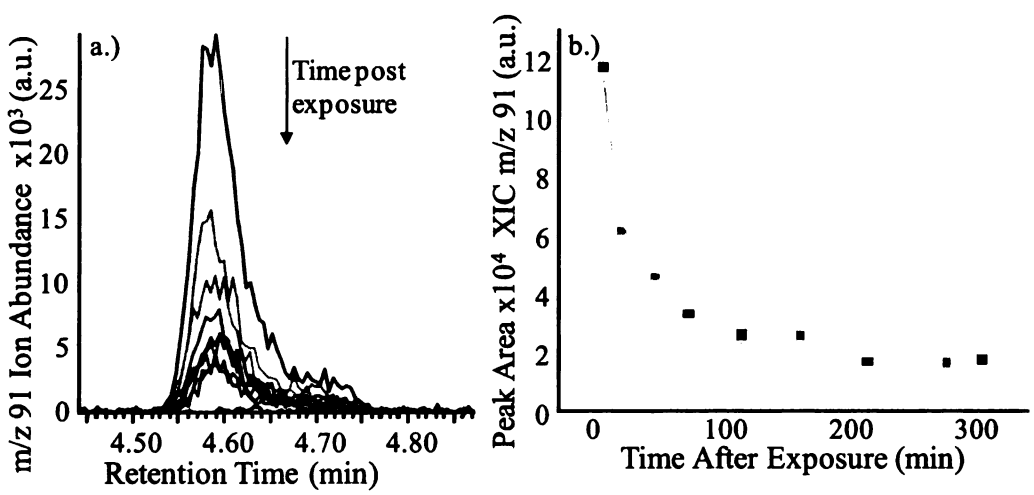

Figure 4- 3: (a) Selected window of GC-MS XIC for m/z 91showing the peak due to toluene in breath before (no peak detected) and, 11, 25, 52, 79, 121, 168, 222, 285, and 313 minutes after salon exposure. (b)Decay of the area of the peak due to toluene fit to an exponential process (R^2=0.960). (Image originally in color)

4-5-1: Headspace Analysis of Manicured Hands

In order to support the hypothesis that the subject was being reexposed to the nail salon chemicals as they outgassed from the nails and hands, studies were performed to determine the composition of the localized headspace surrounding the hands. At 301 minutes after exposure at the nail salon, one hand of the subject was placed in a resealable plastic bag with a SPME fiber for 5 minutes, allowing the VOCs outgassing from the nails and hands to be collected. The resulting TIC is shown in Figure 4- 4.

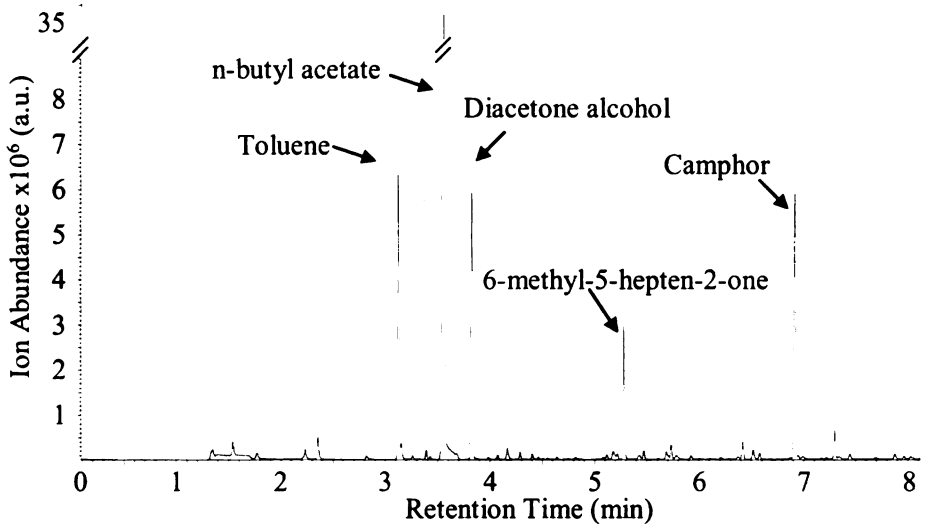

Figure 4- 4: GC-MS total ion chromatogram obtained by exposing a SPME fiber to the manicured hand inside a plastic bag 5 hours, 1 minute after salon exposure. Note that chemicals indicative of the nail polish are still present in the headspace of the nails.

Many chemicals were measured in this sample, including toluene, n-butyl acetate, diacetone alcohol, 6-methyl-5-hepten-2-one, and camphor, common ingredients in nail polish and listed as hazardous ingredients in nail care products by the EPA.[24] That these

chemicals remain in the headspace of the fingernails over 5 hours after exposure in the salon indicates that the products used in nail salons release numerous VOCs to which nail salon workers and clients can be continually exposed, even outside of the salon. Thus, the localized environment from which the inhaled air of a subject giving a breath sample is taken is important to consider in studies such as these.

4-6: Hardware Store Study

The decay in abundance of levels of inhaled volatile chemicals has also been seen post-exposure in hardware store exposures to VOCs. Breath samples (EBC) were obtained from two human subjects before they spent an hour in a local hardware store. After returning to the sampling area, 3 additional breath samples were obtained from each subject over the course of 2 hours. Samples were obtained from subject A at 18, 70, and 125 min after leaving the hardware store; samples were obtained from subject B at 4, 28, and 37 min after leaving the hardware store. Figure 4- 5shows a selected area of the XIC (m/z 105) obtained from each breath sample of the 2 subjects. This peak has been tentatively identified as 1-methoxyethyl benzoate, an ingredient in furniture stain that is sold at the hardware store. The same compound was detected in a direct SPME sample taken of the air inside the hardware store for 10 minutes (data not shown). Given that the compound was present in the air source of the subjects, and the breath of both individuals shows a rise and fall in the concentration of this compound, these data show that breath analysis using GC-MS is an appropriate way to measure and monitor chemical exposure, with detectable signal remaining for hours after exposure. A small signal was detected in

the breath samples obtained before exposure; however this is not unexpected given the ubiquitous nature of furniture stain in an office/laboratory setting.

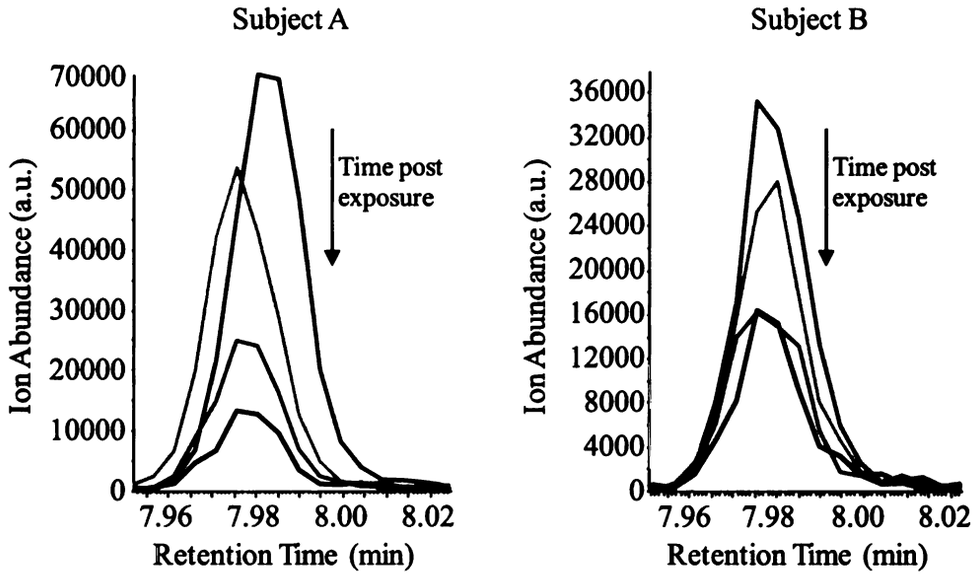

Figure 4- 5: (a.) Selected window of XICs (m/z 105) obtained from Subject A before exposure (black) in the hardware store and 8, 70, and 125 minutes after leaving the hardware store. (b.) Selected window of XICs (m/z 105) obtained from Subject B before exposure (black) and 4, 28, and 37 minutes after leaving the hardware store. The source of the peak was tentatively identified as an ingredient in furniture stain, 1-methoxyethyl benzoate. This chemical was also detected in a SPME sample of the ambient air in the hardware store. (Image originally in color)

4-7: Lemonade Study

A control breath sample was taken prior to lemonade consumption and then many samples were collected after lemonade consumption. A breath sample taken before lemonade consumption does show a detectable but low-level signal in the GC-MS TIC and XIC (m/z 93) from monoterpenes and terpenoid compounds; however, this signal is dwarfed by the contribution of these compounds in a post-lemonade sample. Many of the monoterpenes and terpenoids are consumed in food products or inhaled from the ambient

air due to their abundance in the environment from natural and synthetic sources, presumably causing this initial signal. In fact, estimates of the average per capita combined exposure of α-limonene, terpinolene, and β-myrcene approach 1.3 mg/day.[30] Figure 4- 6 shows an XIC obtained before consuming original lemonade compared to one obtained 3 minutes after lemonade consumption, offset for clarity.

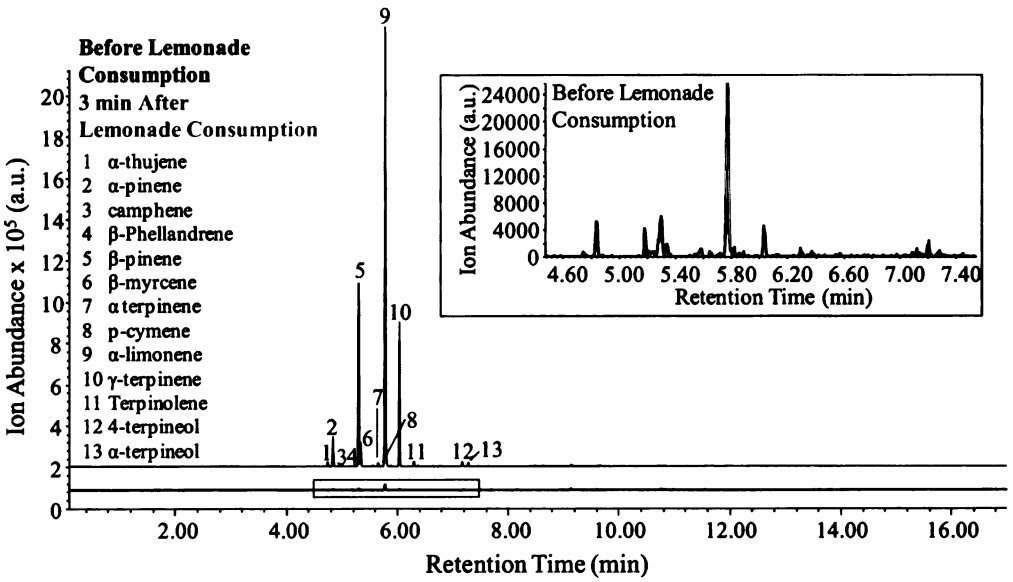

Figure 4- 6: Extracted Ion Chromatograms (XICs) of the m/z 93 ion in breath samples obtained before lemonade consumption (black trace) and 3 min after original lemonade consumption (red trace) offset for clarity. Inset shows magnification of boxed area of the sample taken before lemonade exposure. 13 terpenes and terpenoid compounds of interest are identified. (Image originally in color)

The 13 monoterpenes and terpenoid compounds of interest are labeled, and their structures, molecular weights, and retention times (RT) are shown in Table 4- 1. The signal post-consumption ranges from 1.6-57 times that seen in the sample before consumption. The inset shows a magnification of the boxed area in the figure. Although

these compounds are present in the sample before consuming lemonade, this background contribution to the compounds' level measured after lemonade consumption is minimal. This background contribution is corrected for in peak area calculations for all measurements made after lemonade consumption.

Table 4- 1: Molecular weights, structures, and GC retention times (RT) of 13 terpenes and terpenoid compounds studied. Average decay values, tau, for a single subject (n=5) after consumption of original lemonade, modeling compound decay in breath to a single phase decay are also shown.

Compound	Structure	RT (min)	Average Tau n=5 (min, SEM)
α–Thujene MW 136.23	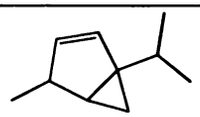	4.75	85.9(13.9) tau_{abs}=1.0
α–Pinene MW 136.23	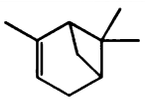	4.84	129.1(12.57) tau_{abs}=2.0
Camphene MW 136.23	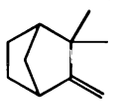	5.03	213.1 (44.6) tau_{abs}=1.5
β–Phellandrene MW 136.23	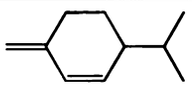	5.23	129.9 (25.7)‡ tau_{abs}=0.1
β–Pinene MW 136.23	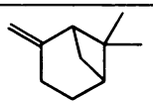	5.30	118.2 (17.6) tau_{abs}=1.5
β–Myrcene MW 136.23	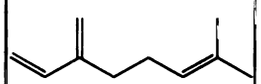	5.34	81.3(10.2) tau_{abs}=0.1
α–Terpinene MW 136.23	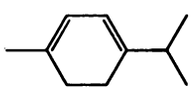	5.66	60.2(13.8) tau_{abs}=0.1
p–Cymene MW 134.22	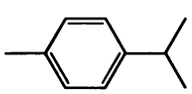	5.73	186.0(25.6)† tau_{abs}=1.0
α–Limonene MW 136.23	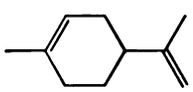	5.78	86.6 (5.7) tau_{abs}=0.2
γ–Terpinene MW 136.23	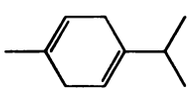	6.04	62.6 (4.3) tau_{abs}=0.0

Table 4-1 (cont'd).

Compound	Structure	RT (min)	Average Tau n=5 (min, SEM)
Terpinolene MW 136.23	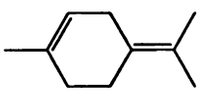	6.30	56.1(12.1) tau_{abs}=0.0
4–Terpineol MW 154.25	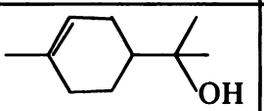	7.17	12.3(2.9) tau_{abs}=0.0
α–Terpineol MW 154.25	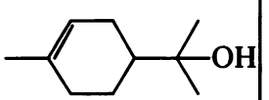	7.29	8.6 (01.7) tau_{abs}=0.2

†n=4, ‡n=3

4-7-1: Reproducibility of Single Subject Drinking Original Lemonade

Figure 4- 7a-b show the XIC region containing the peak identified as α-limonene from 19 breath samples obtained from a single subject after original lemonade consumption. The XIC trace from the pre-consumption sample is also shown.

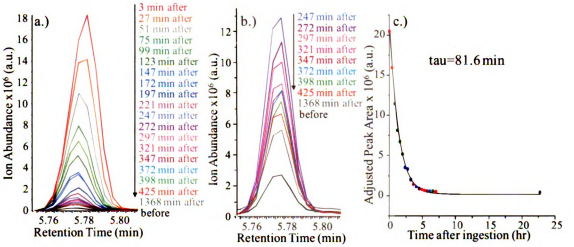

Figure 4- 7: (a) XICs (m/z 93) of peak identified as α-limonene in breath samples obtained before and 3-1368 minutes after original lemonade consumption. (b.) Magnifiea view of XICs shown in (a) obtained 247-1368 minutes after original lemonade consumption, c) Area of peak due to α-limonene corrected for initial area before lemonade consumption plotted versus time after ingestion. These data are fit to a single phase exponential uptake and decay model. (Image originally in color)

In the sample obtained 3 minutes after lemonade consumption, a 77-fold increase in the peak area above background level is observed. An additional experiment in which the subject gargled with lemonade without swallowing and completed the described rinsing procedure demonstrated that a minimal amount of this increase is due to residuals in the mouth and/or throat. Figure 4- 7c shows the α-limonene peak area from each time point. α-Limonene, as well as α-pinene and β-pinene, has previously been shown to follow a triphasic elimination, with a short half life immediately after exposure and longer half lives as the elimination processes progress.[26, 31, 32] This slow elimination is thought to be caused by the high lipophilicity of the compounds which causes the compounds to preferentially partition in fatty tissue, assuming they are not first metabolized.[26, 33] Indeed, previous reports have shown that metabolic products of monoterpenes excreted

through the kidneys reach maximum levels approximately 5 days after exposure, even after hemoperfusion, suggesting storage and slow metabolism in the fatty tissues.[29] While many studies have fit terpene data to a two- or three- component exponential decay process,[11, 28] the data presented in this study do not reveal the first phase of elimination in the α-limonene data as the reported half-life of this phase is 3 min,[34] and the initial breath sample in this study was obtained from 3-13 minutes after exposure. The current data fits most accurately to a model including a single exponential rise (absorption) and a single exponential decay (elimination) model:

$$y = y_o + A_1 e^{(-x/tau_1)} - A_1 e^{(-x/tau_{abs})}$$

Equation 4- 1: Exponential rise and decay with a y-offset

where y_0 is the offset of the fit, A_1 is the concentration remaining in the body, tau_1 is the half-life of the decay, and tau_{abs} is the half-life of the absorption process. tau_{abs} was held constant at 0.2 min for the fit, yielding a half-life (tau_1) of 86.6 min for α-limonene.

Figure 4- 8a-b shows the XIC region for the peak identified as containing γ-terpinene from the same breath samples previously discussed. The pre-consumption sample contained only a trace amount of γ-terpinene, so the sample obtained 3 minutes after consumption showed a 149-fold increase in peak area compared to this value. Figure 4-8c shows the decay in peak area for this peak fit to a single exponential rise and decay (Equation 4- 1). The half-life of absorption was held constant at 0 min, and the half-life

of elimination was determined to be 62.6 minutes. Similar curve peak area analysis and curve fitting was performed for all peaks (See Appendix B).

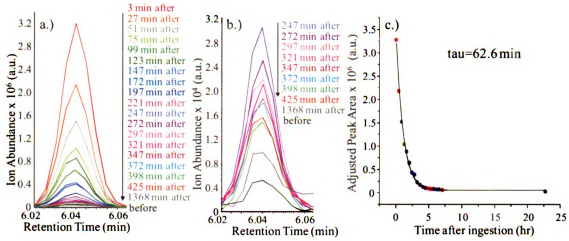

Figure 4- 8: (a) GC-MS XICs (m/z 93) of peak identified as γ-terpinene in breath samples obtained before and 3-1368 minutes after original lemonade consumption, (b) Magnified view of XICs shown in Figure 4a obtained 247-1368 minutes after original lemonade consumption, (c) Area of peak due to γ-terpinene versus time after ingestion. These data are fit to a single phase exponential uptake and decay model. (Image originally in color)

Calculated half-lives are shown in Table 4- 1 for 5 replicates of a single subject except where noted. The standard error of the mean (SEM) is surprisingly low for many of the monoterpenes and terpenoids monitored. This particular subject had a consistent exercise and diet schedule during the study which was thought to affect the consistency of the data. The half-lives of the monoterpene alcohols were determined to be significantly lower than those of the other monoterpenes and terpenoids using Welch's t-test ($p<0.001$). This may be due to the higher water solubility and lower saturated vapor pressure of the alcohols,[35-38] causing them to quickly partition into the water vapor that dominates the components in human breath. The monocyclic monoterpenes' half-lives

were also significantly lower than those of the bicyclic monoterpenes ($p < 0.001$), and the aromatic monoterpene, p-cymene ($0.001 < p < 0.01$). The linear monoterpene's half-life was also significantly different from that of the aromatic monoterpene ($0.01 < p < 0.02$, Student's t-test), which may also be due to the different solubilities of the compounds.[36, 37, 39] Table 4- 2 shows the tau values calculated for 3 subjects after drinking original lemonade. Similar relative values for half-lives of the different compounds were observed for data obtained from 3 subjects after consumption of original lemonade.

Table 4- 2: Half-lives (tau) for single exponential decay of 13 terpenes and terpenoid compounds in breath after original lemonade consumption by 3 subjects.

	Tau (n=3 subjects)	
Compound	Average	SEM
α - Thujene	62.5	26.4
α - Pinene	56.0	29.5
Camphene	76.3	34.7
β - Phellandrene	43.4	27.9
β - Pinene	47.7	31.2
β - Myrcene	39.6	20.7
α - Terpinene	35.7	18.8
p - Cymene	105.7	10.4
α - Limonene	43.6	22.9
γ - Terpinene	32.5	15.6
Terpinolene	32.6	15.1
4 - Terpineol	12.5	2.3
α - Terpineol	15.6	3.6

4-7-2: Concentration Dependence of Terpene Signal in Breath

Other concentrations and types of lemonade were also used to analyze the uptake and decay kinetics of the terpenes and terpenoid compounds. Concentrated lemonade was prepared from the same lot of frozen lemonade concentrate as the original lemonade but with less dilution. Mediterranean lemonade was made from fresh lemons in an effort to further increase the terpene and terpenoid concentration consumed. Figure 4- 9 shows the α-limonene XIC peak area (m/z 93) versus time after consumption of each type of lemonade for a single subject. The highest XIC peak area reached in a sample increases linearly with the α-limonene concentration measured in each lemonade sample: 0.696 mM, 1.93 mM and 5.96 mM for the original, concentrated, and Mediterranean varieties, respectively (R^2=0.993), previously seen with monoterpenes.[25, 31] This trend is also apparent in the other monoterpenes and terpenoid compounds.

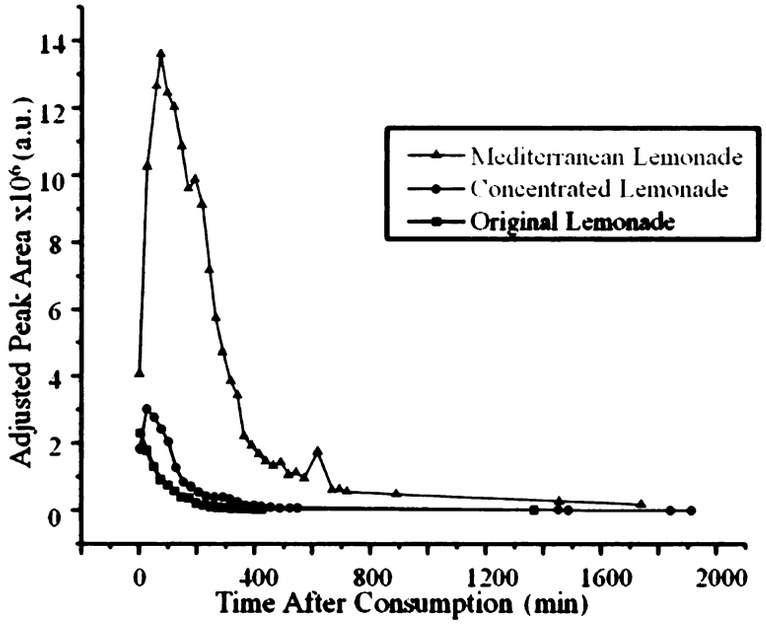

Figure 4- 9: α-Limonene peak area versus time after consumption for original, concentrated, and Mediterranean lemonade. Note the higher t_{max} for higher lemonade concentrations as well as the appearance of the uptake curve of the α-limonene. (Image originally in color)

The maximum peak area of each terpene and terpenoid compound measured in breath after consumption of each lemonade sample was normalized to the maximum peak area measured in breath after consumption of the original lemonade for comparison. Similarly, the peak area of each terpene and terpenoid compound in the actual (neat) lemonade samples was normalized to its area in the original lemonade. Figure 4- 10 shows these relative peak areas for the 13 compounds monitored in the actual (neat) lemonade samples (Figure 4- 10a) as well as the maximum peak area measured in breath after consumption of each type of lemonade (Figure 4- 10b). All terpene analytes show a

significant increase in peak area in breath as the concentration of the lemonade consumed increases, similar to the peak area increase of the terpenes measured in the neat lemonade samples of increasing concentrations. The only exception is the terpene alcohols, 4-terpineol and α-terpineol, where no significant increase in signal in breath samples with increasing concentration of lemonade consumed is seen; this is possibly due to the quick elimination of terpene alcohols from the body.

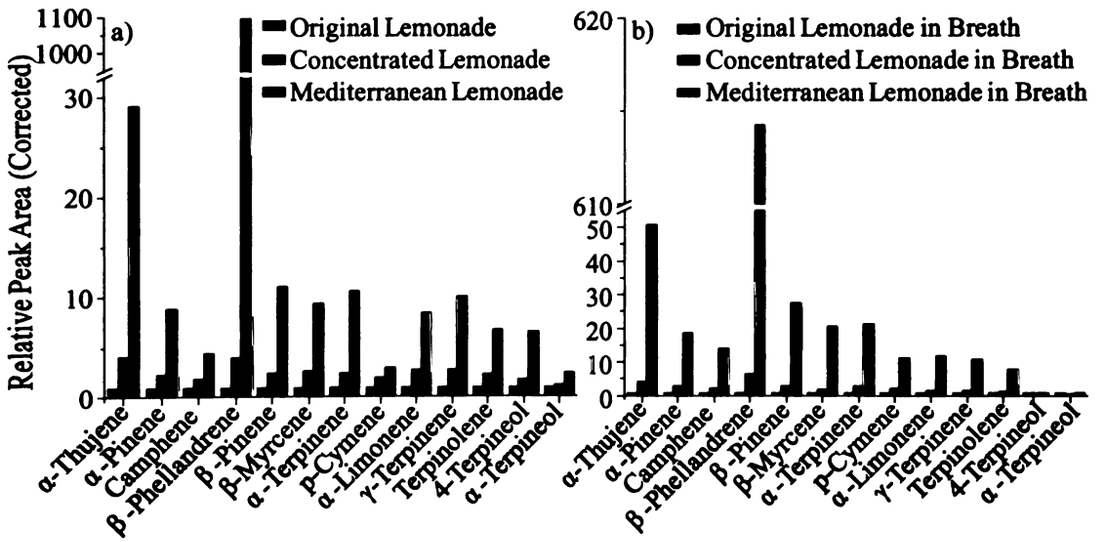

Figure 4- 10: Relative peak areas of 13 terpene and terpenoid compounds in (a) neat samples of original, concentrated, and Mediterranean lemonade, and (b) breath samples after consumption of original, concentrated, and Mediterranean lemonade. Peak areas are normalized to the original lemonade peak area for each compound, and the breath sample obtained at t_{max} was used. (Image originally in color)

More information about the uptake of the monoterpenes and terpenoids is gleaned when higher concentrations of lemonade are consumed. Figure 4- 9 also demonstrates that the maximum peak area, thus, concentration in breath, is reached at later times when the terpene concentrations in lemonade are greater. This finding also supports the conclusion

that residual compounds in the mouth are not causing the signal seen in the breath samples as the signal continues to rise long after consumption. In the original lemonade, the initial breath sample taken 3 minutes after consumption (t_{max}) yielded the highest α-limonene concentration. In the concentrated lemonade this t_{max} was not reached until 52 minutes after consumption, and in the Mediterranean lemonade, 73 minutes after consumption. After exposure, a chemical is first distributed through the body, and then eliminated. These processes are not exclusive of each other; elimination begins while the chemical is still being distributed. In the experiment presented, chemical exposure proceeds through ingestion, so the kinetics of an additional absorption step must be considered. The terpenes and terpenoids are first absorbed through the digestive tract, passed into the blood and distributed to various tissues based on their lipid and water solubilities.[40] Absorption and distribution also occur concurrently. The terpenes and terpenoids pass from the blood into the lung via the alveolar pulmonary membrane and attempt to establish equilibrium between the two compartments. Exhalation pushes the compounds out of the lung, which are subsequently replaced through the constant shift towards equilibrium. The higher the concentration of lemonade consumed, the longer it takes for the absorption and distribution processes to occur, yielding a rise followed by the decay of the peak area due to monoterpenes and terpenoid compounds as previously described.[28] With higher concentration of monoterpenes and terpenoids, absorption and distribution take a longer time, yielding the increased t_{max}, and describing that the absorption or distribution processes have been saturated, and that further terpenes cannot be absorbed until elimination has removed some from circulation. The extended time

period bef

monoterpe

allows the

were obta

Mediterra

parameter

Figure
lemona

Becaus

lemona

The dat

triphasic

period before elimination becomes the primary process in the uptake and decay of the monoterpenes and terpenoid compounds after consumption of Mediterranean lemonade allows the compound uptake to become more apparent in the data, as several data points were obtained before t_{max} was reached. The data from the consumption of the Mediterranean lemonade was fit to Equation 4- 1, and is shown in Figure 4- 11. Fit parameters are shown in Table 4- 3.

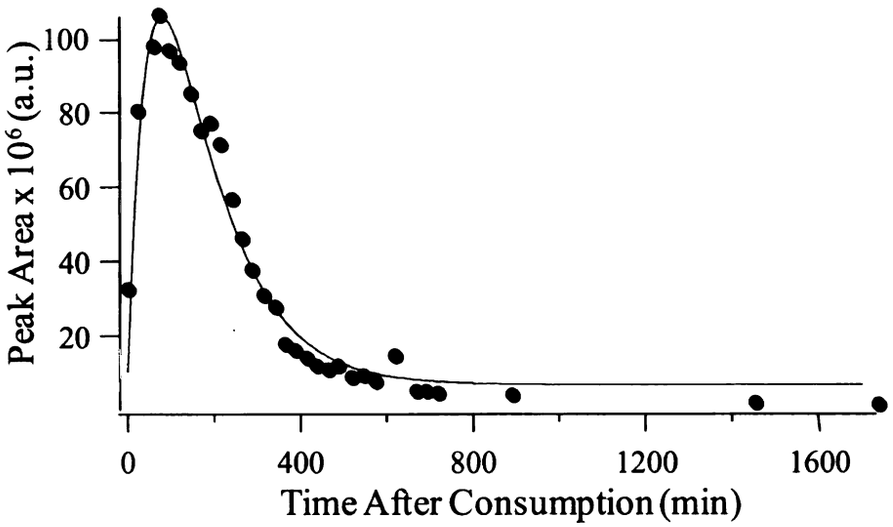

Figure 4- 11: Uptake and decay of α-limonene after consumption of Mediterranean lemonade fit to Equation 4- 1.Equation 4- 2 Fit parameters are shown in Table 4- 3.

Because of the deviation seen in this fit, the data from consumption of the Mediterranean lemonade was fit to a higher order model using the method of residuals (Figure 4- 12).[27] The data was fit to the following equation which describes the first order uptake, and triphasic decay of α-limonene:

$y = A_1 e^{(-}$

Equation 4-

where y is th

constants of

the first orde

and slow el

Equation 4-

that these d

Figure 4-
lemonade
Table 4- 3

$$y = A_1 e^{(-x/tau_1)} + A_2 e^{(-x/tau_2)} + A_3 e^{(-x/tau_3)} - U\, e^{(-x/tau_{abs})}$$

Equation 4- 2: Model of uptake and triphasic decay for monoterpenes and terpenoids

where y is the peak area of the compound detected in breath, A_1, A_2, A_3, and U are the constants of the three phases of decay and uptake, respectively, tau_{abs} is the half-life of the first order absorption process, and tau_1, tau_2, and tau_3 are the first order fast, medium, and slow elimination half-lives. These fit values are also shown in Table 4- 3. Neither Equation 4- 1 nor Equation 4- 2 describe the data in an acceptable manner. It is thought that these data require a much more complicated fit, which may be pursued in the future.

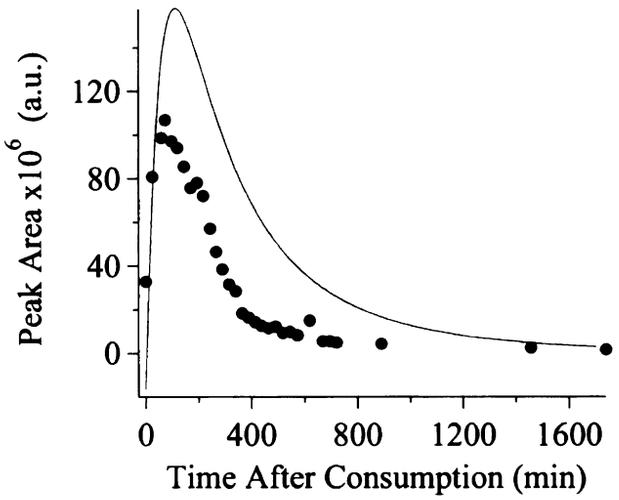

Figure 4- 12: Uptake and decay of α-limonene after consumption of Mediterranean lemonade fit to Equation 4- 2 using the method of residuals. Fit parameters are shown in Table 4- 3

Table 4- 3: Coefficients and half-lives obtained after fitting the uptake and decay of α-limonene in breath after consumption of Mediterranean lemonade to Equation 4- 1 and Equation 4- 2.

Fit to Equation 4-1			
A		tau_{abs}	tau_1
3.70×10^8		57.0	120
Fit to Equation 4-2			
Uptake		Decay	
U	tau_{abs}	A_1	tau_1
3.54×10^8	55.2	1.10×10^7	968
		A_2	tau_2
		1.93×10^8	171
		A_3	tau_3
		1.28×10^8	365

A deviation from exponential decay is seen for many of the monoterpenes and terpenoids across all subjects. Approximately 5 hours after lemonade consumption, the peak area of the terpenes and terpenoids in breath plateaus or increases slightly, rather than continuing to decrease exponentially (see Figure 4- 9 and Appendix B). After approximately 1 hour, peak areas measured in breath samples return to the exponential decay. This is thought to be a real effect, as all samples were analyzed using the same GC-MS method and the deviation is consistently observed for all terpenes and across subjects. A similar plateau phenomenon has been previously reported for several VOCs measured in breath, specifically 1,1,1-trichloroethane,[11] and was thought to be due to changes in activity, blood flow, or diet. Several subjects in this study fasted while participating, eliminating

immediate effects of diet variation as a cause of this effect, however changes in activity, blood flow, or changes in metabolism due to fasting are viable possibilities and will be considered further in the future.

4-8: Drug Studies

4-8-1: Sudafed

Studies were performed to determine if oral ingestion of an OTC drug would be detectable on breath. If so, this method may have applications to drug testing, or even diagnostics in an emergency room setting where a patient may have overdosed on an unknown drug. Two subjects participated in this study. A breath sample was collected in the morning, followed by the subject consuming two 30 mg pseudoephedrine tablets. Breath samples were then collected at several times after ingestion. Breath samples were analyzed using Selected Ion Monitoring (SIM) mode of the GC-MS, monitoring m/z 58, the ion corresponding to the base peak in the mass spectrum of pseudoephedrine. For retention time and mass spectral confirmation, a pseudoephedrine tablet was crushed and 26.6 mg of the powder was dissolved in 5 mL of water. A SPME fiber was directly exposed to the water for 1 min, and analyzed using the method previously described and well as in scan mode. The mass spectrum obtained was consistent with that in the NIST mass spectral database, and the retention time was determined to be 8.61 min.

Results were variable across subjects and even between different exposures of a single subject. Figure 4- 13 shows the 'best case' data of exposure of a single subject. Figure 4- 13a shows the chromatographic peak attributed to pseudoephedrine in breath samples

obtained before and at eight intervals after ingestion. Figure 4- 13b shows the same data, without the 10 min after consumption sample, for clarity. A significant increase in peak area is seen in the breath sample obtained 10 minutes after pseudoephedrine consumption relative to that seen in the breath sample obtained before consumption. Over several hours, the area of this peak decays to values near that seen in the sample obtained before consumption. The decay can be fit to an exponential model (R^2=0.9989) with a half-life of 13.4 minutes. This is a preliminary experiment, and the reproducibility of the rise and decay of the pseudoephedrine peak after consumption has not been determined. In repeated experiments, the pseudoephedrine peak area in a breath sample obtained approximately 10 minutes after consumption was lower than that shown below, and is not seen in samples obtained approximately an hour after consumption, thus preventing study of the decay of the compound in these additional experiments. This could be due to variation in diet of the subject as it was not regulated, illness of the subject as medication was only taken when symptoms were present, or other variation in metabolism and digestion.

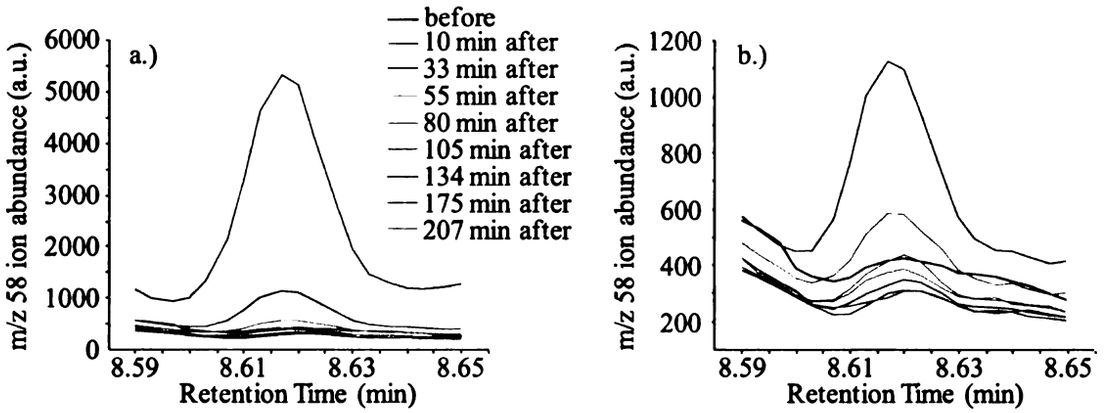

Figure 4- 13: Selected window of the m/z 58 chromatogram obtained in SIM mode before and after ingestion of 60 mg of pseudoephedrine. The peak has been identified as pseudoephedrine. (a) shows all breath samples obtained, (b) shows a zoomed in view of the samples excluding that obtained 10 min after consumption for clarity. (Image originally in color)

The signal seen in the chromatograms obtained from breath after consumption of pseudoephedrine is 4 orders of magnitude less than that previously observed for terpenes after lemonade consumption. The amount consumed is actually higher; 60 mg of pseudoephedrine were consumed in this study while ~45 mg of α-limonene were consumed in the original lemonade sample. The vapor pressure of limonene at 25 °C is 20 torr,[41] much higher than that of pseudoephedrine, which is listed as a non-volatile solid.[42] Indeed, pseudoephedrine is typically derivatized prior to GC-MS analysis in order to increase its volatility. In order for the pseudoephedrine to be detected in breath, it must be absorbed and distributed into the blood which then passes by the alveolar pulmonary membrane, where the pseudoephedrine must partition into the alveolar air and be exhaled. With a low vapor pressure, partitioning into the alveolar air would be slight; whereas the higher vapor pressure of limonene would allow significant partitioning across the membrane. A recent study has used breath analysis to monitor levels of

propofol, an intravenous anesthetic, during surgery by sampling breath directly from the endotracheal tube in the patient.[43] In this study, exhaled breath was analyzed and the propofol signal was correlated to the concentration measured in blood. Although the vapor pressure of propofol is still relatively low (0.142 torr at 20 °C), it was reported that its low water solubility results in a measurable quantity of the drug in the gas phase near a hydrophilic solution.[43]

Investigation into the detection of ibuprofen ingestion was also pursued, but no signal was detected in breath after ingestion. The vapor pressure of ibuprofen is reported as < 1 torr.[44] Ibuprofen undergoes minimal first pass metabolism in the liver; however, it experiences very high binding to plasma proteins.[45] It is reported that only 0.3-0.5% of ibuprofen remains unbound when a low concentration, as used in this study, is consumed.[45] A combination of little free ibuprofen being available to partition across the alveolar pulmonary membrane, as well as the benefit of derivatizing the molecule for GC-MS analysis which was not done in these studies may be responsible for the lack of signal in this study.

4-9: Explosive Studies

4-9-1: Hexamine

Studies were performed to determine if explosive-related compounds could be detected in human breath. Comparisons were made between samples collected using EBC and EBV. A single breath sample was obtained from a subject in the morning. The subject then poured approximately 10 g of hexamine, a common precursor in the synthesis of RDX, between 2 100 mL plastic beakers on the laboratory benchtop for 10 min. Subsequent

breath samples were then collected. Samples were analyzed via GC-MS which was operated in selected ion monitoring (SIM) mode to specifically detect the m/z 140 and 42 ions, the molecular ion and base peak in the hexamine mass spectrum, respectively, with greater sensitivity. For retention time and mass spectrometric confirmation, a sample of vapors from the hexamine powder was obtained by suspending a SPME fiber in the headspace of the jar for 1 minute and analyzing for hexamine using the method previously described and well as with the GCMS in scan mode. The mass spectrum obtained was consistent with that in the NIST mass spectral database, and the retention time was determined to be 7.64 min.

Figure 4- 14a shows the peak due to hexamine in the m/z 140 XIC for EBC samples obtained before and 26 minutes after exposure to hexamine. Figure 4- 14b shows the peak due to hexamine in the m/z 140 XIC for EBV samples obtained before and 30 minutes after exposure to hexamine from the sample subject. Note the difference in the y-axis for the samples. Although they both show an increase in signal after exposure to hexamine, the signal from the EBV is much higher than that from the EBC. The difference in signal may be partially explained by whether the hexamine is inhaled in vapor or aerosol form. The vapor pressure of hexamine is reported to be 0.0035 mbar,[46] which makes it unlikely that it would be present in the vapor phase. Aerosol particles of hexamine may have been inhaled and then exhaled and collected by the SPME fiber. Even a single particle collected in this manner would provide significant signal. Another possible explanation is differences in actual exposure, as the only parameter that was controlled was the length of exposure; the actual exposure, breathing rate and depth were not easily controlled.

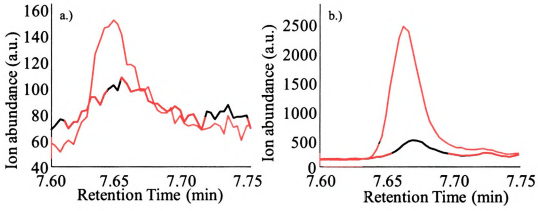

Figure 4- 14: (a) Selected window of GC-MS XIC (m/z 140) for breath samples (EBC) obtained before (black) and 26 min after (red) exposure to hexamine, (b) Selected window of XIC (m/z 140) for breath samples (EBV) obtained before (black) and 30 min after (red) exposure to hexamine. (Image originally in color)

A study was then performed to investigate the rate at which hexamine was cleared from the body via the breath. A single EBV sample was again obtained in the morning, and the subject poured the hexamine back and forth between plastic beakers. Breath samples were then obtained 1, 30, 61, and 82 minutes after exposure. Figure 4- 15a shows the peak due to hexamine in these samples obtained by monitoring m/z 140 and m/z 42. Peak areas were calculated from the XIC of m/z 140. Figure 4- 15b shows the change in peak area versus time after exposure for the samples. The four samples taken after exposure were fit to an exponential decay (R^2=0.994), and the half-life was determined to be 15.6 minutes. This provides initial evidence that an RDX precursor can be detected on breath, and may remain on breath for a period of time after exposure.

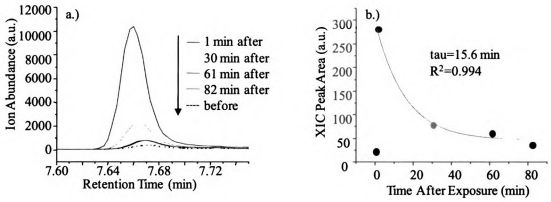

Figure 4- 15: (a) Selected window of TIC (SIM, m/z 140, 42) from breath samples (EBV) of a single subject before and after exposure to hexamine, (b) Exponential decay, R^2= 0.994, of the area of the peak due to hexamine, calculated from the XIC (m/z 140) (chromatogram not shown). (Image originally in color)

As 10 minutes of exposure to 10 g of hexamine provides a relatively low exposure level, a study was performed to determine if a longer exposure would provide a higher signal from the breath samples. A single EBV breath sample was obtained from a subject in the morning. The subject then poured ~10 g of hexamine between the plastic beakers for 10 min. An additional breath sample was collected, and the subject then repeated the 10 min hexamine pour on the benchtop. This procedure was repeated for over 5 hours, resulting in 8, 10 min exposures and the collection of 12 breath samples. All breath samples were analyzed using selected ion monitoring of ions at m/z 140 and 42, the molecular ion and base peak fragment ion in a mass spectrum of pure hexamine, respectively. Figure 4- 16 shows the increase and decay of the area of the hexamine peak in the XIC m/z 140 chromatograms over time. The red bars represent the time the subject was exposed to the hexamine. As the subject's exposure increased, so did the concentration of hexamine on the breath. When exposure ceased, the concentration of hexamine began to decay. The

subject in this study was handling only 10 g hexamine in a well-ventilated environment, while wearing goggles, nitrile gloves, and a laboratory coat for a combined time of 80 minutes; it is hypothesized that clandestine synthesis and/or handling of explosives such as RDX would involve longer exposures to higher concentrations of the precursors in less than ideal environments, allowing for detection on a longer timescale.

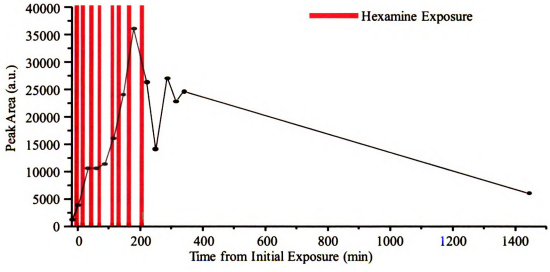

Figure 4- 16: Integrated area of GC-MS XIC m/z 140 peak attributed to hexamine at RT=7.69 min in chromatograms obtained in SIM mode (m/z 140 and 42) of breath samples from a single subject before, during, and after several 10 min exposures (shown in red) to hexamine. Note the increase in hexamine on the breath during exposure and the gradual decay after exposure. Hexamine was still detected on breath 24 hrs after the initial exposure. (Image originally in color)

4-9-2: Field Studies

In order to demonstrate the real-world ability of this technique to detect exposure to industrial chemicals, field studies were performed with six volunteers who participated in exercises designed to accurately simulate the clandestine building of devices. These subjects participated in daily activities that included packing, preparing, and transporting

the materials. Breath samples (EBV) were collected from the subjects each morning before these activities began, and each afternoon after the simulation was completed. Although details of these studies are sensitive and cannot be shared, it was confirmed that exposure to these industrial materials can indeed be measured based on signatures measured in breath samples.

4-10: Conclusions

The detection of chemicals for hours after exposure can serve as proof of concept for a detection protocol for chemical exposure. In the data presented here, the presence of key chemicals, such as camphor, on the breath of an individual can suggest the prior environment of the subject, such as the nail salon. These data are also important in measuring chemical exposures, intentional or accidental, as in the case of a chemical spill. The environment and exposure that occurs in a hardware store are also described, which also provides data on the chemicals that could relate an individual to that location. Even though these locations may not be of forensic interest, this work demonstrates that the prior location of an individual may be determined based on residual signatures of VOCs indicative of that location in human breath. Exposure via ingestion is also described in the uptake and elimination of terpenes and terpenoid compounds after oral exposure to a mixed terpenoid beverage (lemonade). The elimination of each compound is modeled and fit to an exponential decay in order for comparisons to be made between the different compound classes. The uptake and triphasic decay of α-limonene on breath was modeled after consumption of a high concentration lemonade sample. The effect of concentration on the elimination process is also described. These data support the

hypothesis that longer exposures or higher concentration exposures will increase the signal of a chemical measured on breath, therefore providing a larger time scale of detection.

The detection of drugs and chemicals used in the synthesis of explosives is also shown, allowing for the monitoring of illicit activity. Field studies presented an opportunity to test the breath analysis technique on real-world samples from industrial chemical workers, proving the success of the technique and methods that were developed.

4-11: References

(1) Pleil, J. D.; Fisher, J. W.; Lindstrom, A. B. *Environ. Health Perspect.* **1998**, 106, 573-580.

(2) Goldoni, M.; Catalani, S.; De Palma, G.; Manini, P.; Acampa, O.; Corradi, M.; Bergonzi, R.; Apostoli, P.; Mutti, A. *Environ. Health Perspect.* **2004**, 112, 1293-1298.

(3) Maniscalco, M.; De Laurentiis, G.; Pentella, C.; Mormile, M.; Sanduzzi, A.; Carratu, P.; Sofia, M. *Biomarkers* **2006**, 11, 233-240.

(4) Pleil, J. D.; Lindstrom, A. B. *Clin. Chem.* **1997**, 43, 723-730.

(5) Poet, T. S.; Thrall, K. D.; Corley, R. A.; Hui, X.; Edwards, J. A.; Weitz, K. K.; Maibach, H. I.; Wester, R. C. *Toxicol. Sci.* **2000**, 54, 42-51.

(6) Corley, R. A.; Gordon, S. M.; Wallace, L. A. *Toxicol. Sci.* **2000**, 53, 13-23.

(7) Gargas, M. L.; Tyler, T. R.; Sweeney, L. M.; Corley, R. A.; Weitz, K. K.; Mast, T. J.; Paustenbach, D. J.; Hays, S. M. *Toxicol. Appl. Pharmacol.* **2000**, 165, 63-73.

(8) Corley, R. A.; Bormett, G. A.; Ghanayem, B. I. *Toxicol. Appl. Pharmacol.* **1994**, 129, 61-79.

(9) Corley, R. A.; English, J. C.; Hill, T. S.; Fiorica, L. A.; Morgott, D. A. *Toxicol. Appl. Pharmacol.* **2000**, 165, 163-174.

(10) Wallace, L. A. *Annual Review of Energy and the Environment* **2001**, 26, 269-301.

(11) Raymer, J. H.; Pellizzari, E. D.; Thomas, K. W.; Cooper, S. D. *J. Expo. Anal. Environ. Epidemiol.* **1991**, 1, 439-451.

(12) Wallace, L.; Buckley, T.; Pellizzari, E.; Gordon, S. *Environ. Health Perspect.* **1996**, 104, 861-869.

(13) Wallace, L. A.; Nelson, W. C. Measurements of Exhaled Breath Using a New Portable Sampling Method, Environmental Protection Agency, EPA/600/S3-90/049, **1990**.

(14) Wallace, L.; Pellizzari, E.; Gordon, S. *J. Expo. Anal. Environ. Epidemiol.* **1993**, 3, 75-102.

(15) Pellizzari, E. D.; Wallace, L. A.; Gordon, S. M. *J. Expo. Anal. Environ. Epidemiol.* **1992**, 2, 341-355.

(16) Wallace, L. A.; Nelson, W. C.; Pellizzari, E. D.; Raymer, J. H. *J. Expo. Anal. Environ. Epidemiol.* **1997**, 7, 141-163.

(17) Lindstrom, A. B.; Pleil, J. D. *Biomarkers* **2002**, 7, 189-208.

(18) Lindstrom, A. B.; Pleil, J. D.; Berkoff, D. C. *Environ. Health Perspect.* **1997**, 105, 636-642.

(19) Jo, W. K.; Weisel, C. P. L., P.J. *Risk Anal.* **1990**, 10, 575-580.

(20) Spencer, A. B.; Estill, C. F.; McCammon, J. B.; Mickelsen, R. L.; Johnston, O. E. Control of Ethyl Methacrylate Exposures During the Application of Artificial Fingernails at Moore's University of Hair Design, Cincinnati, Ohio U. S. Department of Health and Human Services. Public Health Services, Centers for Disease Control and Prevention, National Institute for Occupational Safety and Health, Engineering Control Technology Branch. Report No.: ECTB 171-22a.

(21) Gosselin, R. E.; Smith, R. P.; Hodge, H. C. *Clinical Toxicology of Commercial Products*; Williams and Wilkins Press: Baltimore, MD, **1984**.

(22) Spencer, A. B.; Estill, C. F.; McCammon, J. B.; Mickelsen, R. L.; Johnston, O. E. *Am. Ind. Hyg. Assoc. J.* **1997**, 58, 214-218.

(23) Maxfield, R.; Howe, H. L. Silica Exposure in Artificial Nail Application Salons. Epidemiologic Report Series 97:8. Springfield, Il: Illinois Department of Public Health: November 1997.

(24) Protecting the Health of Nail Salon Workers: EPA no. 744-F-07-001. March 2007.

(25) Levin, J.; Eriksson, K.; Falk, A.; Lof, A. *Int. Arch. Occup. Environ. Health* **1992**, 63, 571-573.

(26) Falk-Filipsson, A. *Occup. Environ. Med.* **1996**, 53, 100-105.

(27) Gibaldi, M.; Perrier, D. *Pharmacokinetics*, 2nd Edition ed.; Marcel Dekker, Inc.: New York, **1982**.

(28) Chen, H.; Chan, K. K.; Budd, T. *J. Pharm. Biomed. Anal.* **1998**, 17, 631-640.

(29) Koppel, C.; Tenczer, J.; Tonnesmann, U.; Schirop, T.; Ibe, K. *Arch. Toxicol.* **1981**, 49, 73-78.

(30) Test Plan for Monoterpene Hydrocarbons; The Flavor and Fragrance High Production Volume Consortia: Washington, D.C., **2002**.

(31) Falk, A.; Hagberg, M. T.; Lof, A. E.; Wigaeus-Hjelm, E. M.; Zhiping, W. *Scandinavian Journal of Work, Environment &Health* **1990**, 16, 372-378.

(32) *Safety evaluation of certain food additives* In WHO Food Additives Series, 54, Geneva, **2006**.

(33) Falk, A.; Gullstrand, E.; Lof, A.; Wiggaeus-Hjelm, E. *Br. J. Ind. Med.* **1990**, 47, 62-64.

(34) Falk-Filipsson, A.; Lof, A.; Hagberg, M.; Hjelm, E. W.; Wang, Z. *J. Toxicol. Environ. Health* **1993**, 38, 77-88.

(35) Copolovici, L. O.; Filella, I.; Llusia, J.; Niinemets, U.; Penuelas, J. *Plant Physiol.* **2005**, 139, 485-496.

(36) Li, J.; Perdue, E. M.; Pavlostathis, S. G.; Araujo, R. *Environment International* **1998**, 24, 353-358.

(37) "Aqueous Solubility and Henry's Law Constants of Organic Compounds" In CRC Handbook of Chemistry and Physics, 88th Edition (Internet Version 2008); Lide, D. R., Ed.; CRC Press/Taylor & Francis Boca Raton, FL.

(38) Niinemets, U.; Reichstein, M. *Global Biogeochemical Cycles* **2002**, 16, 1-26.

(39) Howard, P. H. Handbook of Environmental Fate and Exposure Data for Organic Chemicals, Vol. V; CRC Press: Boca Raton, FL., **1997**.

(40) Refat, M.; Moore, T. J.; Kazui, M.; Risby, T. H.; Perman, J. A.; Schwarz, K. B. *Pediatr. Res.* **1991**, 30, 396-403.

(41) MSDS d-limonene (Cas=5989275), California Environmental Protection Agency, **2009**.

(42) Salocks, C.; Kaley, K. B. Technical Support Document: Toxicology Clandestine Drug Labs/Methamphetamine, California EPA, **2003**.

(43) Hornuss, C.; Praun, S.; Villinger, J.; Dornauer, A.; Moehnle, P.; Dolch, M.; Weninger, E.; Chouker, A.; Feil, C.; Briegel, J.; Thiel, M.; Schelling, G. *Anesthesiology* **2007**, 106, 665-674.

(44) Ibuprofen, Mallinckrodt Inc., **2002**.

(45) "Metabolism and Pharmacokinetics of Ibuprofen" In Aspirin and Related Drugs; Rainsford, K. D., Ed.; CRC Press, **2004**.

(46) "Hexamethylenetetramine" In Synthetic Nitrogen Products; Springer US, **2005**, pp 333-336.

CHAPTER 5: Conclusions and Thoughts for the Future

5-1: Conclusions

5-1-1: Single Particle Aerosol Mass Spectrometry

This dissertation has presented an evaluation of the performance of Single Particle Aerosol Mass Spectrometry (SPAMS) for the detection of active ingredients in over-the-counter (OTC) drug tablets. In order to analyze these solid tablets, a sampling vial was developed that could create particles from the tablets because of collisions with the vial walls or other tablets. This novel sampling system was coupled easily to SPAMS, and benefited from the slight vacuum at the inlet of SPAMS pulling the aerosolized particles into the instrument.

The forensic implications of the current work are vast. The active ingredients in OTC tablets were identified without destroying the identifying marks on the exterior of the tablet, and even in the presence of filler materials in the tablets. The alarm algorithm developed for use with SPAMS relies on rules trees alone, and was successful in identifying the active ingredients in single ingredient and multi-ingredient tablets, as well as a sample containing multiple tablets of different drugs. The ability for the sampling mechanism to be used for *in situ* sampling out of an original drug bottle is another forensic attribute. This suggests the ease at which a new sample could be presumptively screened for the presence of illicit material, without the need for separating each tablet, extracting the active ingredient, and testing each one individually. The active ingredient could even be detected from the residual particles left on the walls of a container after it had been emptied. This means that even if a drug sample was discarded in order to prevent detection or arrest, identification may still be made.

5-1-2: Breath Analysis

Breath analysis has been developed as a method of detecting chemical exposure based on the identification of signature compounds in the breath. Significant attention was paid to developing a method for sampling the breath, testing both exhaled breath condensate (EBC) and exhaled breath vapor (EBV) obtained at two different temperatures, using GC-MS for analyte detection. EBV was found to be superior for the analysis of most compounds, and thus used for many of the studies. The importance of the localized breathing environment was demonstrated with studies involving chemicals used in a nail salon. The rebreathing of chemicals outgassing from the fingernails was avoided by incorporating a respirator cartridge or plastic tubing to remove contaminants from the inhaled air, or provide it from a different environment, respectively. Both methods were effective at reducing the contamination by the localized environment.

Extensive studies were also completed to analyze the breath of a human subject after ingestion or inhalation exposure to chemicals, in particular terpenes and terpenoid compounds. An immediate rise in signal, followed by decay back to near baseline over several hours was measured for 13 compounds. This decay was successfully fit to a model describing a single exponential uptake and decay. The effects of different doses of compounds on their levels in exhaled breath were then tested by varying the concentration of the lemonade consumed in the study. An increased signal was measured for constituents in breath which corresponded to the increase in concentration of each compound in the lemonade sample. Several subjects were sampled, and several replicates were obtained from a single subject, providing relatively similar signals over time. When more concentrated forms of lemonade were consumed, the kinetics of the

uptake and distribution process of the terpenes and terpenoids could be assessed based on levels exhaled in the breath. Fitting these data to an established model presented substantial challenges, but these measurements provide information that can be used to assess the exposure of individuals to volatile chemicals.

Results from this work indicate that the prior location or prior activity of a subject may be indicated by the presence of chemicals signatures of a particular environment or activity on the breath. The chemical signatures of volatiles present in a nail salon and hardware store were described and detected in breath sampled for several hours after exposure. Chemicals indicative of exposure to explosive-related compounds were also detected on breath for several hours after even a short exposure. These results, although preliminary, indicate that breath analysis will be a powerful technique for identifying subjects of interest when investigating possible criminal and terrorist activities.

5-2: Thoughts for the Future

5-2-1: Single Particle Aerosol Mass Spectrometry

Single Particle Aerosol Mass Spectrometry has already been established as a reliable detection system capable of identifying biological agents, chemical agents, radiological material, and explosives. Its ability to operate autonomously and sound alarms in the presence of a user-defined number of identified particles in time has also been defined. The current work has expanded these applications to include the detection of OTC drugs. The future of SPAMS shows promise in expanding this drug application also to illicit drug testing.

The detection of illicit drugs with SPAMS is a natural extension of the current work. Forensic laboratories would benefit from this ability. In the future, illicit drug samples could be obtained from the Drug Enforcement Agency and analyzed in small quantities using SPAMS. Alarm files could be created from these data and unknown drug samples could be analyzed and characterized using alarm files. However, cutting agents, filler materials, synthetic impurities and byproducts may be present in the 'real world' drug samples. These additives are problematic in that they may interfere with the alarm identification, but are useful in that they may provide information on the synthetic origin of a sample, useful for forensic attribution.[1] Therefore, standard cutting agents, impurities, and byproducts should also be tested, alarm files created for these compounds, and the illicit drug alarm files adjusted to allow identification in these complex matrices. Some common cutting materials in illicit drugs include pseudoephedrine, caffeine, procaine, baking soda, evaporated milk, and salt, some of which have been previously studied with SPAMS.

Once alarm files are operable, SPAMS could become a powerful tool for drug detection in a forensic laboratory. The National Forensic Laboratory Information System (NFLIS), reports that U.S. state and local laboratories analyzed ~1.9 million drug items in 2006.[3] The Census of Publicly Funded Forensic Crime Laboratories reported in 2002 that the overwhelming number of requests caused a backlog of 233,000 samples. The fast analysis time, as well as the ability to perform *in situ* analyses of SPAMS would be beneficial in reducing this massive caseload.

Further development of SPAMS may benefit from modification of the solid tablet sampling apparatus. The current device is made from a glass sampling vial; however, the

transport efficiency of aerosol particles can be influenced by the charge of the particles and interactions of particles with the container. Thus, a non-glass sample introduction device is expected to yield a higher efficiency of particles for SPAMS characterization.

5-2-2: Breath Analysis

This work was initially approached with a single overarching goal: develop a detection scheme that can be used to identify an individual that has been using illicit materials (e.g. explosives) based on characteristic compounds in their breath. This goal was set based on the current political climate and needs of the United States military and government to protect its citizens, soldiers, and innocent civilians, from terrorist attacks, specifically those involving improvised explosive devices (IEDs). Unfortunately, as fast as science and technology evolve on the defense and detection side, so too do they evolve on the side of those who wish to use science and technology with malicious intention. The constant battle waged by U.S. government-funded defense science of the 21st century is to evolve at a faster pace than the evolution of malicious science. But evolution speed is not the only important factor in such a research project. A fundamental understanding of the processes being studied as well as the analytical thoroughness of the work and its place in a larger context are also crucial. Thus, a technique developed without attention to these factors may be doomed to failure in the future if the fundamentals are not also studied.

This work began with a two-fold approach – seek out subjects who may have exposure to explosives who can serve to provide initial signatures and proof of concept results to determine if breath analysis will be successful at detecting explosive markers on breath,

and perform more fundamental studies into what constituents are present in breath, how they can best be detected, and what useful results can be obtained from this relatively understudied matrix. This two-fold approach focused on both the speed of evolution and the analytical thoroughness in parallel.

This research has developed and evaluated a breath analysis technique that has been proven effective at detecting explosives and explosive-related compounds in human breath after exposure to these substances. The technique uses commercial instrumentation which would allow it to be disseminated and used in any lab with a standard GC-MS almost instantaneously. The original goal of the project has therefore been met. But along the way, the dual nature of the scientific approach to this problem allowed additional useful information to be discovered from studies involving unintentional chemical exposure at nail salons, in hardware stores, and from dietary intake, which contributed to the development of a stronger detection method, and added more confidence in the results obtained from the exposures to explosives.

The future of this work must then build upon current results pertinent to explosives detection. In order to advance breath analysis for the detection of explosive makers, enhancements to the sampling and detection system should be made to allow for a field-deployable device. The constant push for deployable systems requires a smaller size both in footprint and weight, low power consumption, higher sensitivity and selectivity, and a shorter analysis time. In order to meet these criteria, significant changes will need to be made to the analytical scheme.

In order to reduce the size of the device, the detector may need to be changed. While GC-MS is a powerful analytical tool, it does not serve well for miniaturization. Mini-GCs have been developed and show remarkable efficiencies and resolving power; however, miniaturizing a mass spectrometer has been more challenging. Although miniature mass analyzers have been developed,[2-5] it is the remainder of the system, including the electronics, power supplies, and vacuum systems that are difficult to miniaturize while retaining functionality and the pumping speeds necessary to maintain the required vacuum. GC-GC, and GC-DMS have been successfully miniaturized, and may show promise for the future of breath analysis. Another aspect that will have to be miniaturized and incorporated into a hand-held system is the preconcentrating device, currently the SPME fiber. The ideal system would incorporate the preconcentrator in an in-line manner, so the sample could be obtained, preconcentrated, and analyzed in a single action. Options for miniaturized preconcentrators are plentiful, as even the polymer on the SPME fibers used in the current study could be incorporated in a high-surface area manner onto different miniaturized structures. Carbon nanotubes or micropore or micropillar technologies are also in development at various laboratories, and these technologies may be useful for a future breath analyzer. The preconcentrator may also be adapted to increase the sensitivity and control the selectivity of a future instrument by selecting materials that would preferentially absorb the compounds of interest. These preconcentrating materials could perhaps be arranged in a consecutive fashion so that multiple materials specific to particular compounds could be used and serve as a crude separation step in the analysis.

In order to reduce the analysis time, the time of sampling must be reduced. If this time is to be cut, attention must be paid to what part of a breath is sampled. Figure 5- 1 shows a typical time capnogram which can be used to describe the respiration pattern of a healthy adult. Carbon dioxide is used as a tracer gas, and the capnogram shows at what points of respiration the concentration of CO_2 is the highest in the respiratory gas.[6]

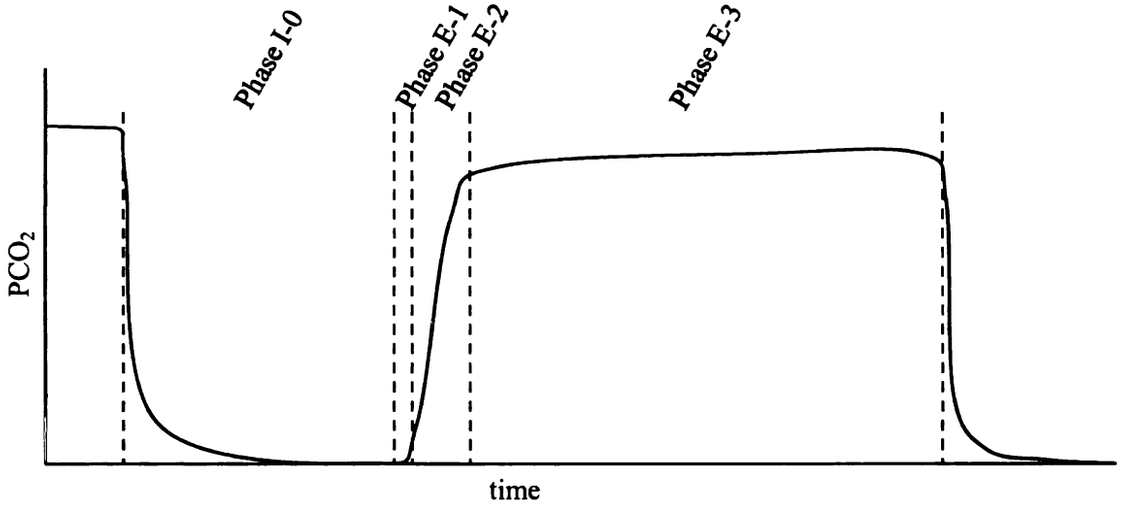

Figure 5- 1: Diagram of a typical time capnogram, which displays the concentration of carbon dioxide in respiratory gas. Inhalation is represented by Phase I-0, exhalation is represented by Phases E-1, E-2, and E-3, corresponding to exhalation of deadspace (CO_2 free) air, a mixture of dead space and alveolar air, and primarily alveolar air, respectively. Adapted from reference 6.

The present work sampled breath from all phases of respiration. It can be seen from the figure that the highest concentration of CO_2, and therefore other VOCs that diffuse across the pulmonary alveolar membrane, occurs during Phase E-3, when the exhalate contains primarily alveolar air. If the time during which a breath sample is obtained is reduced, efforts must be made to sample during Phase E-3, and not Phase E-1 or E-2, to ensure the sample is collected while the concentrations of VOCs are the highest. If the sensitivity

and surface area of the preconcentration material is improved, reducing the sampling time to this window should still provide enough signal for detection. Figure 5- 2 shows a potential schematic for a future breath analysis device, incorporating all of these modifications.

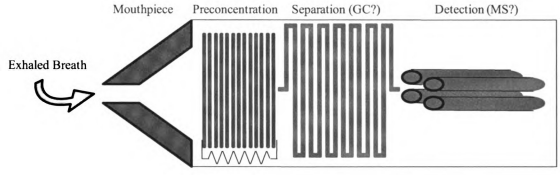

Figure 5- 2: Diagram of possible handheld breath analyzer. Breath is exhaled into the mouthpiece where it passes into a thermally controlled preconcentration region. After a predetermined period of time, the temperature of the preconcentrator is quickly ramped, desorbing the analytes of interest and allowing them to pass into the separation region, possibly a miniaturized GC where separation occurs. The eluent then passes into a detection system, possibly a miniaturized MS where the analytes are identified and a signal is reported to the user (signal digitization not shown).

This technique should not only be pursued for the detection of explosives on breath. This work demonstrated proof of concept data for the use of breath analysis for detecting the prior location of an individual based upon chemical signatures of breath constituents; however, this information also demonstrates a non-invasive way to monitor chemical exposure. Another promising avenue of research may be found in the oral exposure studies that were pursued. This presents breath analysis as a method for assessing the dynamics of the metabolic processes in an individual. The ability to visualize the absorption and uptake phase of exposure would also provide valuable pharmacokinetic

data if similar behaviors were measured for other orally ingested drugs or compounds. Using breath to monitor intravenous exposure to drugs or chemicals would also present potential applications for breath analysis, but would require subjects to already be undergoing medical treatment, and may be difficult to justify to an Institutional Review Board.

Several avenues of research should be pursued to improve the breath research field. There is no accepted and standardized method for breath collection and analysis. This makes it difficult to compare results with those of another laboratory using a different system. It is hoped that the future will hold some standardization practices and recommendations. This should include the temperature and time of breath collection, flow rate of breathing, type of sampling (alveolar versus total air), material of the collection device, and preconcentration methods. The field would also benefit from the existence of a breath reference standard. Figures of merit and analytical method performance are difficult to establish without a standard breath, and no two human breaths are exactly alike. Although an EBC standard would not be ideal for experiments involving the collection of EBV, condensate may be a more reliable standard, as a real breath would contain a mixture of vapor and suspended aerosols that would not be amenable to storage, and condensate could be refrigerated or frozen for stability. In whatever form, this standard would have to contain a complex matrix similar to that of human breath, resulting in hundreds of compounds being necessary. Once a standard is developed it would be a logical step to spike this breath sample with target compounds to determine more reliable limits of detection. Such fundamental studies would allow data

to be more easily compared across research groups, and would improve the possibility of successful applications of breath analysis.

5-3: References

(1) Peterson, J. L.; Hickman, M. J. In *Bureau of Justice Statistics Bulletin*; U.S. Department of Justice, **2005**.

(2) Henry, C. M. *Chemical and Engineering News* **2002**, *80*, 34-35.

(3) Laughlin, B. C.; Mulligan, C. C.; Cooks, R. G. *Anal. Chem.* **2005**, *77*, 2928-2939.

(4) Badman, E. R.; Cooks, R. G. *J. Mass Spectrom.* **2000**, *35*, 659-671.

(5) Fico, M.; Yu, M.; Ouyang, Z.; Cooks, R. G.; Chappell, W. J. *Anal. Chem.* **2007**, *79*, 8076-8082.

(6) Bhavani-Shankar, K.; Philip, J. H. *Anesth. Analg.* **2000**, *91*, 973-977.

APPENDIX A – Additional Rules Trees for Drug Identification Using SPAMS

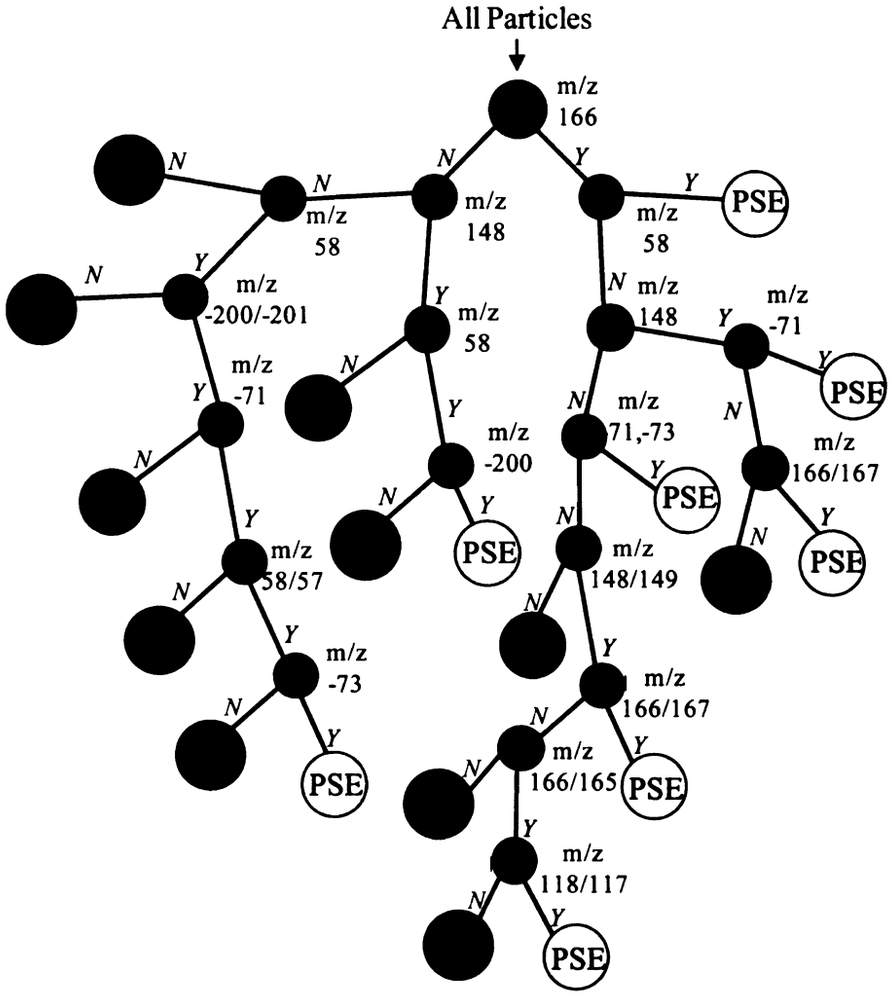

Figure A- 1: Rules tree for classification of pseudoephedrine. The mass vectors probed at each branch division are shown, with 'Y' indicating a positive response and 'N' indicating a negative response. Circles labeled 'PSE' indicate a positive identification for pseudoephedrine; circles labeled 'Null' indicate a negative response.

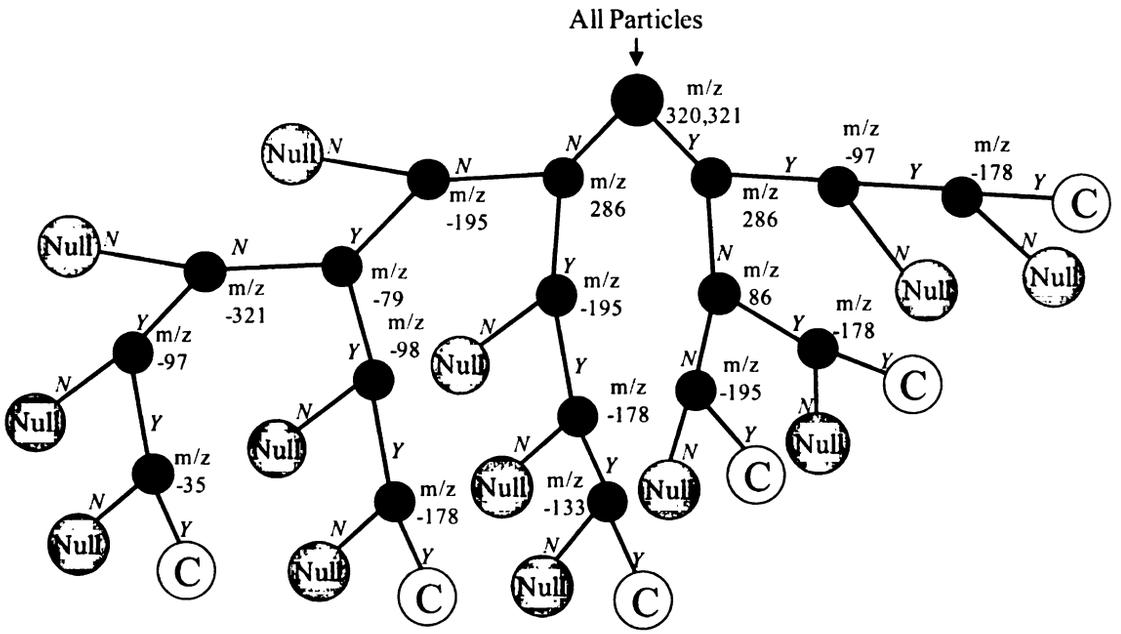

Figure A- 2: Rules tree for classification of Coricidin. The mass vectors probed at each branch division are shown, with 'Y' indicating a positive response and 'N' indicating a negative response. Circles labeled 'C' indicate a positive identification for Coricidin; circles labeled 'Null' indicate a negative response.

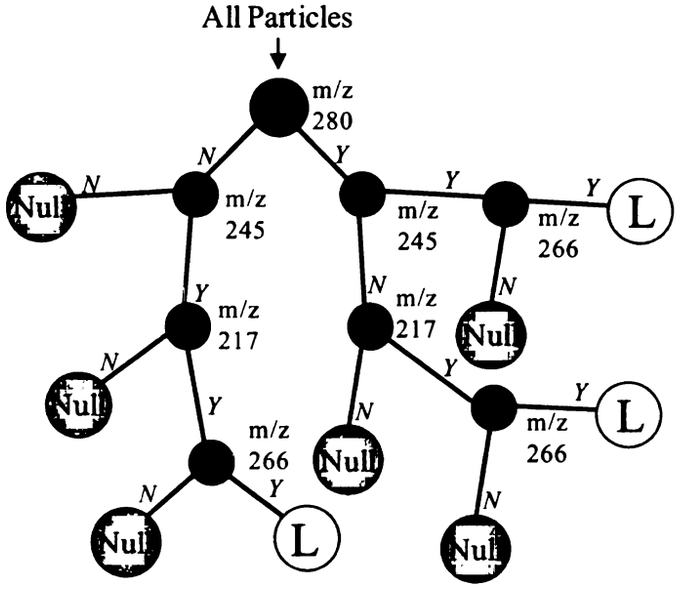

Figure A- 3: Rules tree for classification of loratadine. The mass vectors probed at each branch division are shown, with 'Y' indicating a positive response and 'N' indicating a negative response. Circles labeled 'L' indicate a positive identification for loratadine; circles labeled 'Null' indicate a negative response.

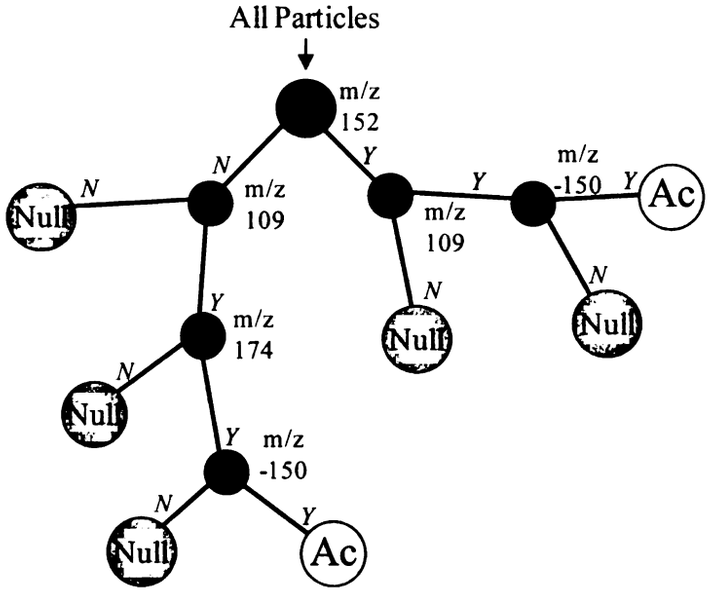

Figure A- 4: Rules tree for classification of acetaminophen. The mass vectors probed at each branch division are shown, with 'Y' indicating a positive response and 'N' indicating a negative response. Circles labeled 'Ac' indicate a positive identification for acetaminophen; circles labeled 'Null' indicate a negative response.

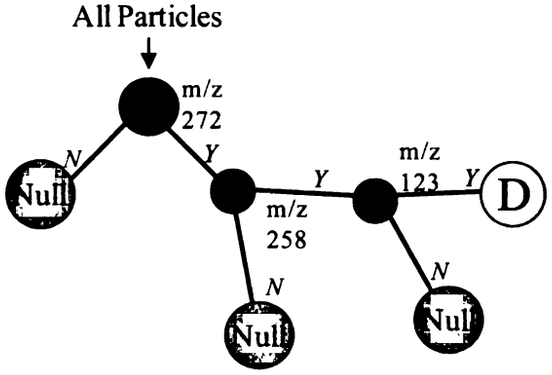

Figure A- 5: Rules tree for classification of dextromethorphan. The mass vectors probed at each branch division are shown, with 'Y' indicating a positive response and 'N' indicating a negative response. Circles labeled 'D' indicate a positive identification for dextromethorphan; circles labeled 'Null' indicate a negative response.

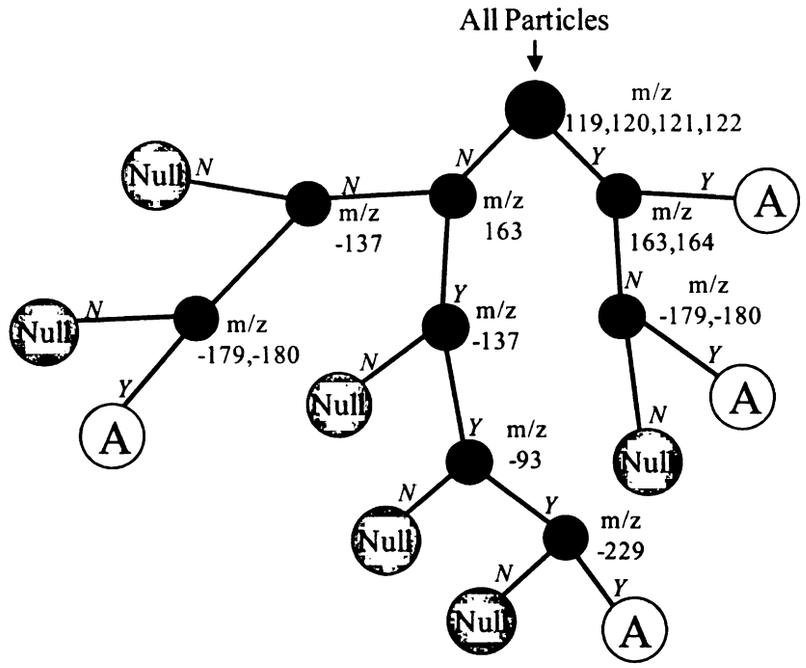

Figure A- 6: Rules tree for classification of aspirin. The mass vectors probed at each branch division are shown, with 'Y' indicating a positive response and 'N' indicating a negative response. Circles labeled 'A' indicate a positive identification for aspirin; circles labeled 'Null' indicate a negative response.

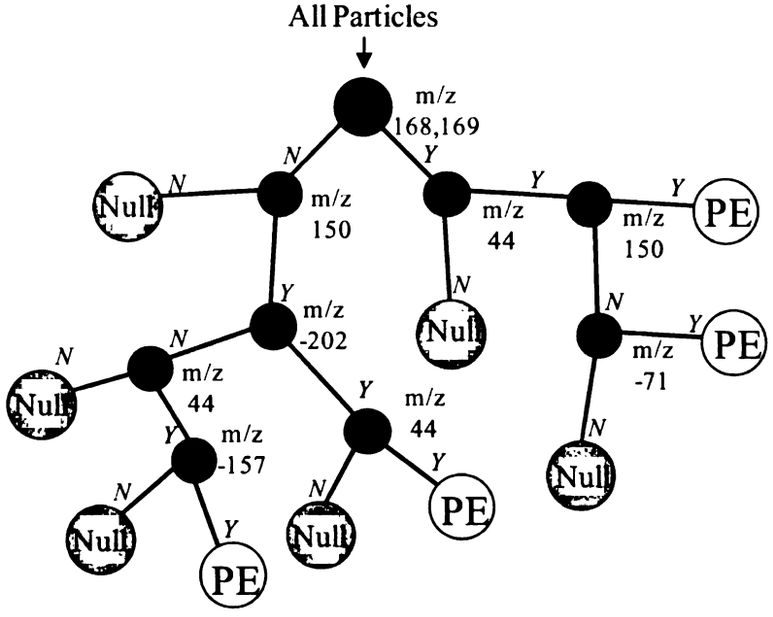

Figure A- 7: Rules tree for classification of phenylephrine. The mass vectors probed at each branch division are shown, with 'Y' indicating a positive response and 'N' indicating a negative response. Circles labeled 'PE' indicate a positive identification for phenylephrine; circles labeled 'Null' indicate a negative response.

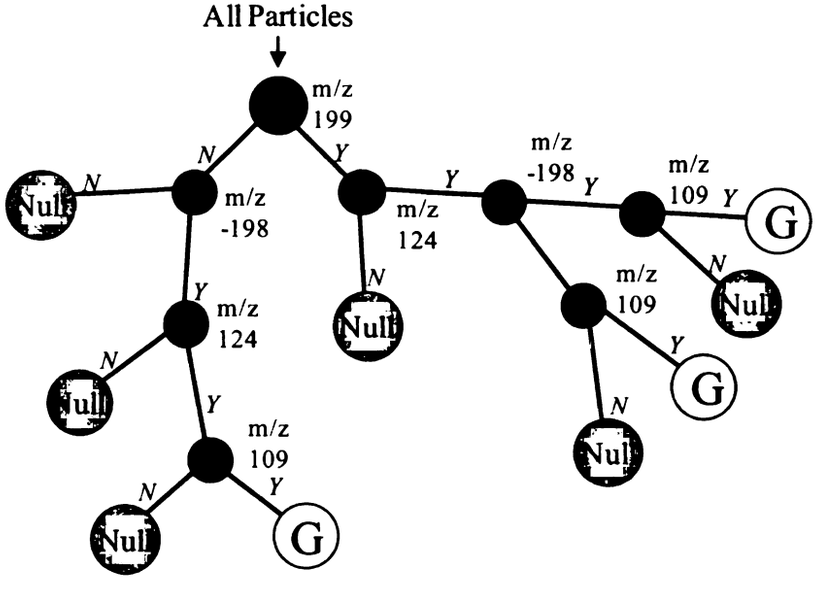

Figure A- 8: Rules tree for classification of guaifenesin. The mass vectors probed at each branch division are shown, with 'Y' indicating a positive response and 'N' indicating a negative response. Circles labeled 'G' indicate a positive identification for guaifenesin; circles labeled 'Null' indicate a negative response.

APPENDIX B - Additional Terpene and Terpenoid Data from Lemonade Consumption

Included herein are the data obtained from several subjects after consumption of original, concentrated, and Mediterranean lemonade. Thirteen terpenes and terpenoid compounds were monitored; peaks due to each compound in the TIC of each breath sample were integrated, and the area plotted versus time after lemonade consumption. The resulting curves were fit to Equation 4-1, describing the rise and decay in each compound. See Chapter 4 for additional information.

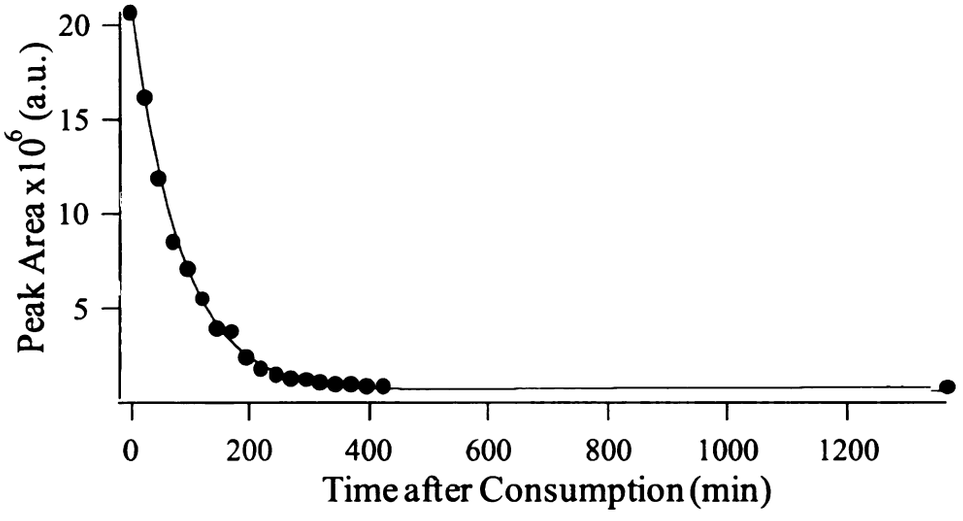

Figure B- 1: Integrated area of the peak attributed to α-limonene in chromatograms obtained from the breath of subject A on the first day of original lemonade consumption. The data has been fit with an exponential rise and decay (Equation 4-1). See Table B- 1 for fit parameters.

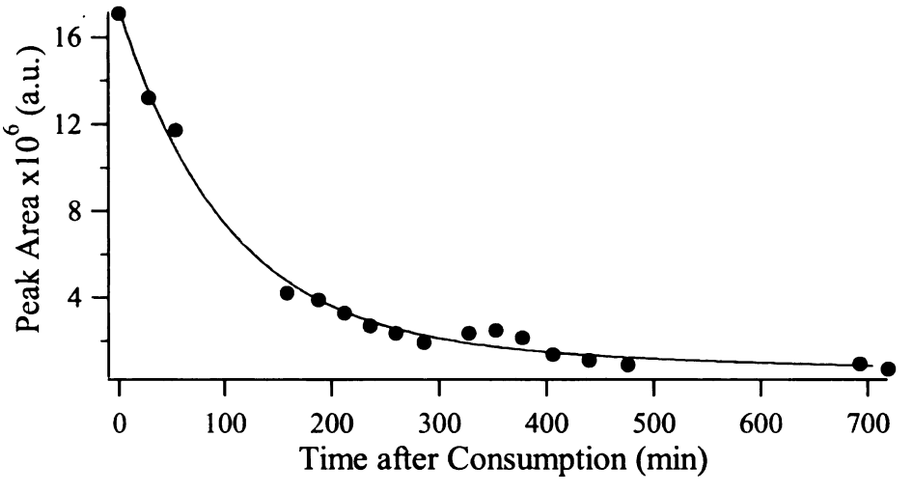

Figure B- 2: Integrated area of the peak attributed to α-limonene in chromatograms obtained from the breath of subject A on the second day of original lemonade consumption. The data has been fit with an exponential rise and decay (Equation 4-1). See Table B- 1 for fit parameters.

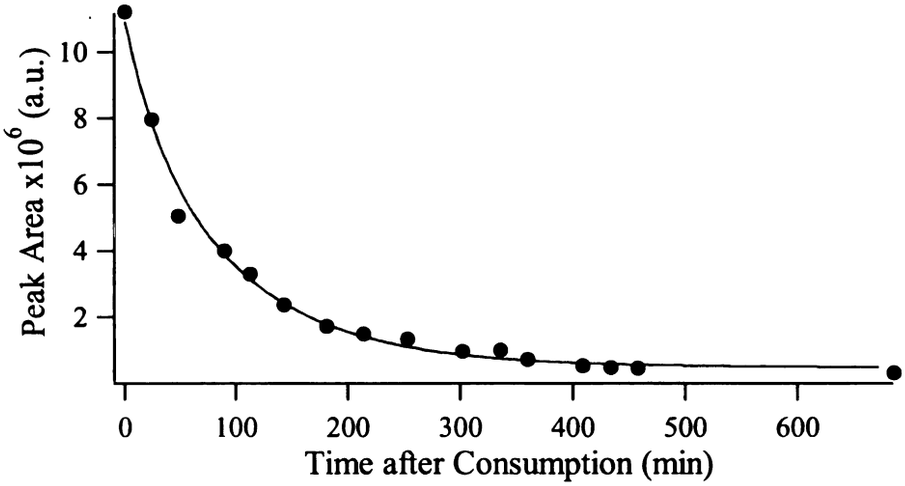

Figure B- 3: Integrated area of the peak attributed to α-limonene in chromatograms obtained from the breath of subject A on the third day of original lemonade consumption. The data has been fit with an exponential rise and decay (Equation 4-1). See Table B- 1 for fit parameters.

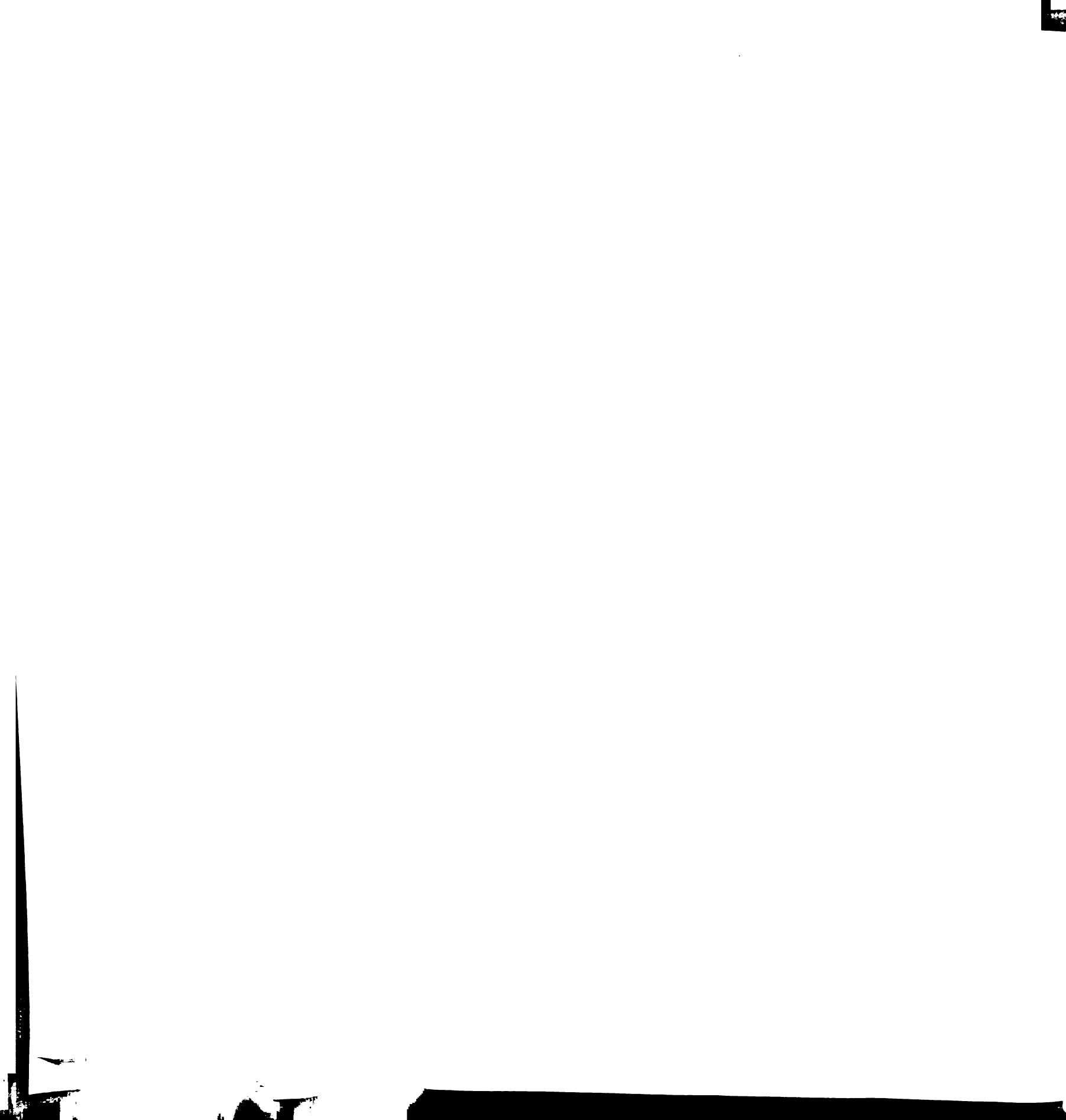

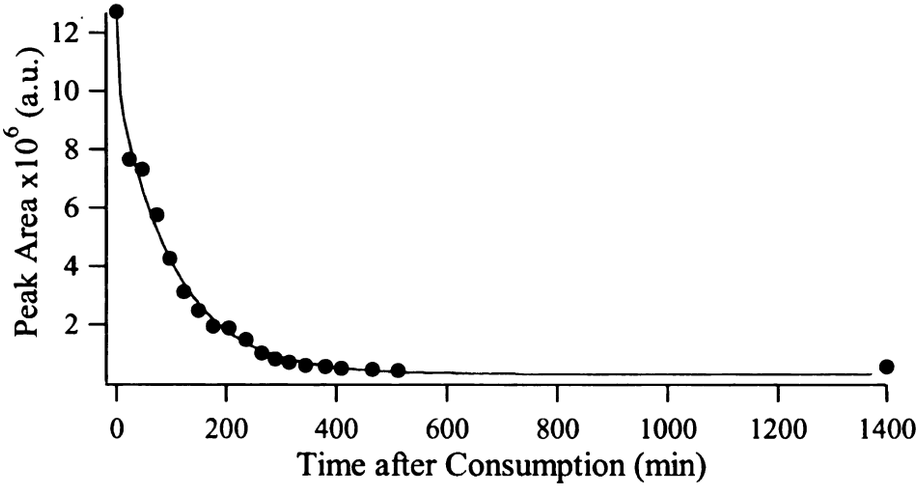

Figure B- 4: Integrated area of the peak attributed to α-limonene in chromatograms obtained from the breath of subject A on the fourth day of original lemonade consumption. The data has been fit with an exponential rise and decay (Equation 4-1). See Table B- 1 for fit parameters.

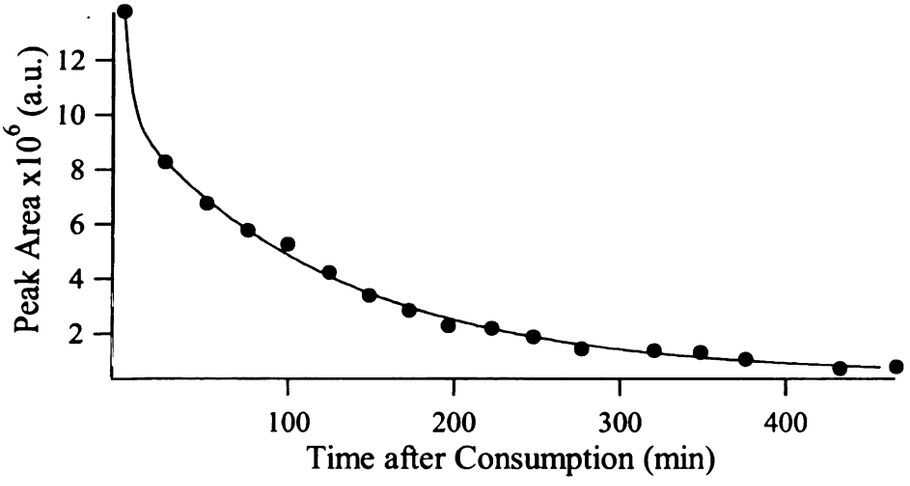

Figure B- 5: Integrated area of the peak attributed to α-limonene in chromatograms obtained from the breath of subject A on the fifth day of original lemonade consumption. The data has been fit with an exponential rise and decay (Equation 4-1). See Table B- 1 for fit parameters.

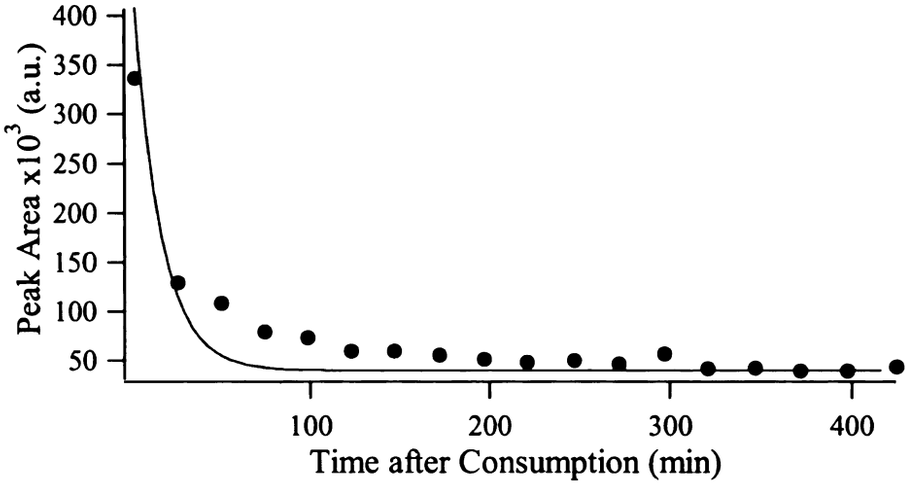

Figure B- 6: Integrated area of the peak attributed to 4-terpineol in chromatograms obtained from the breath of subject A on the first day of original lemonade consumption. The data has been fit with an exponential rise and decay (Equation 4-1). See Table B- 1 for fit parameters.

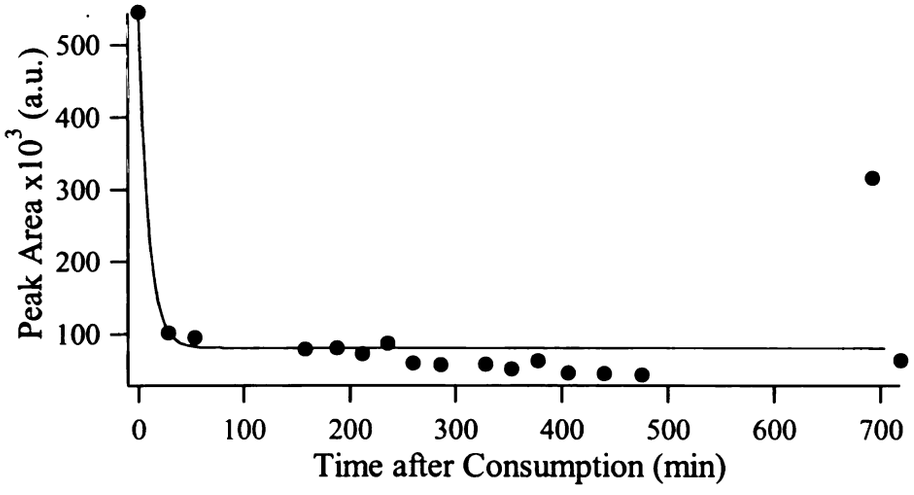

Figure B- 7: Integrated area of the peak attributed to 4-terpineol in chromatograms obtained from the breath of subject A on the second day of original lemonade consumption. The data has been fit with an exponential rise and decay (Equation 4-1). See Table B- 1 for fit parameters.

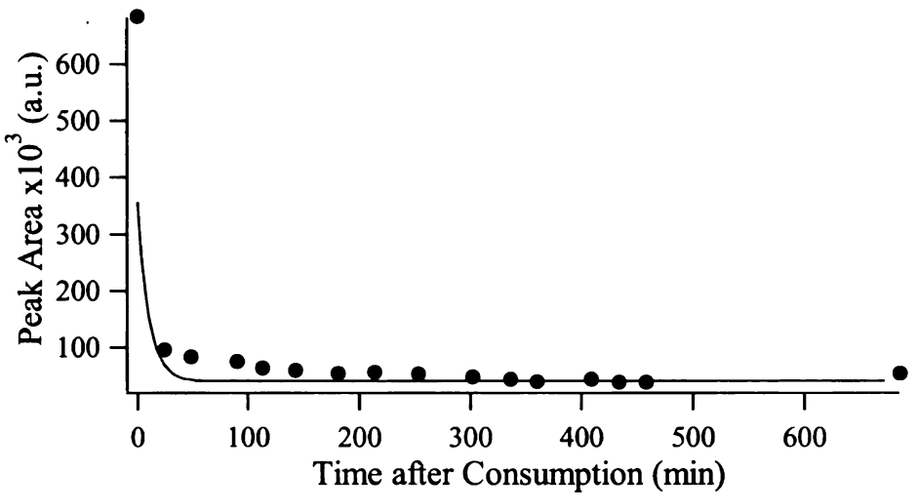

Figure B- 8: Integrated area of the peak attributed to 4-terpineol in chromatograms obtained from the breath of subject A on the third day of original lemonade consumption. The data has been fit with an exponential rise and decay (Equation 4-1). See Table B- 1 for fit parameters.

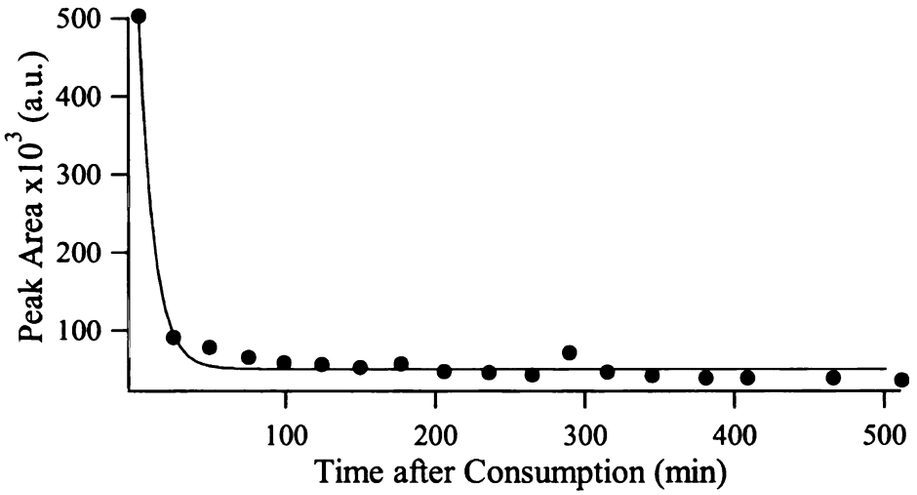

Figure B- 9: Integrated area of the peak attributed to 4-terpineol in chromatograms obtained from the breath of subject A on the fourth day of original lemonade consumption. The data has been fit with an exponential rise and decay (Equation 4-1). See Table B- 1 for fit parameters.

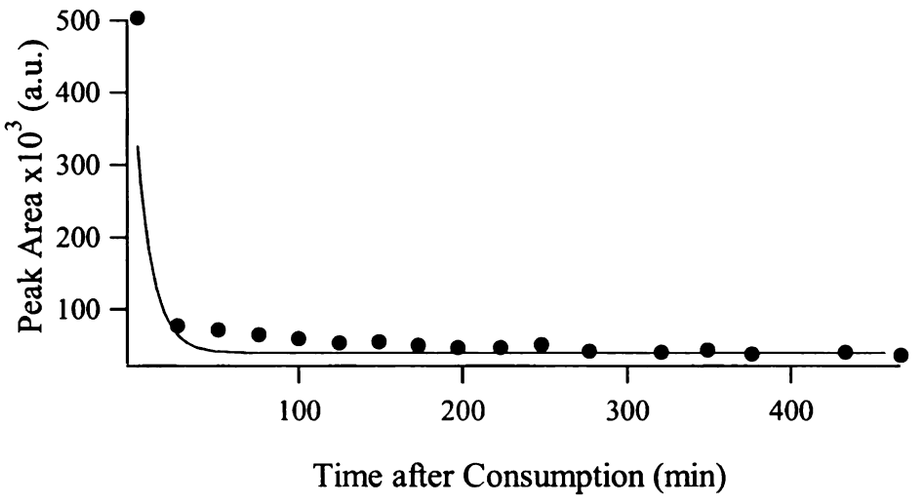

Figure B- 10: Integrated area of the peak attributed to 4-terpineol in chromatograms obtained from the breath of subject A on the fifth day of original lemonade consumption. The data has been fit with an exponential rise and decay (Equation 4-1). See Table B-1 for fit parameters.

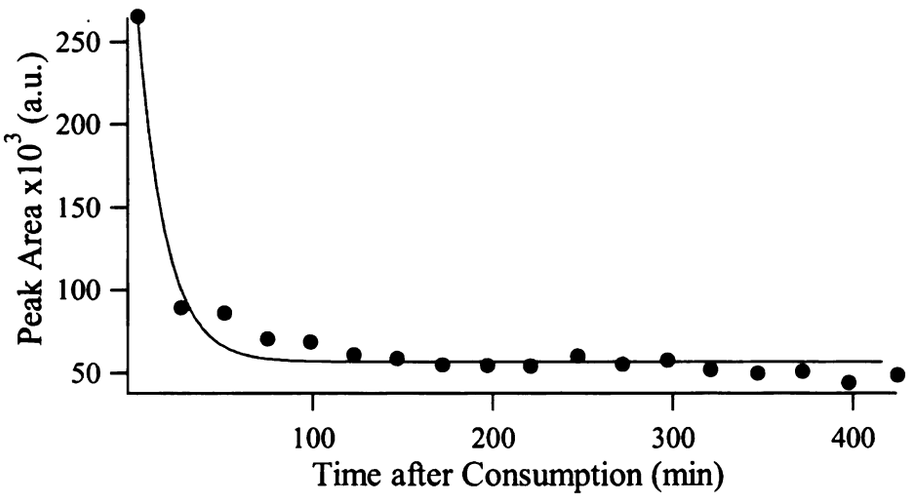

Figure B- 11: Integrated area of the peak attributed to α-terpineol in chromatograms obtained from the breath of subject A on the first day of original lemonade consumption. The data has been fit with an exponential rise and decay (Equation 4-1). See Table B-1 for fit parameters.

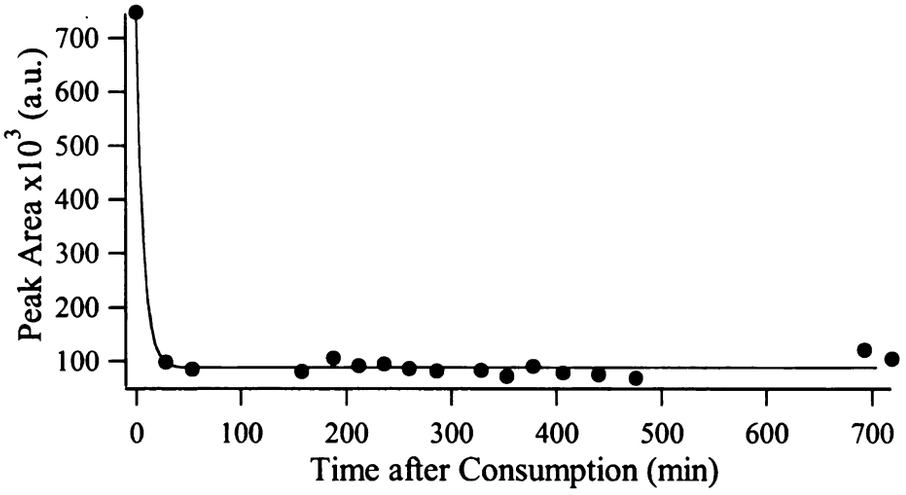

Figure B- 12: Integrated area of the peak attributed to α-terpineol in chromatograms obtained from the breath of subject A on the second day of original lemonade consumption. The data has been fit with an exponential rise and decay (Equation 4-1). See Table B-1 for fit parameters.

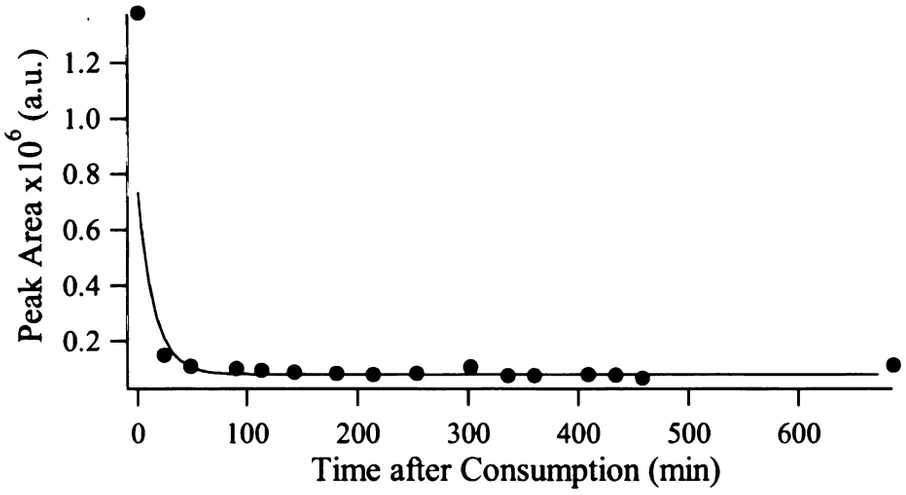

Figure B- 13: Integrated area of the peak attributed to α-terpineol in chromatograms obtained from the breath of subject A on the third day of original lemonade consumption. The data has been fit with an exponential rise and decay (Equation 4-1). See Table B-1 for fit parameters.

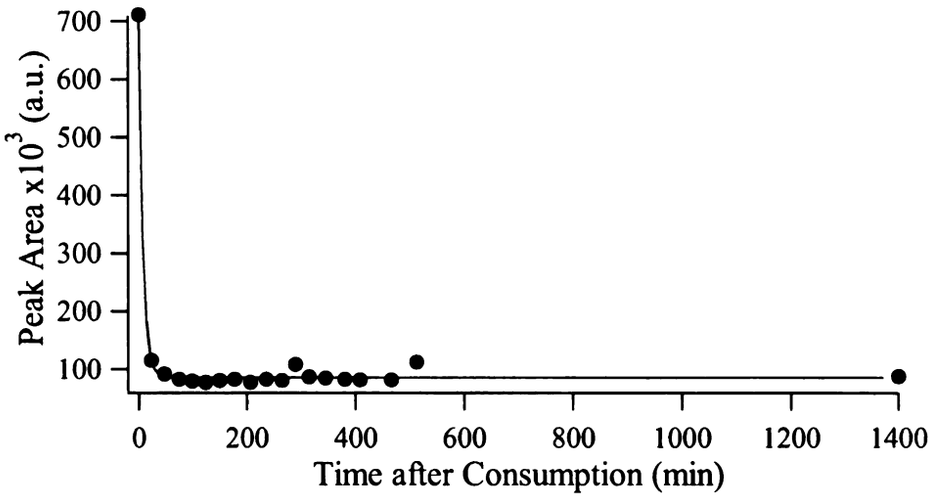

Figure B- 14: Integrated area of the peak attributed to α-terpineol in chromatograms obtained from the breath of subject A on the fourth day of original lemonade consumption. The data has been fit with an exponential rise and decay (Equation 4-1). See Table B-1 for fit parameters.

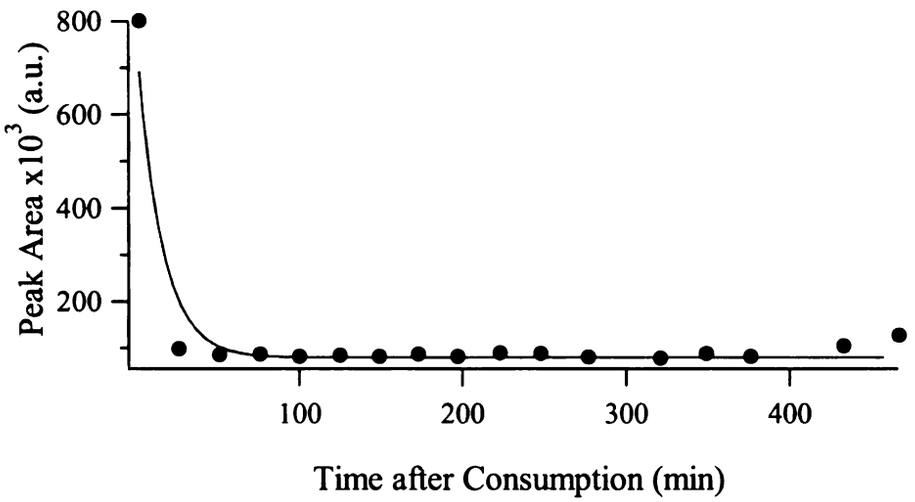

Figure B- 15: Integrated area of the peak attributed to α-terpineol in chromatograms obtained from the breath of subject A on the fifth day of original lemonade consumption. The data has been fit with an exponential rise and decay (Equation 4-1). See Table B-1 for fit parameters.

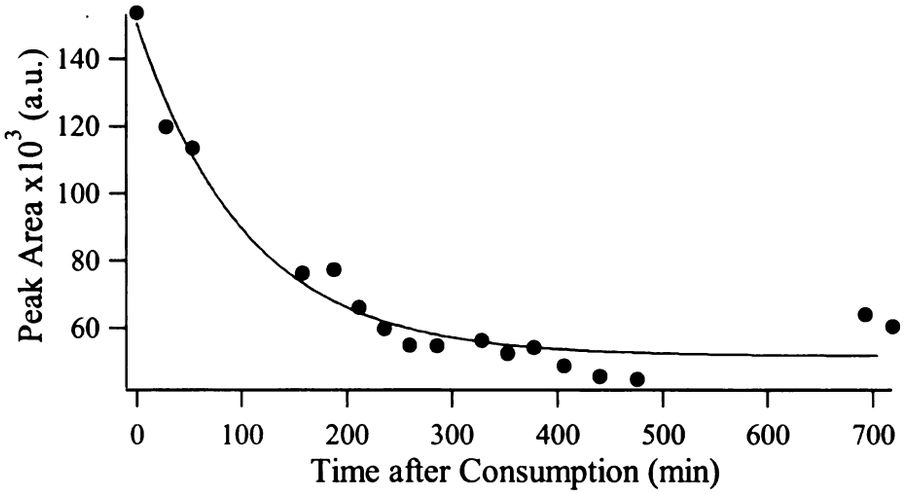

Figure B- 16: Integrated area of the peak attributed to α-terpinene in chromatograms obtained from the breath of subject A on the first day of original lemonade consumption. The data has been fit with an exponential rise and decay (Equation 4-1). See Table B-1 for fit parameters.

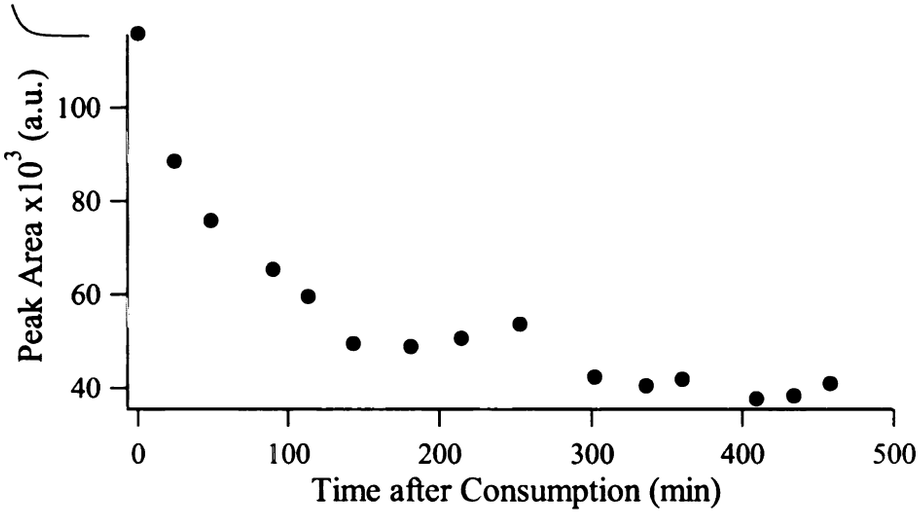

Figure B- 17: Integrated area of the peak attributed to α-terpinene in chromatograms obtained from the breath of subject A on the second day of original lemonade consumption. The data has been fit with an exponential rise and decay (Equation 4-1). See Table B-1 for fit parameters.

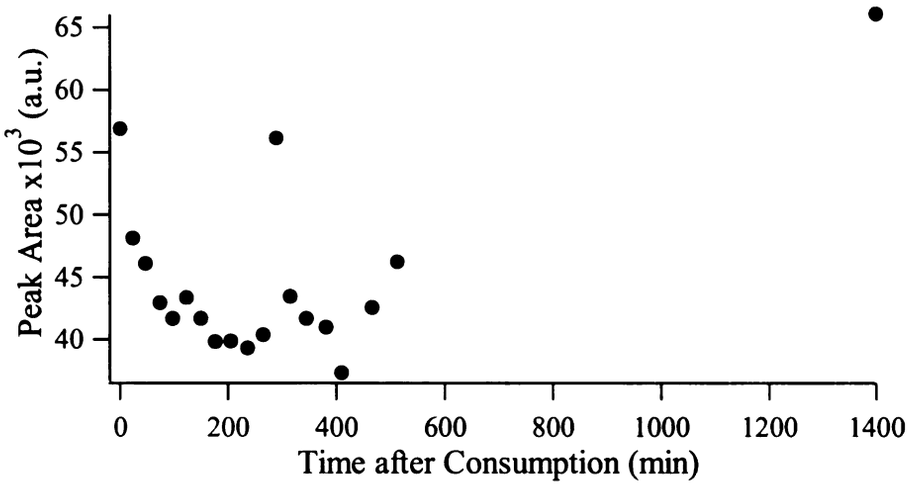

Figure B- 18: Integrated area of the peak attributed to α-terpinene in chromatograms obtained from the breath of subject A on the third day of original lemonade consumption. See Table B-1 for fit parameters.

Figure B- 19: Integrated area of the peak attributed to α-terpinene in chromatograms obtained from the breath of subject A on the fourth day of original lemonade consumption. The data has been fit with an exponential rise and decay (Equation 4-1). See Table B-1 for fit parameters.

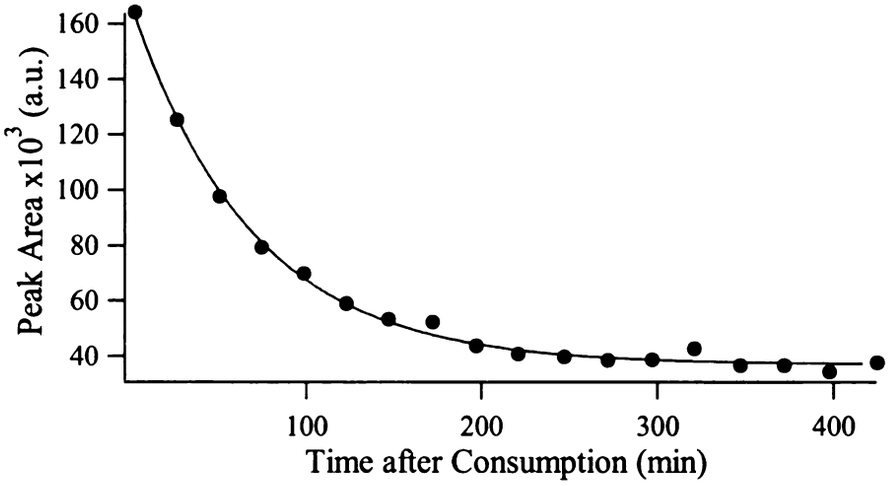

Figure B- 20: Integrated area of the peak attributed to α-terpinene in chromatograms obtained from the breath of subject A on the fifth day of original lemonade consumption. The data has been fit with an exponential rise and decay (Equation 4-1). See Table B-1 for fit parameters.

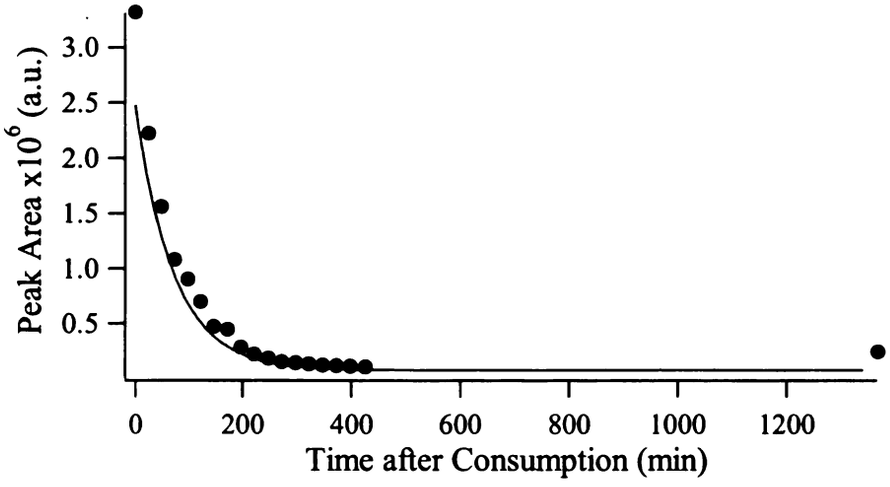

Figure B- 21: Integrated area of the peak attributed to γ-terpinene in chromatograms obtained from the breath of subject A on the first day of original lemonade consumption. The data has been fit with an exponential rise and decay (Equation 4-1). See Table B-1 for fit parameters.

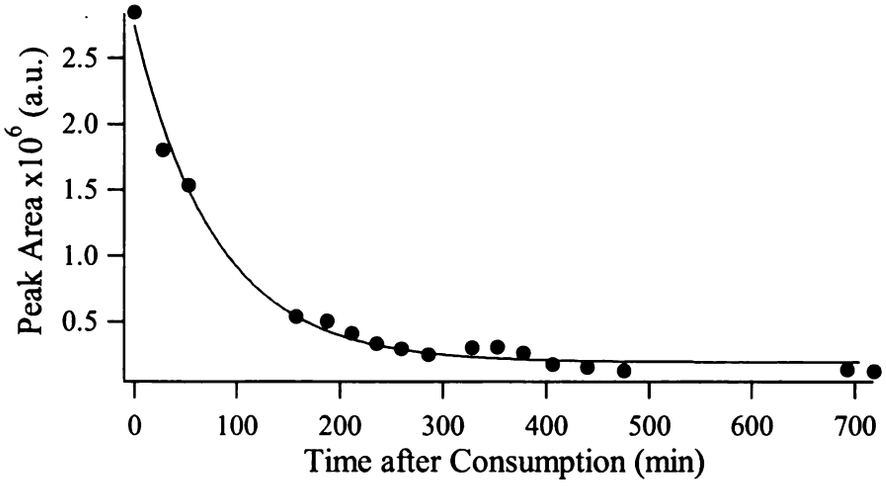

Figure B- 22: Integrated area of the peak attributed to γ-terpinene in chromatograms obtained from the breath of subject A on the second day of original lemonade consumption. The data has been fit with an exponential rise and decay (Equation 4-1). See Table B-1 for fit parameters.

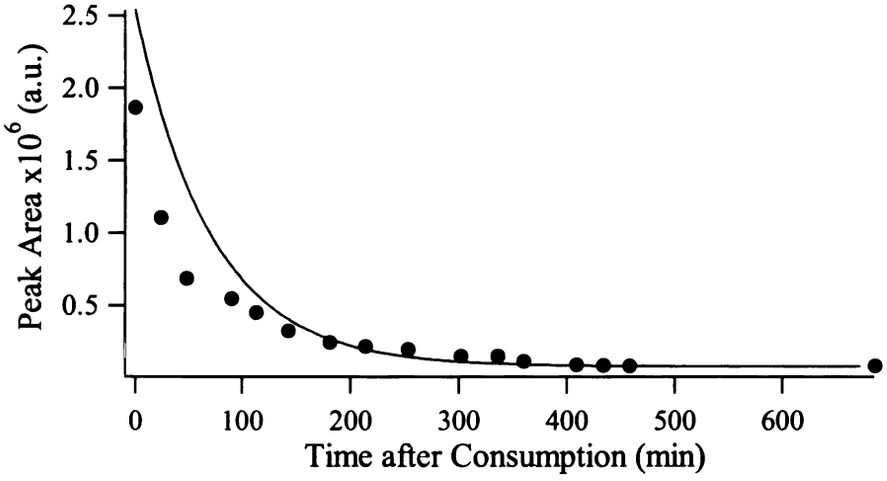

Figure B- 23: Integrated area of the peak attributed to γ-terpinene in chromatograms obtained from the breath of subject A on the third day of original lemonade consumption. The data has been fit with an exponential rise and decay (Equation 4-1). See Table B-1 for fit parameters.

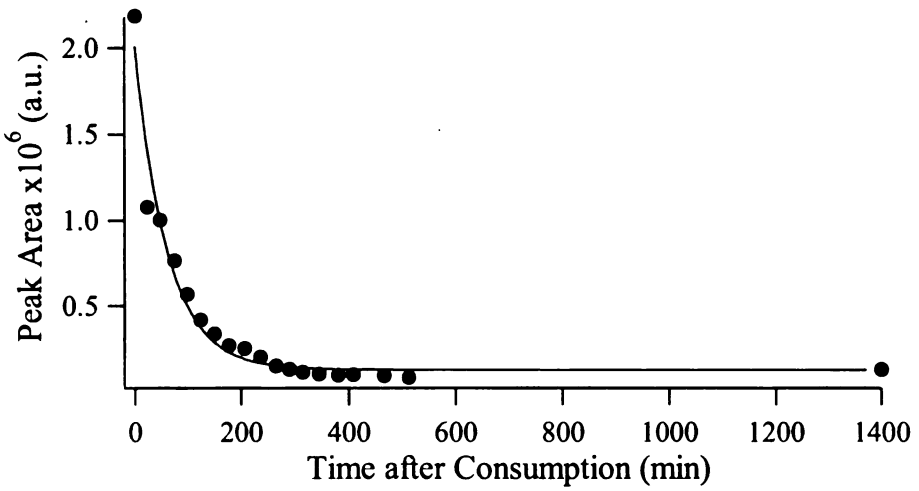

Figure B- 24: Integrated area of the peak attributed to γ-terpinene in chromatograms obtained from the breath of subject A on the fourth day of original lemonade consumption. The data has been fit with an exponential rise and decay (Equation 4-1). See Table B-1 for fit parameters.

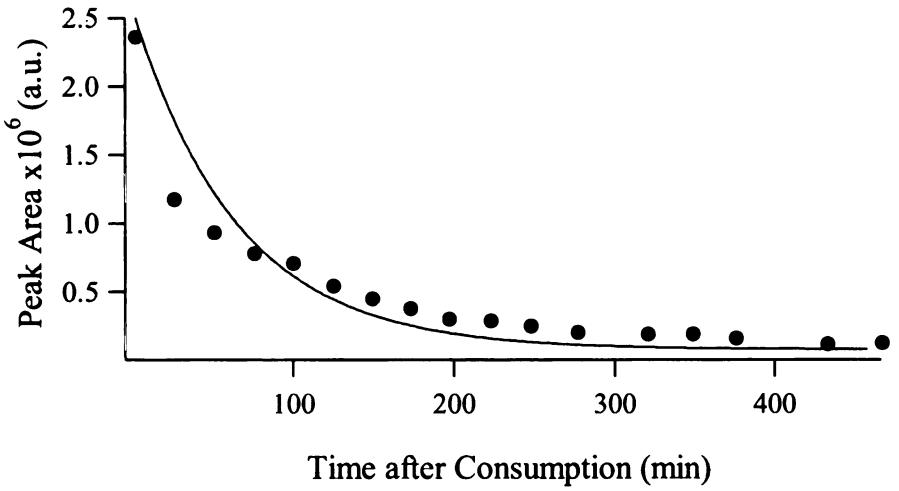

Figure B- 25: Integrated area of the peak attributed to γ-terpinene in chromatograms obtained from the breath of subject A on the fifth day of original lemonade consumption. The data has been fit with an exponential rise and decay (Equation 4-1). See Table B-1 for fit parameters.

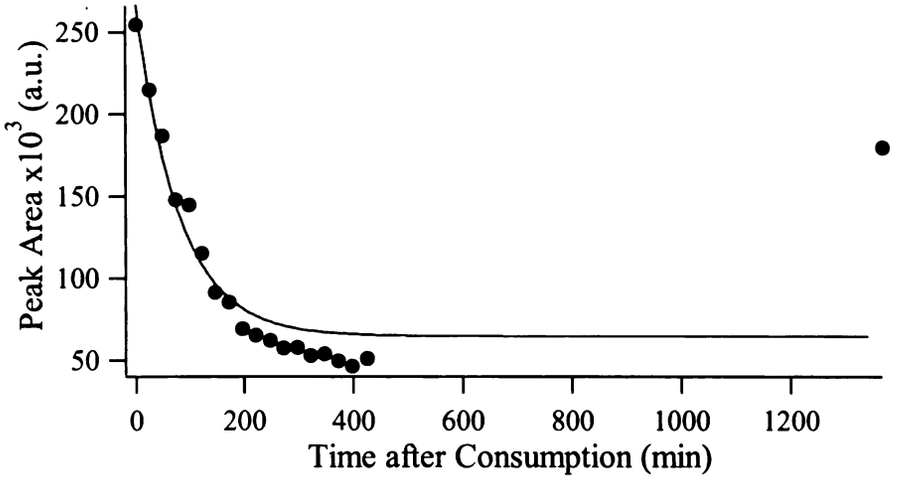

Figure B- 26: Integrated area of the peak attributed to terpinolene in chromatograms obtained from the breath of subject A on the first day of original lemonade consumption. The data has been fit with an exponential rise and decay (Equation 4-1). See Table B-1 for fit parameters.

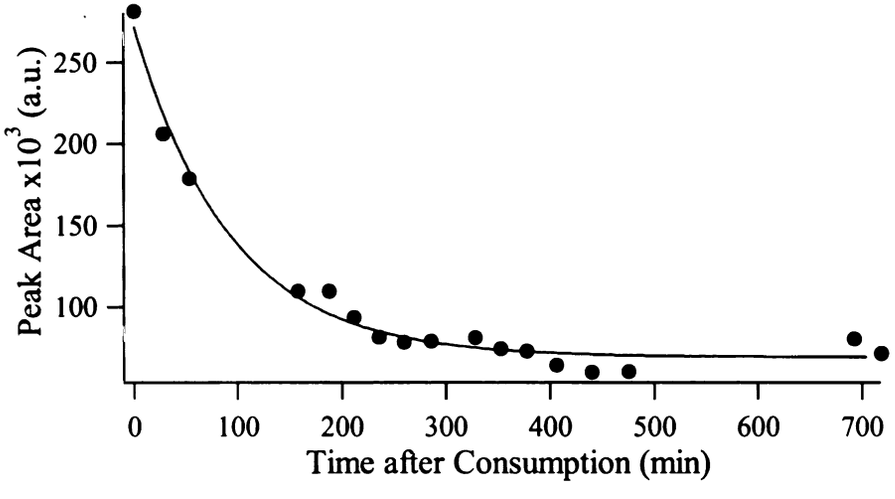

Figure B- 27: Integrated area of the peak attributed to terpinolene in chromatograms obtained from the breath of subject A on the second day of original lemonade consumption. The data has been fit with an exponential rise and decay (Equation 4-1). See Table B-1 for fit parameters.

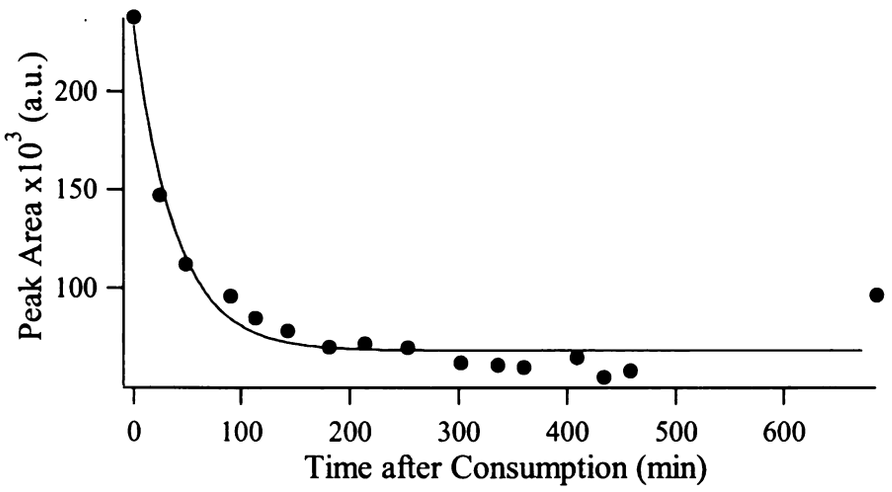

Figure B- 28: Integrated area of the peak attributed to terpinolene in chromatograms obtained from the breath of subject A on the third day of original lemonade consumption. The data has been fit with an exponential rise and decay (Equation 4-1). See Table B-1 for fit parameters.

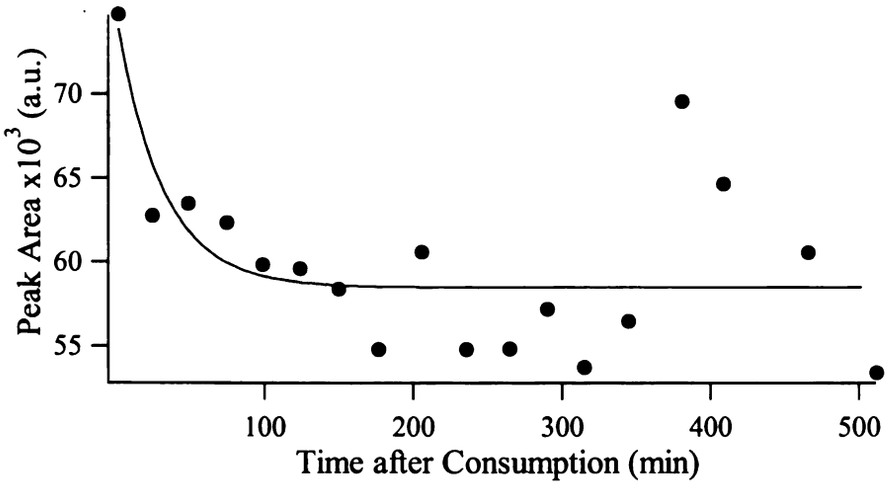

Figure B- 29: Integrated area of the peak attributed to terpinolene in chromatograms obtained from the breath of subject A on the fourth day of original lemonade consumption. The data has been fit with an exponential rise and decay (Equation 4-1). See Table B-1 for fit parameters.

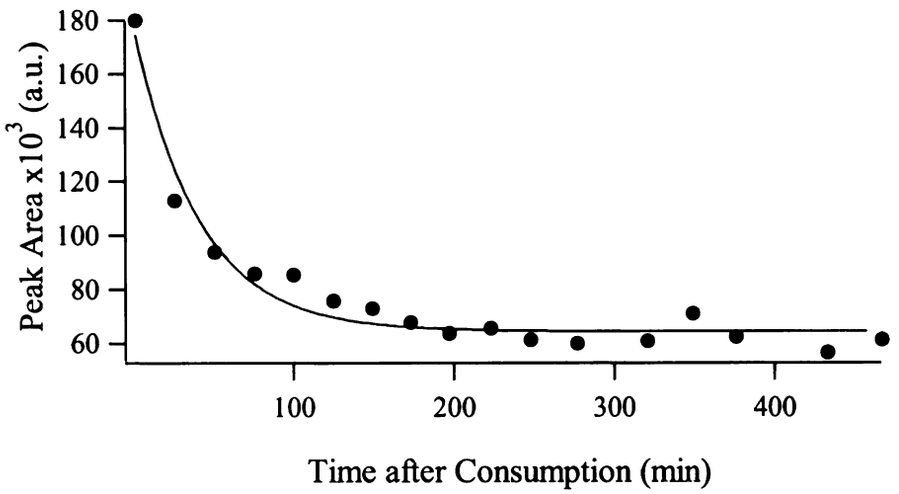

Figure B- 30: Integrated area of the peak attributed to terpinolene in chromatograms obtained from the breath of subject A on the fifth day of original lemonade consumption. The data has been fit with an exponential rise and decay (Equation 4-1). See Table B-1 for fit parameters.

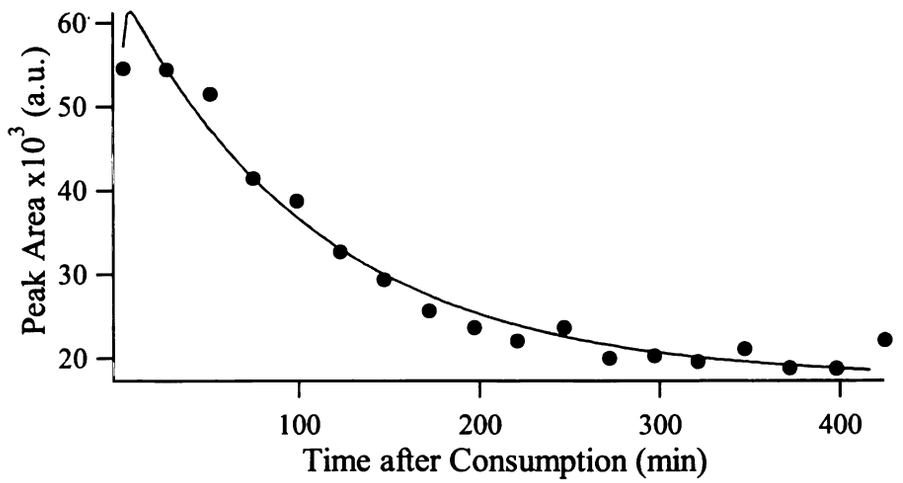

Figure B- 31: Integrated area of the peak attributed to camphene in chromatograms obtained from the breath of subject A on the first day of original lemonade consumption. The data has been fit with an exponential rise and decay (Equation 4-1). See Table B-1 for fit parameters.

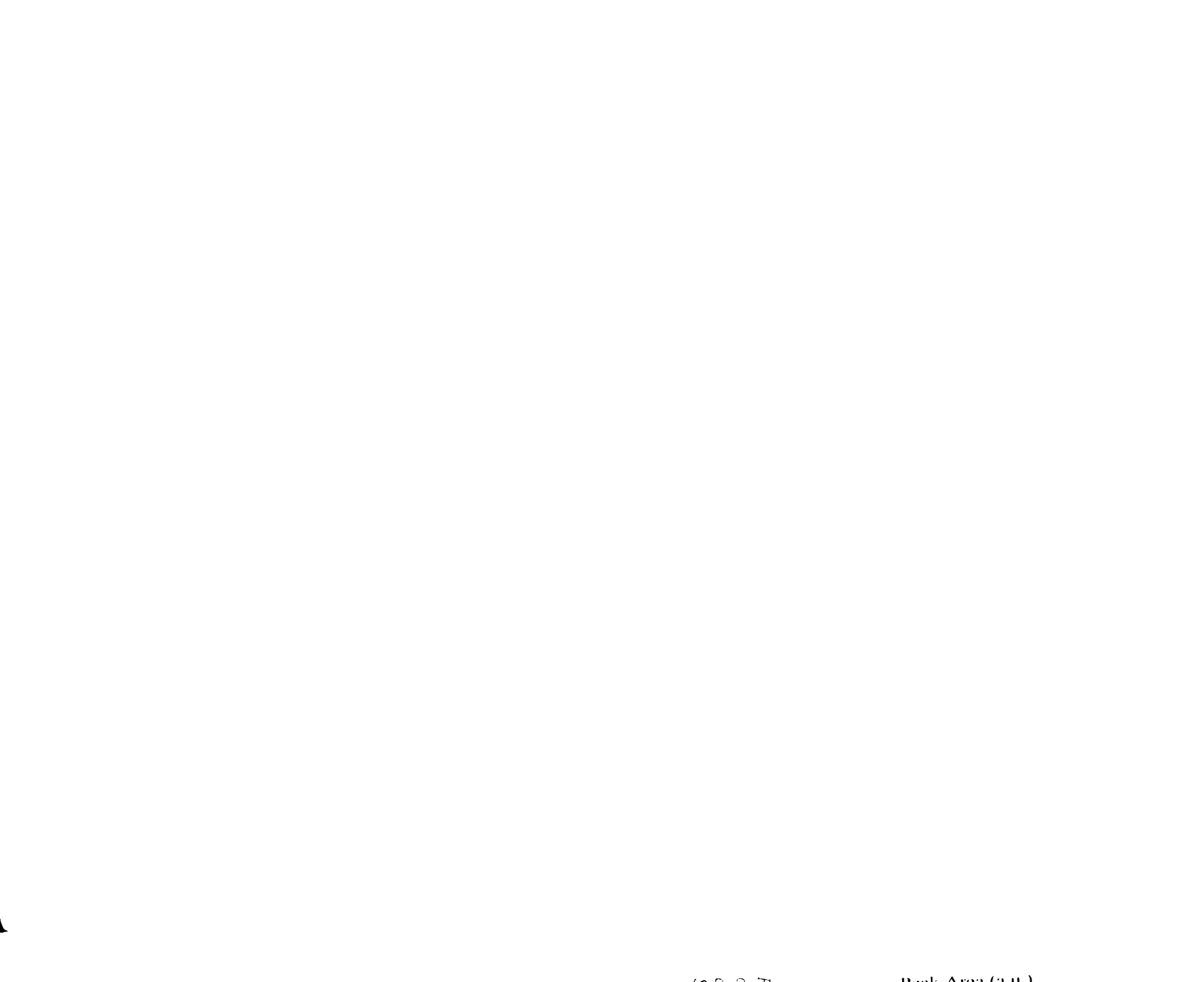
Bank Area (sq.ft.)

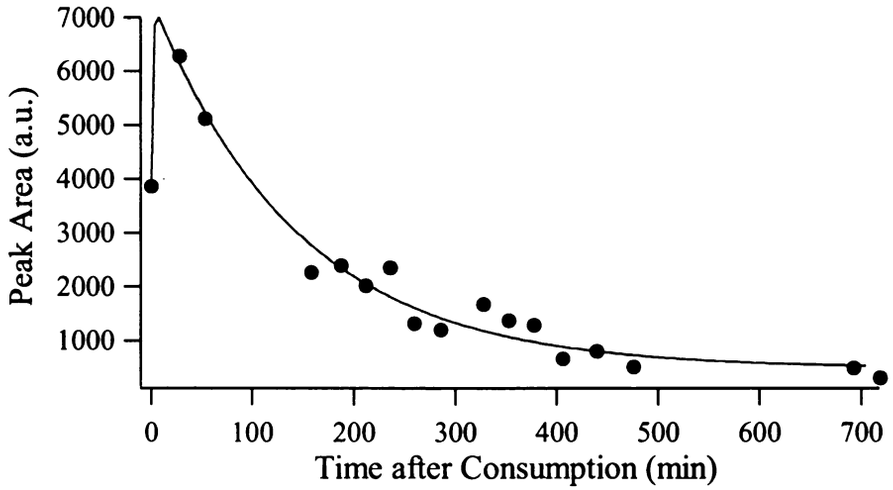

Figure B- 32: Integrated area of the peak attributed to camphene in chromatograms obtained from the breath of subject A on the second day of original lemonade consumption. The data has been fit with an exponential rise and decay (Equation 4-1). See Table B-1 for fit parameters.

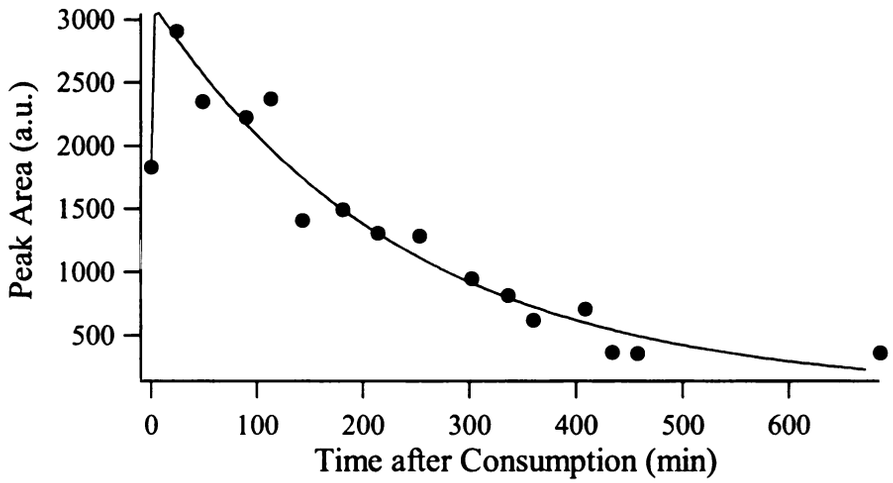

Figure B- 33: Integrated area of the peak attributed to camphene in chromatograms obtained from the breath of subject A on the third day of original lemonade consumption. The data has been fit with an exponential rise and decay (Equation 4-1). See Table B-1 for fit parameters.

Peak Area (a.u.)

Fig
ob
co
Se

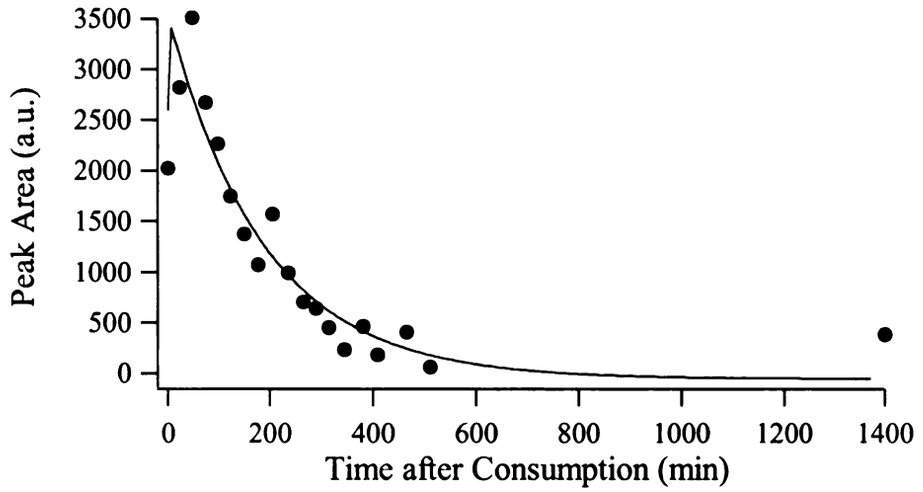

Figure B- 34: Integrated area of the peak attributed to camphene in chromatograms obtained from the breath of subject A on the fourth day of original lemonade consumption. The data has been fit with an exponential rise and decay (Equation 4-1). See Table B-1 for fit parameters.

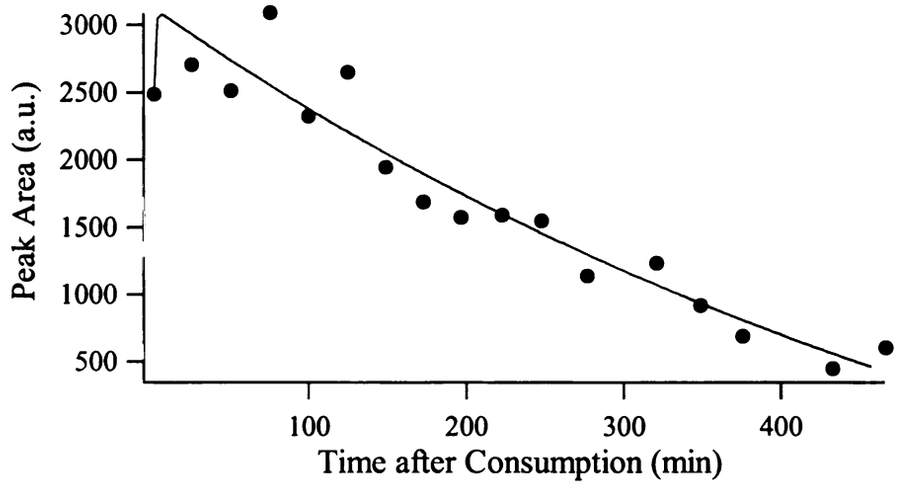

Figure B- 35: Integrated area of the peak attributed to camphene in chromatograms obtained from the breath of subject A on the fifth day of original lemonade consumption. The data has been fit with an exponential rise and decay (Equation 4-1). See Table B-1 for fit parameters.

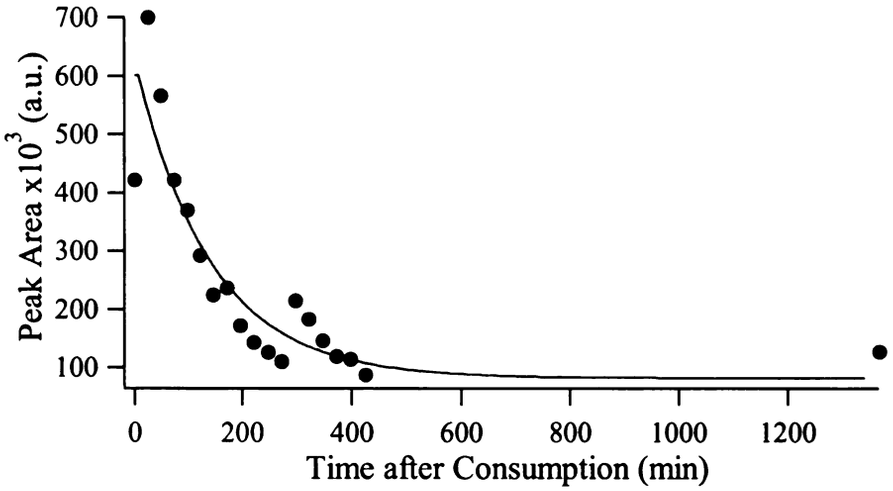

Figure B- 36: Integrated area of the peak attributed to p-cymene in chromatograms obtained from the breath of subject A on the first day of original lemonade consumption. The data has been fit with an exponential rise and decay (Equation 4-1). See Table B-1 for fit parameters.

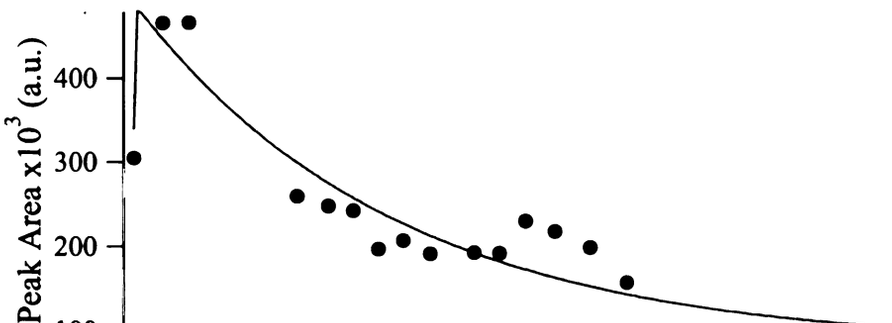

Figure B- 37: Integrated area of the peak attributed to p-cymene in chromatograms obtained from the breath of subject A on the second day of original lemonade consumption. The data has been fit with an exponential rise and decay (Equation 4-1). See Table B-1 for fit parameters.

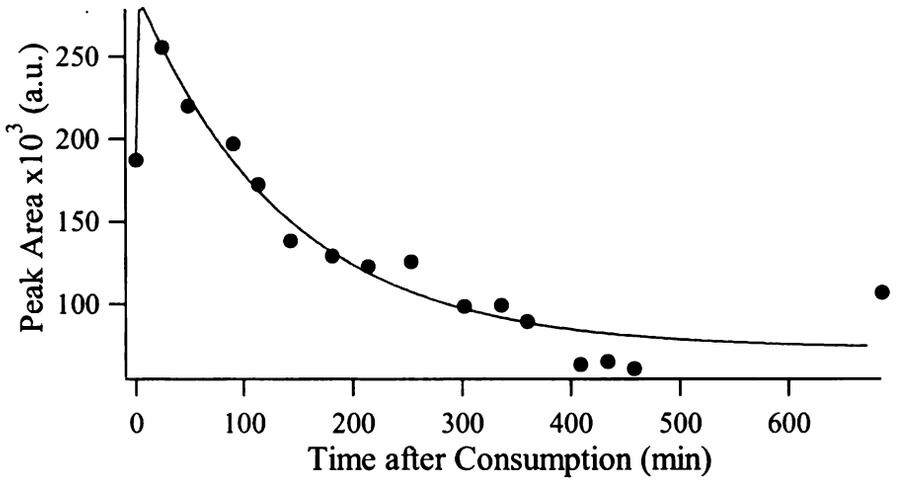

Figure B- 38: Integrated area of the peak attributed to p-cymene in chromatograms obtained from the breath of subject A on the third day of original lemonade consumption. The data has been fit with an exponential rise and decay (Equation 4-1). See Table B-1 for fit parameters.

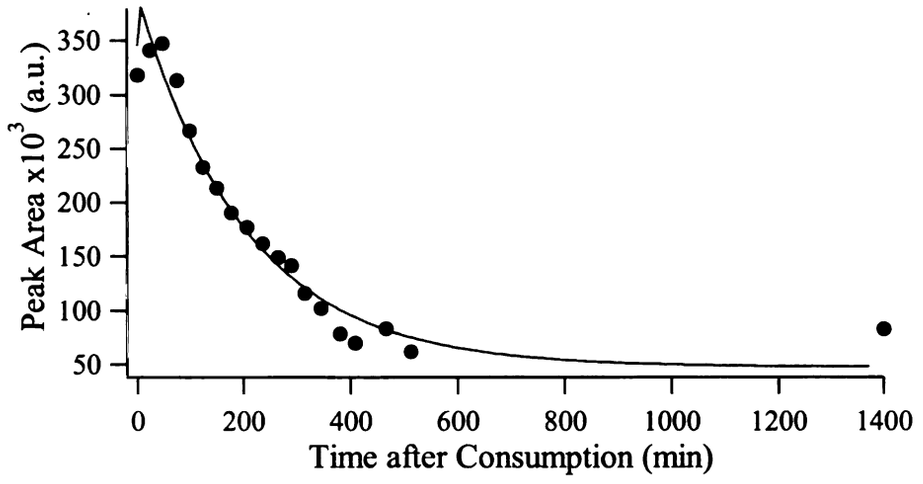

Figure B- 39: Integrated area of the peak attributed to p-cymene in chromatograms obtained from the breath of subject A on the fourth day of original lemonade consumption. The data has been fit with an exponential rise and decay (Equation 4-1). See Table B-1 for fit parameters.

Peak Area x10^3 (a.u.)

35
30
25
20
15
1

Figu
obta
The
for

Peak Area x10^3 (a.u.)

Fi
ob
T
fo

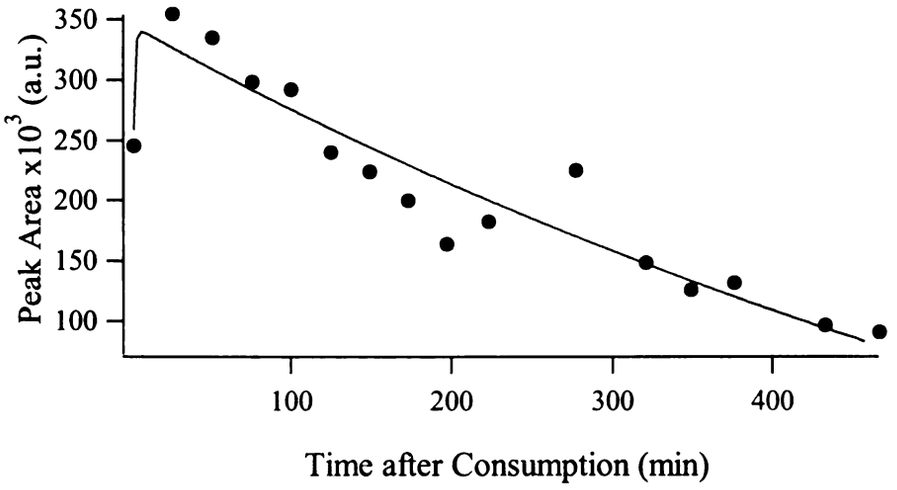

Figure B- 40: Integrated area of the peak attributed to p-cymene in chromatograms obtained from the breath of subject A on the fifth day of original lemonade consumption. The data has been fit with an exponential rise and decay (Equation 4-1). See Table B-1 for fit parameters.

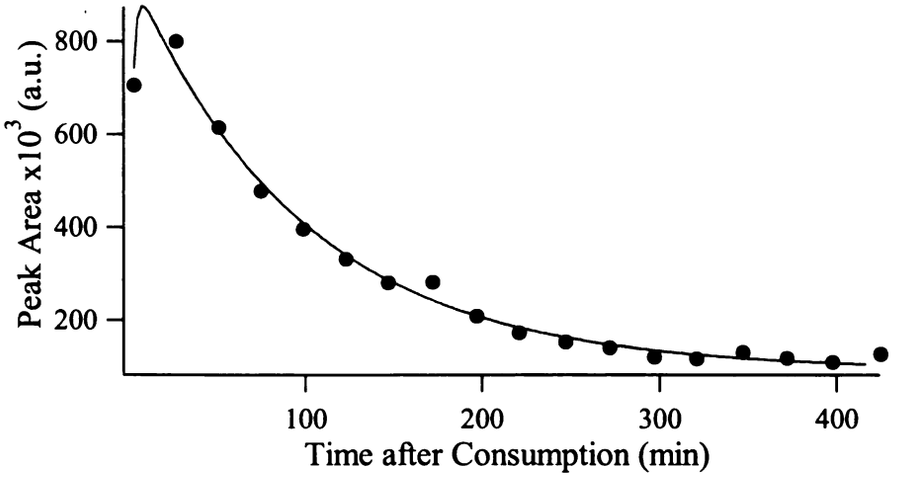

Figure B- 41: Integrated area of the peak attributed to α-pinene in chromatograms obtained from the breath of subject A on the first day of original lemonade consumption. The data has been fit with an exponential rise and decay (Equation 4-1). See Table B-1 for fit parameters.

Fig
ob
co
Se

Peak Area x10^3 (a.u.)

Figu
obta
The
for

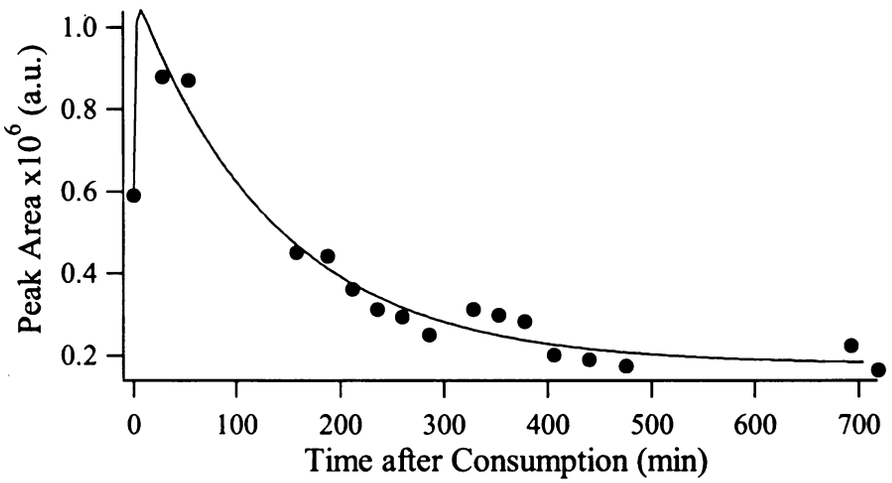

Figure B- 42: Integrated area of the peak attributed to α-pinene in chromatograms obtained from the breath of subject A on the second day of original lemonade consumption. The data has been fit with an exponential rise and decay (Equation 4-1). See Table B-1 for fit parameters.

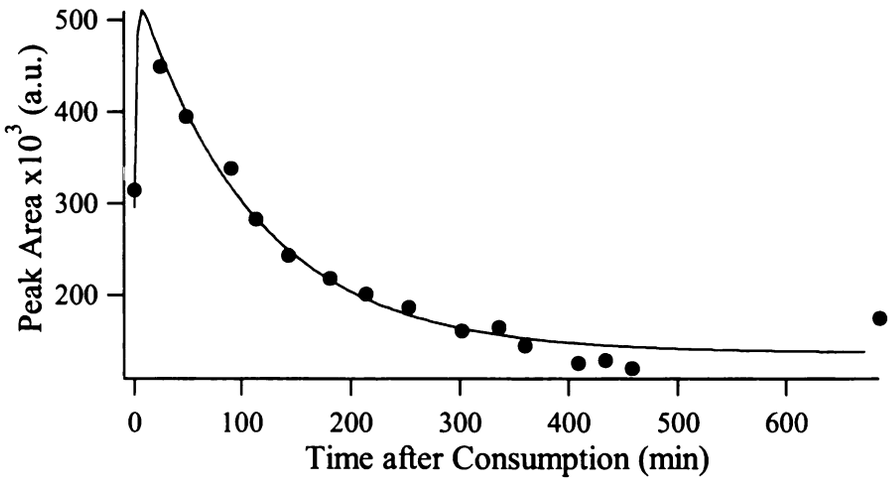

Figure B- 43: Integrated area of the peak attributed to α-pinene in chromatograms obtained from the breath of subject A on the third day of original lemonade consumption. The data has been fit with an exponential rise and decay (Equation 4-1). See Table B-1 for fit parameters.

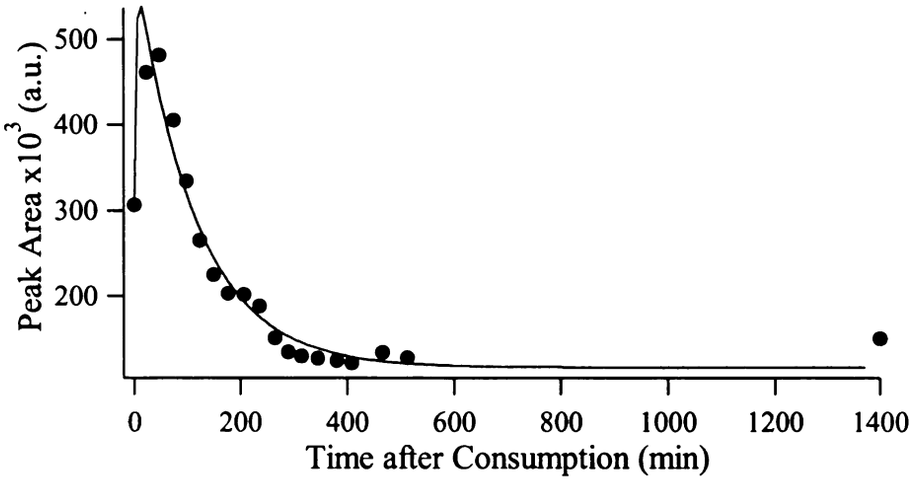

Figure B- 44: Integrated area of the peak attributed to α-pinene in chromatograms obtained from the breath of subject A on the fourth day of original lemonade consumption. The data has been fit with an exponential rise and decay (Equation 4-1). See Table B-1 for fit parameters.

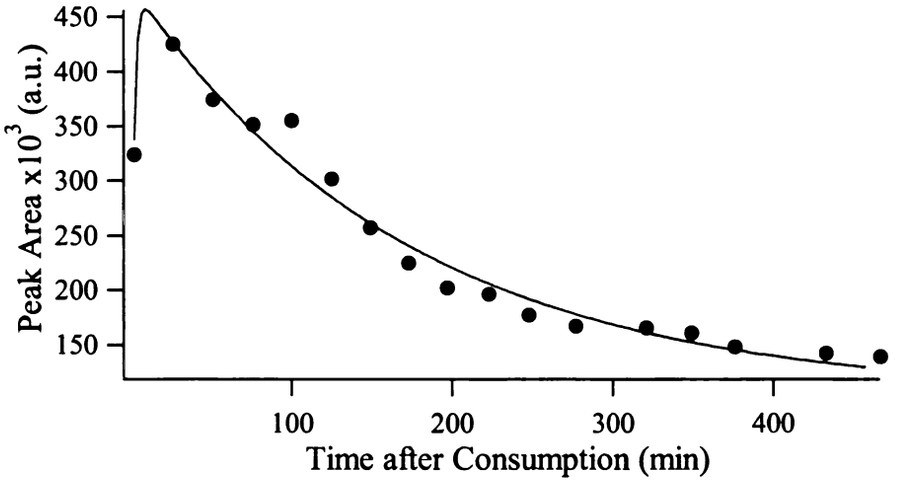

Figure B- 45: Integrated area of the peak attributed to α-pinene in chromatograms obtained from the breath of subject A on the fifth day of original lemonade consumption. The data has been fit with an exponential rise and decay (Equation 4-1). See Table B-1 for fit parameters.

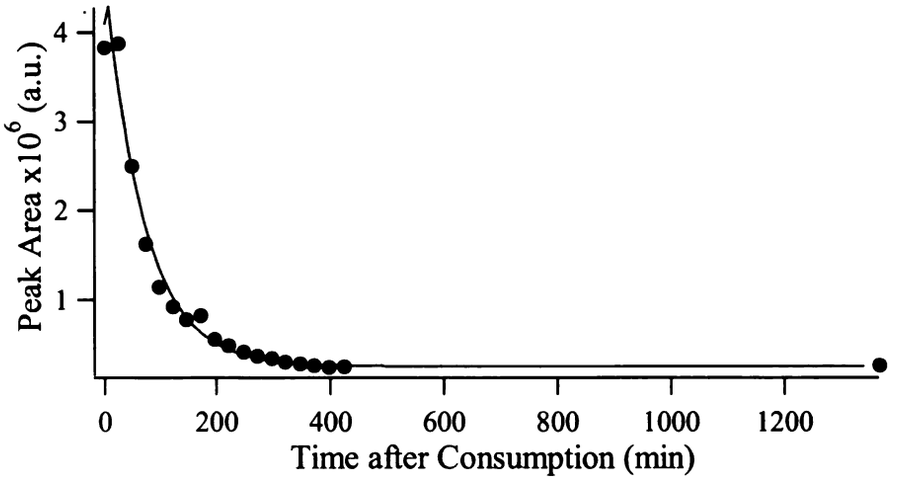

Figure B- 46: Integrated area of the peak attributed to β-pinene in chromatograms obtained from the breath of subject A on the first day of original lemonade consumption. The data has been fit with an exponential rise and decay (Equation 4-1). See Table B-1 for fit parameters.

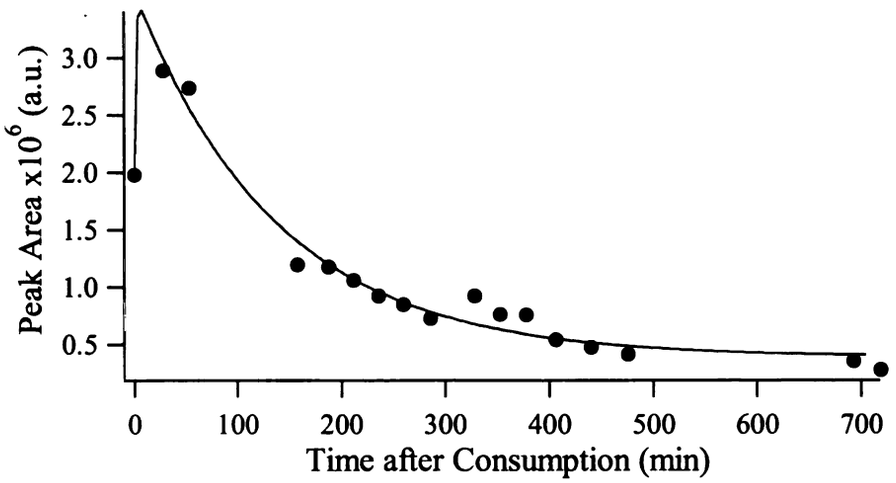

Figure B- 47: Integrated area of the peak attributed to β-pinene in chromatograms obtained from the breath of subject A on the second day of original lemonade consumption. The data has been fit with an exponential rise and decay (Equation 4-1). See Table B-1 for fit parameters.

Peak Area x10^6 (a.u.)

Fig
obt
The
for

Fig
obt
con
See

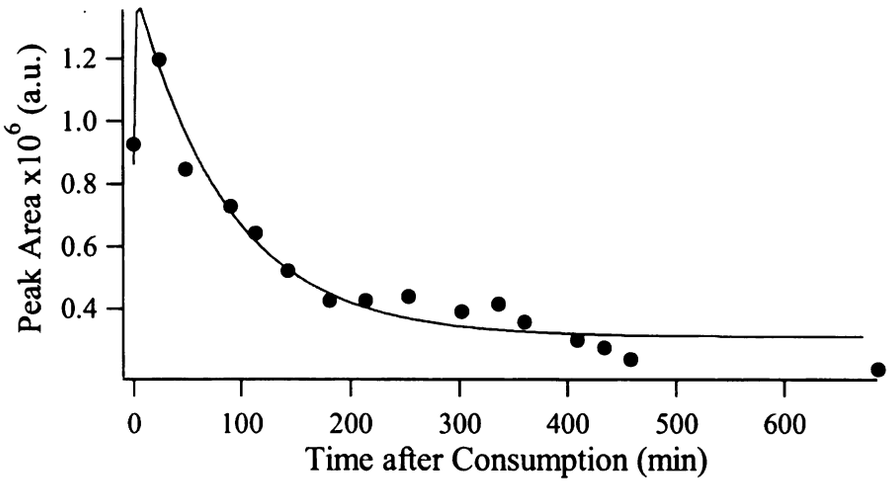

Figure B- 48: Integrated area of the peak attributed to β-pinene in chromatograms obtained from the breath of subject A on the third day of original lemonade consumption. The data has been fit with an exponential rise and decay (Equation 4-1). See Table B-1 for fit parameters.

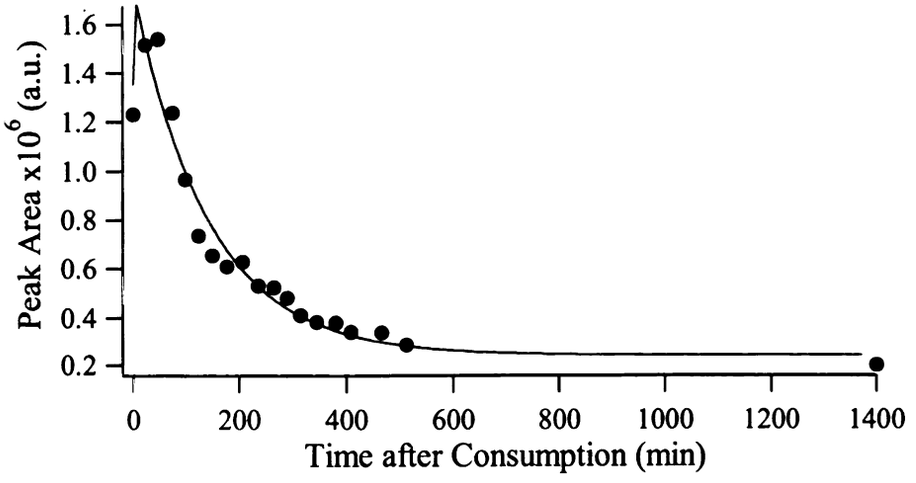

Figure B- 49: Integrated area of the peak attributed to β-pinene in chromatograms obtained from the breath of subject A on the fourth day of original lemonade consumption. The data has been fit with an exponential rise and decay (Equation 4-1). See Table B-1 for fit parameters.

Peak Area x 10^6 (a.u.)

Fig
obt
The
for

Peak Area x 10^3 (a.u.)

Fig
obt
The
for

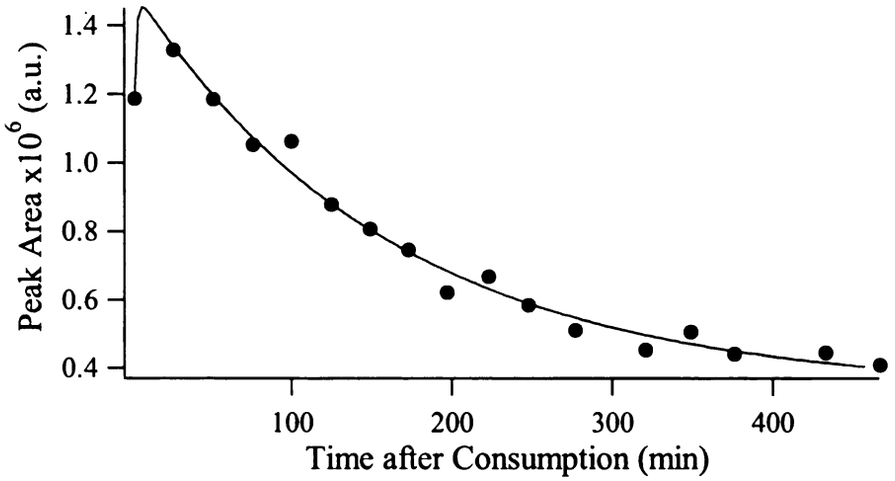

Figure B- 50: Integrated area of the peak attributed to β-pinene in chromatograms obtained from the breath of subject A on the fifth day of original lemonade consumption. The data has been fit with an exponential rise and decay (Equation 4-1). See Table B-1 for fit parameters.

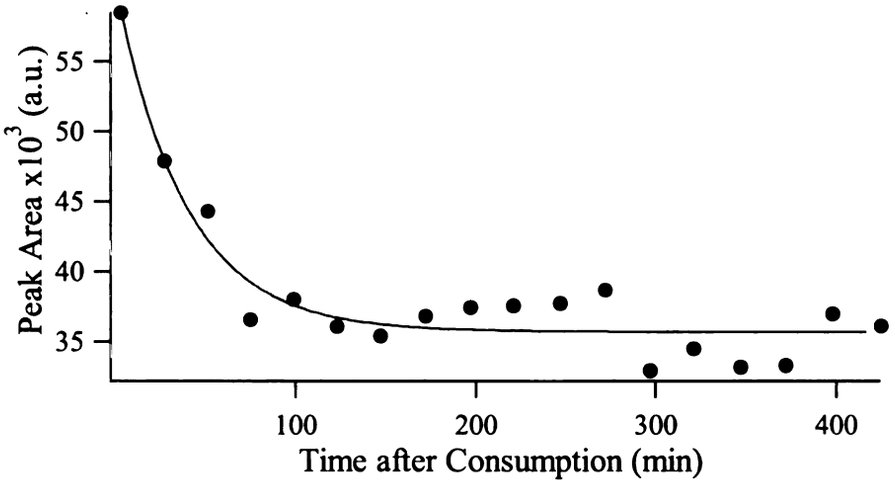

Figure B- 51: Integrated area of the peak attributed to β-phellandrene in chromatograms obtained from the breath of subject A on the first day of original lemonade consumption. The data has been fit with an exponential rise and decay (Equation 4-1). See Table B-1 for fit parameters.

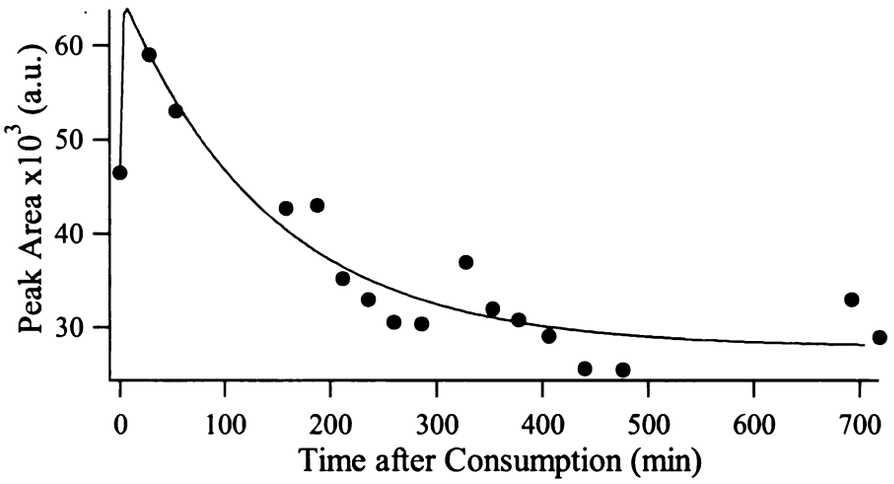

Figure B- 52: Integrated area of the peak attributed to β-phellandrene in chromatograms obtained from the breath of subject A on the second day of original lemonade consumption. The data has been fit with an exponential rise and decay (Equation 4-1). See Table B-1 for fit parameters.

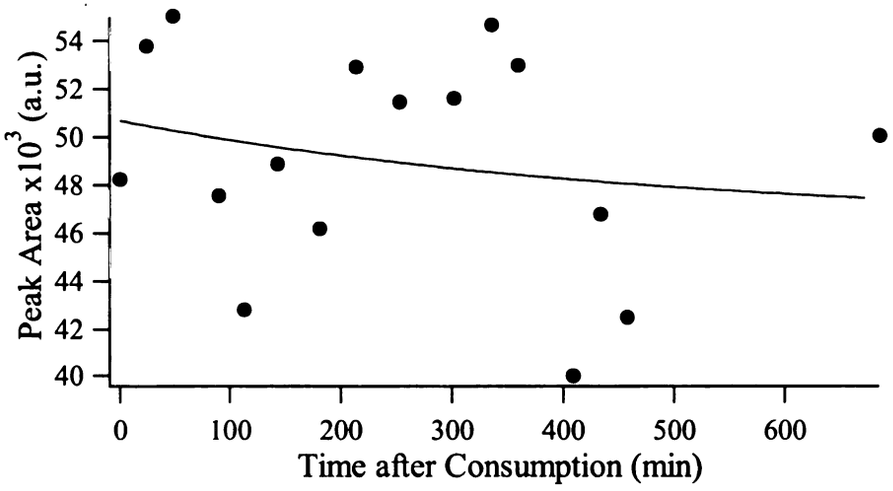

Figure B- 53: Integrated area of the peak attributed to β-phellandrene in chromatograms obtained from the breath of subject A on the third day of original lemonade consumption. The data has been fit with an exponential rise and decay (Equation 4-1). See Table B-1 for fit parameters.

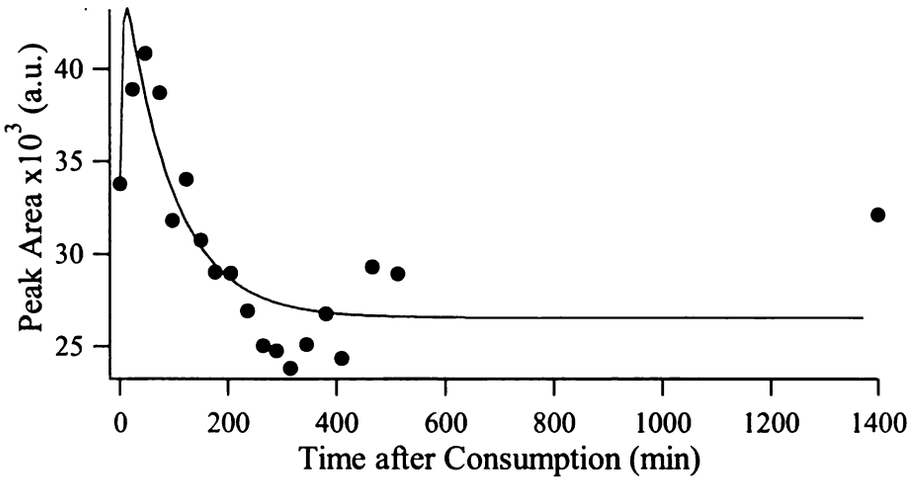

Figure B- 54: Integrated area of the peak attributed to β-phellandrene in chromatograms obtained from the breath of subject A on the fourth day of original lemonade consumption. The data has been fit with an exponential rise and decay (Equation 4-1). See Table B-1 for fit parameters.

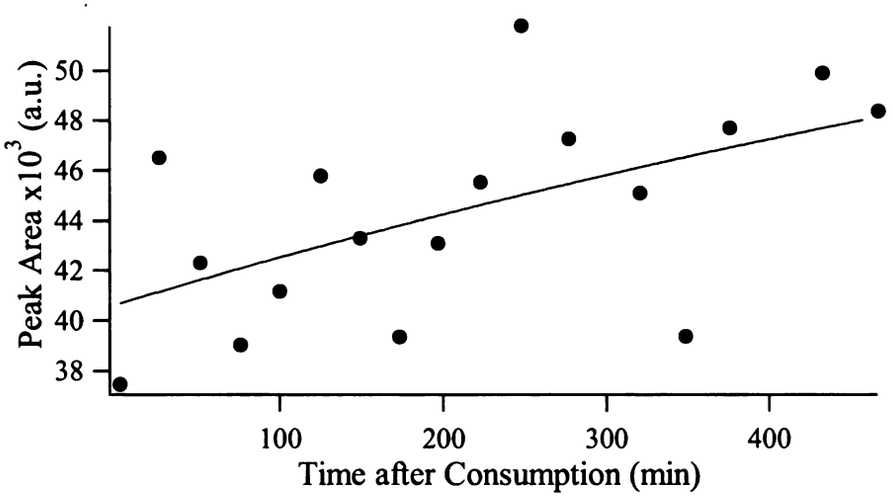

Figure B- 55: Integrated area of the peak attributed to β-phellandrene in chromatograms obtained from the breath of subject A on the fifth day of original lemonade consumption. The data has been fit with an exponential rise and decay (Equation 4-1). See Table B-1 for fit parameters.

Peak Area x10^3 (a.u.)

Peak Area x10^3 (a.u.)

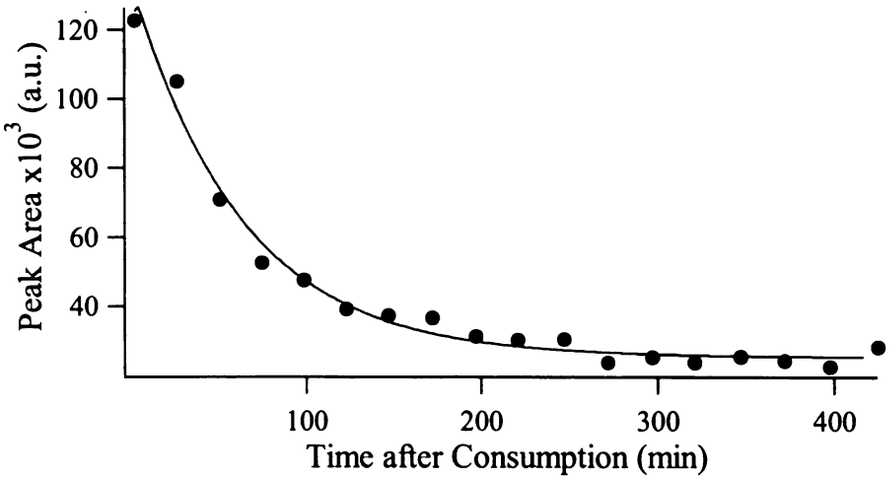

Figure B- 56: Integrated area of the peak attributed to α-thujene in chromatograms obtained from the breath of subject A on the first day of original lemonade consumption. The data has been fit with an exponential rise and decay (Equation 4-1). See Table B-1 for fit parameters.

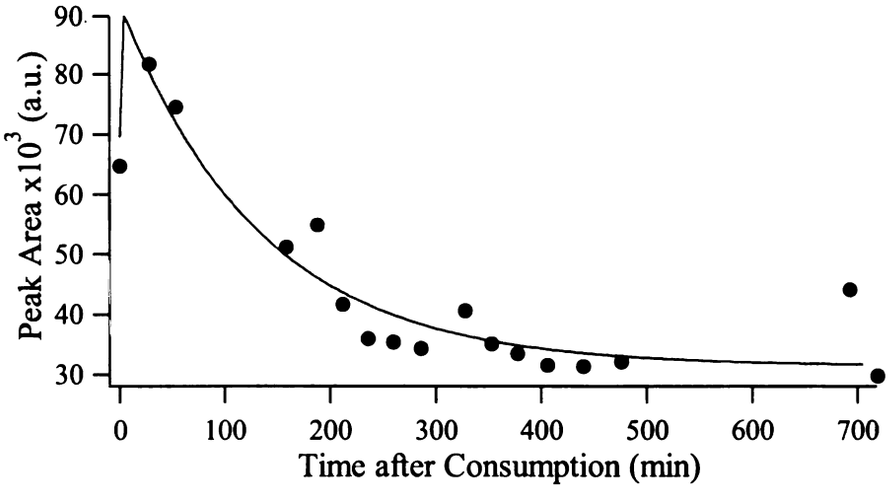

Figure B- 57: Integrated area of the peak attributed to α-thujene in chromatograms obtained from the breath of subject A on the second day of original lemonade consumption. The data has been fit with an exponential rise and decay (Equation 4-1). See Table B-1 for fit parameters.

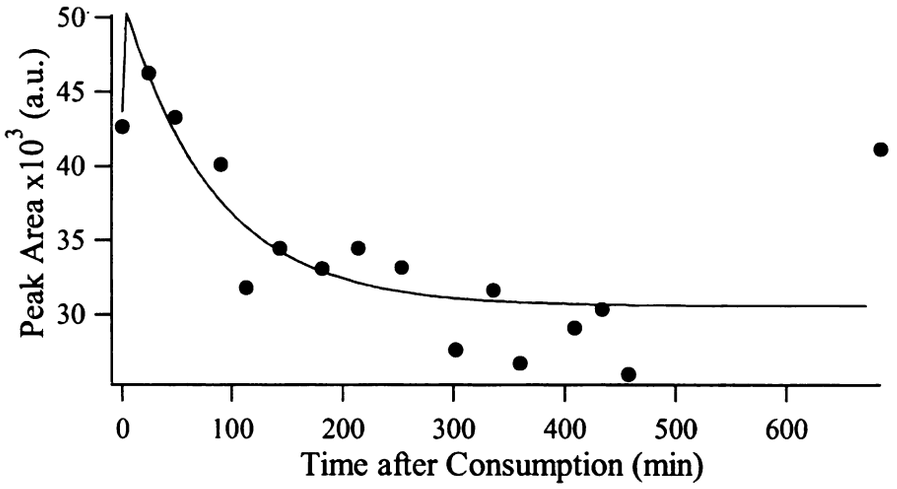

Figure B- 58: Integrated area of the peak attributed to α-thujene in chromatograms obtained from the breath of subject A on the third day of original lemonade consumption. The data has been fit with an exponential rise and decay (Equation 4-1). See Table B-1 for fit parameters.

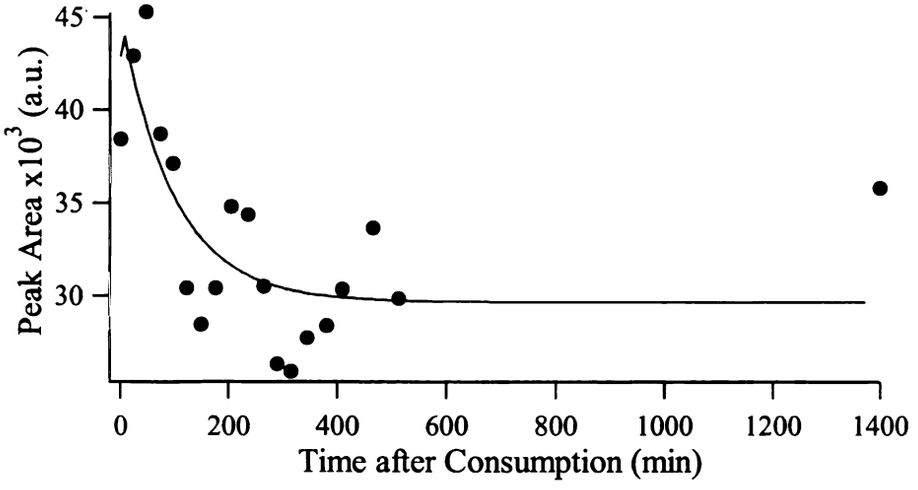

Figure B- 59: Integrated area of the peak attributed to α-thujene in chromatograms obtained from the breath of subject A on the fourth day of original lemonade consumption. The data has been fit with an exponential rise and decay (Equation 4-1). See Table B-1 for fit parameters.

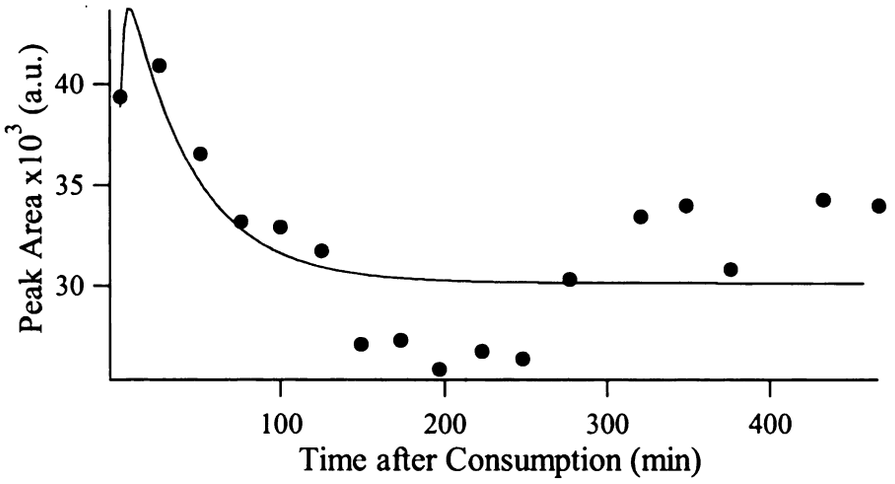

Figure B- 60: Integrated area of the peak attributed to α-thujene in chromatograms obtained from the breath of subject A on the fifth day of original lemonade consumption. The data has been fit with an exponential rise and decay (Equation 4-1). See Table B-1 for fit parameters.

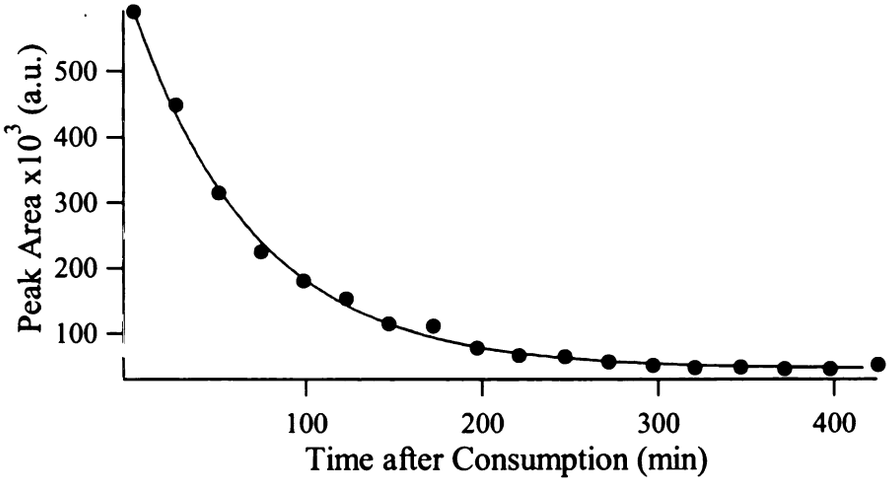

Figure B- 61: Integrated area of the peak attributed to β-myrcene in chromatograms obtained from the breath of subject A on the first day of original lemonade consumption. The data has been fit with an exponential rise and decay (Equation 4-1). See Table B-1 for fit parameters.

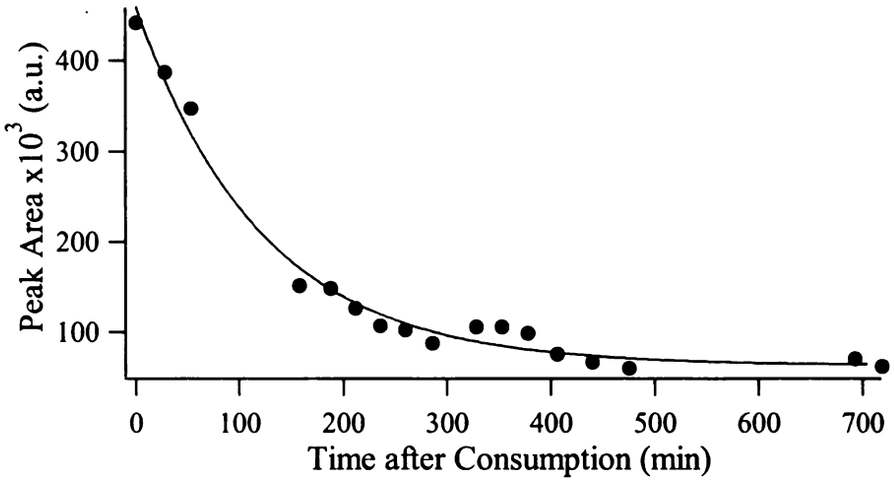

Figure B- 62: Integrated area of the peak attributed to β-myrcene in chromatograms obtained from the breath of subject A on the second day of original lemonade consumption. The data has been fit with an exponential rise and decay (Equation 4-1). See Table B-1 for fit parameters.

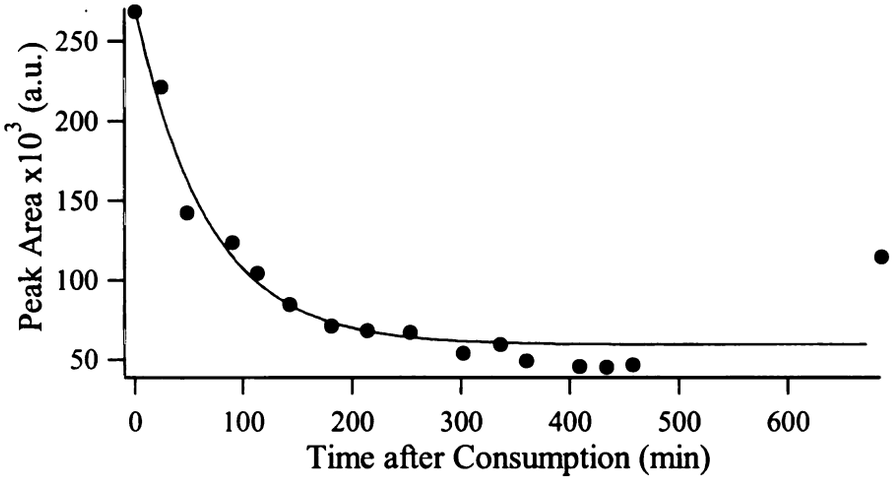

Figure B- 63: Integrated area of the peak attributed to β-myrcene in chromatograms obtained from the breath of subject A on the third day of original lemonade consumption. The data has been fit with an exponential rise and decay (Equation 4-1). See Table B-1 for fit parameters.

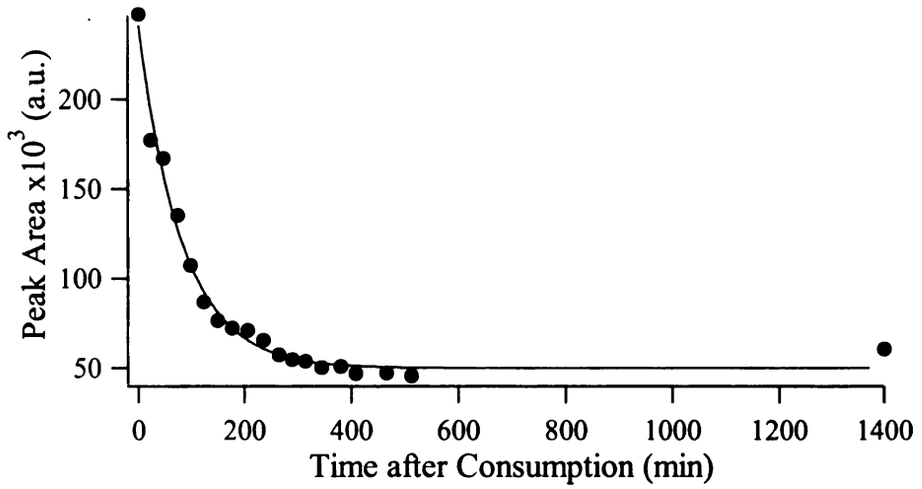

Figure B- 64: Integrated area of the peak attributed to β-myrcene in chromatograms obtained from the breath of subject A on the fourth day of original lemonade consumption. The data has been fit with an exponential rise and decay (Equation 4-1). See Table B-1 for fit parameters.

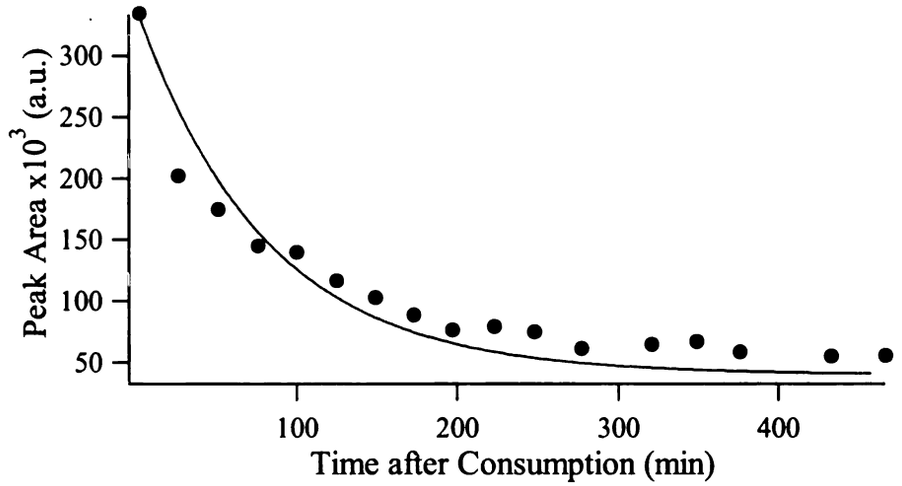

Figure B- 65: Integrated area of the peak attributed to β-myrcene in chromatograms obtained from the breath of subject A on the fifth day of original lemonade consumption. The data has been fit with an exponential rise and decay (Equation 4-1). See Table B-1 for fit parameters.

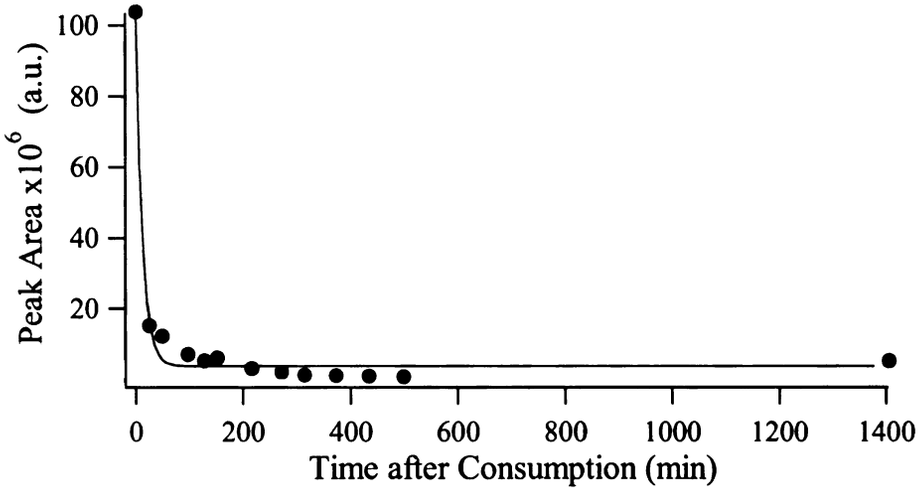

Figure B- 66: Integrated area of the peak attributed to α-limonene in chromatograms obtained from the breath of subject B on the first day of original lemonade consumption. The data has been fit with an exponential rise and decay (Equation 4-1). See Table B-1 for fit parameters.

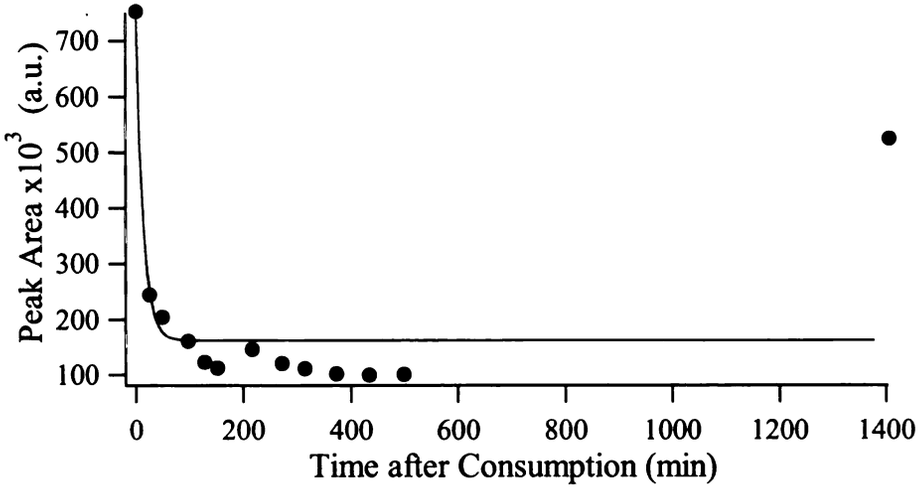

Figure B- 67: Integrated area of the peak attributed to 4-terpineol in chromatograms obtained from the breath of subject B on the first day of original lemonade consumption. The data has been fit with an exponential rise and decay (Equation 4-1). See Table B-1 for fit parameters.

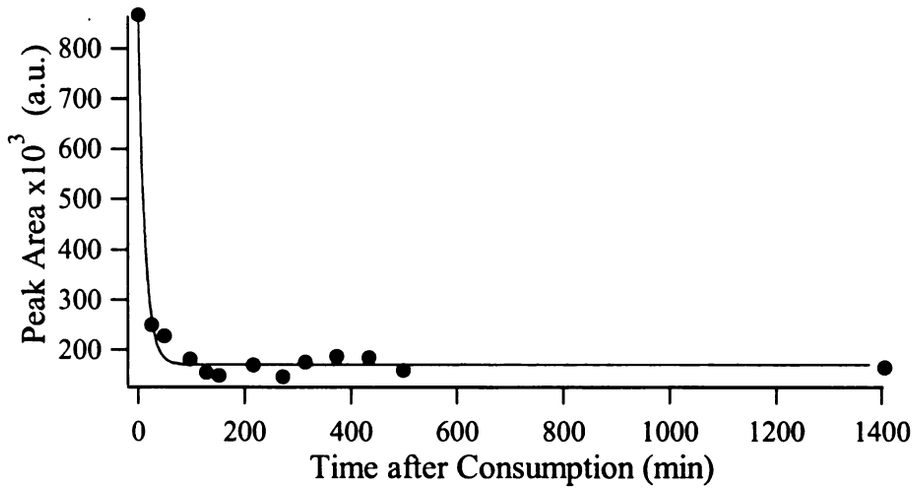

Figure B- 68: Integrated area of the peak attributed to α-terpineol in chromatograms obtained from the breath of subject B on the first day of original lemonade consumption. The data has been fit with an exponential rise and decay (Equation 4-1). See Table B-1 for fit parameters.

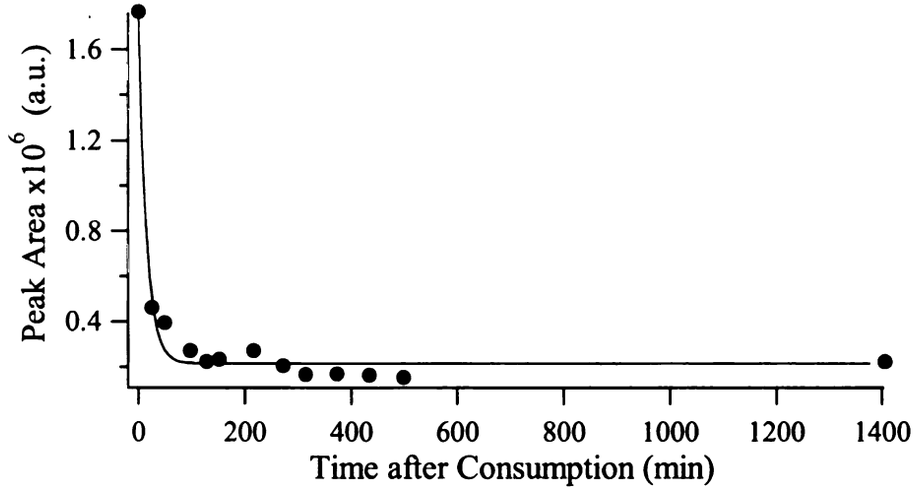

Figure B- 69: Integrated area of the peak attributed to terpinolene in chromatograms obtained from the breath of subject B on the first day of original lemonade consumption. The data has been fit with an exponential rise and decay (Equation 4-1). See Table B-1 for fit parameters.

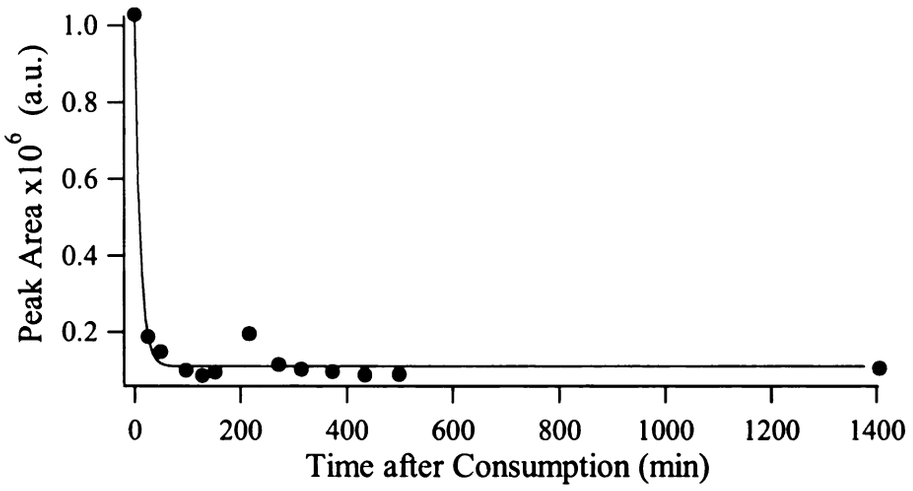

Figure B- 70: Integrated area of the peak attributed to α-terpinene in chromatograms obtained from the breath of subject B on the first day of original lemonade consumption. The data has been fit with an exponential rise and decay (Equation 4-1). See Table B-1 for fit parameters.

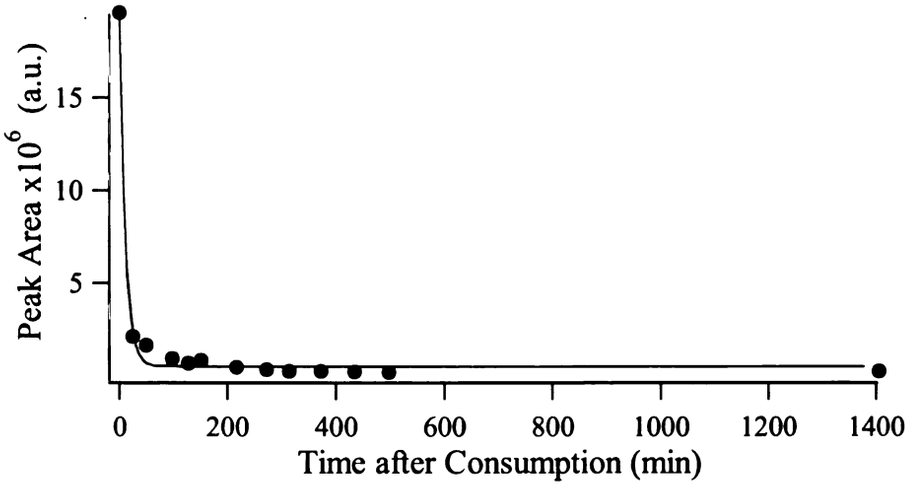

Figure B- 71: Integrated area of the peak attributed to γ-terpinene in chromatograms obtained from the breath of subject B on the first day of original lemonade consumption. The data has been fit with an exponential rise and decay (Equation 4-1). See Table B-1 for fit parameters.

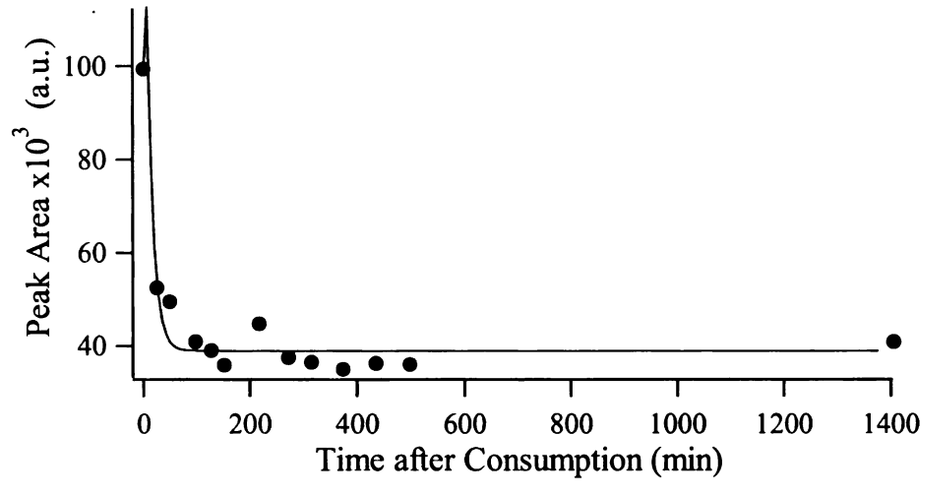

Figure B- 72: Integrated area of the peak attributed to camphene in chromatograms obtained from the breath of subject B on the first day of original lemonade consumption. The data has been fit with an exponential rise and decay (Equation 4-1). See Table B-1 for fit parameters.

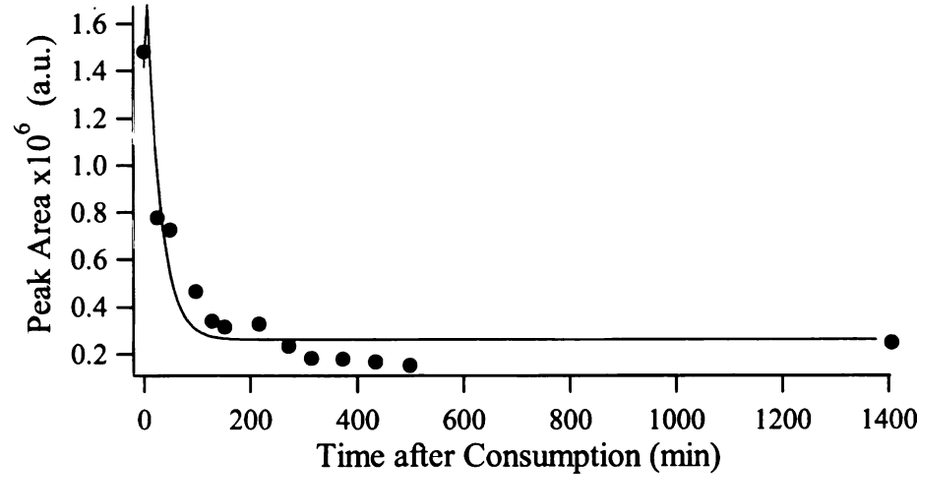

Figure B- 73: Integrated area of the peak attributed to p-cymene in chromatograms obtained from the breath of subject B on the first day of original lemonade consumption. The data has been fit with an exponential rise and decay (Equation 4-1). See Table B-1 for fit parameters.

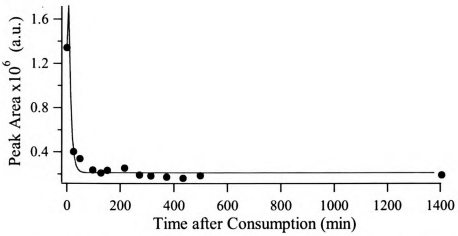

Figure B- 74: Integrated area of the peak attributed to α-pinene in chromatograms obtained from the breath of subject B on the first day of original lemonade consumption. The data has been fit with an exponential rise and decay (Equation 4-1). See Table B-1 for fit parameters.

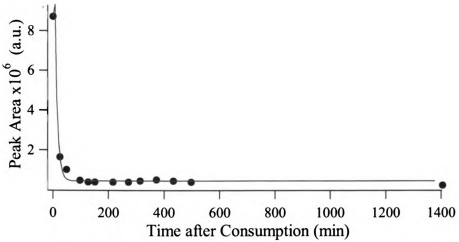

Figure B- 75: Integrated area of the peak attributed to β-pinene in chromatograms obtained from the breath of subject B on the first day of original lemonade consumption. The data has been fit with an exponential rise and decay (Equation 4-1). See Table B-1 for fit parameters.

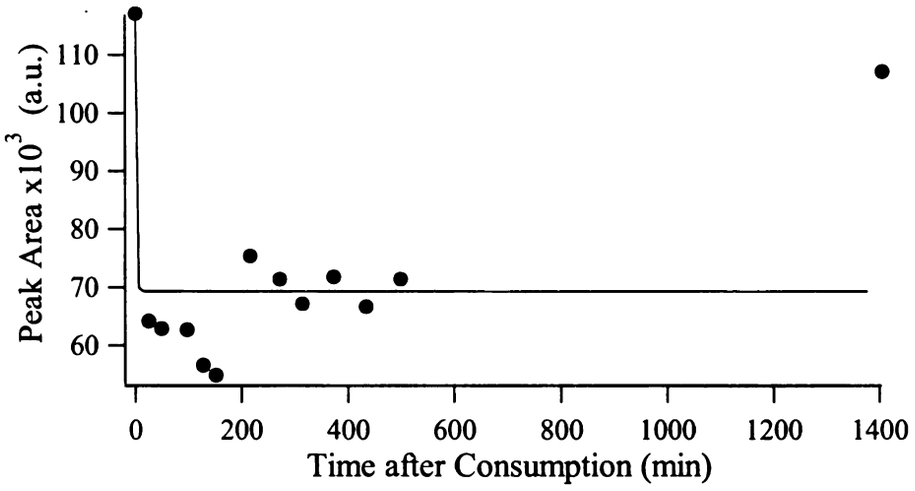

Figure B- 76: Integrated area of the peak attributed to β-phellandrene in chromatograms obtained from the breath of subject B on the first day of original lemonade consumption. The data has been fit with an exponential rise and decay (Equation 4-1). See Table B-1 for fit parameters.

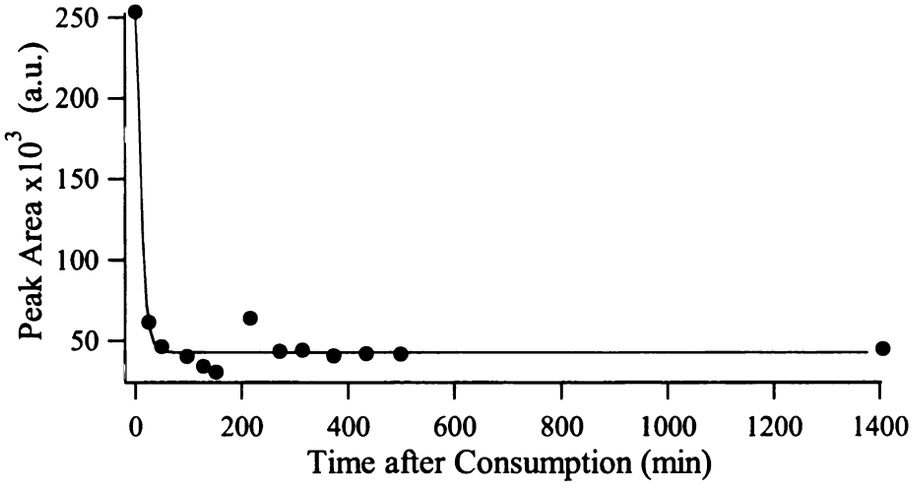

Figure B- 77: Integrated area of the peak attributed to α-thujene in chromatograms obtained from the breath of subject B on the first day of original lemonade consumption. The data has been fit with an exponential rise and decay (Equation 4-1). See Table B-1 for fit parameters.

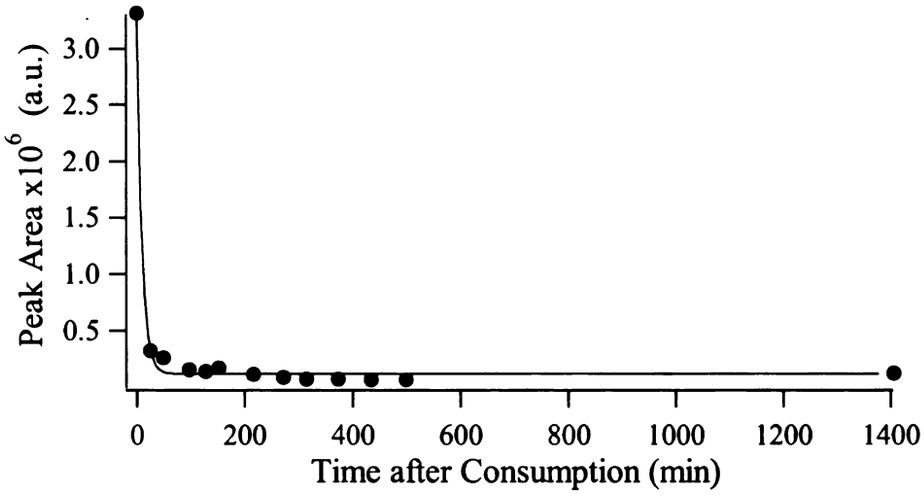

Figure B- 78: Integrated area of the peak attributed to β-myrcene in chromatograms obtained from the breath of subject B on the first day of original lemonade consumption. The data has been fit with an exponential rise and decay (Equation 4-1). See Table B-1 for fit parameters.

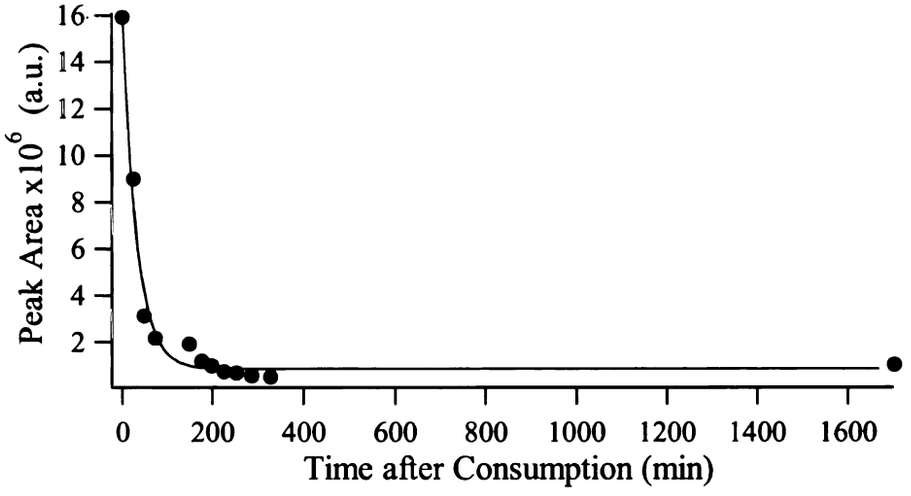

Figure B- 79: Integrated area of the peak attributed to α-limonene in chromatograms obtained from the breath of subject C on the first day of original lemonade consumption. The data has been fit with an exponential rise and decay (Equation 4-1). See Table B-1 for fit parameters.

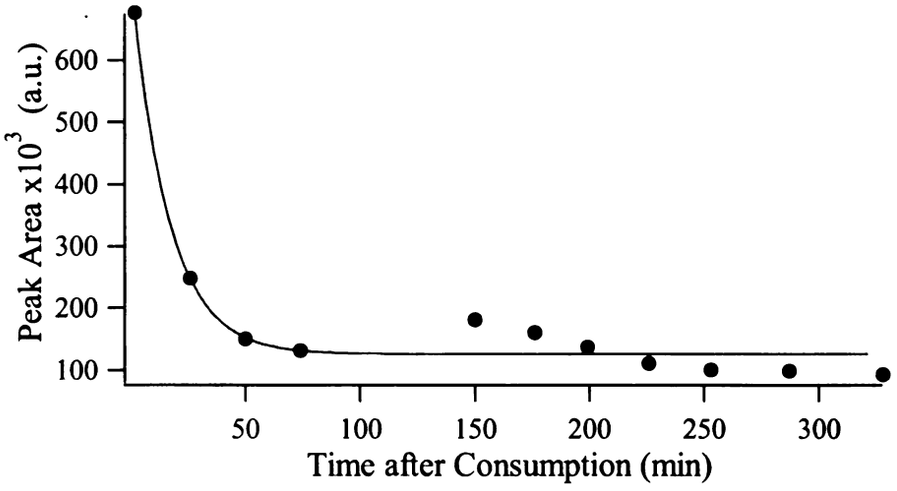

Figure B- 80: Integrated area of the peak attributed to 4-terpineol in chromatograms obtained from the breath of subject B on the first day of original lemonade consumption. The data has been fit with an exponential rise and decay (Equation 4-1). See Table B-1 for fit parameters.

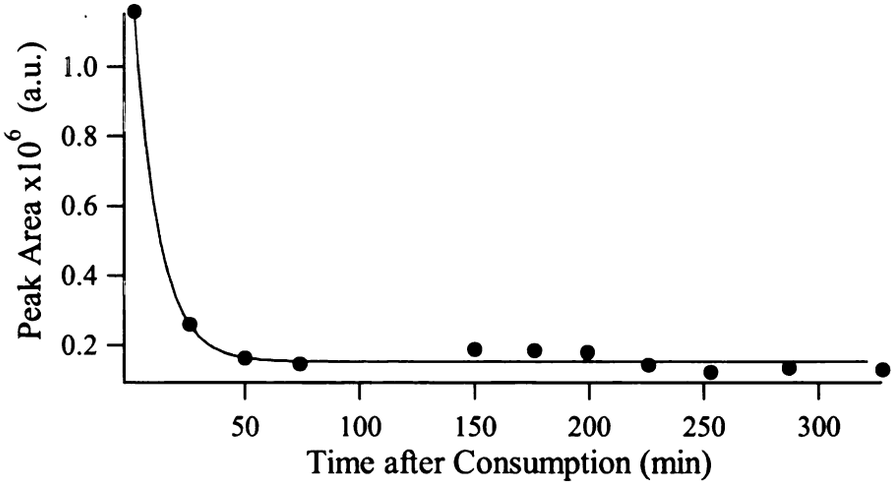

Figure B- 81: Integrated area of the peak attributed to α-terpineol in chromatograms obtained from the breath of subject C on the first day of original lemonade consumption. The data has been fit with an exponential rise and decay (Equation 4-1). See Table B-1 for fit parameters.

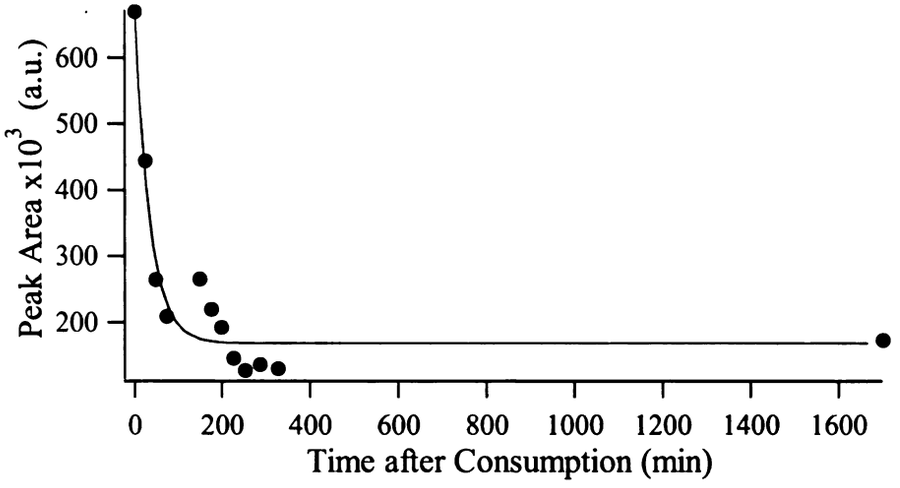

Figure B- 82: Integrated area of the peak attributed to terpinolene in chromatograms obtained from the breath of subject C on the first day of original lemonade consumption. The data has been fit with an exponential rise and decay (Equation 4-1). See Table B-1 for fit parameters.

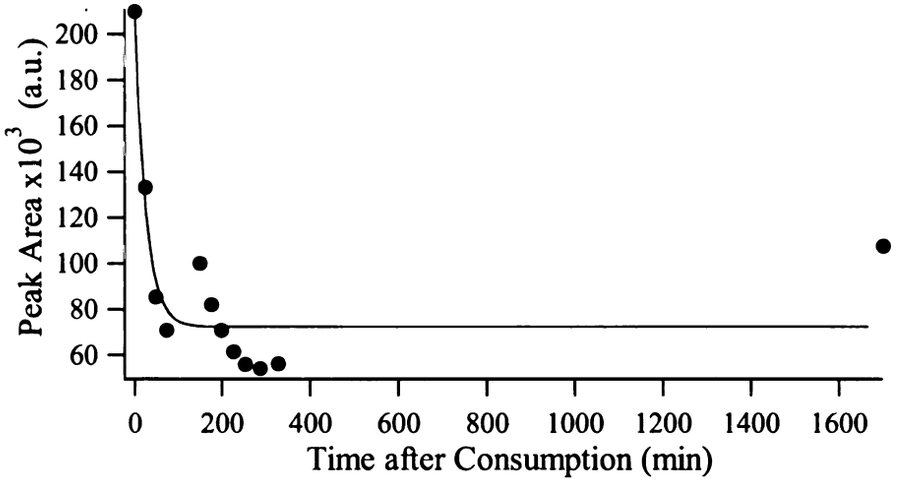

Figure B- 83: Integrated area of the peak attributed to α-terpinene in chromatograms obtained from the breath of subject C on the first day of original lemonade consumption. The data has been fit with an exponential rise and decay (Equation 4-1). See Table B-1 for fit parameters.

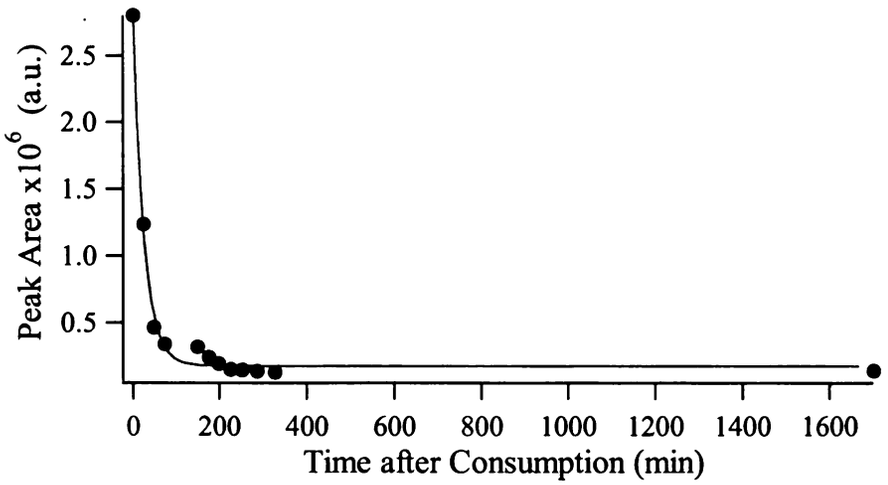

Figure B- 84: Integrated area of the peak attributed to γ-terpinene in chromatograms obtained from the breath of subject C on the first day of original lemonade consumption. The data has been fit with an exponential rise and decay (Equation 4-1). See Table B-1 for fit parameters.

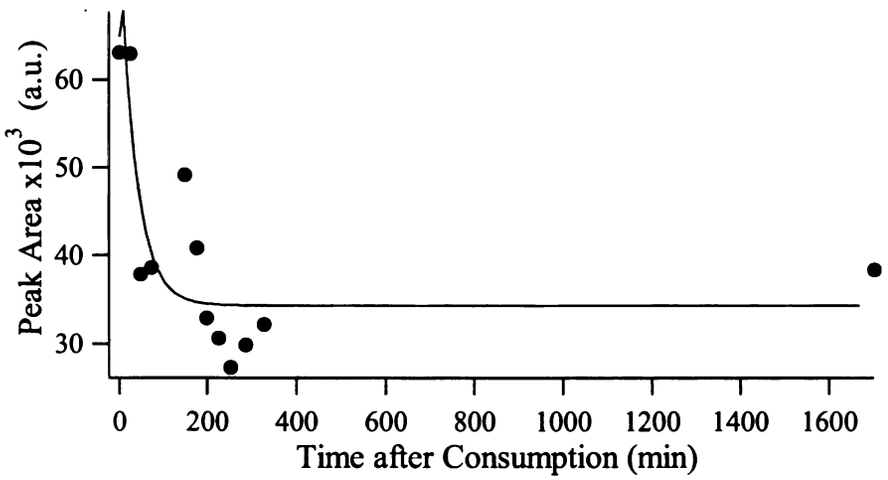

Figure B- 85: Integrated area of the peak attributed to camphene in chromatograms obtained from the breath of subject C on the first day of original lemonade consumption. The data has been fit with an exponential rise and decay (Equation 4-1). See Table B-1 for fit parameters.

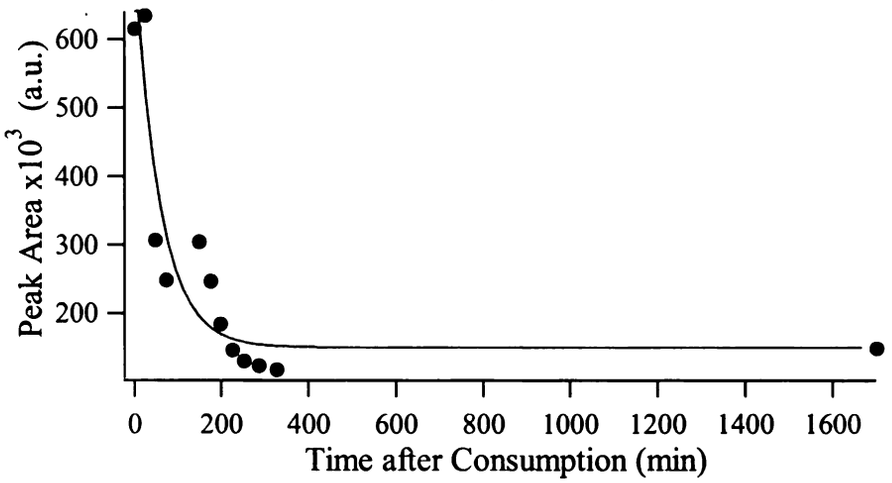

Figure B- 86: Integrated area of the peak attributed to p-cymene in chromatograms obtained from the breath of subject C on the first day of original lemonade consumption. The data has been fit with an exponential rise and decay (Equation 4-1). See Table B-1 for fit parameters.

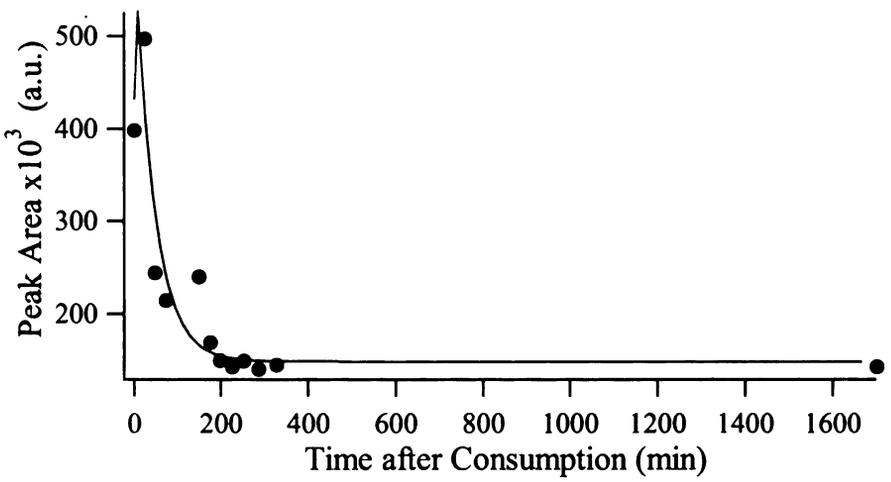

Figure B- 87: Integrated area of the peak attributed to α-pinene in chromatograms obtained from the breath of subject C on the first day of original lemonade consumption. The data has been fit with an exponential rise and decay (Equation 4-1). See Table B-1 for fit parameters.

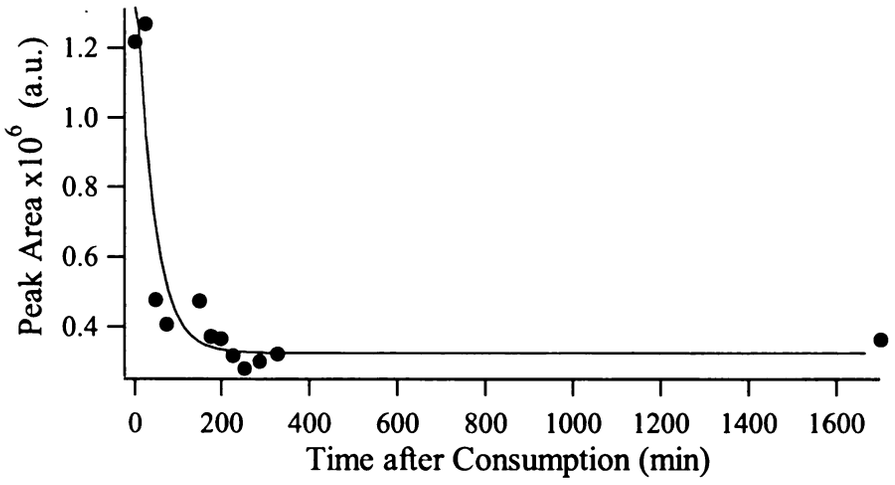

Figure B- 88: Integrated area of the peak attributed to β-pinene in chromatograms obtained from the breath of subject C on the first day of original lemonade consumption. The data has been fit with an exponential rise and decay (Equation 4-1). See Table B-1 for fit parameters.

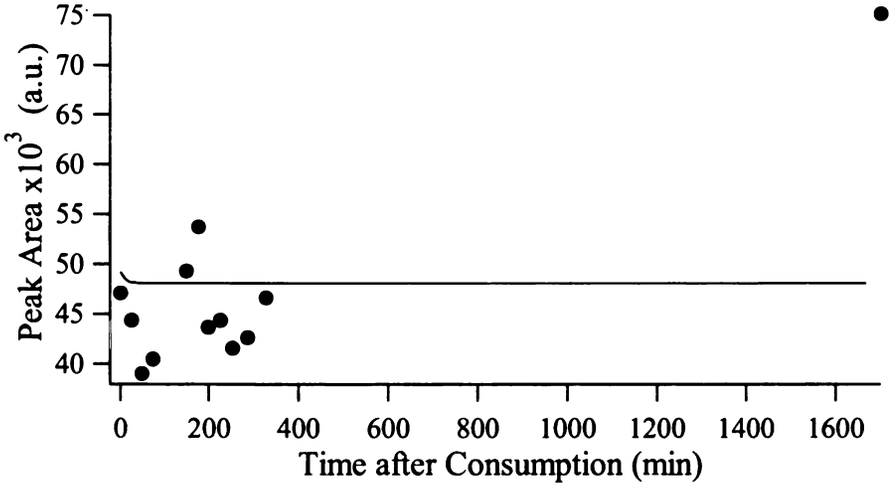

Figure B- 89: Integrated area of the peak attributed to β-phellandrene in chromatograms obtained from the breath of subject C on the first day of original lemonade consumption. The data has been fit with an exponential rise and decay (Equation 4-1). See Table B-1 for fit parameters.

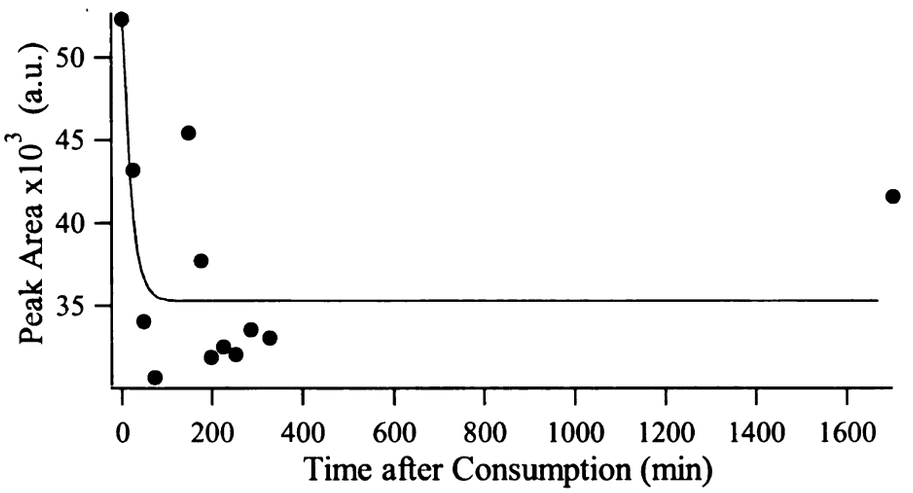

Figure B- 90: Integrated area of the peak attributed to α-thujene in chromatograms obtained from the breath of subject C on the first day of original lemonade consumption. The data has been fit with an exponential rise and decay (Equation 4-1). See Table B-1 for fit parameters.

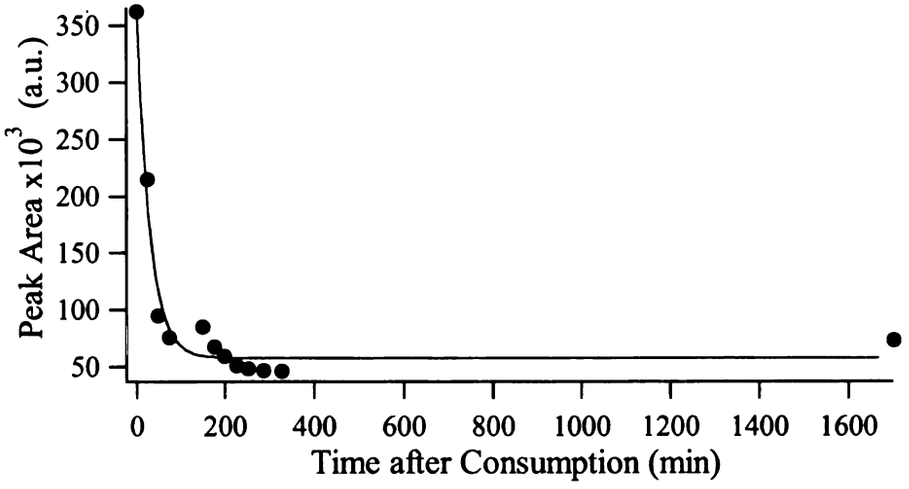

Figure B- 91: Integrated area of the peak attributed to β-myrcene in chromatograms obtained from the breath of subject C on the first day of original lemonade consumption. The data has been fit with an exponential rise and decay (Equation 4-1). See Table B-1 for fit parameters.

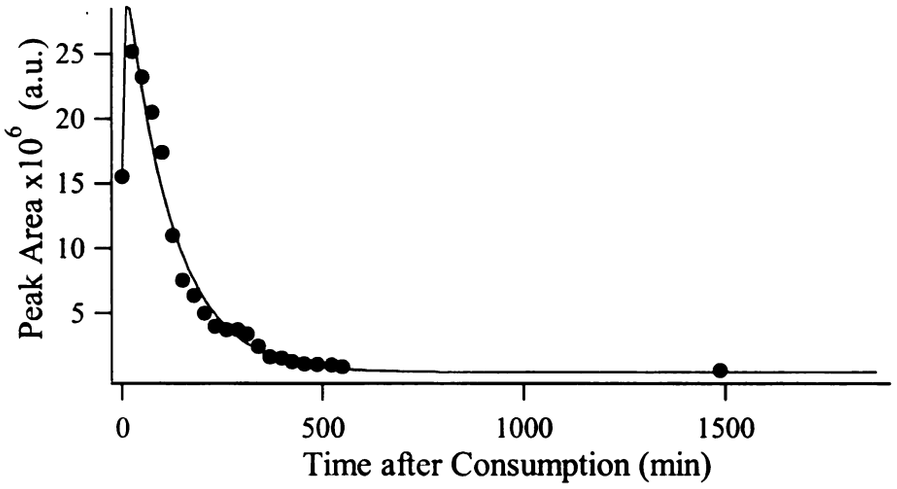

Figure B- 92: Integrated area of the peak attributed to α-limonene in chromatograms obtained from the breath of subject A on the first day of concentrated lemonade consumption. The data has been fit with an exponential rise and decay (Equation 4-1). See Table B-1 for fit parameters.

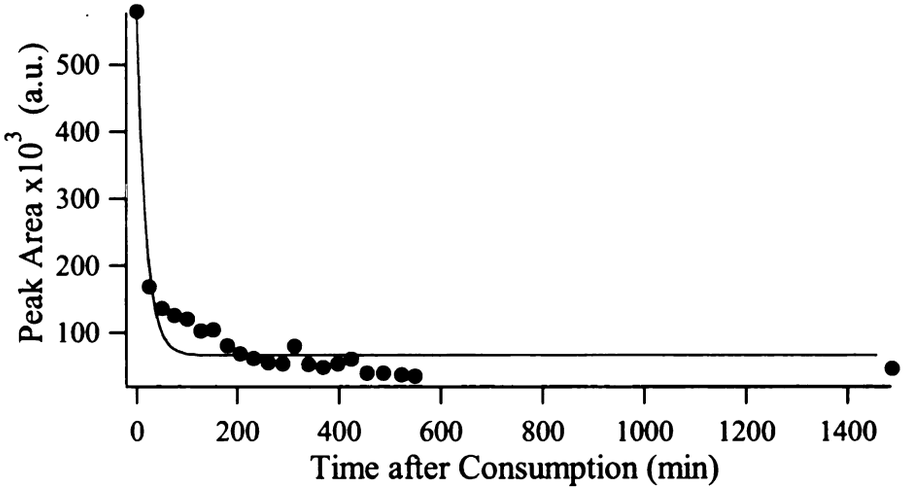

Figure B- 93: Integrated area of the peak attributed to 4-terpineol in chromatograms obtained from the breath of subject A on the first day of concentrated lemonade consumption. The data has been fit with an exponential rise and decay (Equation 4-1). See Table B-1 for fit parameters.

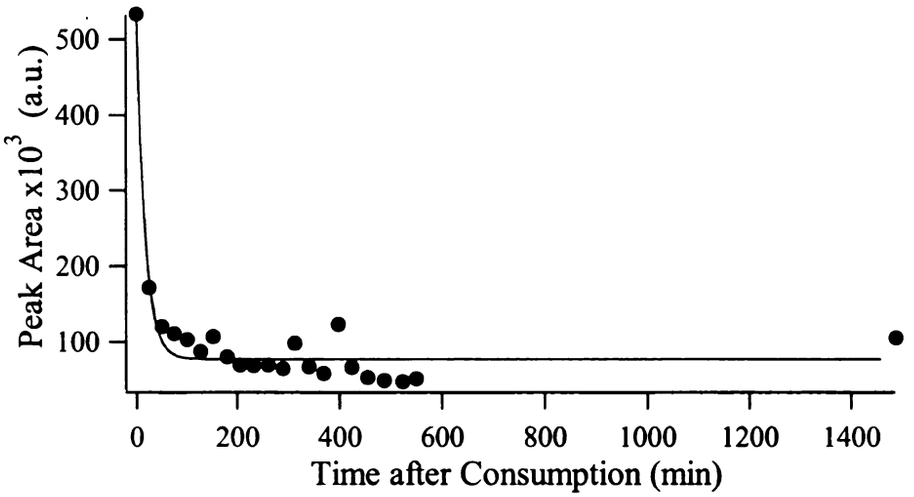

Figure B- 94: Integrated area of the peak attributed to α-terpineol in chromatograms obtained from the breath of subject A on the first day of concentrated lemonade consumption. The data has been fit with an exponential rise and decay (Equation 4-1). See Table B-1 for fit parameters.

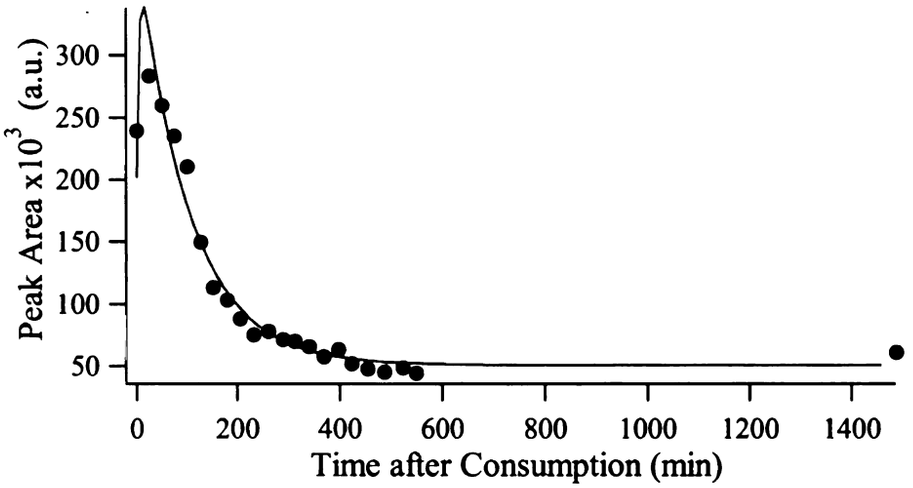

Figure B- 95: Integrated area of the peak attributed to terpinolene in chromatograms obtained from the breath of subject A on the first day of concentrated lemonade consumption. The data has been fit with an exponential rise and decay (Equation 4-1). See Table B-1 for fit parameters.

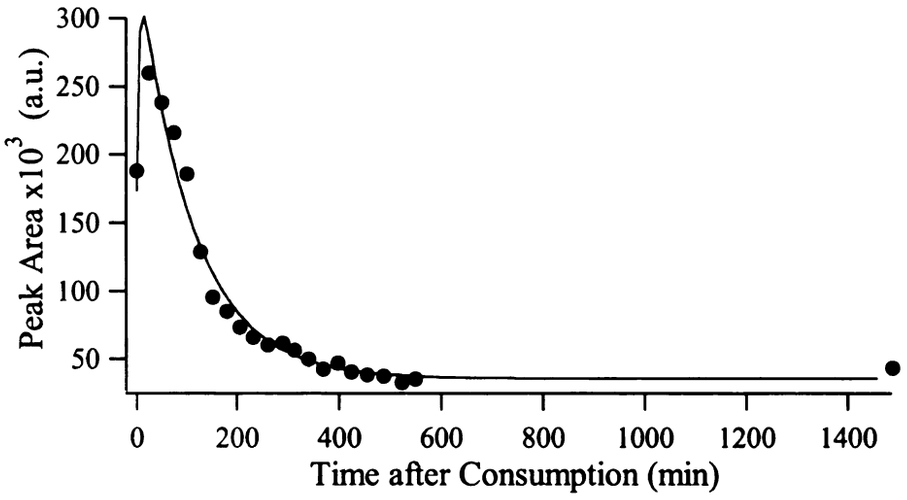

Figure B- 96: Integrated area of the peak attributed to α-terpinene in chromatograms obtained from the breath of subject A on the first day of concentrated lemonade consumption. The data has been fit with an exponential rise and decay (Equation 4-1). See Table B-1 for fit parameters.

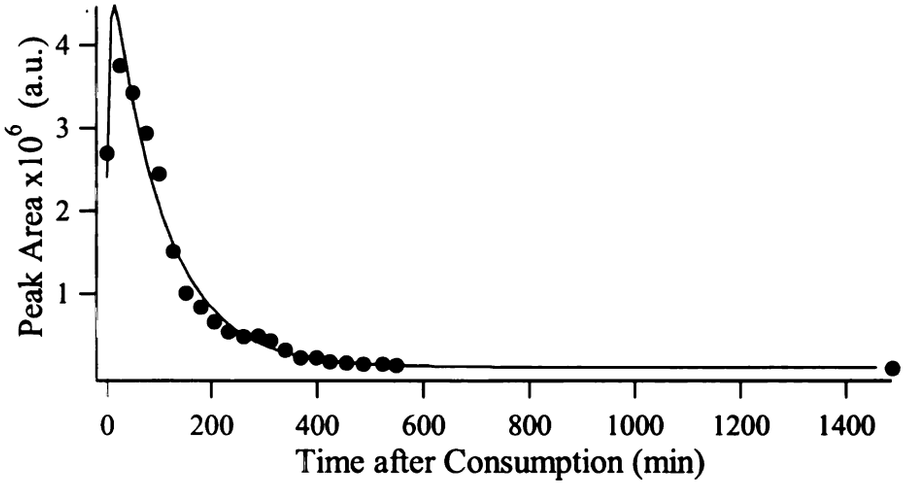

Figure B- 97: Integrated area of the peak attributed to γ-terpinene in chromatograms obtained from the breath of subject A on the first day of concentrated lemonade consumption. The data has been fit with an exponential rise and decay (Equation 4-1). See Table B-1 for fit parameters.

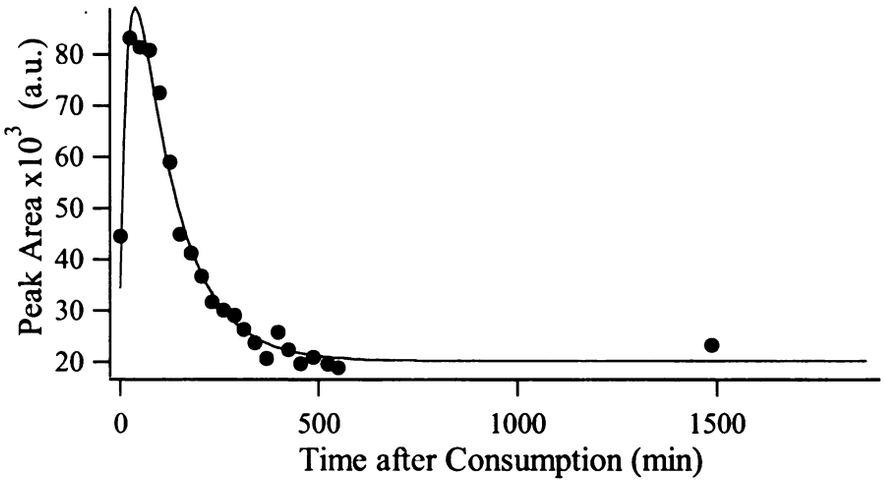

Figure B- 98: Integrated area of the peak attributed to camphene in chromatograms obtained from the breath of subject A on the first day of concentrated lemonade consumption. The data has been fit with an exponential rise and decay (Equation 4-1). See Table B-1 for fit parameters.

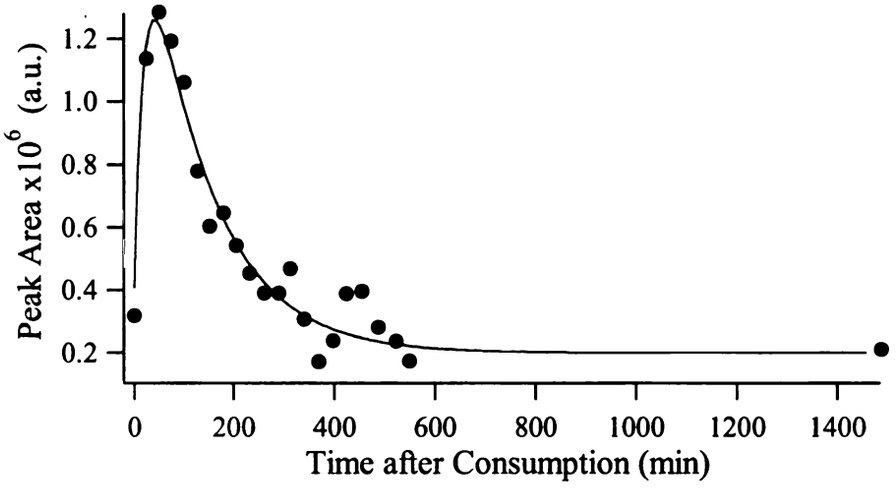

Figure B- 99: Integrated area of the peak attributed to p-cymene in chromatograms obtained from the breath of subject A on the first day of concentrated lemonade consumption. The data has been fit with an exponential rise and decay (Equation 4-1). See Table B-1 for fit parameters.

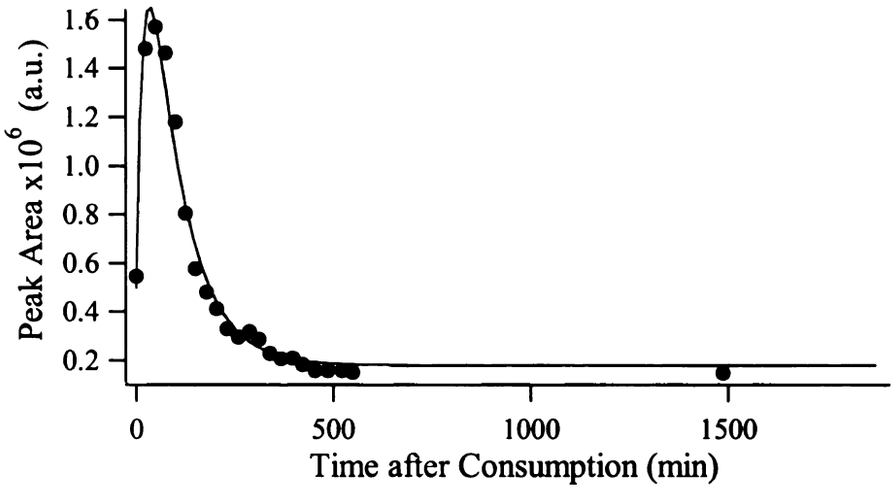

Figure B- 100: Integrated area of the peak attributed to α-pinene in chromatograms obtained from the breath of subject A on the first day of concentrated lemonade consumption. The data has been fit with an exponential rise and decay (Equation 4-1). See Table B-1 for fit parameters.

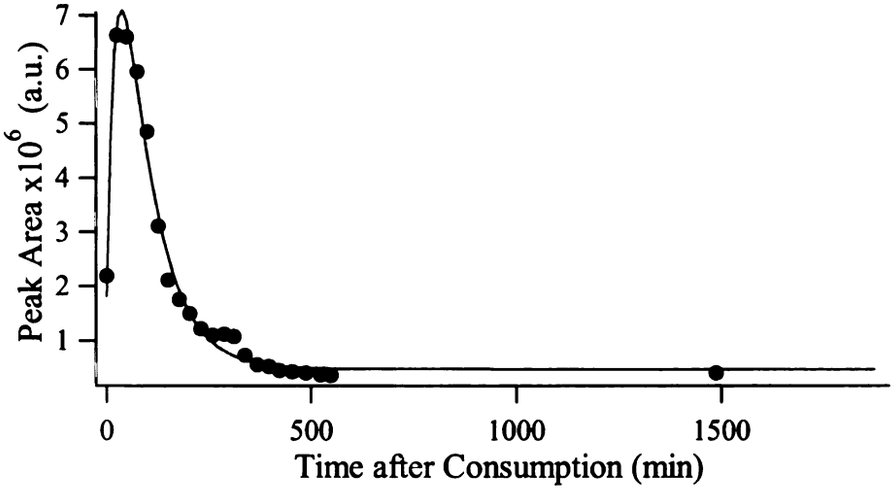

Figure B- 101: Integrated area of the peak attributed to β-pinene in chromatograms obtained from the breath of subject A on the first day of concentrated lemonade consumption. The data has been fit with an exponential rise and decay (Equation 4-1). See Table B-1 for fit parameters.

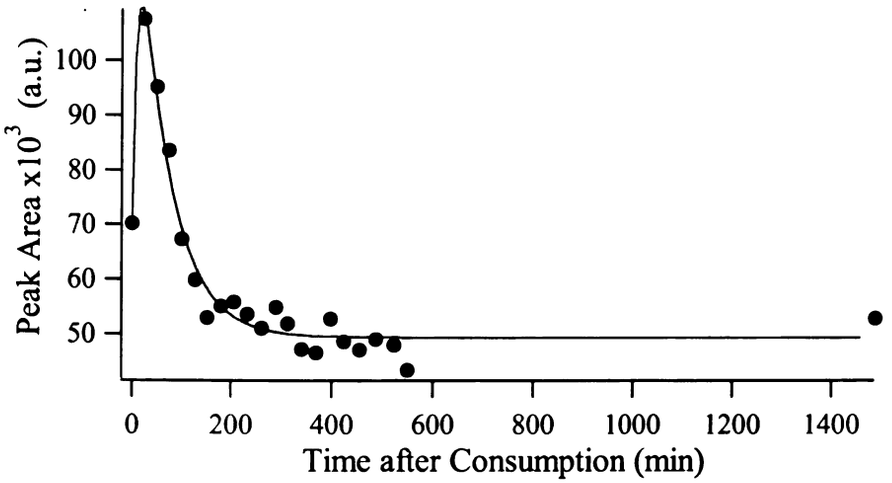

Figure B- 102: Integrated area of the peak attributed to β-phellandrene in chromatograms obtained from the breath of subject A on the first day of concentrated lemonade consumption. The data has been fit with an exponential rise and decay (Equation 4-1). See Table B-1 for fit parameters.

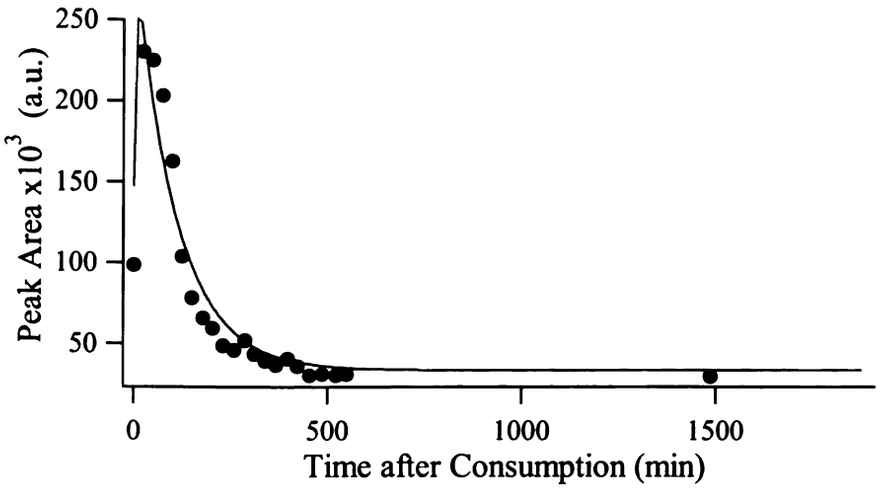

Figure B- 103: Integrated area of the peak attributed to α-thujene in chromatograms obtained from the breath of subject A on the first day of concentrated lemonade consumption. The data has been fit with an exponential rise and decay (Equation 4-1). See Table B-1 for fit parameters.

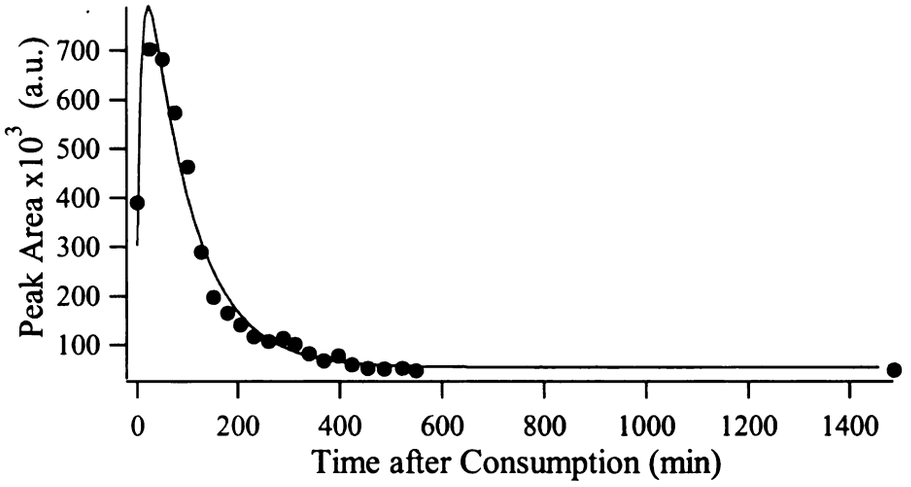

Figure B- 104: Integrated area of the peak attributed to β-myrcene in chromatograms obtained from the breath of subject A on the first day of concentrated lemonade consumption. The data has been fit with an exponential rise and decay (Equation 4-1). See Table B-1 for fit parameters.

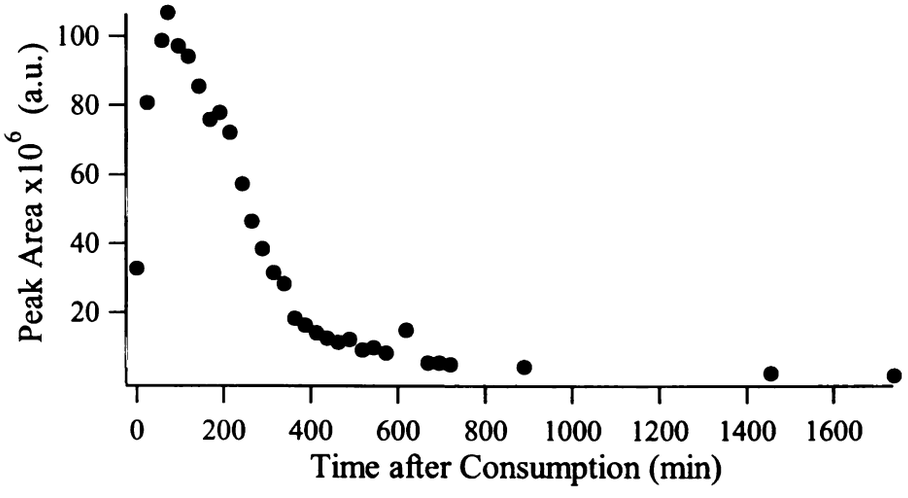

Figure B- 105: Integrated area of the peak attributed to α-limonene in chromatograms obtained from the breath of subject A on the first day of Mediterranean lemonade consumption.

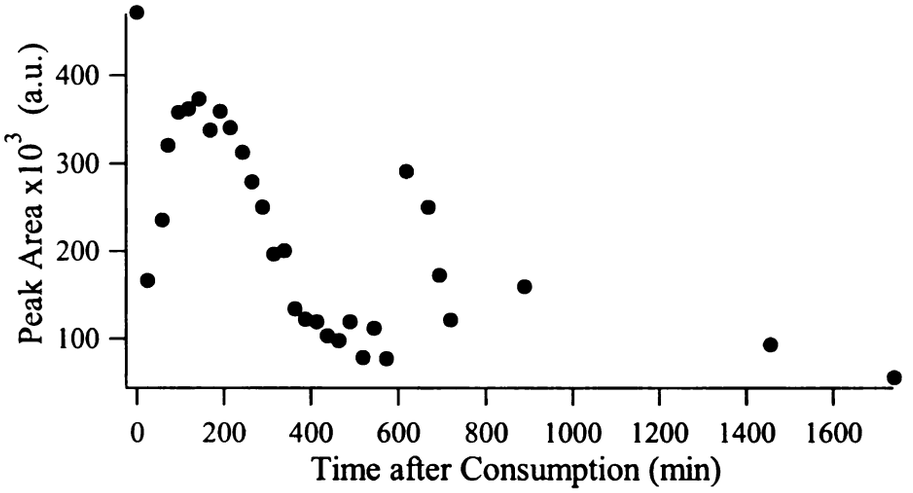

Figure B- 106: Integrated area of the peak attributed to 4-terpineol in chromatograms obtained from the breath of subject an on the first day of Mediterranean lemonade consumption.

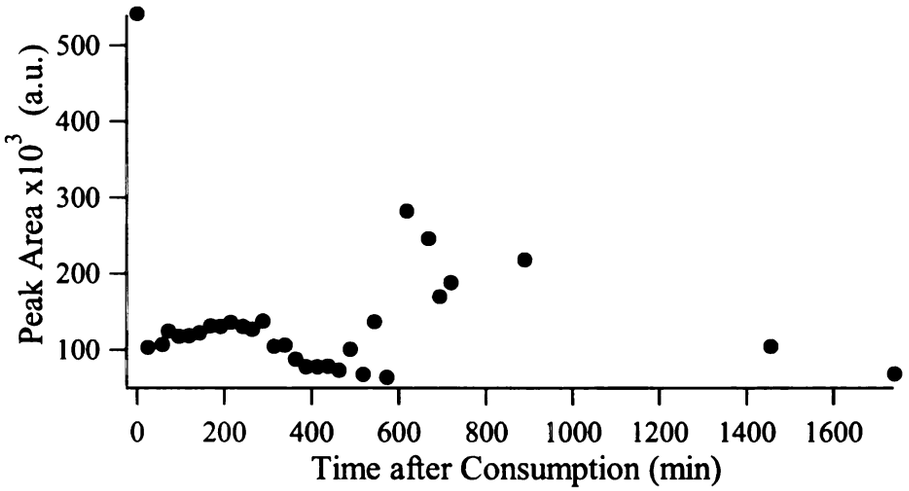

Figure B- 107: Integrated area of the peak attributed to α-terpineol in chromatograms obtained from the breath of subject A on the first day of Mediterranean lemonade consumption.

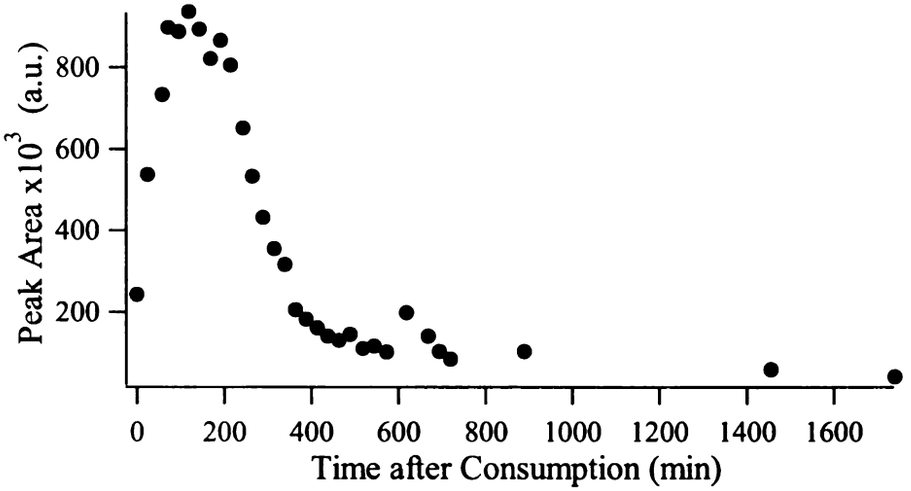

Figure B- 108: Integrated area of the peak attributed to terpinolene in chromatograms obtained from the breath of subject A on the first day of Mediterranean lemonade consumption.

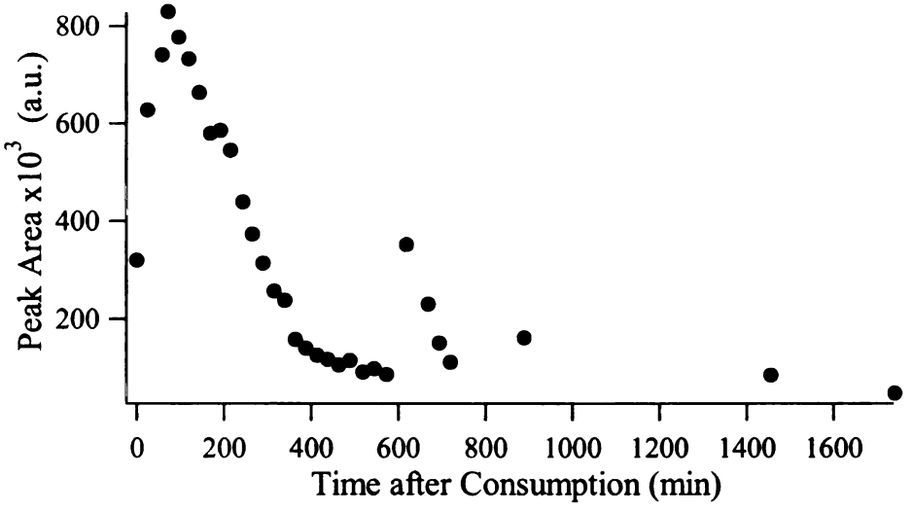

Figure B- 109: Integrated area of the peak attributed to α-terpinene in chromatograms obtained from the breath of subject A on the first day of Mediterranean lemonade consumption.

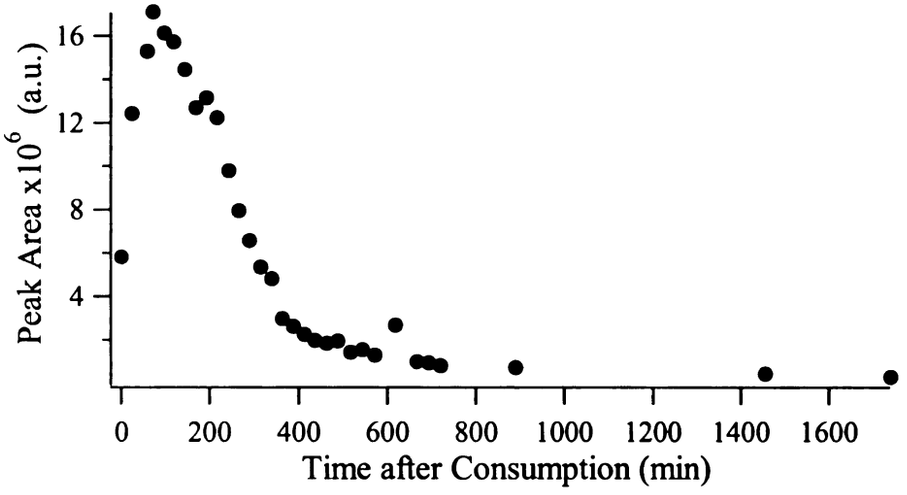

Figure B- 110: Integrated area of the peak attributed to γ-terpinene in chromatograms obtained from the breath of subject A on the first day of Mediterranean lemonade consumption.

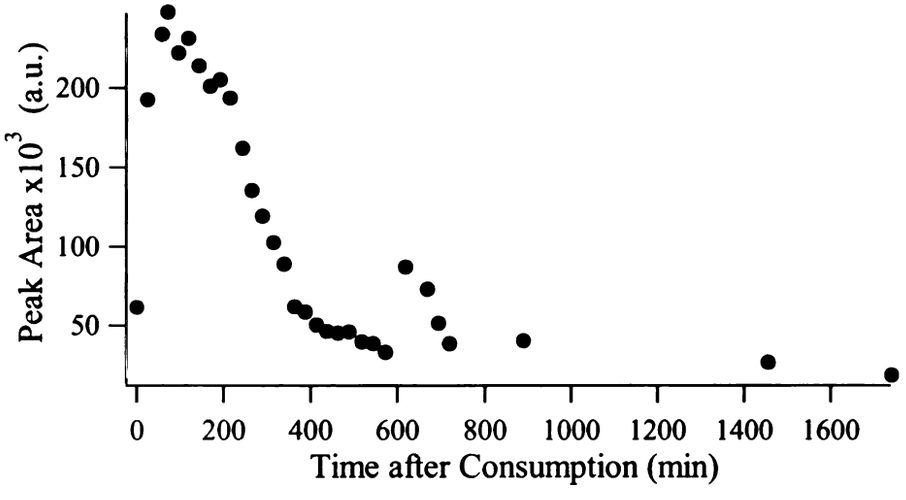

Figure B- 111: Integrated area of the peak attributed to camphene in chromatograms obtained from the breath of subject A on the first day of Mediterranean lemonade consumption.

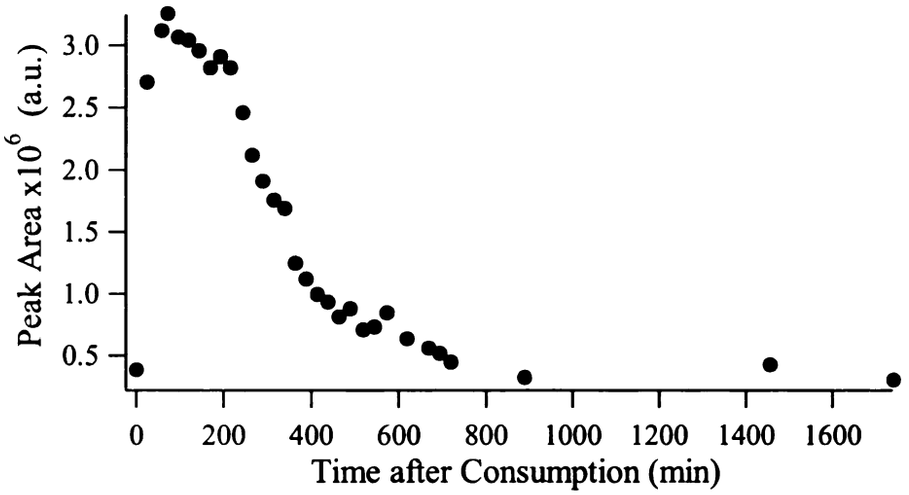

Figure B- 112: Integrated area of the peak attributed to p-cymene in chromatograms obtained from the breath of subject A on the first day of Mediterranean lemonade consumption.

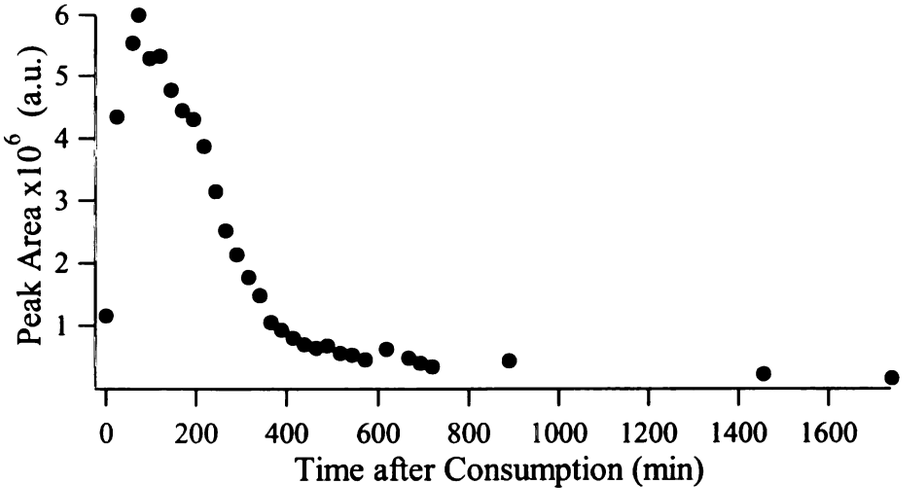

Figure B- 113: Integrated area of the peak attributed to α-pinene in chromatograms obtained from the breath of subject A on the first day of Mediterranean lemonade consumption.

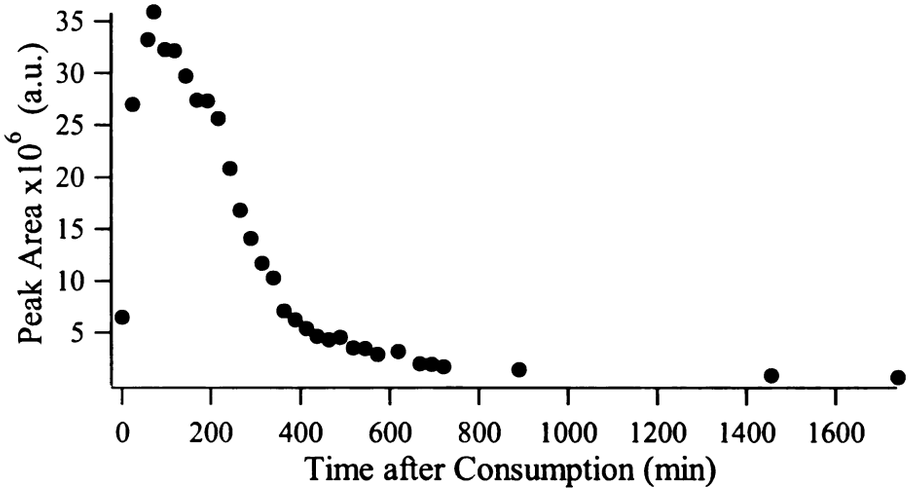

Figure B- 114: Integrated area of the peak attributed to β-pinene in chromatograms obtained from the breath of subject A on the first day of Mediterranean lemonade consumption.

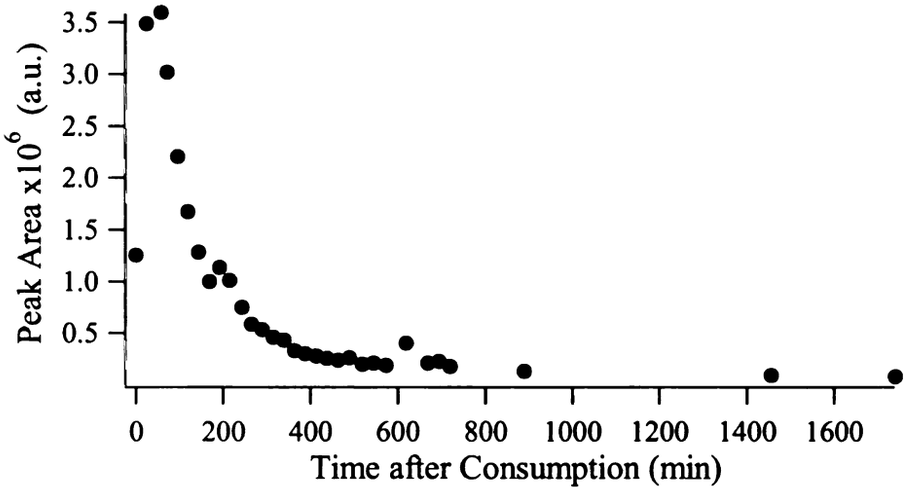

Figure B- 115: Integrated area of the peak attributed to β-phellandrene in chromatograms obtained from the breath of subject A on the first day of Mediterranean lemonade consumption.

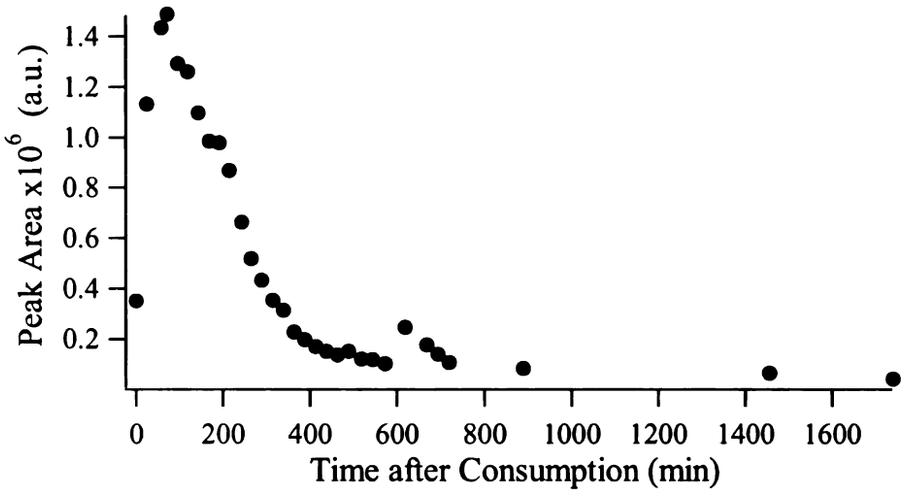

Figure B- 116: Integrated area of the peak attributed to α-thujene in chromatograms obtained from the breath of subject A on the first day of Mediterranean lemonade consumption.

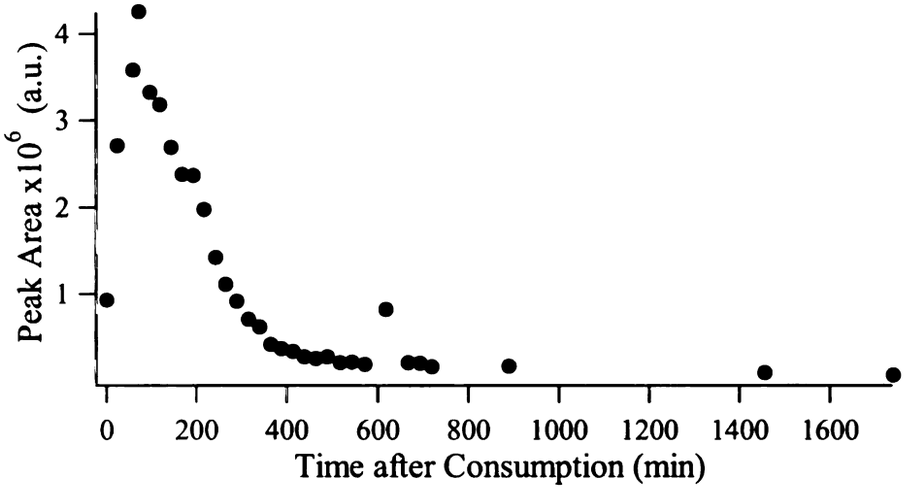

Figure B- 117: Integrated area of the peak attributed to β-myrcene in chromatograms obtained from the breath of subject A on the first day of Mediterranean lemonade consumption.

Table B- 1: Fit Parameters for the terpenes and terpenoid compounds monitored in breath. The data after lemonade consumption were fit according to Equation 4-1.

		Subject A Original First	Subject A Original Second	Subject A Original Third	Subject A Original Fourth	Subject A Original Fifth	Subject B Original First	Subject C Original First	Subject A Concentrated First
α-limonene	y_o	544310	1021000	661590	491670	1089600	3790200	874680	424470
	A_1	21034000	16377000	10373000	11691000	11822000	109160000	16273000	34604000
	tau_1	81.564	108.4	74.521	85.105	83.484	12.349	31.422	114.03
	tau_{ka}	0.2	0.2	0.2	0.2	0.2	0.2	0.2	5
4-terpineol	y_o	51083	80935	53062	50923	49537	163310	125720	65881
	A_1	317930	517310	703930	552660	567080	634550	625420	601010
	tau_1	23.896	9.2733	9.1991	9.9467	8.9428	13.349	15.902	18.076
	tau_{ka}	0.000001	0.000001	0.000001	0.000001	0.000001	0.000001	1E-07	0.001
α-terpineol	y_o	56696	87705	88101	85451	89343	170800	154040	77308
	A_1	252460	767850	1465000	816210	1013100	753710	1212800	542880
	tau_1	15.268	6.6357	7.985	7.5243	5.6561	12.365	10.641	16.807
	tau_{ka}	0.01	0.000001	0.000001	0.000001	1	0.01	1E-07	0.2
terpineolene	y_o	64617	69237	68144	58483	64372	216010	167190	50995
	A_1	209800	204870	169450	16317	115580	1652000	536590	356460
	tau_1	78.108	91.896	38.416	31.751	40.248	15.107	34.455	99.715
	tau_{ka}	0.001	0.001	0.001	0.001	0.001	0.001	0.001	5
α-terpinene	y_o	36958	51700	46303	44039	44389	110570	67407	35795
	A_1	131740	99934	68834	14414	41738	1009800	154460	325180
	tau_1	68.593	103.75	60.344	18.312	50.149	10.478	27.205	106.02
	tau_{ka}	0.1	0.1	0.1	0.1	0.1	0.1	0.1	5
γ-terpinene	y_o	141540	193150	139900	129970	216150	507560	176230	115050
	A_1	3274900	2588000	1674100	1945500	2033800	20981000	2854200	5411600
	tau_1	63.624	78.745	54.905	60.109	55.548	10.638	24.828	99.381
	tau_{ka}	0.001	0.001	0.001	0.001	0.001	0.001	0.001	5

Table B- 1 (cont'd).

		Subject A Original First	Subject A Original Second	Subject A Original Third	Subject A Original Fourth	Subject A Original Fifth	Subject B Original First	Subject C Original First	Subject A Concentrated First
camphene	y_o	17514	484.92	189.55	-53.236	-459.81	38904	34352	20197
	A_1	47217	6917.7	3083.4	3642.6	3792.7	149140	44602	127360
	tau_1	110.64	143.19	206.24	185.91	349.4	11.6	36.913	102.43
	tau_{ka}	1.5	1.5	1.5	1.5	1.5	1.5	1.5	20
p-cymene	y_o	82408	82563	68480	47475	-370770	261000	150230	199970
	A_1	557820	408760	211550	348540	718880	1936800	589630	1785100
	tau_1	137.65	250.73	153.15	202.34	1032.7	26.01	58.287	125.94
	tau_{ka}	1	1	1	1	1	1	1	20
α-pinene	y_o	93362	189450	137520	101760	103430	213250	148260	179430
	A_1	867400	942450	409330	446750	377030	3934900	480570	3026700
	tau_1	98.043	128.98	110.21	137.08	171.21	8.8082	45.438	84.163
	tau_{ka}	2	2	2	2	2	2	2	20
β-pinene	y_o	252950	388570	310790	246720	336370	443750	326810	107140
	A_1	4671600	3229900	1156400	1533400	1178800	21566000	1442200	8452400
	tau_1	68.442	136.25	85.069	139.58	161.39	9.1774	35.176	132.87
	tau_{ka}	1.5	1.5	1.5	1.5	1.5	1.5	1.5	5
β-phellandrene	y_o	35710	26337	46418	25998	62417	69373	48093	49434
	A_1	24723	29399	4273.9	13625	-21769	89102	1383.9	102570
	tau_1	38.561	207.12	479.66	144.13	1107.3	1.6004	9.1121	62.239
	tau_{ka}	0.1	0.1	0.1	0.1	0.1	0.1	0.1	10
α-thujene	y_o	25208	31416	30556	29669	30051	42818	35280	33511
	A_1	1.1101	60926	21087	15648	13470	404250	23081	268620
	tau_1	61.854	131.9	82.485	99.071	54.184	8.4933	17.735	106.93
	tau_{ka}	1	1	1	1	1	1	1	5
β-myrcene	y_o	46828	63287	59473	49877	63215	115540	57665	54613
	A_1	572360	400240	215380	196240	255320	3555100	331510	1098000
	tau_1	69.242	120.56	66.424	81.517	68.671	9.3712	29.104	88.277
	tau_{ka}	0.1	0.1	0.1	0.1	0.1	0.1	0.1	10